Springer Protocols

Methods in Molecular Biology 611

Histology Protocols

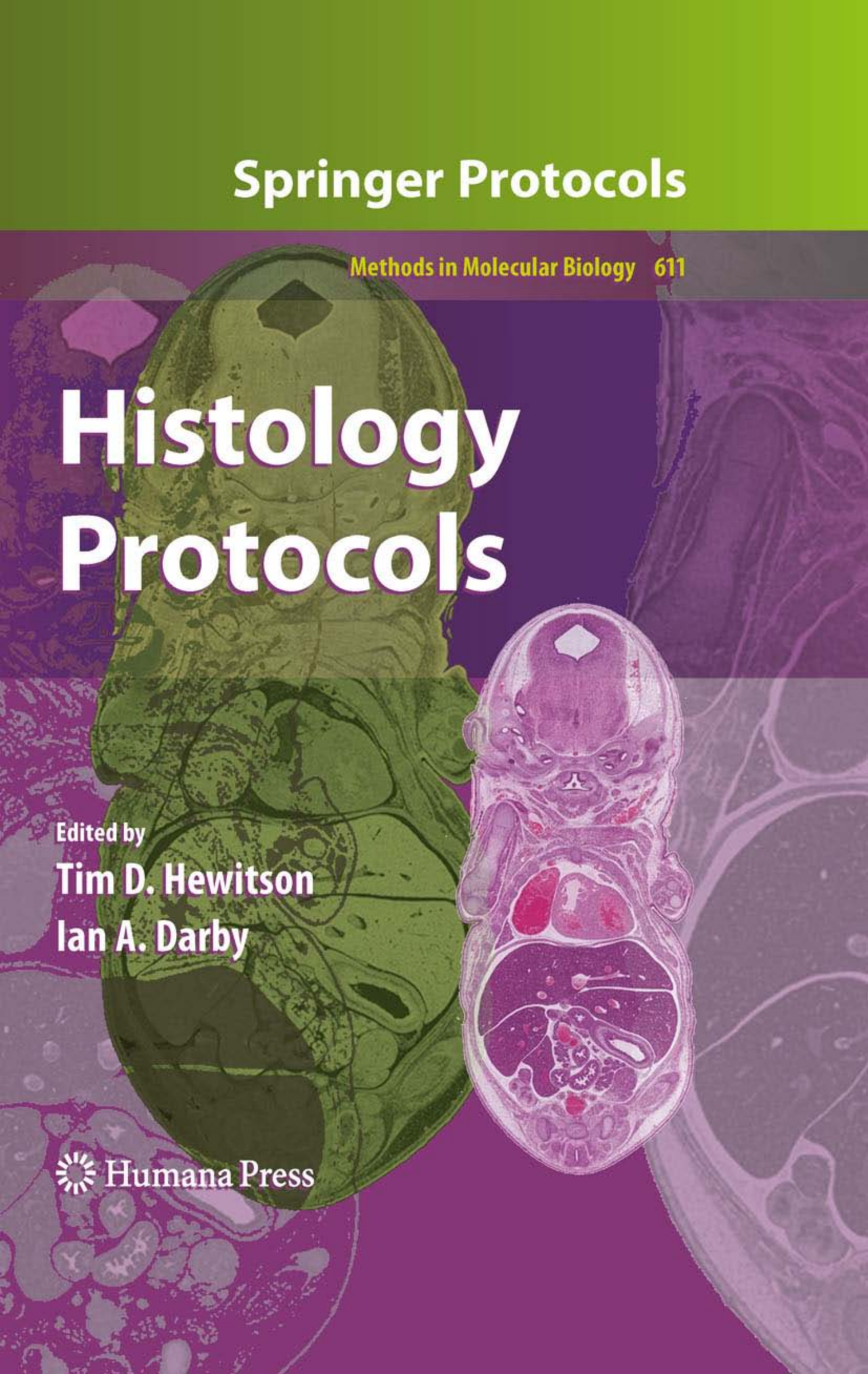

Edited by

Tim D. Hewitson

Ian A. Darby

Humana Press

METHODS IN MOLECULAR BIOLOGY™

Series Editor
John M. Walker
School of Life Sciences
University of Hertfordshire
Hatfield, Hertfordshire, AL10 9AB, UK

For other titles published in this series, go to
www.springer.com/series/7651

Histology Protocols

Edited by

Tim D. Hewitson

Royal Melbourne Hospital and University of Melbourne, Melbourne, VIC, Australia

Ian A. Darby

RMIT University, Bundoora, VIC, Australia

Humana Press

Editors
Tim D. Hewitson
Department of Nephrology
Royal Hospital Melbourne
Grattan Street, Melbourne VIC 3050
Australia
tim.hewitson@mh.org.au

Ian A. Darby
School of Medical Sciences
Cancer & Tissue Repair Research Group
RMIT University
Plenty Road, Melbourne VIC 3083
Australia
ian.darby@rmit.edu.au

ISSN 1064-3745 e-ISSN 1940-6029
ISBN 978-1-60327-344-2 e-ISBN 978-1-60327-345-9
DOI 10.1007/978-1-60327-345-9

Library of Congress Control Number: 2009939928

Printed on acid-free paper

springer.com

Preface

So much of what we know about the pathogenesis of human disease has come from the systematic and careful study of histological material. Indeed, every internal medicine discipline has its landmark papers describing the clinico-pathological correlations. However, increasingly, it is molecular and cellular biology that provides the necessary mechanistic insights. For many years, it was thought that the two skill sets were mutually exclusive, but we hope that this book shows that this is not necessarily so.

Implicit in the science of histology is the preservation and archiving of tissue. Part I of the book concentrates on the preparation of tissue, providing an overview of fixation, embedding, and processing (**Chapter 1**), and in **Chapters 2** and **3**, the required techniques for the retrieval of RNA from histological sections. Both routine and specialist histological staining techniques are provided in Part II. These include protocols for immuno (**Chapters 4–7**), lectin (**Chapter 8**), and hybridization (**Chapter 9**) histochemistry, histological staining (**Chapters 10** and **11**), as well as specific methods for the in situ identification of hypoxia (**Chapter 12**) and apoptosis (**Chapter 13**). Finally, Part III details advances in imaging (**Chapters 14–16**) and image analysis (**Chapter 17**).

It is hoped that this volume will provide molecular biologists with the basic histochemical techniques and histologists with the molecular techniques to realise the potential of their resource. We are indebted to the authors for their generosity in sharing these protocols.

Tim D. Hewitson
Ian A. Darby
Melbourne, Australia
October 2009

Contents

Contributors

Marcia Barbosa Aguila • *Laboratory of Morphometry and Cardiovascular Morphology, Institute of Biology, Biomedical Center, State University of Rio de Janeiro, Rio de Janeiro, Brazil*

Emilio Badoer • *School of Medical Sciences, RMIT University, Melbourne, VIC, Australia*

Gavin J. Becker • *Department of Nephrology, The Royal Melbourne Hospital, and Department of Medicine, University of Melbourne, Melbourne, VIC, Australia*

Joon-Yong Chung • *Tissue Array Research Program, Laboratory of Pathology, Center for Cancer Research, National Cancer Institute; National Institutes of Health, Bethesda, MD, USA*

Luís Cristóvão de Moraes Sobrino Porto • *Tissue Repair Laboratory, Histology and Embryology Department, State University of Rio de Janeiro, Rio de Janeiro, Brazil*

Ian A. Darby • *Cancer and Tissue Repair Research Group, School of Medical Sciences, RMIT University, Melbourne, VIC, Australia*

Alexis Desmoulière • *Department of Physiology, and EA 3842, Institut Fédératif de Recherche 145, Faculté de Médecine et de Pharmacie, Université de Limoges, Limoges, France*

Amanda J. Edgley • *Department of Medicine, St. Vincent's Hospital, University of Melbourne, Melbourne, VIC, Australia*

Caroline Fernandes-Santos • *Laboratory of Morphometry and Cardiovascular Morphology, Institute of Biology, Biomedical Center, State University of Rio de Janeiro, Rio de Janeiro, Brazil*

Renae M. Gow • *Department of Medicine, St Vincent's Hospital, University of Melbourne, Fitzroy, Melbourne, VIC, Australia*

Tim D. Hewitson • *Department of Nephrology, The Royal Melbourne Hospital; and Department of Medicine, University of Melbourne, Melbourne, VIC, Australia*

Stephen M. Hewitt • *Tissue Array Research Program, Laboratory of Pathology, Center for Cancer Research, National Cancer Institute, National Institutes of Health, Bethesda, MD, USA*

Boris Hinz • *CIHR Group in Matrix Dynamics, Laboratory of Tissue Repair and Regeneration, Faculty of Dentistry, University of Toronto, Toronto, ON, Canada; and Laboratory of Cell Biophysics, Ecole Polytechnique Fédérale de Lausanne (EPFL), Lausanne, Switzerland*

Jin K. Jeong • *Department of Brain and Cognitive Sciences, University of Rochester, Rochester, NY, USA*

G. Allan Johnson • *Center for In Vivo Microscopy, Duke University, Durham, NC, USA*

Darren J. Kelly • *Department of Medicine, St. Vincent's Hospital, University of Melbourne, Melbourne, VIC, Australia*

Carlos Alberto Mandarim-de-Lacerda • *Laboratory of Morphometry and Cardiovascular Morphology, Institute of Biology, Biomedical Center, State University of Rio de Janeiro, Rio de Janeiro, Brazil*

Andreas Möller • *Research Division, Cancer Genomics and Biochemistry Laboratory, Peter MacCallum Cancer Centre, Melbourne, VIC, Australia*

Andréa Monte-Alto-Costa • *Tissue Repair Laboratory, Histology and Embryology Department, State University of Rio de Janeiro, Rio de Janeiro, Brazil*

Christian Mühlfeld • *Institute of Anatomy and Cell Biology, Justus-Liebig-University Giessen, Giessen, Germany*

Alexandra Petiet • *Neurospin, CEA Saclay, Gif-sur-Yvette, France*

Raphael Pinaud • *Department of Brain and Cognitive Sciences; Center for Visual Science and Center for Navigation and Communication Sciences, University of Rochester, Rochester, NY, USA*

Jörg Piper • *Clinic Meduna, Bad Bertrich, D-56864 Bad Bertrich, Germany*

Simon Potocnik • *School of Medical Sciences, RMIT University, Melbourne, VIC, Australia*

Chrishan S. Samuel • *Howard Florey Institute, The University of Melbourne, Melbourne, VIC, Australia*

Vincent Sarrazy • *Faculté de Médecine et de Pharmacie, EA 3842, Institut Fédératif de Recherche 145, Université de Limoges, Limoges, France*

Josiane Smith-Clerc • *Laboratory of Cell Biophysics, Ecole Polytechnique Fédérale de Lausanne (EPFL), Lausanne, Switzerland*

Martin Stebbing • *School of Medical Sciences, RMIT University, Melbourne, VIC, Australia*

Belinda Wigg • *Department of Nephrology, The Royal Melbourne Hospital, Melbourne, VIC, Australia*

Verena C. Wimmer • *Ion Channels and Disease Group, Howard Florey Institute, The University of Melbourne, Melbourne, VIC, Australia*

Catherine Winbanks • *Baker IDI Heart and Diabetes Institute, Melbourne, VIC, Australia*

Su Ee Wong • *Department of Nephrology, The Royal Melbourne Hospital, Melbourne, VIC, Australia*

Pinglu Ye • *School of Medical Sciences, RMIT University, Melbourne, VIC, Australia*

Richard J. Young • *Research Division, Translational Research Laboratory, Peter MacCallum Cancer Centre, Melbourne, VIC, Australia*

Part I

Tissue Processing

Chapter 1

Tissue Preparation for Histochemistry: Fixation, Embedding, and Antigen Retrieval for Light Microscopy

Tim D. Hewitson, Belinda Wigg, and Gavin J. Becker

Abstract

A number of techniques have been developed to use chemical, immunological, and molecular biology assays in histological material. Collectively termed histochemistry, these techniques have allowed us to better understand tissue and organ biology in situ. Success with each of these methods is dependent on the adequate preparation of material. In this article, we describe the basic steps required to prepare tissue for routine histochemical analysis.

Histochemical techniques routinely use frozen and paraffin-embedded tissue as a basis for cellular and morphological analysis. Freezing tissue results in less alteration to epitopes and therefore may offer improved staining characteristics compared to techniques based on paraffin embedding. As in conventional histology, the use of fixation and embedding in more rigid media such as wax offers a number of potential advantages related to improved structural detail. Improvements in morphology may however be offset by a loss of antigens. The careful application of antigen retrieval techniques may overcome these deficiencies.

Key words: Histochemistry, fixative, histology, antigen retrieval.

1. Introduction

For more than three decades, a variety of techniques have been developed to use chemical, immunological, and molecular biology assays in histological material. Collectively termed histochemistry, these techniques have allowed us to better understand tissue and organ biology in situ.

In its simplest form, histochemistry uses sections of unfixed frozen tissue to maximize the accessibility of antigens, proteins, and genetic material. However, as in conventional histology, the use of fixation and embedding in more rigid media, such as wax, offers a number of potential advantages related to improved morphology (1, 2).

T.D. Hewitson, I.A. Darby (eds.), *Histology Protocols*, Methods in Molecular Biology 611,
DOI 10.1007/978-1-60327-345-9_1,

1.1. Fixation

Fixation confers chemical stability on tissue, hardens tissue for sectioning, and, most importantly, halts autolysis and degradation. Chemical fixatives preserve tissue by denaturing proteins through coagulation (e.g., acetone, methyl Carnoy's), cross-linking (e.g., formaldehyde), or both (e.g., mercuric formalin). Changes to the molecular form mean that fixation is often therefore a compromise between retention and preservation. It also alters tissue penetration and antigen exposure, which may be advantageous or disadvantageous.

A number of different individual fixatives are in use. The most common routine fixatives for histology are formaldehyde-based fixatives such as neutral buffered formalin (NBF) and 4% paraformaldehyde (4% PFA). Aldehydes stabilize proteins by cross-linking amino acid side chains. NBF offers good preservation and ease of use. Four percent PFA is popular for immunostaining, but unlike NBF, it needs to be freshly prepared. Periodate–lysine–paraformaldehyde (PLP) is a variation of PFA, where the addition of periodate oxidizes polysaccharide chains and forms lysine-mediated cross-links (3). Bouin's fixative is particularly useful for soft and delicate tissues (such as brain and embryos) and small pieces of tissue. It is a good preservative of glycogen and nuclei (4), but penetrates slowly, and distorts kidney tissue and mitochondria. Fixation in mercuric formalin gives excellent nuclear staining and is widely used in lymph nodes, bone marrow, and other tissues to obtain superior nuclear detail (5). Finally, our laboratory has found methyl Carnoy's (6) particularly useful for immunoperoxidase staining of extracellular matrix constituents.

Chemical fixatives may be administered in two ways: immersion and perfusion via the circulation. Immersion fixation refers to the immersion of dissected tissue in fixative; fixation therefore occurs via diffusion and is directly related to the size of tissue. In experimental studies, in situ perfusion fixation may also be possible. In this case, fixative is infused through the blood flow of an anesthetized animal by cannulation of the aorta. Although in situ fixation of highly vascularized organs such as the kidney is far better (**Fig. 1.1**), perfusion fixation is time consuming and means that only a single fixative can be used for each animal.

1.2. Embedding

Most tissue for histochemistry is embedded in paraffin wax. In tissues with complex cellular structures such as the renal glomerulus, embedding in more rigid media such as wax or plastic resin means that thinner sections can be cut and therefore much greater microscopic detail can be obtained.

A combination of cross-linking fixatives with paraffin embedding produces excellent morphology, but there are significant problems with both the loss of epitopes through cross-linking and degradation after prolonged exposure to high-temperature

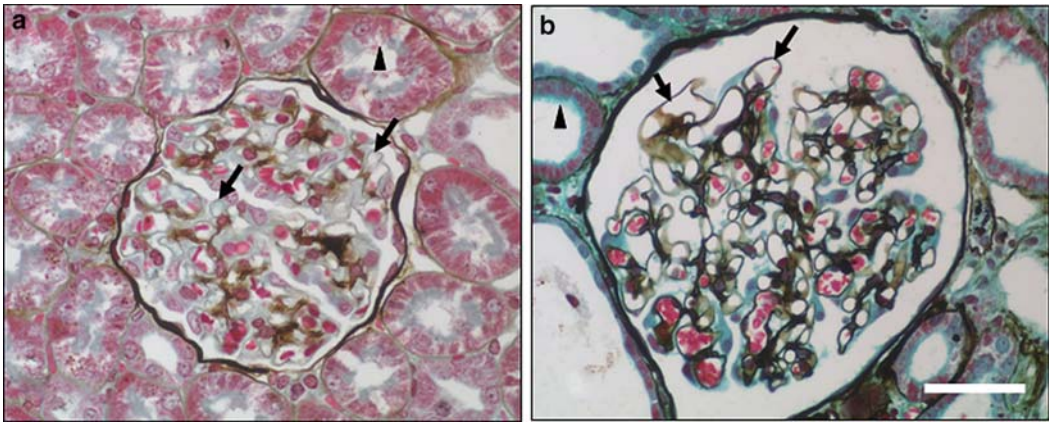

Fig. 1.1. Comparison of silver methenamine-Masson trichrome staining of rat kidney tissue after (**a**) immersion and (**b**) perfusion fixation. Perfusion results in both improved preservation and greater patency of glomerular capillary loops (*arrows*). Likewise fixation of tubules is much improved; *arrowheads* highlight preservation of the proximal tubule brush border. Bar=100 μm. (*see* **Chapter 10** for a discussion of trichrome staining).

wax during embedding. The temperature effect is particularly problematic with in situ hybridization studies due to the instability of RNA. Furthermore, the infiltration of a hydrophobic embedding matrix such as paraffin wax provides support but also further inhibits chemical, antibody, and probe penetration. Incomplete removal of wax before staining is therefore a potential artifact. An alternative strategy is to freeze the tissue after fixation in 4% PFA, a fixative that only mildly cross-links proteins. The compromise between fixation and embedding offers some improvement in morphology, without excessive cross-linking and heat exposure.

1.3. Antigen Retrieval

After sectioning, antigen retrieval is often necessary in order to expose antigens that have been masked by the fixation and embedding process (7). Formalin or other aldehyde fixation forms protein cross-links that mask the antigenic sites in tissue specimens, thereby giving weak or falsely negative immunohistochemical staining (8). The purpose of antigen retrieval is therefore to break the protein cross-links, unmask the antigens and epitopes in formalin-fixed and paraffin-embedded tissue sections, and thereby enhance the staining intensity of antibodies. There are two main techniques that can be used for antigen retrieval: proteolytic (enzymatic) digestion and heat-induced antigen retrieval.

Proteolytic digestion is thought to enzymatically break the protein cross-links. A number of proteolytic enzymes are used for this purpose and include, but are not limited to, trypsin, proteinase K, pepsin, and collagenase. Although protease pretreatment of sections can result in a dose- and time-dependent

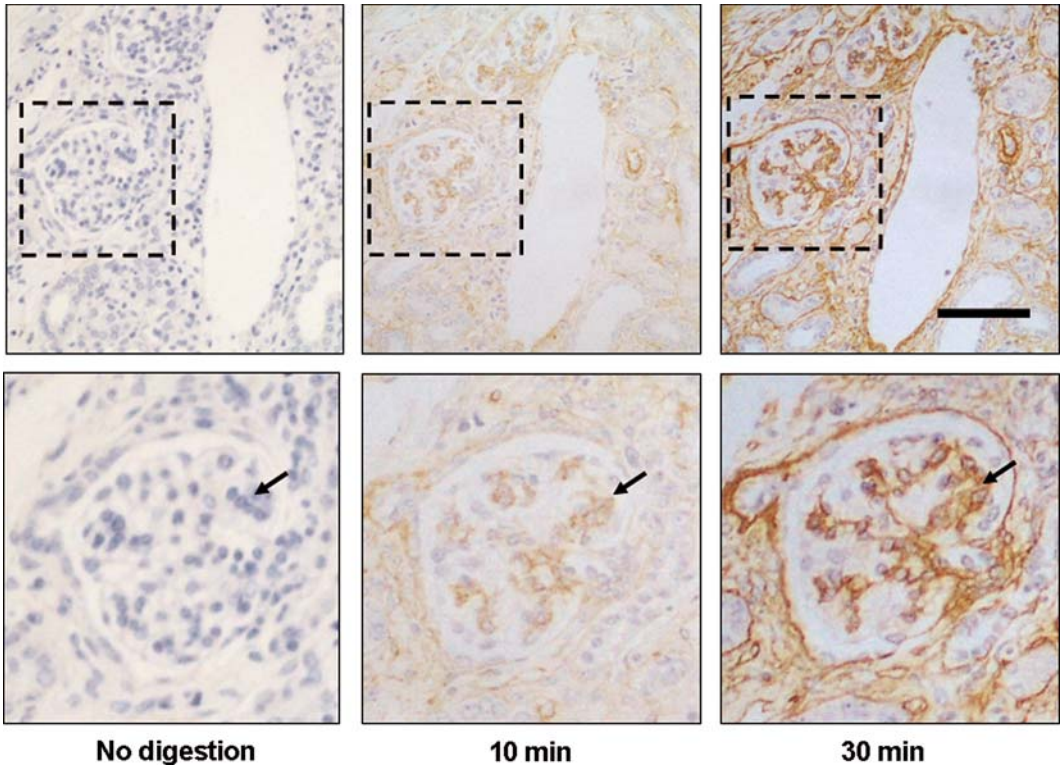

Fig. 1.2. Effect of increasing digestion time on immunostaining for the extracellular matrix protein collagen IV. Serial sections of rat kidney tissue from an animal with interstitial fibrosis and glomerulosclerosis. Undigested fixed tissue shows no immunostaining for collagen IV. Digestion with proteinase K (20 mg/mL) results in a time-dependent increase in staining, as highlighted by the *arrows*. Bar=200 μm.

increase in staining (**Fig. 1.2**), over-digestion can just as easily destroy both epitopes and tissue structure (morphology) and may increase false-positive and background staining.

Heat is hypothesized to cause protein denaturation based on the observation that some antigens may be lost after the heat treatment, and heat induces reversal of various chemical modifications of the protein structure that results from fixation (7–9). Heat-induced epitope retrieval (HIER) (sometimes termed decloaking or unmasking) was initially achieved by microwaving, although a number of methods are now used. These include pressure cookers, autoclaving, and even the standard laboratory water bath, where temperatures of less than 100°C are required.

While it is generally accepted that heat is the key factor in microwave retrieval, the rapidly oscillating electromagnetic field of microwaves may itself directly affect chemical reactions and protein structure. Microwave energy may also have the added advantage of mobilizing the last traces of paraffin that may not have been extracted by section rehydration. Some have suggested using a combination of both heat and enzymatic retrieval methods to produce the desired staining intensity.

Optimal preservation, embedding, and pre-treatment of tissue are therefore the essential first steps for successful histology, immunochemistry, and hybridization chemistry. What follows are our suggested protocols for the preparation of tissue for microscope slide-based histochemistry.

2. Materials

2.1. Fixatives

The following is a list of commonly used fixatives. Selection of the appropriate fixative may need to be determined by trial and error, as all fixatives influence antigenicity in the tissue to some extent.

2.1.1. Neutral Buffered Formalin (NBF)

Ten percent v/v neutral buffered formalin: 100 mL formalin (~40% aqueous solution of formaldehyde) (BDH, Poole, UK), 4 g NaH_2PO_4 (monohydrate), 6.5 g Na_2HPO_4 (anhydrous), deionized water (dH_2O) to 1 L (*see* **Notes 1** and **2**).

2.1.2. Paraformaldehyde (PFA)

1. Phosphate buffered saline (PBS): Prepare a 10 × stock by dissolving 80 g of NaCl, 2.0 g of KCl, 14.4 g of Na_2HPO_4 and 2.4 g of KH_2PO_4 in 900 mL of dH_2O. Adjust to pH 7.4 and make up to 1 L. Dilute 1:10 for a 1 × working concentration (1 × PBS).
2. 4% PFA: Add 4 g paraformaldehyde (BDH) to 100 mL phosphate buffered saline (PBS) pH 7.4, heat to a maximum of 60°C with stirring, and add 5–10 drops of 1 M NaOH to clear (*see* **Note 2**).

2.1.3. Paraformaldehyde–Lysine–Periodate (PLP)

1. Stock A: Dissolve 1.827 g L-lysine HCl in 50 mL dH_2O. After adjusting the pH to 7.4 with 0.1 M Na_2HPO_4, the solution is made up to 100 mL with 0.1 M $NaPO_4$, pH 7.4. This solution can be stored at 4°C for up to 10 days.
2. Stock B: Mix 8.0 g of paraformaldehyde (*see* **Note 2**) in 100 mL of distilled water and heat to 60°C with stirring. One to five drops of 1 M NaOH are added slowly until the mixture turns clear. After passing through filter paper, this solution can be stored at 4°C for up to 1 day.
3. Finally, when required, PLP is prepared by combining three parts of stock A solution with one part of stock B solution and adding sodium *m*-periodate to a final concentration of 0.01 M.

2.1.4. Bouin's Fixative

Bouin's solution: Combine 75 mL saturated (1.2% w/v) aqueous picric acid (Sigma-Aldrich, St. Louis, MI, USA), 25 mL formalin (~40% w/v aqueous solution of formaldehyde) (BDH), and 5 mL of glacial acetic acid (*see* **Notes 2** and **3**).

2.1.5. Mercuric Formalin

1. Mercuric formalin fixative: Combine 100 mL formalin (~40% w/v aqueous solution of formaldehyde) (BDH) (*see* **Note 2**), 9 g NaCl, 900 mL dH_2O, and add HgCl (*see* **Note 2**) with stirring until saturated. Store with residual undissolved HgCl to maintain saturation (*see* **Note 4**).
2. Lugol's iodine: 2% w/v iodine in 70% ethanol.
3. 5% w/v sodium thiosulfate in dH_2O.

2.1.6. Methyl Carnoy's

Methyl Carnoy's fixative: 60% methanol, 30% chloroform, 10% glacial acetic acid v/v/v.

2.2. Additional Materials for Perfusion Fixation

1. Anesthetic: sodium pentobarbital (Nembutal™; Boehringer Ingelheim, Sydney, NSW, Australia).
2. Scalpel, scissors, forceps for general surgical procedures.
3. Small forceps with fine claws for clamping aorta.
4. Surgical tape.
5. Small vials (10–20 mL) with lids for storing specimens.
6. 0.9% saline.
7. Two 1-L reservoirs for holding perfusion fluids (saline, fixative) (**Fig. 1.3**). These need to be equipped so that they can be held approximately 1 m above the bench for a gravity-fed flow.

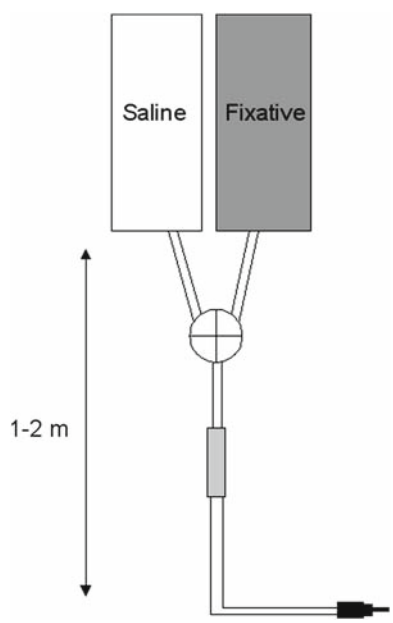

Fig. 1.3. Schematic drawing of a typical perfusion apparatus showing arrangement of reservoirs, and the position of three-way stopcock to allow a rapid change between saline and fixative.

8. Perfusion apparatus assembled from perfusion set with drip chamber and luer-lock connectors, as used for intravenous blood infusions.
9. Blunt short syringe needle for perfusion of aorta, length about 50 mm, outer diameter 1.3–1.5 mm. Blunted 18-G needles are ideally suited and can be prepared in a workshop by cutting and grinding syringe needles. Putting a slight bend in the needle makes cannulation easier.

2.3. 3-Aminopropyltriethoxysilane (APES)-Coated Slides

1. Microscope slides.
2. Laboratory detergent, e.g., Pyroneg™ (Johnson Diversey Australia Pty Ltd., Smithfield, Australia).
3. Ethanol.
4. Hair dryer.
5. Acetone.
6. 2% freshly prepared solution of APES (Sigma-Aldrich) (*see* **Note 2**) in dry acetone (w/v).

2.4. Tissue Freezing and Sectioning

1. Small bowl filled with isopentane (2-methylbutane).
2. Polystyrene box.
3. Dry ice (*see* **Note 2**).
4. Forceps.
5. 1 × PBS (*see* **Section 2.1.2**).
6. Sucrose wash buffer: 7% w/v sucrose in PBS.
7. OCT (Tissue-Tek™; Sakura Finetek, Torrance, CA, USA) or equivalent cryogenic tissue-embedding compound.
8. Embedding molds (Simpot, Beloeil, QC, Canada) (*see* **Note 5**).
9. APES-coated microscope slides (*see* **Section 2.3**).
10. Cryostat.
11. Acetone (if post-fixing after cutting).
12. Sealed plastic slide boxes with desiccant.

2.5. Paraffin Embedding and Sectioning

1. Labeled glass vials.
2. Graded ethanol: 50, 70, 95, and 100% v/v mixture of ethanol and water.
3. Chloroform.
4. Paraplast™ paraffin-embedding medium (McCormick Scientific, St. Louis, MO, USA), or equivalent low-temperature embedding wax.
5. Embedding molds and cassettes (Simpot).
6. Scalpel and no. 22 blade.
7. Small bowl.

8. Artist's paint brush.
9. Shallow bowl filled with a 20% v/v mixture of ethanol and water.
10. Microtome.
11. Uncoated microscope slides.
12. APES-coated microscope slides (*see* **Section 2.3**).
13. Histological water bath.
14. Slide racks.

2.6. Antigen Retrieval

Listed below are a number of commonly used enzymes and antigen retrieval buffers. The appropriate solution depends on individual circumstances.

2.6.1. Protease Digestion

1. Protease digest: Dissolve 0.0125 g protease VIII (bacteria from *Bacillus licheniformis*; Sigma-Aldrich) in 50 mL (1 × PBS) (*see* **Section 2.1.2**).
2. 1 × PBS.
3. Coplin jar (staining jar with internal ridges to hold slides apart).

2.6.2. Trypsin Digestion

1. Trypsin digest: Add 100 mg trypsin (type II porcine pancreas trypsin; Sigma-Aldrich) to 100 mL of dH_2O pre-heated to 37°C and stir gently. When dissolved, add 100 mg $CaCl_2$ and adjust to pH 7.8 with 0.1 M NaOH. Keep at 37°C and use within 30 min.
2. Coplin jar.

2.6.3. Hydrochloric Acid (HCl) Solution

1. 0.2 M HCl: Add 20 mL 10 N (concentrated) HCl to 80 mL dH_2O and mix. pH should be around 0.6–0.9.
2. Coplin jar.
3. 1 × PBS (*see* **Section 2.1.2**).

2.6.4. Citrate Buffer Antigen Retrieval Solution (pH 6.0)

1. Citrate buffer: 0.01 M citric acid monohydrate in dH_2O. Adjust to pH 6.0 with 2 M NaOH and make up to 1 L.
2. Plastic film (domestic food wrap).
3. Plastic coplin jar (microwavable staining jar with internal ridges to hold slides apart).
4. 1 × PBS (*see* **Section 2.1.2**).

2.6.5. Tris–EDTA Buffer Antigen Retrieval Solution (pH 9.0)

1. 10 mM Tris–1 mM EDTA: Add 1.21 g of Tris and 0.37 g of EDTA in 900 mL of dH_2O. Add Tween 20 at 0.05% v/v and adjust to pH 9 if necessary. Make up to 1 L.
2. Plastic film (domestic food wrap).
3. Plastic coplin jar (microwavable staining jar with internal ridges to hold slides apart).
4. 1 × PBS (*see* **Section 2.1.2**).

3. Methods

3.1. Immersion Fixation

For many purposes, adequate fixation is obtained by simple immersion of small tissue pieces into the fixative solution. This is the only mode of fixation possible for many tissues, and if it is necessary to process in multiple fixatives.

The appropriate fixative depends on a number of factors including the nature of the antigen and antibody, and any other anticipated usage of tissue (e.g., simultaneous study of protein and mRNA expression). For immersion fixation, keep tissue in fixative for 4–24 h depending on the size of tissue. As a guide, biopsy-sized tissue is fixed for 4 h, 1 cm^2 portions for 18 h.

3.1.1. NBF, Mercuric Formalin, or Bouin's Fixative

1. Immerse tissue in fixative, ensuring that the fixative is at least 10 × the volume of tissue.
2. Store at room temperature until embedding.

3.1.2. 4% PFA and PLP

1. Immerse in cold freshly prepared fixative, 10 × the volume of tissue.
2. Store at 4°C for 2–18 h, depending on size of tissue.
3. If tissue is to be frozen, wash overnight at 4°C in sucrose wash buffer (7% sucrose in PBS) (*see* **Note 6**).

3.1.3. Methyl Carnoy's

1. Immerse tissue in cold, freshly prepared fixative, 10 × volume of tissue.
2. Store at 4°C until processing and embedding.

3.2. Perfusion Fixation

Under in situ conditions, vascular perfusion of fixative results in a more uniform and rapid dissemination of fixative into all parts of the tissue via the vascular bed, resulting in an increased depth and rate of actual fixation. The following procedures provide a generic protocol for fixation of most rat organs with 4% paraformaldehyde.

1. Fill reservoirs with saline and fixative, and assemble the perfusion set. The volume of fixative should be scaled to the size of animal with a minimum of 200–300 mL per 200 g rat. Connect perfusion needle.
2. Run approximately 100 mL of saline through the tubing to clean and remove any air bubbles. Adjust to a slow steady drip (20 mL/min) and then close valve.
3. Induce anesthesia with an intraperitoneal (ip) injection of pentobarbital at the recommended injectable dose. Use the pinch-response method to determine the depth of anesthesia. Allow 10–15 min for anesthesia to occur, indicated by the loss

of sensory/reflex response, i.e., non-response to tail pinching and no eye reflex. The animal must be unresponsive before proceeding with the next steps.

4. Once the animal is under anesthetised, place it on the operating table with its abdomen exposed. It often helps to use tape to hold the appendages so that the animal is securely fixed.
5. Open the abdominal cavity by a long midline incision with lateral extension and move the intestines to the left side of the animal.
6. Carefully expose the aorta below the origin of the renal arteries and very gently free the aorta from overlaying adipose and connective tissues.
7. Hold the wall of the aorta firmly with fine forceps with claws, about 0.5–1.0 cm from its distal bifurcation. Insert the perfusion needle into the lumen of the aorta, facing the heart and close to the forceps.
8. In very rapid succession (a) cut a hole in the inferior caval vein with fine scissors, (b) start perfusion with saline solution, and (c) clamp the aorta below the diaphragm, but above the origin of the renal arteries.
9. The kidney surface should turn a uniform pale color immediately. Adjust the height of the perfusion reservoirs so that the gravity-fed flow rate is maintained. Perfuse for 2–3 min until about 60 mL of saline has been used and the vessels are cleared of blood.
10. Quickly switch between saline solution and fixative. Perfuse for 3–4 min.
11. Stop the perfusion, excise and trim the required tissues. Store the tissue in vials and immersion-fix in the same fixative (post-fixation step) for between 2 and 12 h. If necessary (e.g., paraformaldehyde fixation), tissue should be kept at 4°C until processing (*see* **Note 7**).
12. Ensure that exsanguination has been sufficient for cessation of heart beat and death of animal.
13. Empty the perfusion apparatus and run approximately 200 mL of distilled H_2O through to remove residual fixative and salts.

3.3. Freezing Tissue

1. Fill a small container with isopentane (*see* **Note 8**), add dry ice to make a slurry (*see* **Note 9**), and place in a polystyrene container half filled with dry ice to chill to –80°C.
2. Place sections in molds containing a thin layer of embedding compound. When properly orientated, cover section completely with OCT, ensuring that there are no air bubbles.

3. Freeze tissue and compound by immersion in isopentane (*see* **Note 8**).
4. Once frozen, store at –80°C.

3.4. Tissue Embedding in Paraffin Wax

A number of different automated machines are routinely used for tissue processing. If these are not available, tissue can easily be infiltrated with embedding wax using a simple manual protocol described below.

1. Transfer tissue to labeled glass vials.
2. Dehydrate tissue through graded alcohols (50, 70, 95, 100%) and clear in two changes of chloroform (45 min to 1 h each). Rotate tissue throughout processing to ensure thorough penetration.
3. Infiltrate tissue with two changes of molten paraffin wax (approximately 56°C) for a total of 4–6 h (*see* **Note 10**).
4. Orientate and embed tissue in fresh wax using warm molds and embedding cassettes.
5. Place tissue and molds in a –20°C freezer for a minimum of 2 h before separating the block from the mold.

3.5. Preparation of APES-Coated Slides

Proper preparation of microscope slides is required to prevent the loss of tissue during antigen retrieval techniques. We routinely coat microscope slides with APES to ensure maximum section adhesion and minimum section loss during incubation and washing.

1. Wash slides in diluted laboratory detergent overnight (e.g., 1% solution w/v of Pyroneg™ in tap water).
2. Collect slides in histology staining racks and wash in running tap water for 3 h (slides must be fully immersed).
3. Wash twice in dH_2O, 5 min each.
4. Wash in freshly prepared 95% alcohol $\times$ 2 for 5 min each.
5. Dry with hair dryer.
6. Immerse slides for 10 s in a staining jar filled with a 2% w/v solution of APES in acetone.
7. Wash twice in dry acetone for 5 min each.
8. Rinse twice in dH_2O.
9. Air-dry in hot oven at 37°C for 12 h.
10. Store in a covered dust-free container at room temperature.

3.6. Sectioning of Frozen Tissue

Sections of frozen tissue are cut using a freezing microtome (cryostat). A number of different cryostats exist, from a variety of manufacturers. The operator should therefore be guided by the manufacturer's instructions for that machine. As with all histology,

the correct set-up and use of the microtome will greatly influence the outcome. What follows is a general guide to the preparation of sections.

1. Place frozen tissue block in cryostat chamber (–20°C) for 30 min to reach equilibrium temperature.
2. Cut and collect serial 5–10 μm sections on labeled APES-coated slides in accordance with manufacturer's instructions.
3. Place slides on dry ice. If tissue was unfixed at the time of freezing, fix sections by immersion in 4°C acetone for 5 min.
4. After fixation, air-dry for 20 min at room temperature.
5. Store slides in a rack, place in a sealed box with desiccant, and store at –20°C for up to 4 weeks.

3.7. Sectioning of Paraffin-Embedded Tissue

1. Heat histological water bath to 56°C.
2. Prepare a transfer bath by filling a shallow bowl with 20% v/v ethanol in water.
3. Cut 2–5 μm ribbon sections of paraffin-embedded tissue with a microtome in accordance with the manufacturer's instructions.
4. Use a scalpel to divide ribbon in two to three section pieces. Using the edge of the blade, transfer to the 20% ethanol bath. The section should flatten.
5. Transfer to the heated histological water bath using an uncoated glass slide.
6. Collect sections on labeled APES-coated slides and stand upright to drain. After 5–10 min, transfer to a slide rack and dry overnight in an oven at 40°C.
7. Store sections in a dry, dust-free environment until use.

3.8. Antigen Retrieval (Enzyme Digestion, Acid Treatment, and Heat-Induced Epitope Retrieval)

In some cases, antigen retrieval (or antigen recovery) may be necessary to expose or retrieve antigens masked by the tissue fixation and embedding process. There are various protocols available; some apply enzymes while others make use of heat-induced epitope retrieval. Different combinations of fixation and retrieval methods may actually increase background staining, so the most appropriate combination of techniques may need to be determined by trial and error. Unfixed frozen tissue sections are particularly prone to proteolytic damage, which often leads to substantial loss of architecture. To avoid this, frozen sections are usually treated with heat-based antigen retrieval protocols.

3.8.1. Enzyme Digestion

Enzyme digestion improves accessibility of antigenic determinants. Enzymes that can be used include pepsin, pronase E, protease VIII, and trypsin. The requirement for digestion, the optimal concentration, and time needed may have to be determined by trial and error for individual antibodies (**Fig. 1.2**).

3.8.1.1. Protease VIII Digestion

1. Fill a coplin jar with protease digest and pre-heat to 37°C in a water bath.
2. Deparaffinize sections by loading a slide rack with microscope slides and immersing in two changes of xylene for 5 min each.
3. Rehydrate paraffin-embedded sections by passing slides through two changes of 100% ethanol for 2 min each and 95, 70, and 50% ethanol for 1 min each.
4. Rinse in dH_2O.
5. Incubate de-waxed and rehydrated sections in enzyme for 3 min at 37°C.
6. Wash in 1 × PBS for 5 min.

3.8.1.2. Trypsin Digestion

1. De-wax and rehydrate sections (*see* **Section 3.8.1.1,** steps 2–4).
2. Incubate in trypsin digest for 10–30 min at 37°C.
3. Wash in 1 × PBS for 5 min.

3.8.2. Acid Treatment

Treatment with hydrochloric acid is commonly used in antibody labeling of bromodeoxyuridine (BrdU) incorporation, a marker of cell proliferation (10). BrdU is a thymidine analogue and is selectively incorporated into replicating DNA. Therefore, animals pulsed with BrdU before sacrifice incorporate BrdU in replicating nuclei. Acid treatment denatures DNA and improves accessibility of BrDU to the antibody.

1. Deparaffinize and rehydrate sections, rinse in dH_2O (*see* **Section 3.8.1.1,** steps 2–4).
2. Incubate sections with 2 M HCl solution for 10–20 min (optimal incubation time should be determined by the user).
3. Rinse sections twice in 1 × PBS for 2 min each.

3.8.3. Heat-Induced Epitope Retrieval

Pre-treatment of sections by boiling in buffer using a microwave oven (*see* **Note 11**) is employed as an alternative to enzymatic digestion with some antibodies.

A number of different buffers have been utilized for antigen retrieval, including, but not limited to, citrate buffer and Tris–EDTA. Citrate buffer at pH 6.0 is the most popular solution for heat antigen retrieval and is thought to be effective by destroying cross-links with calcium ions and proteins (8).

Different pH values (3.0, 9.0) can also be utilized, and in some cases improved antigen retrieval may be demonstrated (7). In fact, the pH of a buffer may be as important as the actual composition. The pH dependency of heat antigen retrieval suggests that as well as cleaving polypeptide chains, heating causes conformational changes to the structure, which are not reversed after cooling (8).

The length of incubation time required by each of the different retrieval methods needs to be determined and optimized and may also be dependent on the antibody being used.

1. De-wax paraffin-embedded sections by immersing slides in two changes of xylene (*see* **Section 3.8.1.1**, step 2).
2. Rehydrate in graded ethanol (*see* **Section 3.8.1.1**, step 3).
3. Wash in dH_2O for 5 min.
4. Place in coplin jar filled with retrieval buffer and cover with plastic film.
5. Boil for 3 min. Refill coplin jar with buffer or dH_2O at 1 min intervals.
6. Leave in coplin jar at room temperature for 20 min.
7. Wash in 0.1 M 1 × PBS before continuing with an immunostaining protocol.

3.8.4. Quality Control

In most laboratories, fixation time, processing conditions, and antigen retrieval are by far the greatest variables in histochemistry. In each step, therefore, the key to reproducible results is the standardization of procedures. Antigen retrieval presents a number of specific challenges. The use of enzymatic digestion and heat may unmask numerous antigens. Consistency is particularly difficult to maintain with microwaving techniques; there is often poor adherence to temperature and time control. In this regard, the reader is referred to Tacha et al. (11) for a useful protocol to calibrate microwave ovens.

Once sections are prepared, the use of appropriate controls is an essential, and often neglected, part of histology and histochemistry.

4. Notes

1. Pre-prepared neutral buffered formalin, complete with pH indicator, is readily available from commercial suppliers.
2. Many of the fixatives and solvents in histochemistry are highly toxic. Refer to material safety data sheets (MSDS) for correct and safe handling.
3. Picric acid crystals are highly explosive when dry. It is therefore best handled as a commercially prepared saturated aqueous solution.
4. The deposition of mercuric pigments is a confounding artifact with mercuric formalin fixation. These pigments appear as a fine brown granular deposit. Most laboratories routinely treat mercuric formalin-fixed tissue sections with Lugol's iodine

and sodium thiosulfate before staining. Iodine treatment oxidizes mercuric chloride to form a mercuric iodine complex which is soluble in water. Free brown iodine left is removed by the sodium thiosulfate step, resulting in an improved histological appearance. However, it is important to remember that pre-treatment to remove mercuric pigment can in itself affect immunoperoxidase staining (5).

5. Small pieces of tin foil folded into the shape of a boat can be substituted for commercial molds.
6. Infiltration of sucrose acts as a cryoprotectant when freezing.
7. Because of the unavoidable leakage of fixative, all perfusion fixation needs to be performed in a fume cabinet.
8. Isopentane chilled to –80°C results in rapid freezing of tissue without the formation of ice crystals. If isopentane is not available, other hydrocarbons such as hexane or acetone may be substituted. If none are available, placing the mold directly on the dry ice is possible, albeit slower. Although rapid freezing of tissue is required, immersion in liquid nitrogen is not recommended, as a layer of gaseous nitrogen can form at the sample surface, slowing the rate of heat transfer. Furthermore, the use of very low temperature cryogens such as liquid nitrogen can overcool the block and result in cracking.
9. It is easier to make an isopentane slurry when the dry ice is in pellet form.
10. Many antigens are easily destroyed by high temperature and therefore prolonged exposure to molten wax. Infiltrate tissue with wax at the lowest possible temperature to keep it molten.
11. Alternative methods of heating include pressure cooker, autoclaving, and even the standard laboratory water bath, when temperatures of less than 100°C are required.

References

1. Cook, J.D. (2006) *Cellular pathology: introduction to techniques and applications* (2nd Edition). Scion, Bloxham, Oxfordshire.
2. Kiernan, J.A. (2000) *Histological and histochemical methods: theory and practice*. Butterworth-Heinemann, Oxford.
3. McLean, I.W. and Nakane, P.K. (1974) Periodate-lysine-paraformaldehyde fixative. A new fixation for immunoelectron microscopy. *J. Histochem. Cytochem.* **22**, 1077–1083.
4. Ananthanarayanan, V., Pins, M.R., Meyer, R.E., and Gann, P.H. (2005) Immunohistochemical assays in prostatic biopsies processed in Bouin's fixative. *J. Clin. Pathol.* **58**, 322–324.
5. Wan, X., Cochran, G., and Greiner, T.C. (2003) Removal of mercuric chloride deposits from B5-fixed tissue will affect the performance of immunoperoxidase staining of selected antibodies. *Appl. Immunohistochem. Mol. Morphol.* **11**, 92–95.
6. Puchtler, H., Sweat Waldrop, F., Conner, H.M., and Terry, M.S. (1968) Carnoy fixation: practical and theoretical considerations. *Histochemie* **16**, 361–371.
7. Leong, T.Y.-M. and Leong, A.S.-Y. (2007) How does antigen retrieval work? *Adv. Anat. Pathol.* **14**, 129–131.

8. Shi, S.-R., Imam, S.A., Young, L., Cote, R.J., and Taylor, C.R. (1995) Antigen retrieval immunohistochemistry under the influence of pH using monoclonal antibodies. *J. Histochem. Cytochem.* **43**, 193–201.
9. Yamashita, S. (2006) Heat-induced antigen retrieval: mechanisms and application to histochemistry. *Prog. Histochem. Cytochem.* **41**, 141–200.
10. Hewitson, T.D., Wu, H.L., and Becker, G.J. (1995) Interstitial myofibroblasts in experimental renal infection and scarring. *Am. J. Nephrol.* **15**, 411–417.
11. Tacha, D.E. and Chen, T. (1994) Modified antigen retrieval procedure: calibration technique for microwave ovens. *J. Histotechnol.* **17**, 365–366.

Chapter 2

An Optimized RNA Extraction Method from Archival Formalin-Fixed Paraffin-Embedded Tissue

Joon-Yong Chung and Stephen M. Hewitt

Abstract

Formalin-fixed and paraffin-embedded (FFPE) tissue is one of the most valuable resources available for molecular biological analysis on tissue after diagnostic histopathological examination. Gene expression profiles of FFPE can provide insights into molecular mechanisms of disease but are difficult due to the high level of cross-linking of biomolecules by formalin fixation. Despite advances in molecular technologies, the quality of RNA obtained from FFPE tissue remains variable. We have optimized a reliable RNA extraction method for FFPE tissue. This approach is based on deparaffinization at high temperature coupled with a 3-day lysis at 65°C. The average total RNA yield is 4.5–5.5 ng per 1 mm^3 of archival FFPE tissue and 260/280 ratios are between 1.80 and 1.95. The extracted RNA has a modal fragment length between 100 and 200 nucleotides by bioanalyzer analysis. Although modal lengths of RNA fragments were shorter, reverse transcription and polymerase chain reaction was able to amplify amplicons in the range of 300 base pairs. This optimized method improves the utility of FFPE tissue for molecular profiling studies.

Key words: Formalin-fixed, paraffin-embedded, tissue, RNA isolation, RT-PCR.

1. Introduction

Gene profiling of formalin-fixed, paraffin-embedded (FFPE) specimens is a powerful tool for biomarker discovery in translational research. However, the recovery of RNA from archival FFPE tissues is challenging because RNA from FFPE tissue suffers from strand breakage and cross-linking by formalin fixation. Cross-linking not only complicates isolation of nucleic acid but also inhibits polymerase during PCR-based molecular assay. To overcome these problems, a number of alternative fixatives and approaches have been examined and discussed (1). Unfortunately,

T.D. Hewitson, I.A. Darby (eds.), *Histology Protocols*, Methods in Molecular Biology 611,
DOI 10.1007/978-1-60327-345-9_2,

all alternative fixation methods have limitations either in diagnostic histomorphologic interpretation or in other molecular assays such as immunohistochemistry (1).

Despite excellent RNA extraction methods, RNA quality from FFPE specimens remains variable. RNA isolated from FFPE tissue samples was first described in 1988 by Rupp and Locker (2). Previous studies on RNA extraction have reported varying degrees of success but have used relatively large amounts of tissue for a limited number of specific genes or relatively abundant genes (3–7). No consensus isolation method exists and the data on optimization of protocols are limited. Currently, a limited number of groups routinely isolate RNA from FFPE tissue, and all acknowledge that there is extensive degradation by the formalin fixation process and extraction methodologies are poorly optimized (6). It is therefore imperative that more robust methods of extraction of RNA from FFPE tissue be developed that are compatible and integrated with the current methods used in pathology laboratories around the world.

Currently RT-PCR-based assays are performed on FFPE tissue; however, they require extensive optimization and rely on short amplicons. The introduction of real-time RT-PCR has overcome some of the difficulties of analyzing short RNAs (8, 9). However, the quality of the results of real-time RT-PCR using FFPE tissue depends critically upon the quality and quantity of extracted RNA. For expression profiling to reach its potential in clinical care, the reduction to application on FFPE tissue is essential. Many new methods have been developed and evaluated to address this challenge, with varying degrees of success. In this context, we have established a reliable RNA extraction methodology for archival FFPE tissue (10, 11). The recovery of the RNA is linked to the deparaffinization process, and the capacity to extract the RNA from the paraffin-impregnated tissue. As a fundamental molecular tool, we believe that this new RNA protocol can provide reliable starting material for gene profiling studies via array or RT-PCR-based methodologies.

2. Materials

2.1. Deparaffinization

1. Aqueous dewaxer reagent (AutoDewaxer™; OpenBiosystem, Huntsville, AL, USA) (*see* **Note 1**).
2. Autoalcohol™ (OpenBiosystem).
3. Microcentrifuge tubes.
4. Disposable safety scalpels (Miltex Inc., Bethpage, NY, USA).
5. Thermomixer™ (Eppendorf, Westbury, NY, USA).

2.2. RNA Extraction

1. Disposable pellet mixers and cordless motor (VWR, West Chester, PA, USA).
2. Stock solution of RNA lysis buffer: 4 M guanidine isothiocyanate, 25 mM sodium acetate, 0.5% sodium lauryl sarcosinate, pH 5.5 (*see* **Note 2**). Store at room temperature.
3. Working solution of RNA lysis buffer: Add 10 μL 14.4 M β-mercaptoethanol per 1 mL lysis buffer before use. The lysis buffer is stable for 1 month after addition of β-mercaptoethanol (*see* **Note 2**).
4. Thermomixer™ (Eppendorf).
5. Phenol–chloroform–isoamyl alcohol (PCI): Combine phenol (pH 4.3), chloroform, and isoamyl alcohol in the ratio of 25:24:1 (v/v/v) (*see* **Note 3**).
6. Chloroform–isoamyl alcohol (CI): Combine chloroform and isoamyl alcohol in the ratio of 49:1 (v/v) (*see* **Note 3**).
7. 3 M sodium acetate (pH 5.2) (Quality Biological Inc., Gaithersburg, MD, USA).
8. 100 and 75% ethyl alcohol (Warner-Graham, Cockeysville, MD, USA).
9. DEPC-treated DW: DEPC (Di-ethyl-pyro-carbonate)-treated water (Quality Biological Inc.).
10. RNase ZAP™ wipes (Ambion, Austin, TX, USA).

2.3. Assessment of the Quality and Quantity of Total RNA

1. NanoDrop™ ND-1000 Spectrophotometer (NanoDrop Technologies Inc., Wilmington, DE, USA).
2. Agilent 2100 Bioanalyzer™ (Agilent Technologies, Palo Alto, CA, USA).
3. RNA 600 LabChip™ kit (Agilent Technologies).

2.4. cDNA Synthesis and RT-PCR

1. Random primers (Promega, Madison, WI, USA).
2. SuperScript™ II Reverse Transcriptase (Invitrogen, Carlsbad, CA, USA).
3. dNTP Mix (10 mM each, Invitrogen).
4. 0.1 M DTT (Invitrogen).
5. RNasin™ (Promega).
6. RNase H (Invitrogen).
7. PCR SuperMix™ (Invitrogen).
8. Specific primers (sense and antisense).
9. DNase (Promega).
10. PCR tubes (Applied Biosystems, Foster City, CA, USA).
11. PCR machine 9700 (Applied Biosystems).

12. ReadyAgarose™ Mini Gel: 1% agarose with ethidium bromide (Bio-Rad, Hercules, CA, USA) (*see* **Note 4**).
13. Ready-load™ 100 bp DNA ladder (Invitrogen).
14. 1 × Tris acetate EDTA (TAE) buffer: 242 g Tris base, 57.1 mL concentrated glacial acetic acid, 100 mL 0.5 M EDTA, pH 8.0.
15. Alpha-Innotech imaging system (Alpha Innotech Corporation, San Leandro, CA, USA).

3. Methods

The ability to isolate nucleic acid from archived tissue samples provides a powerful molecular analysis tool in retrospective studies of diseased tissue. This method is not novel; rather the approach is based on empiric optimization of existing protocols. The basic protocols are largely derived from other protocols, typically histochemical protocols for staining tissue, and those for the recovery of RNA from fresh or frozen tissue. Our methodology has demonstrated that the deparaffinization step is a significant issue in RNA recovery from FFPE tissue and remains the least optimized step in the RNA extraction process (10). In addition, the RNA yield of our refined methodology was two to threefold higher compared with previous studies and allowed a high purity and quality of RNA (10). This protocol was designed based on two sections of 10-μm thickness archival FFPE tissue specimen (*see* **Note 5**).

3.1. Deparaffinization

1. Cut two 10-μm sections from FFPE tissue blocks using a microtome. Place the tissue sections in a microcentrifuge tube (*see* **Note 6**).
2. Add 1 mL of AutoDewaxer™ to the sample and vortex briefly to mix.
3. Centrifuge briefly to bring the tissue that is stuck to the sides of the tube down into the AutoDewaxer™.
4. Incubate the tube for 15 min at 95°C with vigorous mixing condition (800 rpm) using the Thermomixer™.
5. Centrifuge the sample for 1 min at room temperature with maximum speed in a microcentrifuge. Remove carefully the AutoDewaxer™ solution without disturbing the tissue pellet. Repeat three times from Steps 2 to 5.
6. Add 1 mL of AutoAlcohol™ to the sample and centrifuge the tube for 1 min at room temperature with maximum speed in a microcentrifuge. Remove carefully the AutoAlcohol™ solution without disturbing the tissue pellet.
7. Dry the sample for 5 min at room temperature (*see* **Note 7**).

3.2. RNA Extraction

1. Add 300 μL of RNA lysis buffer to the deparaffinized tissue. Homogenize immediately using the disposable pellet mixers and cordless motor until the sample is uniformly homogeneous.
2. Add an additional 300 μL of RNA lysis buffer (final to 600 μL) to the sample. Vortex thoroughly for 1 min to get homogeneous solution (*see* **Note 8**).
3. Incubate the reaction tube for 72 h at 60°C with mild mixing condition (500 rpm) using the Thermomixer™.
4. Add 600 μL of equilibrated PCI to the tube. Vortex vigorously for 30 s.
5. Centrifuge the tube at 16,000*g* for 10 min at 4°C in a microcentrifuge. Transfer as much as is easily possible of the upper, aqueous phase to a fresh tube (*see* **Note 9**).
6. Add an equal volume of CI to the tube. Vortex vigorously for 30 s.
7. Centrifuge the tube at 16,000*g* for 10 min at 4°C and then transfer the upper aqueous phase to a fresh tube.
8. Add 0.1 volume of 3 M sodium acetate buffer (pH 5.2) and 3.0 volume of 100% chilled ethanol. Mix well and allow the RNA to precipitate at –20°C overnight.
9. Centrifuge at 16,000*g* for 30 min at 4°C. Discard the supernatant.
10. Add 1 mL of 75% chilled ethanol to the pellet and then centrifuge the tube at 16,000*g* for 10 min at 4°C. Discard the supernatant.
11. Dry the precipitated RNA for 5–10 min at room temperature.
12. Dissolve the RNA in 20 μL of DEPC-treated distilled water (*see* **Note 10**).

3.3. Assessment of the Quality and Quantity of Total RNA

1. Take 1 μL of the sample to measure the concentration and quality of the RNA.
2. Turn on the NanoDrop™ ND-1000 Spectrophotometer and set up a reference using blank solution (DEPC-treated DW).
3. Apply 1 μL of the RNA to the Nanodrop™ and press a measure button (*see* **Note 11**).
4. To check the quantity and quality of the RNA sample (*see* **Note 12**), take 150–200 ng of the RNA sample and apply to Agilent 2100 Bioanalyzer™. An example of the results produced is shown in **Fig. 2.1**.

3.4. cDNA Synthesis and RT-PCR

Synthesize the first-strand cDNAs from the isolated total RNAs using reverse transcriptase and random primers.

3.4.1. Synthesis of First-Strand cDNA

1. Anneal 8 μL (2 μg) total RNA templates with 1 μL (500 ng) random primer in a sterile RNase-free microcentrifuge tube.

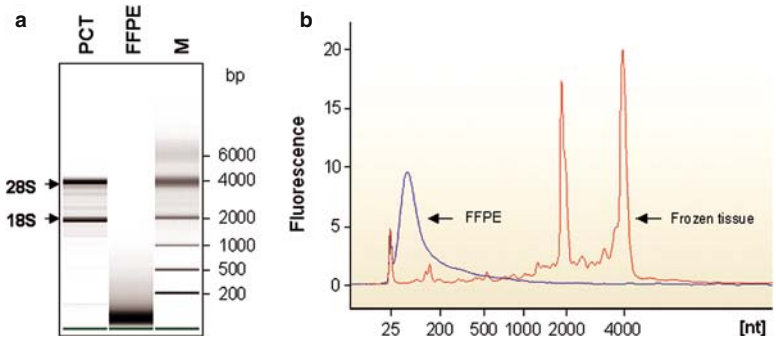

Fig. 2.1. The profiling of total RNA extracted from archival formalin-fixed and paraffin-embedded (FFPE) tissue by microcapillary electrophoresis. We analyzed RNA quality using the Agilent 2100 Bioanalyzer™, using 200 ng of total RNA extracted from rat kidney FFPE tissues. Representative data were presented as a gel-like image (**a**) and an electropherogram (**b**). PCT: positive control (frozen rat kidney); FFPE: formalin-fixed and paraffin-embedded tissue; M: RNA 6000 nano ladder (Agilent Technologies).

2. Heat the tube at 70°C for 5 min and allow it to slowly cool to room temperature to finish annealing. Briefly spin down the mixture to the bottom.
3. To the annealed primer/template, add the following in the order shown. Gently spin well after each addition.
   a. First-strand 5 × buffer (4 μL)
   b. 0.1 M DTT (2 μL)
   c. 10 mM dNTP mix (2.5 mM each) (2 μL)
   d. RNasin™ (1 μL)
   e. SuperScript™ II (2 μL)
4. Incubate the tube at 42°C for 2 h and place on ice (*see* **Note 13**).
5. Inactivate the reaction by heating at 70°C for 15 min and store the tube on ice for 2 min. Briefly spin down the mixture to the bottom.
6. Add 1 μL (two units) of RNase H and briefly spin down the mixture. Incubate the tube at 37°C for 20 min.
7. Add 80 μL of RNase-free water to the mixture and store at –20°C until amplification by PCR.

3.4.2. cDNA Amplification

Amplify the specific cDNA of interest by PCR using specific primers.

1. In a sterile RNase-free microcentrifuge tube on ice, add the following in the listed order for amplification of one sample:
   a. PCR SuperMix (45 μL)
   b. Molecular-grade distilled water (3 μL)
   c. Template cDNA (1 μL) (*see* **Note 14**)
   d. Sense primer (200 μM) (0.5 μL)
   e. Antisense primer (200 μM) (0.5 μL)

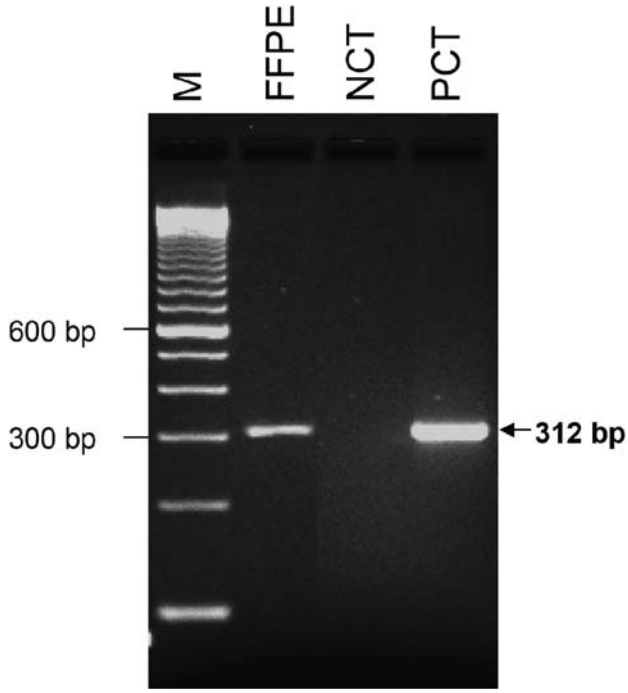

Fig. 2.2. Expression of rat *GAPDH* by RT-PCR analysis in total RNA derived from formalin-fixed paraffin-embedded (FFPE) kidney tissue. cDNA was synthesized using a random hexamer, and amplicons were separated on a 1% ready agarose gel (Bio-Rad). Positive as well as negative controls had been included in the amplification experiments. FFPE: formalin-fixed and paraffin-embedded tissue; NCT: negative control (without cDNA); PCT: positive control (fresh rat kidney); M: ready-load™ 100 bp DNA ladder (Invitrogen).

2. Carry out PCR amplification for 35 cycles in the PCR machine 9700.
3. To confirm the size of PCR amplicons, carry out agarose electrophoresis using 1% ReadyAgarose™ Mini Gel with 1 × TAE buffer. An example of the results produced is shown in **Fig. 2.2**.

4. Notes

1. The aqueous-based dewaxer was as efficient as xylene and allowed the use of higher temperatures than xylene for the deparaffinization steps.
2. 4 M guanidine isothiocyanate and β-mercaptoethanol are strong RNase inhibitors. The RNA lysis buffer is toxic. Wear gloves, a laboratory coat, and eye protection when preparing, handling, or working with solution.

3. These reagents are toxic and should be used in the fume hood. Gloves should be worn when working with these reagents. The remnant of these reagents should be decanted into a special container. Do not discard into sink.
4. EtBr (ethidium bromide) is a neurotoxin. Gloves should always be worn when working with the reagents. The used EtBr solution must be collected in a special container and disposed of in accordance with guidelines. Stock solutions of EtBr should be stored in light-tight bottles at 4°C.
5. This method has been optimized for whole tissue sections. Application to micro-dissected sections has not been validated. Issues with reference to micro-dissected specimens include volume of material as well as previous preparative steps of deparaffinization and staining. Exposure to aqueous states during staining is associated with RNA degradation. Additionally, it should not be assumed that the deparaffinization steps for micro-dissection are sufficient for optimal RNA isolation, and additional deparaffinization should be carried out after micro-dissection.
6. If you are using archival FFPE slide specimens, carefully collect tissue in the microcentrifuge tube using a disposable safety scalpel.
7. The pellet should become white.
8. To minimize contamination by DNA trapped at the interface, avoid taking the lowest part of the aqueous phase.
9. As long as the sample is in RNA lysis buffer, RNase may be inhibited by guanidinium thiocyanate.
10. DEPC is a carcinogen and should be handled with care. Gloves should be worn when handling the reagent.
11. The NanoDrop™ can automatically and simultaneously measure RNA at wavelengths of 260 and 280 nm, and calculate and display RNA concentration together with the ratio of A_{260}/A_{280} reading numbers on the computer screen.
12. The extracted RNA should have a ratio of 1.80 to 1.95 of A_{260}/A_{280} reading numbers. The concentration of the RNA sample is variable depending on FFPE tissue quality.
13. At this stage, the synthesis of the first-strand cDNA is completed and safe for RNase contamination.
14. PCR experiments demonstrate that amplicons up to 300 bp are feasible; however, to achieve these, the investigator must use more cDNA template than required for the same amplicons using RNA from fresh tissues.

Acknowledgments

We acknowledge the technical expertise provided by Ylaya Kris.

References

1. Hewitt, S. M., Lewis, F., Cao, Y., Conrad, R. C., Cronin, M., Danenberg, K. D., Goralski, T. J., Langmore, J. P., Raja, R. G., Williams, P. M., Palma, J. F., and Warrington, J. A. (2008) Tissue handling and specimen preparation in surgical pathology: issues concerning the recovery of nucleic acids from formalin fixed, paraffin embedded tissue. *Arch. Pathol. Lab. Med.* **132**, 1929–1935.
2. Rupp, G. M. and Locker, J. (1988) Purification and analysis of RNA from paraffin embedded tissue. *Biotechniques* **6**, 56–60.
3. Jewell, S. D., Srinivasan, M., McCart, L. M., Williams, N., Grizzle, W. H., LiVolsi, V., MacLennan, G., and Sedmak, D. D. (2002) Analysis of the molecular quality of human tissues: an experience from Cooperative Human Tissue Network. *Am. J. Clin. Pathol.* **118**, 733–741.
4. Stanta, G. and Schneider, C. (1991) RNA extracted from paraffin-embedded human tissues is amenable to analysis by PCR amplification. *Biotechniques* **11**, 304–308.
5. Finke, J., Fritzen, R., Ternes, P., Lange, W., and Dölken, G. (1993) An improved strategy and a useful housekeeping gene for RNA analysis from formalin-fixed, paraffin-embedded tissue by PCR. *Biotechniques* **14**, 448–453.
6. Mizuno, T., Nagamura, H., Iwamoto, K. S., Ito, T., Fukuhara, T., and Tokunaga, M. (1998) RNA from decades-old archival tissue blocks for retrospectives studies. *Diagn. Mol. Pathol.* **7**, 202–208.
7. Krafft, A. E., Duncan, B. W., Bijwaard, K. E., Taubenberger, J. K., and Lichy, J. H. (1997) Optimization of the isolation and amplification of RNA from formalin-fixed, paraffin embedded tissue: the armed forces institute of pathology experience and literature review. *J. Mol. Diagn.* **2**, 217–230.
8. Godfrey, T. E., Kim, S. H., Chavira, M., Ruff, D. W., Warren, R. S., Gray, J. W., and Jensen, R. H. et al. (2000) Quantitative mRNA expression analysis from formalin-fixed, paraffin-embedded tissues using 5′ nuclease quantitative reverse transcription-polymerase chain reaction. *J. Mol. Diagn.* **2**, 84–91.
9. Specht, K., Richter, T., Muller, U., Walch, A., Werner, M., and Hofler, H. (2001) Quantitative gene expression analysis in microdissected archival formalin-fixed and paraffin embedded tumor tissue. *Am. J. Pathol.* **158**, 419–429.
10. Chung, J. Y., Braunschweig, T., and Hewitt, S. M. (2006) Optimization of recovery of RNA from formalin-fixed, paraffin-embedded tissue. *Diagn. Mol. Pathol.* **15**, 229–236.
11. Chung, J. Y., Braunschweig, T., Williams, R., Guerrero, N., Hoffmann, K. M., Kwon, M., Song, Y. K., Libutti, S. K., and Hewitt, S. M. (2008) Factors in tissue handling and processing that impact RNA obtained from formalin-fixed, paraffin-embedded tissue. *J. Histochem. Cytochem.* **56**, 1033–1042.

Chapter 3

Laser-Capture Microdissection and Pressure Catapulting for the Analysis of Gene Expression in the Renal Glomerulus

Amanda J. Edgley, Renae M. Gow, and Darren J. Kelly

Abstract

Investigation into the molecular mechanisms regulating normal renal physiology and pathophysiology has benefited from the development of microdissection techniques enabling sampling of specific cell populations or structures within the kidney. Laser-capture microdissection and pressure catapulting is a relatively new, entirely non-contact microdissection technique that facilitates the assay of mRNA and protein expression in single nephron segments or populations. Herein, we describe methods for sample preparation, microdissection and collection of glomeruli from archival renal biopsies for later analysis of gene expression using real-time PCR. Microdissection of glomeruli from archival renal biopsy sections was carried out using the PALM Microbeam UV laser system from P.A.L.M. Technologies.

Key words: Laser-capture microdissection, pressure catapulting, renal, glomerulus, gene expression.

1. Introduction

Modern molecular analyses including DNA, RNA and protein microarray technologies are strengthened when the sample consists of a specific single cell or cell population. In the kidney, disease often involves selective injury to specific structures such as the glomerulus, tubules, interstitium or blood vessels (e.g. chronic renal disease). Thus, the ability to sample precise cell populations or specific renal structures is crucial for accurate characterization of cellular function and elucidation of the molecular mechanisms of disease (1, 2). Laser microdissection and pressure catapulting technology is a patented and unique way to select and obtain a single cell or a limited region of tissue, thus facilitating pure, homogenous sample preparation and increasing the accuracy of molecular analyses. Laser microdissection techniques can be applied to

T.D. Hewitson, I.A. Darby (eds.), *Histology Protocols*, Methods in Molecular Biology 611,
DOI 10.1007/978-1-60327-345-9_3,

histological specimens, living cells and cell cultures, plant material, chromosome spreads, forensic preparations, formalin-fixed paraffin-embedded (FFPE) or fresh frozen tissues and stained or unstained tissues. Preparations for microdissection can be viewed microscopically under fluorescence or transmitted light.

There are two classes of laser-capture microdissection (LCM): infrared (IR) capture (e.g. PixCell™ II, PixCell™ IIe, AutoPix™ or Veritas Laser Capture Microdissection system from Arcturus Molecular Devices) and ultraviolet (UV) cutting systems (e.g. PALM Microbeam from P.A.L.M. Microlaser Technologies). The main processes of laser microdissection technology are (i) visualization of the cells of interest using a microscope, (ii) laser cutting (known as ablative decomposition) of cells surrounding a selected area (UV system) or, laser activation of a thermoplastic film placed on top of the tissue, creating a polymer-cell composite (IR system), and (iii) removal of the cells of interest from the surrounding tissue section. The following method will describe the use of non-contact microdissection and pressure catapulting for collection of samples for subsequent RNA analysis using the PALM microbeam system.

Laser microdissection uses a pulsed UV-A laser that is focused through a microscope lens down to a spot size of <1 μm in diameter (**Fig. 3.1**). At the focal point of the laser, the energy density created facilitates cutting of the material mounted on a glass slide or culture dish on the microscope stage. The cutting

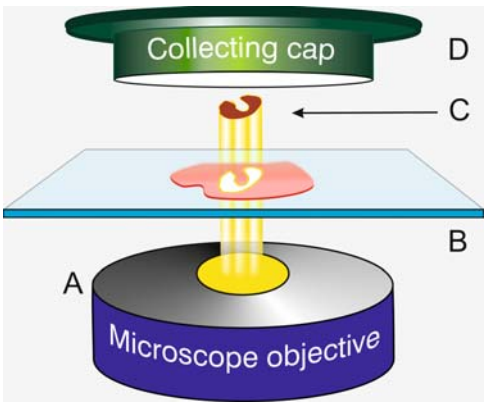

Fig. 3.1. Schematic diagram of the laser microdissection and capture process. (**a**) The microscope lens is used to focus the UV laser light down to a very fine beam (~1 μm in diameter). (**b**) The histological tissue section is mounted on the microscope stage and viewed on computer screen. Computer-assisted software marks out the area to be dissected on the tissue. The laser cuts through the tissue section. (**c**) UV laser pulses directly at the underside of the tissue are used to catapult the excised tissue against gravity into the collecting cap positioned directly above sample. (**d**) The collecting tube is mounted approximately 1 mm above the tissue section using a moved mounting arm connected to the microscope.

process is known as "ablative decomposition" which is a photochemical process initiated by the energy within the narrow laser focal point (3). The energy of the laser is transferred to the microplasma and causes extreme temperature and pressure increases, disrupting chemical bonds in the region and causing the collapse of the microplasma in nanoseconds (3). The material to be sampled is visualized with the aid of the microscope and the area to be excised marked with the aid of computer software, allowing precise manipulation down to the subcellular level without involving neighbouring tissue.

Collection of samples from histological sections using laser pressure catapulting involves activation of the microplasma underneath the sample (i.e. between the slide and the cells of interest) using laser pulses. The resulting pressure waves, combined with the atomic efflux or "photonic cloud" propel the dissected samples against gravity towards a collection vial (3) (**Fig. 3.1**). Depending on the size of the specimen, one single pulse or multiple pulses may be needed to propel the samples into the collection vial.

The main advantage of combining laser microdissection and pressure catapulting of samples is that it provides an entirely non-contact method to isolate cells of interest for analysis; thus there is no risk of contamination of the sample through contact. Historically, LCM has been used to select cells on fixed preparations such as histological tissue sections (FFPE or snap frozen). However, recently, LCM has successfully been used to collect living cells including stem cells (4, 5), with little impact on cell viability after the laser dissection and capture.

One disadvantage of the UV-cutting method is the presence of UV-damaged cells in the final sample. If the perimeter of the cut area is high compared to the overall microdissected area (>10%), then the UV-damaged cells may contribute significantly to the final molecular signal (6). Other disadvantages include the need to identify the cells of interest (no cover slip or immersion oil makes distinguishing cells of interest difficult) and interference of tissue staining and fixing protocols with downstream gene and protein analysis.

2. Materials

2.1. Tissue Collection, Preservation and Preparation

1. Specimens for protein, DNA or RNA analysis.
2. Cryopreservation solution (OCT™; Sakura Finetek Corporation, Torance, CA, USA).
3. Cryomolds (Sakura Finetek Corporation).
4. Dry ice.

5. Isopentane.
6. 10% solution neutral buffered formalin (Merck, Darmstadt, Germany).
7. Embedding cassettes (Sakura Finetek Corporation).
8. Liquid paraffin-embedding wax.
9. Mayer's hematoxylin solution (Sigma-Aldrech, St. Louis, MO, USA).
10. Eosin Y solution, alcoholic (Sigma-Aldrech).
11. Scott's tap water.
12. Milli-Q^{TM}-purified water (Millipore, Billerica, MA, USA) or other type-I reagent-grade water.
13. 70, 95 and 100% ethanol (v/v) in Milli-Q^{TM} – purified water.
14. Diethyl pyrocarbonate-treated (DEPC)-treated water (DEPC-H_2O).
15. Xylene.
16. 70, 90 and 100% DEPC-treated ethanol (v/v) in Milli-Q^{TM} – purified water.

2.2. RNA Extraction and Real-Time PCR (qRT-PCR)

1. RNA lysis buffer: Combine 100 μL of 1 M Tris/HCl pH 8.0, 2 μL of 0.5 M Na_2EDTA pH 8.0, 1,000 μL of 20% w/v SDS and add Milli-Q^{TM} water to 10 mL (final composition 10 mM Tris–HCl, 0.1 mM EDTA, 2% w/v SDS, pH 7.3).
2. DEPC-treated 100% ethanol (Molecular Biology Grade).
3. β-Mercaptoethanol (Sigma-Aldrech).
4. Proteinase K: 10 mg/mL stock (Roche Diagnostics, Mannheim, Germany).
5. Water-saturated phenol (Sigma-Aldrech).
6. Chloroform (Sigma-Aldrech).
7. Isopropanol (Merck).
8. 3M Sodium acetate, ph5.2 (Sigma-Aldrech).
9. Glycogen (Roche Diagnostics).
10. RNase inhibitors (Protector RNase inhibitor; Roche Diagnostics).
11. AMV-Reverse Transcriptase (Roche Diagnostics).
12. dNTPs (Invitrogen, Carlsbad, CA, USA).
13. Taqman^{TM} Universal Master Mix (Applied Biosystems, Foster City, CA, USA).

2.3. Equipment

1. Laser-capture microdissection apparatus: PALM Microbeam with PALM Robosoftware (P.A.L.M. Microlaser Technologies GmbH, Bernried, Germany) (**Fig. 3.1**).
2. Cryostat and/or microtome.

3. Automated tissue processor for paraffin embedding.
4. Uncoated, pre-cleaned glass microscope slides (Menzel-Glaser, Braunschweig, Germany) or PALM polyethylene napthalate-coated membrane slides (1 mm PEN-membrane-covered slides; P.A.L.M. Microlaser Technologies) (*see* **Note 1**).
5. LPC-microfuge tubes (500 μL; P.A.L.M. Microlaser Technologies).

3. Methods

3.1. Sample Collection and Storage

3.1.1. Frozen Tissue

1. Embed tissue directly into a cryomold with OCT solution as soon as possible after the specimen is collected in order to limit RNA and protein degradation. Float cryomold containing OCT-embedded tissue on a bath of isopentane and dry ice to freeze.
2. Once frozen, store at –80°C.

3.1.2. Formalin-Fixed Paraffin-Embedded Tissue

1. Collect specimen (not bigger than 1 cm cubes) into 10% neutral buffered formalin and leave for 20 h at room temperature before processing into paraffin.
2. For processing into paraffin blocks, transfer tissue into a tissue cassette. If available, an automated tissue processing machine can be used to process into paraffin. If this is unavailable, take tissues through the following series of baths.
   a. 70% ethanol, 20 min (× 1)
   b. 95% ethanol, 20 min (× 2)
   c. 100% ethanol, 20 min (× 2)
   d. Xylene, 20 min (× 2)
   e. Paraffin (65°C), 30 min (× 1)
3. Paraffin (65°C), 30 min (× 1) with a vacuum applied
4. Once embedded, tissue can be stored at room temperature indefinitely.

3.2. Tissue Sectioning

3.2.1. Frozen Sections

1. Cut frozen sections at 2–15 μm thickness on a cryostat with a disposable blade and place sections on labeled, uncoated glass microscope slides. Alternatively use PALM polyethylene napthalate-coated membrane slides for recovery of larger sections of tissue with preserved morphology. Position the tissue section near the centre of the slide, avoiding the top and bottom thirds of the slide. Do not allow the tissue section to dry on the slide at room temperature.
2. Place the slide directly on dry ice or keep the slide in the cryostat at –20°C or colder until the slides can be stored at –80°C or immediately stained and microdissected.

3.2.2. Paraffin-Embedded Tissue

1. Cut formalin-fixed, paraffin-embedded tissue samples at 2–15 μm thickness using a microtome and disposable blade and place on uncoated or PEN-coated slides as above (*see* **Section 3.2.1**, step 1).
2. Paraffin sections should then be dewaxed in xylene (coplin jar), 2 × 10 min, rehydrated through subsequent washes with 100, 90 and 70% DEPC-treated ethanol, for 5 min each, then air dried on the bench.

3.3. Hematoxylin and Eosin (H&E) Staining for Frozen Tissue and Paraffin-Embedded Sections

1. Remove fresh tissue slide from freezer and place on dry ice or directly into the 70% ethanol fixative solution (*see* **Note 2**). For paraffin-embedded tissue sections, dewax as described above (*see* **Section 3.2.2**, step 2) and then place in 70% ethanol. Dip the slides, for the time indicated, in each solution as listed below (*see* **Note 3**)
   a. 70% EtOH – 5 min
   b. DEPC H_2O – 2 min
   c. hematoxylin – 15 s
   d. DEPC H_2O – 30 s to 1 min
   e. Scott's tap water – 15 s
   f. 70% EtOH – 2 min
   g. Eosin Y (optional but not necessary for visualization of cells), 3–10 s
   h. 90% EtOH – 2 min
   i. 100% EtOH – 2 min
   j. 100% EtOH – 2 min
   k. Xylene – 2 min (× 2)
2. Air-dry slide as quickly as possible and begin LCM immediately (*see* **Note 4**).

3.4. Microdissection Using the PALM Microbeam UV-Cutting Laser and Pressure Catapulting

Samples are laser microdissected from histological sections following the manufacturer's protocol for the PALM Laser-MicroBeam System with PALM Robosoftware™ for the control of microdissection, laser function and contact-free transport (**Fig. 3.2**). In brief, the UV laser microbeam is coupled to the objective of the microscope. A motorized controlled microscope stage is attached to the inverted microscope and a CCD camera enables the observation of the microscopic image on a computer screen (**Fig. 3.2**).

1. The image is manipulated using a graphical user interface program (PALM Robosoftware™). Thus laser manipulation of tissue is controlled directly on the screen.
2. RNA lysis buffer (30 μL) is added into the lid of a microfuge tube (for paraffin sections), or 35 μL RNA lysis buffer + β-mercaptoethanol (for frozen sections) before the cap is

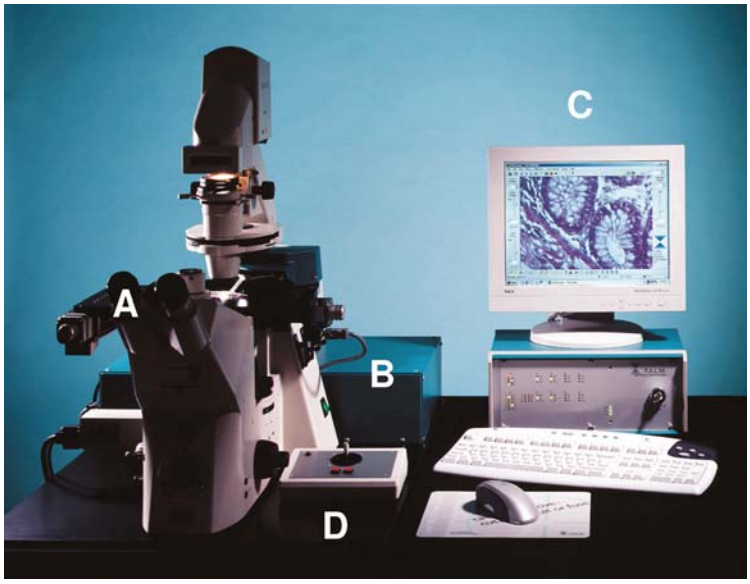

Fig. 3.2. PALM™ LPC-MicroBeam System. PALM™ LPC-Microbeam instrument. (**a**) Inverted light microscope with ×4 to ×100 objective. (**b**) UV Laser control unit; UVa laser (337 nm, 300 μJ, 3 ns). (**c**) PC with live video monitor. PALM Robosoftware™ installed. (**d**) PALM™ Robostage & RoboCapmover.

mounted with the aid of a swinging arm attached to the microscope, and positioned over the area to be microdissected, about 1 mm above the slide.

3. To select and isolate areas of interest, microdissection is performed by cutting around the perimeter of the area of interest with a fine focused laser beam (**Fig. 3.2**).
4. Unwanted cells within the area of interest can selectively be removed with single "shots" of pulsed laser.
5. Following isolation of cells, pulses of the focused laser beam just below the focal plane of the tissue specimen are used to create a pressure wave separating the targeted tissue from the slide, catapulting it against gravity into the microfuge cap (**Figs. 3.1 and 3.3**). The whole procedure takes approximately 1.5 h, and in this time it is possible to collect 50–500 cells.
6. When sampling glomeruli from archival renal biopsy sections, the glomerulus is defined as the area internal to and including Bowman's capsule (**Fig. 3.3**). Glomeruli can be visualized in H&E stained sections under transmitted light at ×40 magnification. Laser-dissected glomeruli from individual biopsies can be pooled for later RNA analysis. In general, we pool 4–10 glomeruli per biopsy for subsequent RNA extraction and PCR.

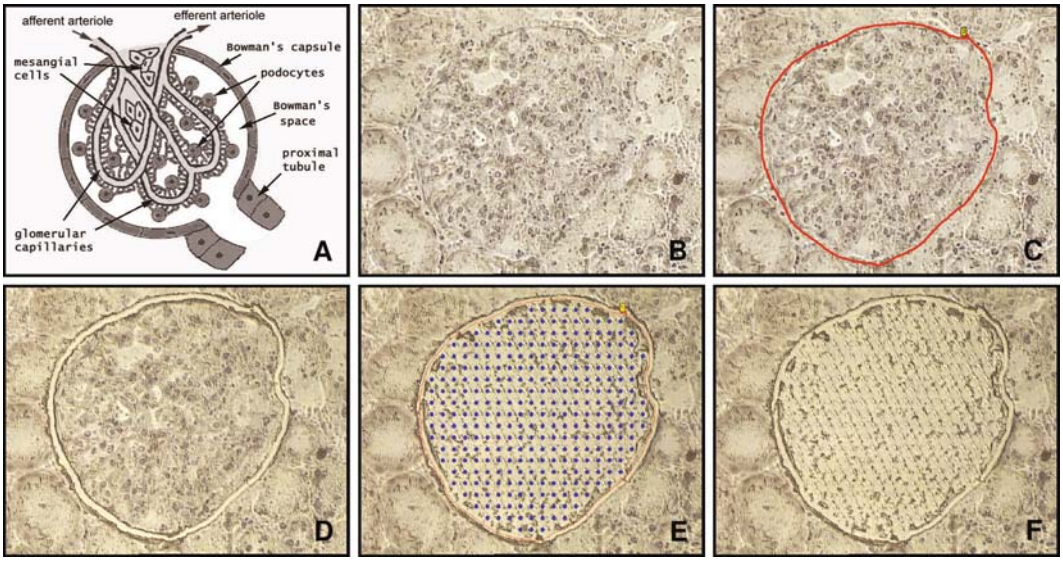

Fig. 3.3. Example of the laser capture process of a single glomerulus from an archival kidney biopsy. (**a**) Schematic diagram of a glomerulus indicating Bowman's capsule (the defining perimeter for microdissection). (Reproduced from www.siumed.edu/~dking2 with permission.) (**b**) Glomerulus as viewed on PALM microbeam screen (× 40 magnification, unstained 4 μm section from a renal biopsy). (**c**) PALM™ software allows user to highlight area to be excised. (**d**) Laser ablates area around glomerulus. (**e**) Entire section is pressure catapulted into microcap. (**f**) Section following LCM removal of glomerulus. Figure 3.3A courtesy of Dr David G. King, School of Medicine & College of Science, University of Illinois, IL, USA.

7. Immediately following the microdissection and capture procedure, a further 170 μL of RNA lysis buffer is added to the microfuge tube, vortexed briefly and centrifuged for 5 min to spin down cells from the lid.
8. The samples are stored in ice or frozen at –80°C for later RNA extraction.

3.5. RNA Extraction for qRT-PCR

1. For microdissected samples taken from paraffin embedded tissue, 500 μg/mL proteinase K should be added to the microfuge tube containing the sample in 200 μL of RNA lysis buffer. The stock of proteinase K is at 10 mg/mL; therefore, add 10 μL (a 1:20 dilution) to the RNA lysis buffer. The sample should then be vortexed to aid digestion and incubated at 60°C for 16 h or overnight until the tissue has completely solubilized (7). RNA extraction of microdissected specimens taken from fresh frozen tissue can commence without incubation with proteinase K.
2. RNA is purified by phenol (water saturated) and chloroform extraction. 200 μL water-saturated phenol and chloroform is added to the collected sample, vortexed and centrifuged for 5 min at 4°C (16,000*g*).

3. Remove supernatant to a fresh tube and add 200 μL phenol/chloroform to repeat extraction, spinning for a further 5 min at 4°C.
4. Remove supernatant again and perform a chloroform extraction by adding 200 μL of chloroform.
5. The final supernatant is removed and the RNA precipitated by adding an equal volume of isopropanol (180 μL) in the presence of 0.1 volume of 3 M sodium acetate (pH 5.2) (19 μL) and 1 μL of 20 mg/mL of carrier glycogen.
6. Precipitate RNA in this solution at –20°C for 4–7 days.
7. To recover RNA, spin for 15 min in 4°C centrifuge (16,000*g*). Remove and discard supernatant (pellet sometimes not visible, therefore take care with pipetting supernatant).
8. Wash RNA pellet with 1 mL cold 70% DEPC-treated ethanol and centrifuge for 10 min at 4°C.
9. Let RNA pellet dry at room temperature and resuspend in 10 μL of RNase-free DEPC-H_2O (*see* **Notes 3** and **5**).

3.6. Microchip Gel Electrophoresis

RNA quality can be determined using a picochip on an Agilent Bioanalyser (Agilent Technologies, Palo Alto, CA, USA); however, due to the very small amounts of RNA recovered from LCM samples, this is rarely performed. Others have shown that RNA quality from formalin-fixed, paraffin-embedded tissue may be fragmented but is suitable for real-time PCR (7).

3.7. cDNA Synthesis from Microdissected Cells

cDNA synthesis is performed from RNA extracted from tissue sections. Depending on the yield of RNA, 1–10 μL of RNA made up to 10 μL with DEPC–H_2O is added to 1 μL of random hexamers (Roche Diagnostics) and incubated at 70°C for 5 min and then cooled on ice for 5 min. A master mix containing 5 μL of 5 × AMV reaction buffer, 2.5 μL of 10 mM dNTP mix, 0.5 μL RNase inhibitor (40 U/μL) (Roche Diagnostics), 0.5 μL AMV reverse transcriptase (25 U/μL) and 4.5 μL of DEPC–H_20 is added to a final volume of 25 μL. The reaction mixture is then heated to 37°C for 60 min to complete cDNA synthesis; then cDNA samples were removed and stored at –20°C (*see* **Note 6**).

3.8. Real-Time PCR

Gene expression is measured and quantified using the ABI Prism 7,000 Sequence detection System (Applied Biosystems) according to the manufacturer's instructions. The following example describes the quantitative analysis of glomerular connective tissue growth factor (CTGF) expression.

1. Sequence-specific primers are designed to span exon–exon boundaries to avoid amplification of contaminating genomic DNA using the Primer Express software v1.5 (Applied Biosystems).

2. Primers are obtained from Sigma-Aldrich and fluorescent probes can be obtained from Applied Biosystems. The primer and probe sequences used to examine CTGF gene expression in laser dissected glomeruli are as follows:

   CTGF forward primer: 5′-TGCACCGCCAAAGATGGT-3′

   CTGF reverse primer: 5′-GGACTCTCCGCTGCGGTAC-3′

   CTGF probe: 5′-CTCCCTGCATCTTCGGTGGTACGG-3′

3. The Taqman™ fluorogenic probe (Applied Biosystems) includes a fluorescence reporter (6-carboxyfluorescein) at the 5′ end and a fluorescent quencher (6-carboxytetramethylrhodamine [TAMRA]) at the 3′ end. A commercial, pre-developed 18S control kit labeled with a fluorescent reporter dye on the 5′ end and the quencher on the 3′ end (Applied Biosystems) is used as the endogenous control.

4. The 25 μL PCR mixture contains 12.5 μl Taqman Universal PCR Master Mix (Applied Biosystems), 500 nM primers (forward and reverse), 100 nM Taqman™ probe and 1 μL of cDNA template. PCR is performed at 50°C for 2 min, 95°C for 10 min and then run for 50 cycles at 95°C for 15 s and 60°C for 1 min.

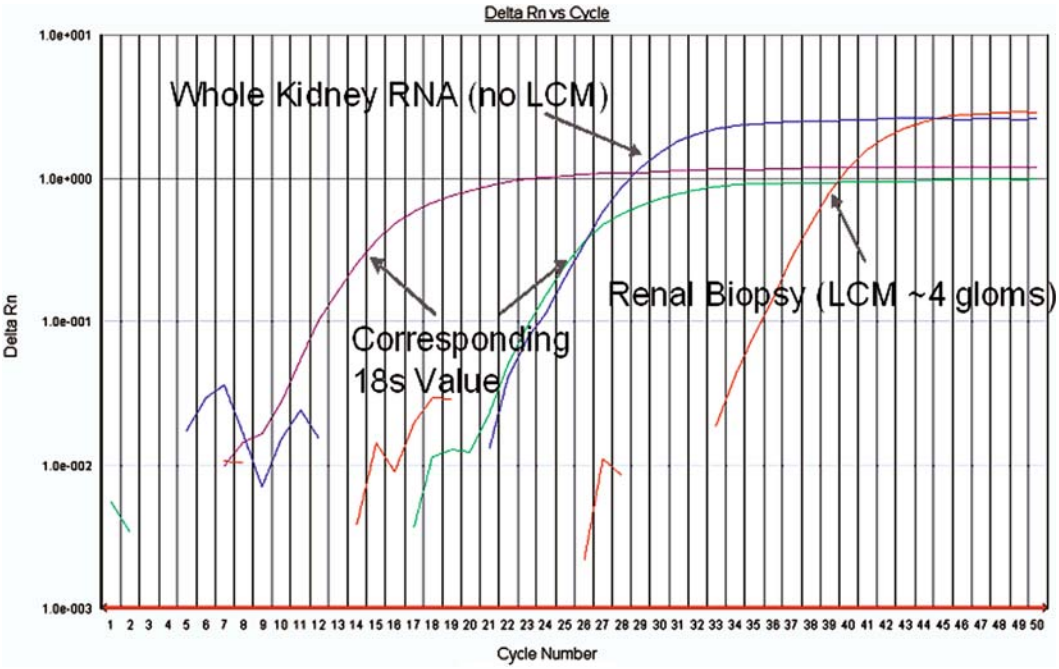

Fig. 3.4. CTGF gene expression in glomeruli collected from fixed paraffin-embedded tissue using laser microdissection. qRT-PCR of whole kidney RNA from a frozen renal biopsy compared to glomeruli collected using laser-capture microdissection (LCM) from a fixed, paraffin-embedded histological section of a renal biopsy. For the laser-capture microdissected sample, four glomeruli were pooled to examine the expression of a gene linked with the development of fibrosis in kidney disease (CTGF).

5. Primer and probe concentrations are optimized before experiments are completed.
6. Amplification efficiencies of the target gene CTGF, and the endogenous control, 18S are approximately equal and can be validated allowing relative quantitation to be performed between the target gene and endogenous control. Comparative cycle threshold (C_T) calculations are all relative to control tissue, with gene expression for CTGF derived using the equation $2{-}\Delta\Delta Ct$ (**Fig. 3.4**).

4. Notes

1. The use of PEN-membrane-covered slides allows recovery of larger, intact fragments of tissue with retained morphology. The membrane supports the underlying tissue and protects the sample from contaminating tissue fragments.
2. Samples for LCM can be stained with any standard chromogenic–histologic, fluorescent or immunohistologic procedure to aid in visualization of the cells of interest. Most LCM systems offer visualization with both standard transmitted light and fluorescence.
3. All procedures should be carried out in RNase-free conditions. The working place and pipettes should be decontaminated. Gloves should be worn at all times and be changed frequently. RNase-free filter pipette tips should be used and if possible, all reagents used should be RNase-free.
4. The quality of the original sample is important for all kinds of RNA analyses. In general, it has been found that fresh, frozen tissues yield more RNA than paraffin-embedded, fixed tissues. When considering the type of fixative to use, it has been shown that fixatives such as ethanol and acetone yield better RNA than cross-linking fixative such as formalin (8, 9). Despite this, there are reports of successful RNA amplification from formalin-fixed and paraffin-embedded tissue using PCR methods (7).
5. We have used a traditional phenol:chloroform protocol to extract RNA from microdissected samples; however, alternative methods of RNA extraction have been used in combination with LCM and later analyses. These include Mini RNA isolation Kits (Stratagene, La Jolla, CA, USA), Qiagen Rneasy™ Micro Kit (Qiagen, Valencia, CA, USA) and TRIzol™ reagent (Invitrogen).

6. When small amounts (<1 ng) of cDNA are expected, purification of cDNA should be considered. This can be performed by phenol extraction.

References

1. Kohda, Y., Murakami, H., Moe, O.W., and Star, R.A. (2000) Analysis of segmental renal gene expression by laser capture microdissection. *Kidney Int.* **57**, 321–331.
2. Nagasawa, Y., Takenaka, M., Matsuoka, Y., Imai, E., and Hori, M. (2000) Quantitation of mRNA expression in glomeruli using laser-manipulated microdissection and laser pressure catapulting. *Kidney Int.* **57**, 717–723.
3. Schutze, K., Niyaz, Y., Stich, M., and Buchstaller, A. (2007) Noncontact laser microdissection and catapulting for pure sample capture. *Methods Cell Biol.* **82**, 649–673.
4. Chaudhary, K.W., Barrezueta, N.X., Bauchmann, M.B., Milici, A.J., Beckius, G., Stedman, D.B., Hambor, J.E., Blake, W.L., McNeish, J.D., Bahinski, A., and Cezar, G.G. (2006) Embryonic stem cells in predictive cardiotoxicity: laser capture microscopy enables assay development. *Toxicol. Sci.* **90**, 149–158.
5. Mayer, A., Stich, M., Brocksch, D., Schutze, K., and Lahr, G. (2002) Going in vivo with laser microdissection. *Methods Enzymol.* **356**, 25–33.
6. Espina, V., Wulfkuhle, J.D., Calvert, V.S., VanMeter, A., Zhou, W., Coukos, G., Geho, D.H., Petricoin, E.F. 3rd, and Liotta, L.A. (2006) Laser-capture microdissection. *Nat. Protoc.* **1**, 586–603.
7. Specht, K., Richter, T., Muller, U., Walch, A., Werner, M., and Hofler, H. (2001) Quantitative gene expression analysis in microdissected archival formalin-fixed and paraffin-embedded tumor tissue. *Am. J. Pathol.* **158**, 419–429.
8. Goldsworthy, S.M., Stockton, P.S., Trempus, C.S., Foley, J.F., and Maronpot, R.R. (1999) Effects of fixation on RNA extraction and amplification from laser capture microdissected tissue. *Mol. Carcinog.* **25**, 86–91.
9. Burgemeister, R., Gangnus, R., Haar, B., Schutze, K., and Sauer, U. (2003) High quality RNA retrieved from samples obtained by using LMPC (laser microdissection and pressure catapulting) technology. *Pathol. Res. Pract.* **199**, 431–436.

Part II

Staining Techniques

Chapter 4

Immunofluorescence Detection of the Cytoskeleton and Extracellular Matrix in Tissue and Cultured Cells

Josiane Smith-Clerc and Boris Hinz

Abstract

"A picture is worth a thousand words" goes the proverb. A poor picture however can be worse than saying nothing at all. This is particularly true for immunofluorescence pictures that in addition to their informative character bear an esthetic component. We here provide a panel of straightforward methods to process tissue sections and cultured cells for immunostaining of cytoskeletal elements, primarily those associated with actin filaments. We want to emphasize to the reader the fact that the choice of the processing method will have an important influence on the outcome of the immunostaining and thus on the interpretation of the results. Fixation of cultured cells with cross-linking reagents such as paraformaldehyde efficiently preserves structural elements at the expense of reduced antigenicity. The degree and timing of cell permeabilization with detergents, along with chemical cross-linking, contributes to the clarity and resolution of distinct structures but can also lead to loss of information. Fixation with organic solvents like methanol will, in most cases, better preserve antigens but will produce a higher background and impact on structural integrity. Therefore, it is recommended to test different protocols for a "new" protein or epitope – the results will pay back your investment.

Key words: Actin, focal adhesion, microtubule, intermediate filament, extracellular matrix, fixation by cross-linking, fixation by precipitation, myofibroblast, wound healing, fibrosis.

1. Introduction

The histochemical detection of specific proteins and structures in tissues and cultured cells by means of epifluorescence microscopy was pioneered by Albert Hewett Coons, being the first to chemically couple antibodies with fluorescein molecules (1, 2). Another milestone in the development of immunofluorescence staining methods was the development of hybridoma cultures to produce monoclonal antibodies in the 1970s (3), a time when it was still possible to publish in high-impact papers with results exclusively based on immunofluorescence images. Now, three decades later,

T.D. Hewitson, I.A. Darby (eds.), *Histology Protocols*, Methods in Molecular Biology 611,
DOI 10.1007/978-1-60327-345-9_4, © Humana Press, a part of Springer Science+Business Media, LLC 2010

immunostaining of cells and tissues is one of the most widely used standard methods in cell biology, having experienced another boost with the significant technical advances made in epifluorescence and confocal microscopy. Given these improvements, it is surprising or indeed sad to see that a considerable number of publications still present poor immunofluorescence images. One reason is suboptimal use of the acquisition equipment, including microscopes, objectives, digital cameras, and the image acquisition/processing software. Another reason is the sometimes careless application of the standardized protocols for immunofluorescence. If the basic material is not well prepared, neither the one-million-dollar total internal reflection fluorescence confocal microscope nor Huygen's deconvolution, three-dimensional rendering, and Adobe Photoshop™ will be able to improve the quality of your image.

Here we describe a selection of easy-to-use techniques to process tissue sections and cultured cells for immunostaining of cytoskeletal elements in less than a day. In our laboratory, these protocols are applied to investigate the so-called myofibroblasts. Myofibroblasts are highly contractile fibroblastic cells that have developed a smooth-muscle-like phenotype in response to tissue injury and remodeling. They contribute to normal wound closure by contracting the wound granulation tissue and are instrumental in causing the tissue deformations characteristic of fibrotic diseases (4). Hallmark features of myofibroblasts are de novo expression of α-smooth muscle actin (α-SMA) (**Fig. 4.1**) in stress fibers, in addition to the cytoplasmic actins present in normal fibroblasts (5), and the formation of unusually large cell-matrix focal adhesions (6).

The cytoskeleton comprises three main filament types: (1) microtubules, (2) intermediate filaments, and (3) microfilaments (actin filaments) and associated proteins (**Fig. 4.2**). Their high abundance, their fundamental importance for a plethora of cell functions, and last but not least the beauty of their organization rendered cytoskeletal proteins one of the earliest targets for immunofluorescence microscopy (7–10). Despite being relatively easy to visualize, the choice of the "right" procedure for processing cells and tissues will influence the interpretation of the cytoskeleton immunofluorescence staining. The fixation procedure to a large extent determines the structural integrity of the tissue or living cell; it generally comprises the use of either chemical cross-linkers such as formaldehyde, paraformaldehyde, and glutaraldehyde or organic solvents, including methanol, ethanol, and acetone. Organic solvents are relatively gentle to antigens and precipitate proteins by cell dehydration, sometimes leading to structural changes. On the other hand, cross-linking reagents form a network of proteins primarily connected via free aldehyde groups. This preserves the structure very well but often at the expense of reduced antigenicity. Moreover, cells have to be permeabilized with detergents to allow antibody access to the specific antigens after

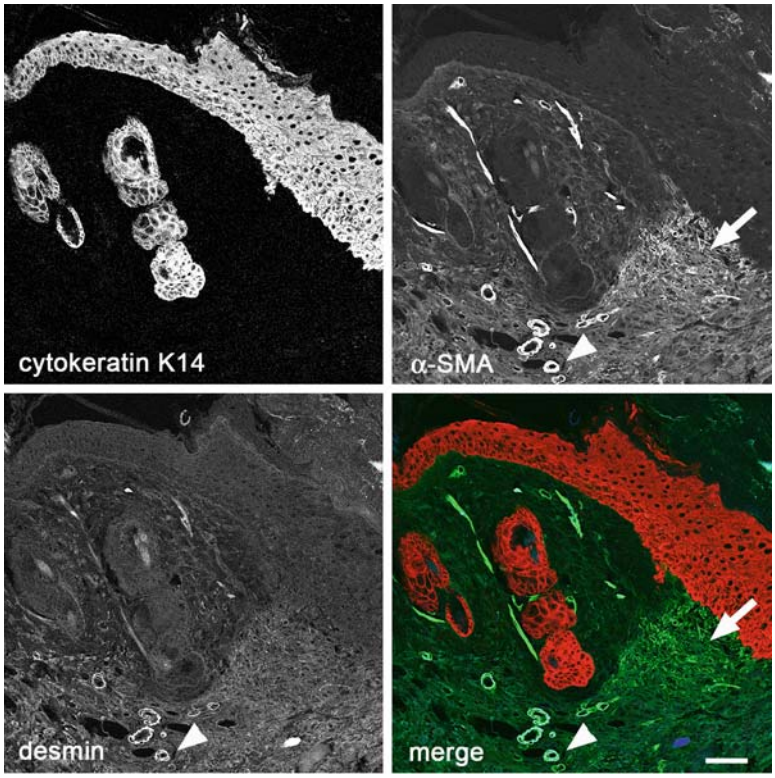

Fig. 4.1. *Distinction of keratinocytes, smooth muscle cells, and myofibroblasts in skin wounds*. Five-day-old full thickness mouse skin wounds are fixed with acetic acid/ethanol and embedded in paraffin (**Section 3.2.2**). Microtome sections of 3 μm thickness are stained using anti-cytokeratin K14 (rabbit, Babco, Richmond, CA, USA; *red*), anti-α-SMA (mouse IgG2a, clone αSM-1, a kind gift of Dr. G. Gabbiani (14); *green*), and anti-desmin (mouse IgG1, clone D33, Dako, Glostrup, Denmark; *blue*). As secondary antibodies, goat anti-rabbit Alexa647 (Molecular Probes, Invitrogen, Carlsbad, CA, USA), goat anti-mouse IgG1-TRITC (Southern Biotechnology, Birmingham, AL, USA), and goat anti-mouse IgG2a-FITC (Southern Biotechnology) are applied. Note that specific expression or specific combinations of cytoskeletal proteins can be used as cell-specific markers. The epithelium at the wound edge (*right*) and of hair follicles specifically stains for cytokeratin K14, myofibroblasts residing under the hyperproliferative epithelium stain exclusively for α-SMA (*arrow*), whereas smooth muscle cells of small vessels co-express α-SMA and desmin (*arrowheads*). Scale bar: 150 μm. (For color figures, see online version).

cross-linking, whereas organic solvents remove the lipid bilayer and fix at the same time. We show that the resistance of the cytoskeleton to detergent treatment can indeed be exploited to reduce background and to specifically reveal cytoskeletal structures.

2. Materials

2.1. Cell Culture

1. 22 × 22 mm glass or tissue culture plastic cover slips.
2. 100% acetone.
3. 100% ethanol.
4. 35 mm tissue culture dishes or six-well plates.

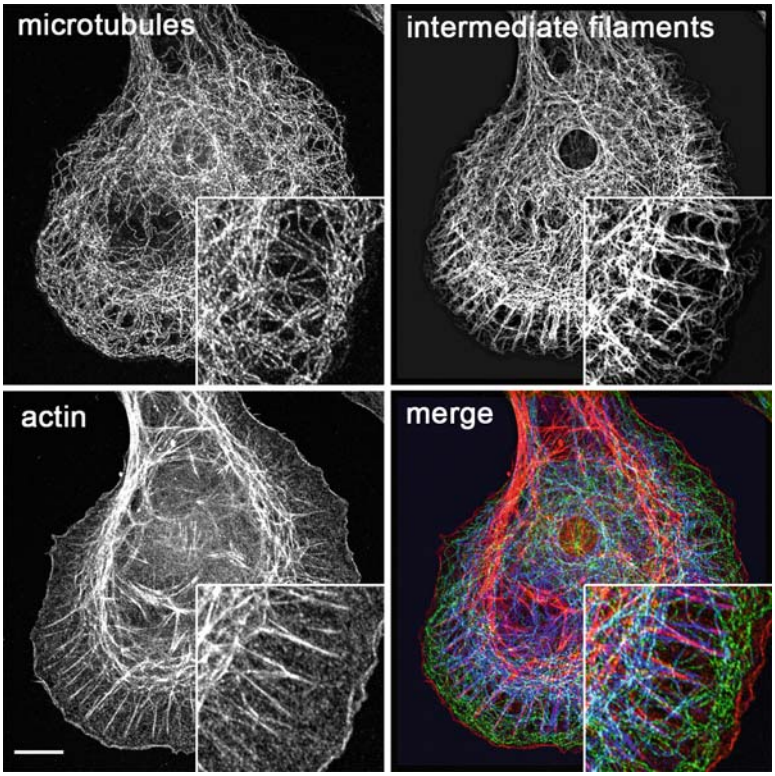

Fig. 4.2. *Filaments of the cytoskeleton.* The three filament types of the cytoskeleton are visualized by scanning confocal microscopy after PFA fixation and permeabilization of cultured rat cardiac fibroblasts (**Section 3.3.1**). Microtubules are immunostained with primary antibodies directed against anti-α-tubulin (rabbit, Abcam, Cambridge, UK; *green*) and intermediate filaments with anti-vimentin (mouse IgG1, clone V9, Dako; *blue*). F-actin is probed with Phalloidin-Alexa568 (Molecular Probes, *red*), applied together with secondary antibodies goat anti-rabbit Alexa488 and goat anti-mouse Alexa647 (Molecular Probes). Scale bar: 10 μm. (For color figures, see online version).

2.2. Tissue Preparation

2.2.1. Cryofixation

1. Embedding compound (e.g., OCT, Tissue Tek™, Zoeterwoude, The Netherlands).
2. Embedding molds (e.g., 15 × 15 Cryomold, Tissue Tek™).
3. 100% pentane (2-methylbutane) in a glass beaker, –20°C.
4. Liquid nitrogen in dewar.
5. Cryomicrotome.
6. 76 × 26 mm microscope slides.

2.2.2. Acetic Acid/Ethanol Fixation

1. Acetic acid.
2. Xylene.
3. 100% ethanol.

4. 100% chloroform.
5. Paraffin embedding material.
6. Microtome.
7. 76 × 26 mm microscope slides.

2.2.3. Formalin Fixation

1. 4% buffered formalin: 45 mM NaH_2PO_4, 33 mM Na_2HPO_4, 35% stock solution of formaldehyde to a final concentration of 4%, pH 7.4, protected from light.
2. 10 mM sodium citrate buffer, pH 6.0.
3. Xylene.
4. 100% ethanol.
5. 100% chloroform.
6. Paraffin embedding material.
7. Microtome.
8. 76 × 26 mm microscope slides.
9. Microwave oven.

2.3. Preparation of Cultured Cells

1. Phosphate-buffered saline (PBS): 150 mM NaCl, 8.06 mM Na_2HPO_4, 1.74 mM NaH_2PO_4, pH 7.4.
2. 20% Triton-X 100 (TX-100), 4°C (*see* **Note 1**).
3. 3% paraformaldehyde (PFA) in PBS (w/v).
4. Cytoskeleton buffer: 60 mM PIPES (1,4-piperazinebis(ethanesulfonic acid)), 25 mM HEPES (4-(2-Hydroxyethyl)piperazine-1-ethanesulfonic acid), 2 mM $MgCl_2$, pH 6.9, 4°C, protected from light.
5. 200 mM Na_3VO_4 (sodium orthovanadate).
6. PMSF (phenylmethanesulfonyl fluoride), room temperature.
7. Desoxycholate (DOC) buffer: 50 mM Tris–HCl, 150 mM NaCl, 0.2% DOC, 4°C.
8. 0.4% NH_4OH in distilled water.
9. 100% methanol, –20°C.
10. 100% acetone, –20°C.

2.4. Immunostaining of Fixed Tissue and Cells

1. Appropriate primary and secondary antibodies.
2. Orbital shaker.
3. PBS.
4. 20% TX-100, 4°C.
5. 3% BSA in PBS (w/v) (optional).
6. PVA (polyvinylalcohol) or other suitable mounting medium.
7. 76 × 26 mm glass microscope slides.

8. Slide racks and tray (for tissue).
9. Staining-dishes with lids, and tissue paper to maintain humidity (for tissue).
10. 22 × 22 mm glass cover slips.

3. Methods

3.1. Cell Culture

For subsequent processing, it is convenient to directly culture cells on glass cover slips, either uncoated or coated with extracellular matrix (ECM) proteins. Depending on the structure and protein of interest, cells are grown sparsely (e.g., to study focal adhesions) or confluent (e.g., to visualize cell–cell junctions). Some cell types grow better on tissue culture plastic which is available with the thickness of cover slips and as special plastic chambers (e.g., Lab-Tek™, Nunc, Roskilde, Denmark). A less expensive solution is to grow and stain cells directly on 35 or 60 mm tissue culture dishes that can then be observed from the top with upright microscopes after mounting samples with glass coverslips. Microscopy with high numerical aperture immersion objectives requires a short working distance to the object (~200 μm); hence, high resolution microscopy is not possible through the cell culture dish bottom or through microscope slides (~1,000 μm).

1. Wipe 22 × 22 mm glass cover slips; clean using 100% acetone.
2. Soak coverslips in 100% ethanol for 10 min and then air-dry in sterile hood.
3. Incubate clean and sterile coverslips in six-wells or 35-mm dishes with 1 mL culture medium containing 10% serum for minimum 60 min at 37°C. With some cell types, it is necessary to coat slides by supplementing medium with 1–10 μg/cm^2 ECM protein (e.g., collagen, fibronectin, vitronectin, laminin) to ensure adherence.
4. Add 1 mL of cell suspension containing ~5,000 cells (5–7 days culture) or ~20,000 cells (1–2 days culture) for sparse conditions. For confluent cell layers, add ~50,000 cells (5–7 days culture) or ~100,000 cells (1–2 days culture). These approximate numbers are given for fibroblastic cell culture in 35-mm diameter dishes and have to be adjusted for the respective cell size and growth rates or when using different culture vessel volumes.

3.2. Tissue Preparation

Protein epitopes (antigens) exhibit different sensitivities to the procedures of tissue fixation, embedding, and tissue sectioning. Three alternative protocols are provided here to be adapted to the

structure and protein of interest. Cryofixation and embedding are most gentle to the antigens but compromise tissue architecture. Formalin fixation and paraffin embedding best preserve tissue structure but can impair epitope antigenicity.

3.2.1. Cryofixation

1. Place and orient tissue in a cryomold filled with cryoembedding compound.
2. Drop mold with the embedded sample into a beaker filled with pentane, cooled to –196°C in liquid nitrogen. Freeze for 2 min and store at –80°C.
3. Cut sections of 2–3 μm thickness using a cyromicrotome and attach tissue sections to microscope slides.
4. Rinse once with PBS at room temperature.
5. Continue with **Section 3.4**.

3.2.2. Acetic Acid/Ethanol Fixation

1. Fix tissue in 95% ethanol/5% acetic acid at 4°C overnight.
2. Transfer to 100% ethanol for 60 min.
3. Rinse in 100% chloroform for 10 min, × 2.
4. Soak tissue in molten paraffin (~56°C) for minimum 4 h.
5. Transfer tissue to fresh molten paraffin for another 4 h.
6. Embed tissue in paraffin using embedding molds. Cool to –20°C for 60 min and remove paraffin block from the mold.
7. Cut tissue slices of 2–3 μm thickness with a microtome and collect sections on microscope slides.
8. Deparaffinize by soaking slides in xylene at room temperature for 5 min, × 2.
9. Rehydrate sections through graded ethanol by immersing in 100 (× 2), 96, 90, 80, 70, 50% (v/v in distilled water) at room temperature for 1 min each.
10. Transfer to distilled water at room temperature for 5 min.
11. Wash with PBS at room temperature for 10 min, × 3.
12. Continue with **Section 3.4**.

3.2.3. Formalin Fixation

1. Fix tissue in 4% buffered formalin at room temperature overnight.
2. Dehydrate tissue through graded ethanol: 50, 70, 95, 100% (v/v in distilled water) at room temperature for 2 min each.
3. Embed, cut, and deparaffinize as in **Section 3.2.2**, steps 3–10.
4. Unmask antigenic sites by microwave incubation in 10 mM sodium citrate buffer, pH 6.0 at 700 Watts for 8 min (11).
5. Continue with **Section 3.4**.

3.3. Preparation of Cultured Cells

As described for tissue samples, protein epitopes in cultured cells exhibit different sensitivities to different fixation procedures. Eight alternative protocols are provided below to be adapted to the structure and protein of interest. These protocols fall into two classes of fixation: (1) Under **Sections 3.3.1–3.3.5**, PFA is used as cross-linking reagent, generating a network of proteins/antigens through free amino groups. In this case, to allow access to the antigen by its specific antibody, the cell membrane needs to be permeabilized or completely extracted using detergents such as TX-100, DOC or by applying an osmotic shock with ammonium hydroxide. (2) Under **Sections 3.3.6–3.3.8**, organic solvents such as methanol, acetone

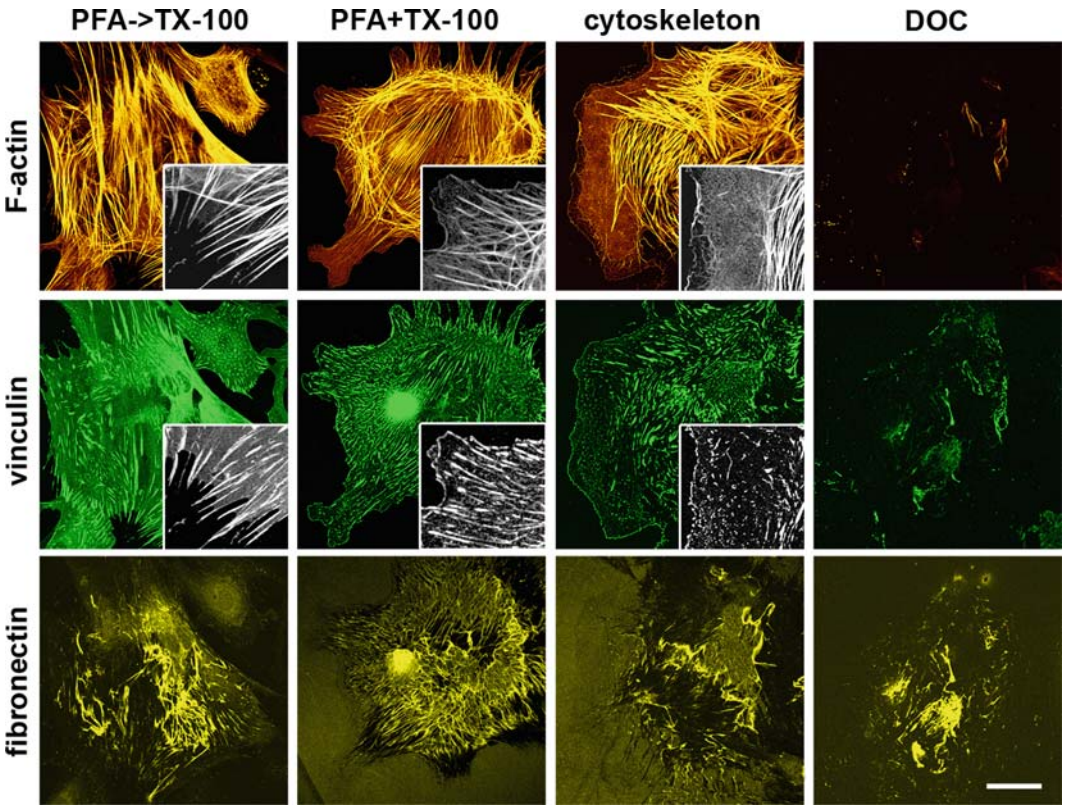

Fig. 4.3. *Different permeabilization procedures in combination with PFA fixation.* Rat cardiac myofibroblasts were cultured for 4 days on fibronectin-coated glass coverslips and processed by (a) PFA fixation followed by 0.2% TX-100 permeabilization (PFA->TX-100, **Section 3.3.1**), (b) simultaneous PFA fixation and 0.2% TX-100 permeabilization (PFA+TX-100, *see* **Section 3.3.2**), (c) extraction with 0.5% TX-100, followed by PFA fixation (cytoskeleton, *see* **Section 3.3.3**), and (d) cell extraction with DOC buffer (DOC, *see* **Section 3.3.4**). Processing was followed by immunostaining for focal adhesions using anti-vinculin antibodies (mouse IgG1, clone hVin-1, Sigma-Aldrich, St Louis, MO, USA) and for ECM with anti-fibronectin (rabbit, Sigma-Aldrich). F-actin was stained using Phalloidin-Alexa568 (Molecular Probes), applied together with secondary antibodies goat anti-rabbit Alexa647 and goat anti-mouse Alexa488 (Molecular Probes). Note that different protocols produce different levels of background fluorescence and differently show cytoskeletal structures, particularly evident for focal adhesion staining. DOC removes the cytoskeleton and only preserves ECM fibers. Scale bar: 20 μm; insets: 10 μm.

or ethanol are used to remove membrane lipids and to dehydrate the cells, thereby precipitating proteins on the cellular architecture. Experimental outcomes of different protocols are compared in **Figs. 4.3** and **4.4** for preserving focal adhesions and stress fibers. To stain cultured cells, follow this master protocol that is as follows:

1. Wash cells with serum-free medium at room temperature, $\times 2$ (*see* **Note 2**).
2. Continue directly with *one* selected protocol under **Sections 3.3.1–3.3.8**.
3. Continue from **Section 3.4**.

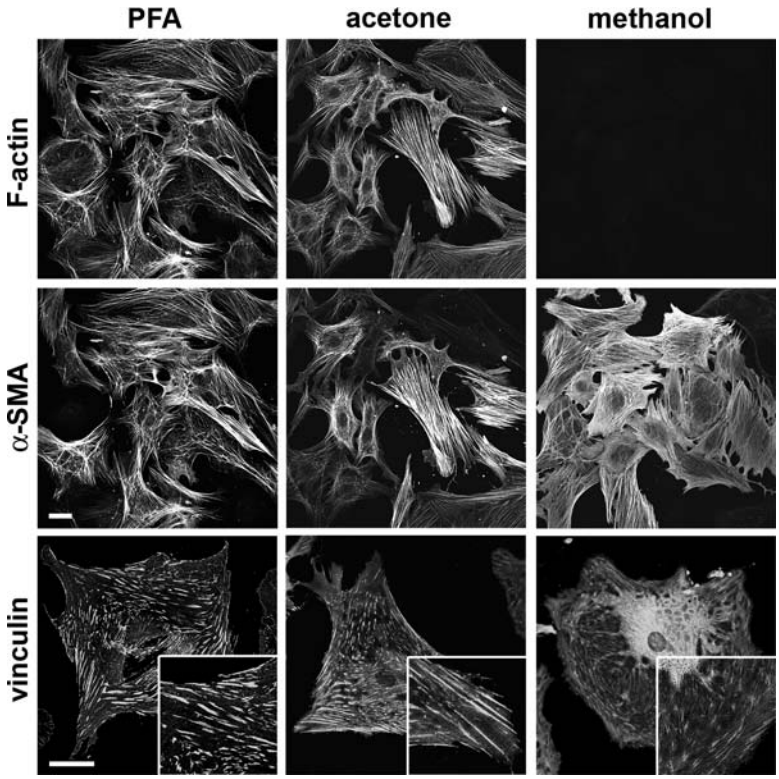

Fig. 4.4. *Use of organic solvents for fixation.* Rat cardiac myofibroblasts were cultured for 4 days on fibronectin-coated glass coverslips and processed by (a) PFA fixation followed by 0.2% TX-100 permeabilization (PFA, *see* **Section 3.3.1**) for cross-linking comparison, (b) acetone treatment (acetone, *see* **Section 3.3.7**), and (c) methanol treatment (methanol, *see* **Section 3.3.6**). Processed cells were immunostained using anti-α-SMA (mouse IgG2a, clone αSM-1) and for focal adhesions using anti-vinculin antibodies (mouse IgG1, clone hVin-1, Sigma-Aldrich). F-actin was stained using Phalloidin-Alexa647 (Molecular Probes), applied together with secondary antibodies goat anti-mouse IgG1-TRITC (Southern Biotechnology) and goat anti-mouse IgG2a-FITC (Southern Biotechnology). Note that methanol fixation reveals α-SMA better than acetone or PFA but is not compatible with the Phalloidin probe and produces high background for focal adhesion staining. Acetone fixation allows high-quality discrimination of stress fibers but relatively poor identification of focal adhesions. Scale bar: 20 μm; insets: 10 μm.

3.3.1. Cell Fixation and Subsequent Permeabilization

1. Fix cells in 3% PFA/PBS at room temperature for 10 min.
2. Rinse once with PBS (*see* **Note 3**).
3. Permeabilize cells in 0.2% TX-100/PBS at room temperature for 5 min.
4. Rinse once with PBS.

3.3.2. Simultaneous Cell Fixation and Permeabilization

1. Fix and permeabilize cells simultaneously in 0.2% TX-100/3% PFA/PBS at room temperature for 10 min.
2. Rinse once with PBS.
3. Post-fix cells in 3% PFA/PBS at room temperature for 5 min.
4. Rinse once with PBS.

3.3.3. Cytoskeleton Preparation

1. Titrate a 200 mM solution of sodium orthovanadate (yellow) to pH 10.0. Boil until the solution turns colorless and then cool to room temperature. Readjust to pH 10.0 and repeat previous steps until the solution is colorless and remains stable at pH 10.0. Portions can be stored at –20°C (*see* **Note 4**).
2. Extract cell membranes and cytosolic compounds with cytoskeleton buffer, supplemented with 0.5% TX-100, 1 mM PMSF, and 1 mM sodium orthovanadate at 4°C for 10 min with mild shaking on ice (*see* **Note 5**).
3. Rinse very gently once with ice-cold cytoskeleton buffer (without TX-100).
4. Fix cytoskeleton preparations in 3% PFA/PBS at room temperature for 5 min.
5. Rinse once with PBS.

3.3.4. ECM Protein Preparation with DOC Buffer

1. Extract cell components with DOC buffer on ice at 4°C for 10 min under mild shaking (*see* **Note 6**).
2. Rinse once with PBS.
3. ECM preparations can be directly processed or air-dried for intermediate storage at 4°C. Fixation in 3% PFA/PBS at room temperature for 5 min is optional for antigens that are not sensitive to fixation.

3.3.5. ECM Protein Preparation with Ammonium Hydroxide (NH_4OH)

1. Remove cellular components by applying hypo-osmotic shock using 0.4% NH_4OH diluted in distilled water on ice at 4°C for 3 min (*see* **Note 6**).
2. Rinse gently with PBS.
3. Equilibrate in 0.02% TX-100/PBS for 10 min.
4. ECM preparations can be directly processed or air-dried for intermediate storage at 4°C. Fixation in 3% PFA/PBS at room temperature for 5 min is optional for antigens that are not sensitive to fixation.

3.3.6. Methanol Precipitation

1. Aspirate medium or buffer thoroughly.
2. Gently add –20°C pre-cooled methanol to extract and precipitate on ice for 5 min.
3. Do *not* remove methanol. Rehydrate gradually by gently adding PBS at 1:1 volume at room temperature for 5 min; repeat this step three times (*see* **Note 7**).
4. Equilibrate in PBS at room temperature for 10 min.
5. Rinse once with 0.02% TX-100/PBS.

3.3.7. Acetone Precipitation

1. As in **Section 3.3.6**, only step 3 differs. Instead of step 3, gently add –20°C pre-cooled 100% acetone to extract and precipitate on ice for 5 min. Acetone is a solvent and not compatible with standard tissue culture plasticware.

3.3.8. Ethanol Precipitation

1. As in **Section 3.3.6**, only step 3 differs. Instead of step 3, gently add –20°C pre-cooled 100% ethanol to extract and precipitate on ice for 5 min.

3.4. Immunostaining of Fixed Tissue and Cells

1. Dilute all primary antibodies for multiple proteins staining in one vial of PBS/0.02% TX-100. Most antibodies work well at final concentrations of 10–50 μg/mL (*see* **Note 8**).
2. Block non-specific antibody binding with 3% BSA/PBS. This step can be omitted for most good quality antibodies used on cultured cells but may be required when staining tissue sections (*see* **Note 9**).
3. Incubate tissue or cell samples with diluted primary antibodies at room temperature for 60 min (*see* **Note 10**). Omit this step in one control sample to test non-specific secondary antibody binding (*see* **Note 11**).
4. Wash with PBS/0.02% TX-100 at room temperature for 10 min, × 3.
5. Dilute all fluorochrome-conjugated secondary antibodies (for multiple colors, staining in one vial) in PBS/0.02% TX-100 (*see* **Note 8**). Continue all the following steps protected from light to reduce fluorochrome bleaching.
6. Incubate with diluted secondary antibodies at room temperature for 60 min.
7. Wash with PBS/0.02% TX-100 at room temperature for 15 min, × 3.
8. Rinse once with distilled water.
9. Mount samples with one drop of PVA or any other suitable mounting medium (*see* **Note 12**). Polymerize PVA at room temperature overnight. Store samples at 4°C afterwards for several months or years.

3.5. Immunostaining of Living Cells for Fixative-Sensitive Extracellular Epitopes

It is often advantageous to incubate living cells with primary antibodies prior to the fixation, if antigens are sensitive to fixatives or organic solvents or when using antibodies that only recognize native protein configurations. Because in this case cells are not permeabilized for primary antibody incubation, the protein epitopes must be extracellular to be accessible, such as ECM proteins and the extracellular portions of cadherins and integrins (**Fig. 4.5**). Cell dynamics may enhance presentation of antigens or even reveal cryptic epitopes. Care must be taken because some antibodies that bind to extracellular epitopes have protein-function blocking activity and will interfere with cell activities.

1. Dilute primary antibodies in culture medium (can contain 10% serum).
2. Incubate living cells with diluted primary antibodies in the incubator for 2 h.
3. Follow one protocol under **Section 3.3**.
4. Continue with **Section 3.4** by omitting steps 1–4.

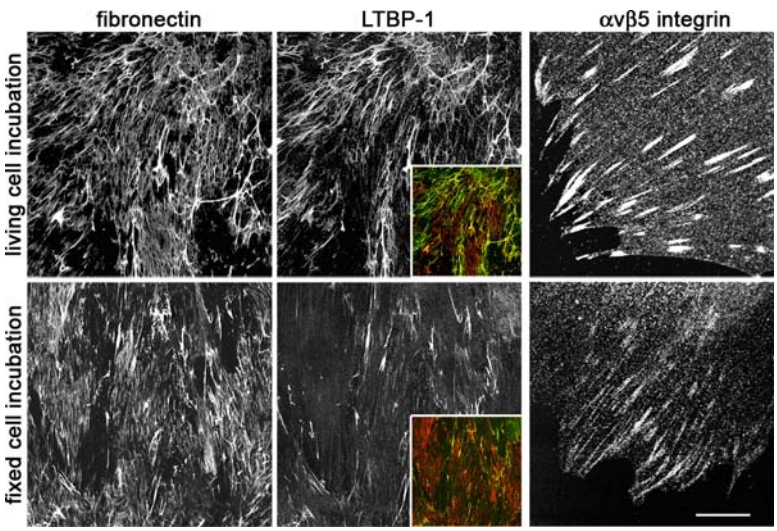

Fig. 4.5. *Probing extracellular epitopes of living cells.* Rat cardiac myofibroblasts were cultured for 4 days on fibronectin-coated glass coverslips. Living cells were incubated for 2 h with primary antibodies diluted in culture medium before fixation (*top row*) (**Section 3.5**). Cells from the same conditions were fixed and permeabilized prior to primary antibody incubation for identical times (**Sections 3.3.1** and **3.4**). As primary antibodies, anti-fibronectin (mouse IgG1, Sigma), anti-latent TGFβ-binding protein 1 (LTBP-1, rabbit Ab39, a kind gift from C.H. Heldin (15)), and anti-αvβ5 integrin (mouse IgG1, clone P1F6, Abcam) were used. Secondary antibodies were goat anti-rabbit Alexa568 and goat anti-mouse Alexa488 (Molecular Probes). Insets show color merge of LTBP-1 (*green*) and fibronectin (*red*). Note that incubation of living cells with primary antibodies significantly improves the signals for the ECM protein LTBP-1 and for the extracellular epitope of αvβ5 integrin but not for fibronectin. Scale bar for first two columns: 25 μm; for third column: 10 μm. (For color figures, see online version).

4. Notes

1. TX-100 is difficult to handle in its pure viscous form and it is not stable in high dilutions (e.g., 0.2%). Prepare 20% stock solution at room temperature and then store at 4°C.
2. Keep living cells as "happy" as possible by washing in serum-free medium or cell culture PBS solutions that have been pre-warmed to at least room temperature. Never pipette directly onto the cells as this may dislodge them even after fixation, but apply solutions to the culture vessel border.
3. Possible steps to suspend the protocol: After fixation, samples can be kept in PBS for approximately 1 week in sterile conditions at 4°C. Because of possible epitope degradation, it is not recommended to store samples for longer periods or to store already-permeabilized cells before the staining procedure.
4. Sodium orthovanadate requires activation and depolymerization of the vanadate to inhibit phosphotyrosyl phosphatases (12).
5. After extraction, cell structures are vulnerable to mechanical challenges (e.g., too rigorous shaking or pipetting); hence, work very gently before fixation.
6. Too long or too harsh treatments with cell-extracting procedures will eventually also remove ECM proteins from the substrate. To fine-tune the timing, control the extraction progress occasionally by phase-contrast microscopy (10 × or 20 × objective).
7. Acetone and methanol are strongly hygroscopic. To prevent dehydration/rehydration artifacts, rehydrate stepwise and always pipette very gently.
8. It is generally possible to mix all primary antibodies (and secondary antibodies, respectively) in one vial for dilution when doing multiple labeling. Some antibody preparations tend to aggregate; such aggregates can be removed by one quick spin in a microcentrifuge and then pipetting only the supernatant onto slides or cells. Make sure to combine for the same sample only polyclonal antibodies that have been produced in different species (e.g., mouse, rabbit, rat, goat). Monoclonal antibodies from one species can be combined by using different isotypes (e.g., combine mouse IgG2a with mouse IgG1). Obviously, secondary antibodies must be specific against these isotypes and the spectra of the fluorochromes must be separable by the microscopy setup.
9. Alternatively to 3% BSA/PBS, 3% fat-free milk powder in PBS can be used for blocking of non-specific antibody binding. Some antibodies may not support the latter. Blocking solutions of 1% BSA or 1% milk powder in PBS can also be used to dilute primary and secondary antibodies.

10. Before applying antibodies, carefully dry a 20-mm diameter region around the sample using a 1,000 μL blue tip (5 mm of tip cut-off), connected to an aspiration vacuum or water-jet pump. When cells are grown on coverslips, dry thoroughly around the coverslip without letting the sample drop dry itself. The dry rim will prevent outflow of the antibody solution and working with 50 μL per 22 × 22 mm cover slip/region is possible. Proceed with one sample at a time; preparing a series before adding antibody dilutions bears the risk of sample dehydration artifacts. It is also possible to incubate with primary antibodies overnight at 4°C; this however increases the risk of sample drying. Most primary antibodies bind efficiently with incubations of no longer than 30 min at room temperature.
11. Tissue sections in particular tend to promote non-specific binding of secondary antibodies and a negative control is obligatory. Regenerating tissues and the immune system contain immune cells that can react with secondary antibodies, if these have been produced in the same species. In this case, it is recommended to use directly labeled primary antibodies.
12. If cells are grown on cover slips, put one drop (~100 μL) of mounting medium on a 76 × 26 mm microscope slide and then place the cell coverslip upside-down. If cells are grown on culture dishes and for stained tissues, put one drop of mounting medium on the sample and then place a clean coverslip upside-down. If too large a volume is used, the mounting medium layer will be too thick and can exceed the working distance of high-resolution objectives. Alternatively to PVA (13), other commercially available mounting media can be used; always verify compatibility with immunofluorescence. For short-term storage at 4°C, samples can be mounted in PBS or in 40% glycerol in PBS with the risk of sample drying.

Acknowledgments

Drs. G. Gabbiani (University of Geneva, Switzerland) and C. Heldin (University of Uppsala, Sweden) are acknowledged for providing antibodies and Dr. S. Werner (Eidegnössische Technische Hochschule Zürich, Switzerland) for providing mouse wound tissue sections. We are grateful to Dr. J.-J. Meister for providing laboratory facilities. This work was supported by the Swiss National Science Foundation, grant #3100A0-113733/1 (to BH).

References

1. Coons, A.H., Creech, H.J., and Jones, R.N. (1941) Immunological properties of an antibody containing a fluorescent group. *Proc. Soc. Exp. Biol. Med.* **47**, 200–205.
2. Coons, A.H., Kaplan, M.H., and Cooper, J.A. (1950) Localization of antigens in tissue cells: improvements in a method for the detection of antigen by means of fluorescent antibody. *J. Exp. Med.* **91**, 1–13.
3. Kohler, G. and Milstein, C. (1975) Continuous cultures of fused cells secreting antibody of predefined specificity. *Nature* **256**, 495–497.
4. Hinz, B., Phan, S.H., Thannickal, V.J., Galli, A., Bochaton-Piallat, M.L., and Gabbiani, G. (2007) The myofibroblast: one function, multiple origins. *Am. J. Pathol.* **170**, 1807–1816.
5. Darby, I., Skalli, O., and Gabbiani, G. (1990) Alpha-smooth muscle actin is transiently expressed by myofibroblasts during experimental wound healing. *Lab. Invest.* **63**, 21–29.
6. Dugina, V., Fontao, L., Chaponnier, C., Vasiliev, J., and Gabbiani, G. (2001) Focal adhesion features during myofibroblastic differentiation are controlled by intracellular and extracellular factors. *J. Cell. Sci.* **114**, 3285–3296.
7. Lazarides, E. and Weber, K. (1974) Actin antibody: the specific visualization of actin filaments in non-muscle cells. *Proc. Natl. Acad. Sci. USA* **71**, 2268–2272.
8. Osborn, M., Franke, W.W., and Weber, K. (1977) Visualization of a system of filaments 7–10 nm thick in cultured cells of an epithelioid line (Pt K2) by immunofluorescence microscopy. *Proc. Natl. Acad. Sci. USA* **74**, 2490–2494.
9. Brinkley, B.R., Fuller, E.M., and Highfield, D.P. (1975) Cytoplasmic microtubules in normal and transformed cells in culture: analysis by tubulin antibody immunofluorescence. *Proc. Natl. Acad. Sci. USA* **72**, 4981–4985.
10. Weber, K., Pollack, R., and Bibring, T. (1975) Antibody against tubulin: the specific visualization of cytoplasmic microtubules in tissue culture cells. *Proc. Natl. Acad. Sci. USA* **72**, 459–463.
11. Mason, D.Y., Micklem, K., and Jones, M. (2000) Double immunofluorescence labelling of routinely processed paraffin sections. *J. Pathol.* **191**, 452–461.
12. Gordon, J.A. (1991) Use of vanadate as protein-phosphotyrosine phosphatase inhibitor. *Methods Enzymol.* **201**, 477–482.
13. Lennette, D.A. (1978) An improved mounting medium for immunofluorescence microscopy. *Am. J. Clin. Pathol.* **69**, 647–648.
14. Skalli, O., Ropraz, P., Trzeciak, A., Benzonana, G., Gillessen, D., and Gabbiani, G. (1986) A monoclonal antibody against alpha-smooth muscle actin: a new probe for smooth muscle differentiation. *J. Cell. Biol.* **103**, 2787–2796.
15. Kanzaki, T., Olofsson, A., Morén, A., Wernstedt, C., Hellman, U., Miyazono, K., Claesson-Welsh, L., and Heldin, C.H. (1990) TGF-beta 1 binding protein: a component of the large latent complex of TGF-beta 1 with multiple repeat sequences. *Cell* **61**, 1051–1061.

Chapter 5

Double Immunohistochemistry with Horseradish Peroxidase and Alkaline Phosphatase Detection Systems

Vincent Sarrazy and Alexis Desmoulière

Abstract

We describe here a protocol optimized for formalin-fixed paraffin-embedded tissue sections that enables the detection of two antigens. This technique allows immunohistochemistry to be performed with detection systems allowing observation by light microscopy. This chapter discusses the choice of appropriate protocols as well as the choice of visualization systems.

In doing so, we provide examples of representative results obtained with this protocol and describe necessary controls; additionally, we discuss common problems associated with this methodology, and detail troubleshooting recommendations. Although this method has been optimized for liver sections, it may be applicable for performing double immunostaining in a variety of tissue samples.

Key words: Horseradish peroxidase, alkaline phosphatase, 3, 3′-diaminobenzidine.

1. Introduction

Abundant studies show that immunohistochemistry has become an important tool for both research and diagnostic purposes. In some situations, and to answer some questions in research, the relative localization of different targets is necessary on the one-tissue section. Multiple staining can be defined as the detection of two or more targets on one slide, thus increasing the information obtained from each section. For this purpose, it is necessary to combine different staining techniques or detection systems in one step or to perform sequential staining. Clearly, it is important to reduce hands-on time, and in this respect, sequential staining seems less than ideal. However, in our experience, the mixing of the primary antibodies and of the detection systems necessary to reduce the number of steps induces problems in many situations

T.D. Hewitson, I.A. Darby (eds.), *Histology Protocols*, Methods in Molecular Biology 611,
DOI 10.1007/978-1-60327-345-9_5,

which are sometimes difficult to solve. Therefore, in this chapter, we will describe a sequential staining method. Multiple staining methods also allow for a reduction in the number of tissue sections; this is particularly attractive when the size of the tissue sample available is small, for example, with human biopsy samples. Today, the development of tissue microarrays, which are a valuable tool for high-throughput molecular profiling of tissue specimens in order to investigate novel targets and potential disease biomarkers, still increases the desirability of developing multiple staining methods for co-localizing multiple targets. The main advantage of the multiple staining method is that this makes it possible to assess the topographical relationship of the target antigens, for example, to determine whether targets are present in different cells, in the same cell, or even in the same cellular compartment. Information can also be obtained on possible cell-to-cell spatial contacts of different cell types.

The use of a multiple fluorophore staining method allows the evaluation of the co-localization of different epitopes in the same location; however, immunofluorescence microscopy is not always available, and furthermore, by immunofluorescence, the general architecture of the tissue is not always well preserved or easily defined.

Obviously, similar information can also be obtained using single staining on serial sections. However, for this to be successful, the sections must be very thin to ensure that all structures or cells are present in the entire series of sections, rendering this job laborious and time consuming. Moreover, multiple staining allows the combination of techniques such as in situ hybridization and immunhistochemistry, giving information about a particular target both at protein level and DNA/mRNA level, although this can be difficult due to treatments required to maintain the quality of both nucleotides and epitopes. This chapter describes a protocol to perform multiple antibody staining, as well as the considerations that have to be made to ensure successful staining.

2. Materials

2.1. Fixation and Tissue Processing

1. 10% neutral buffered formalin, pH 7: Combine 100 mL of formalin (40% formaldehyde), 6.5 g dibasic sodium phosphate (anhydrous), 4.0 g monobasic sodium phosphate (monohydrate) in 900 mL distilled water. Mix, adjust to pH 7.0 and make up to 1 L.
2. Superfrost™ Plus (Menzel-Glaser, Braunschweig, Germany) or suitably coated glass microscope slides.
3. Ethanol.

4. Xylene.
5. Hydrophobic wax pen.
6. Mounting agent.

2.2. Antigen Retrieval

1. Sodium citrate buffer (10 mM sodium citrate, 0.05% Tween 20, pH 6.0): Dissolve 2.9 g of trisodium citrate (dihydrate) in 900 mL of distilled water. Adjust pH to 6.0 with 1 M HCl, add 0.5 mL of Tween 20, mix and make up to 1 L. Store this solution at room temperature for 3 months or at 4°C for longer storage.
2. Citrate buffer (10 mM citric acid, 0.05% Tween 20, pH 6.0): Add 1.92 g citric acid (anhydrous) to 900 mL of distilled water. Mix to dissolve and adjust to pH 6.0 with 1 M NaOH. Add 0.5 mL of Tween 20, mix well and make up to 1 L. Store this solution at room temperature for 3 months or at 4°C for longer storage.
3. Protease digestion solution: 0.1% trypsin (tissue culture grade) and 0.1% calcium chloride (w/v) in 20mM TBS (PH 7.6-8.0).

2.3. Alkaline Phosphate Staining

1. Tris-buffered saline (TBS).
2. Alkaline phosphatase anti-IgG of appropriate class (Dako, Glostrup, Denmark).
3. Alkaline phosphatase anti-alkaline phosphatase complex (APAAP) (Dako).
4. New fuchsin substrate buffer.
   i. Solution A: Mix 18 mL of 0.2 M 2-amino-2-methyl-1,3 propanediol (Sigma-Aldrich, St. Louis, MO, USA) with 50 mL 0.05 M Tris buffer, pH 9.7 and 600 mg sodium chloride. Add 28 mg levamisole (Sigma-Aldrich).
   ii. Solution B: Dissolve 35 mg naphthol AS-BI phosphate disodium salt (Sigma-Aldrich) in 0.42 mL N,N-dimethylformamide.
   iii. Solution C: In a fume hood, mix 0.14 mL of a 5% solution of New Fuchsin (Sigma-Aldrich) dissolved in 2 M HCl with 0.35 mL of freshly prepared 4% sodium nitrite (40 mg in 1 mL distilled water). Stir for 60s.

2.4. Immunoperoxidase Staining

1. Phosphate buffered saline (PBS).
2. Hydrogen peroxide (H_2O_2).
3. 0.05% avidin in PBS (w/v).
4. 0.005% biotin in PBS (w/v).
5. Normal serum/biotinylated secondary antibody – Vectastain™ kit (Vector Laboratories, Burlingame, CA, USA).
   i. Blocking serum: 150 μL stock normal serum in 10 mL of 1 × PBS.
   ii. Biotinylated secondary antibody: 50 μL species-specific biotinylated anti-IgG diluted in 10 mL of 1 × PBS.

6. Primary antibody of interest.
7. PBS/Tween: 1 × PBS with 0.5% v/v Tween 20 (Sigma-Aldrich).
8. Secondary antibody detection kits. ABC Elite™ Reagent (Vectastain™): Combine 100 μL Reagent A and 100 μL Reagent B in 5 mL of PBS. Reagent A and B are supplied in the kit. Prepare it 30 min before use. Similar detection kits are made by a number of manufacturers.
9. Diaminobenzidine-4HCl (DAB) enzyme substrate: Dissolve 6 mg DAB in 10 mL 0.05 M Tris buffer, pH 7.6. Add 0.1 mL 3% hydrogen peroxide. Mix and filter through a 0.2-μm syringe filter if precipitate forms. Solution is stable for 1 h at room temperature.

3. Methods

3.1. Tissue Preparation and Fixation

For most immunohistochemisry procedures, it is imperative that tissue does not dry out. Rapid processing of the tissue samples is important.

1. The area of interest should be selected and cut for fixation into blocks not more than 2 cm^2 by 4 mm thick. Tissue thickness is important because the fixative must penetrate tissue in order to be effective, and fast penetration is necessary.
2. Immerse in fixative. We use buffered formalin which is commonly used in pathology departments. Formalin should always be fresh (with time, formic acid forms and decreases the efficiency of the fixation, *see* **Note 1**), and fixative should be buffered to a pH of 7.0–7.6.
3. After fixation, tissue should be processed for paraffin embedding using routine paraffin processing usually starting at ethanol (50–70%). A period in phosphate buffered saline equivalent to the fixation time can be included to remove some of the residual aldehydes in the tissue.

3.2. Sectioning

1. Five-micron-thick paraffin sections of each sample are cut on a microtome (avoid thicker sections in which multiple layers of cells will be present, making interpretation difficult).
2. When cut, sections are floated on water and picked up on slides. Two to three sections could be mounted on charged Superfrost™ Plus slides (these commercially available slides come with a positive charge that attracts the negative charges of tissue proteins; alternatively, slides can be bought or prepared with a coating of gelatin or poly L-lysine). To avoid detachment during immunostaining processes, sections must be flat without ridges and ripples so that they adhere firmly to the slide.

3.3. Slide Processing

Slides of paraffin-embedded tissue should be dewaxed and rehydrated.

1. Remove paraffin from sections by immersing slides in two changes of xylene, 5 min each.
2. Hydrate in two changes of 100% ethanol for 3 min each, followed by 95 and 80% ethanol for 1 min each.
3. Rinse in distilled water.

3.4. Preliminary Treatments

Formalin or other aldehyde fixation forms protein cross-links that may mask the antigenic sites in tissue specimens, thereby giving weak or false negative staining for immunohistochemical detection of certain proteins. It is therefore often necessary to pre-treat sections by microwaving with antigen retrieval solution or incubating in a protease solution. The most suitable method and solution may need to be determined empirically.

3.4.1. Antigen Retrieval Solution

Treatment in a citrate-based solution is designed to break the protein cross-links, therefore unmasking the antigens and epitopes in formalin-fixed and paraffin-embedded tissue sections, thus enhancing staining intensity of antibodies. We describe here the heat-induced epitope retrieval.

1. Pre-heat steamer or water bath (*see* **Note 2**) with staining dish containing sodium citrate buffer (this buffer is commonly used and works perfectly with many antibodies; it gives very intense staining with very low background) or citrate buffer until the temperature reaches 95–100°C (1, 2).
2. Immerse slides in the staining dish. Place the lid loosely on the staining dish and incubate for 20–40 min. The optimal incubation time should be determined by the user.
3. Turn off steamer or water bath and remove the staining dish to room temperature and allow the slides to cool for 20 min.

3.4.2. Protease Digestion

Enzymatic epitope retrieval is defined as a method used to relax the rigidity of the protein structure that results from the cross-linkages of formalin fixation. Proteolytic enzymes are thought to cleave proteins at specific locations depending on the specificity of the enzyme. If cleavage points are in proximity to a cross-link, then the resulting effect is a relaxation of the rigid protein structure facilitating contact between the primary antibody and the corresponding antigenic determinant. Proteolytic digestion with trypsin compensates for the impermeable nature of non-coagulant fixatives by "etching" tissue and by exposing hidden determinants. Other proteolytic enzymes including bromelain, chymotrypsin, ficin and other proteases have been reported to restore immunoreactivity to tissue antigens with varying success.

Enzyme use may, however, also entail the risk of destroying some epitopes and having a deleterious effect on tissue structure and morphology.

1. Place slides into rack or other suitable container.
2. Incubate the slides for 10 min at room temperature in PBS with occasional agitation to thoroughly hydrate the tissue.
3. Pour off the PBS and incubate the specimen in the protease digestion solution for 5–30 min at room temperature depending upon the thickness and type of tissue (**Table 5.1**). Optimization will be necessary. Typical time is 10 min.
4. Stop the digestion by gently rinsing the slide under cold running water for 5 min, followed by incubation in TBS or PBS.

Table 5.1
Enzymatic reagents and their incubation conditions

Enzyme	Approximate activation temp or range in °Celcius	Incubation time in mins
Proteinase K	25–37	5
Trypsin	37	10
Pepsin	37	5–20
Pronase	25–37	30

3.5. Immunohistochemical Staining

Obviously, single staining protocols and multiple staining protocols show similarities, but multiple staining protocols are more complex. Indeed, some specific points must be considered. To avoid target or species cross-reactivity, complex protocols may be necessary. Spectral differentiation of stain colors may be difficult, especially if the targets are co-localized. If the expression of a target is rare, co-staining with a more abundant target can be difficult, and if colors are mixed due to a co-localization, the analysis is difficult. Then, in many cases, the best antibody concentration and the most appropriate visualization systems to distinguish the targets and to obtain the topographic information desired are necessary. Finally, chromogenic dyes can be used successfully for double staining; however, identifying co-localized targets may be a problem.

In each case, the visualization of antigen binding can be either peroxidase or alkaline phosphatase based (**Figs. 5.1 and 5.2**). In this protocol, we suggest detecting the first antigen with an alkaline phosphatase method, followed by an immunoperoxidase

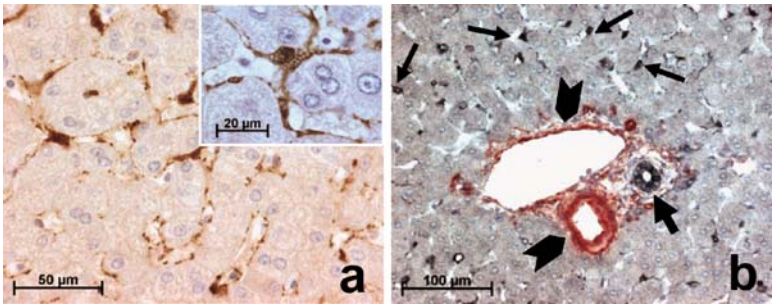

Fig. 5.1. Immunohistochemistry for cellular retinol-binding protein-1 (CRBP-1) expression (**a**) and double immunohistochemistry (**b**) for CRBP-1 (in *black, arrows*) and α-smooth muscle actin (in *red, arrowheads*) in normal liver. In the parenchyma, a strong expression for CRBP-1 is observed in hepatic stellate cells (**a**), underlining cytoplasmic processes along the sinusoids. Hepatic stellate cells expressing CRBP-1 present a typical stellate shape; at higher magnification, lipid droplets of hepatic stellate cells are clearly observed (*inset*). In a portal zone (**b**), double immunohistochemistry shows that biliary epithelial cells (*thick arrow*) express CRBP-1 (in *black*) and vascular smooth muscle cells (*arrowheads*) express α-smooth muscle actin (in *red*); in the parenchyma, hepatic stellate cells (thin arrows) express only CRBP-1 (in *black*). From (4), with the kind permission of the publisher. For double immunohistochemistry, sections were first incubated with anti-α-smooth muscle actin, Envision-alkaline phosphatase (Dako), and New Fuchsin (Dako). Then, the sections were incubated with 3% H_2O_2 in methanol to inhibit endogenous peroxidase. After heating by using a pressure cooker, the sections were incubated with anti-CRBP-1, Envision-horseradish peroxidase anti-rabbit, and detected with 1 mg/ml diaminobenzidine, 2.5 mg/ml nickel, and 0.1% H_2O_2 in 0.05 M Tris–HCl (pH 7.6) at room temperature. After washing with water, the sections were counterstained with hematoxylin and mounted with solvent-based mounting medium.

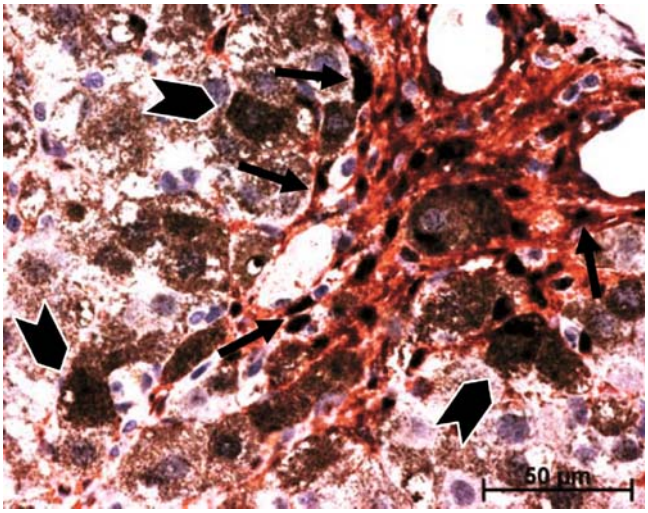

Fig. 5.2. Double immunostaining for α-smooth muscle actin (in *red*) and CRBP-1 (in *dark brown*) after carbon tetrachloride (CCl_4) treatment for 2 weeks. After CCl_4 treatment, the majority of α-smooth muscle actin-positive cells (elongated shape) strongly express CRBP-1 (*arrows*); a slight staining (compared with α-smooth muscle actin-expressing myofibroblastic cells) is observed in hepatocytes (rounded shape), although some hepatocytes close to the proliferating myofibroblasts present a strong staining (*arrowheads*). From (5), with the kind permission of the publisher.

method to detect the second antigen. However, if preferred, the two protocols can just as easily be applied in reverse. Usually, all procedures are conducted at room temperature (*see* **Note 3**).

3.5.1. Endogenous Enzyme Activity

False-positive results can occur because certain cell types have endogenous enzymes that can convert colorless chromogens to colored end products, independently from the antigen–antibody complexes. Endogenous alkaline phosphatase activity is encountered frequently in intestine (mucosa), kidney (proximal tubules), osteoblasts, endothelial cells, neutrophils, stromal reticular cells, lymphoid tissues, and placenta. Most forms of endogenous alkaline phosphatase activity can be quenched by including 5 mM levamisole in the chromogen substrate solution. The intestinal form of alkaline phosphatase is the exception and resists this treatment, but it can be quenched by treating the tissue sections with a weak acid wash prior to the application of the primary antibody (**Table 5.2**).

Table 5.2
Common endogenous enzyme-blocking reagents for horseradish peroxidase and alkaline phosphatase systems

Endogenous enzyme	Blocking agent
Horseradish peroxidise	Hydrogen peroxide
Alkaline phosphatase except intestinal alkaline phosphatase	Levamisole
Alkaline phosphatase including intestinal alkaline phosphatase	Weak acid (0.3 M HCl)

Likewise, endogenous peroxidase activity can be defined as any activity that results in the decomposition of H_2O_2. Such activity is a common property of all hemoproteins, such as hemoglobin, myoglobin, cytochrome, and catalases. Therefore, endogenous peroxidase activity is commonly found in red blood cells, granulocytes, eosinophils, monocytes, muscle, hepatocytes, and kidney. Peroxidase activity also may be encountered in tissue areas adjacent to vessels due to the diffusion of blood prior to fixation. Endogenous peroxidase activity is quenched by pre-treatment of sections (**Table 5.2**).

3.5.2. Detection of the First Antigen (Alkaline Phosphatase Labeling)

1. Outline sections with a hydrophobic wax pen to avoid antibody spreading and possible drying.
2. Incubate sections with the second primary antibody at appropriate dilution in primary antibody dilution buffer for 1 h at room temperature or overnight at 4°C (*see* **Note 3**).
3. Rinse with TBS for 3 × 2 min.

4. Incubate with second primary antibody at room temperature (*see* **Note 3**) for 2 h.
5. Wash twice in 1 × TBS, 5 min each.
6. Incubate for 10 min with a 1:50 dilution of alkaline phosphatase-conjugated anti-IgG antiserum (Dako; species specific for primary antibody).
7. Wash twice in 1 × TBS, 5 min each.
8. Incubate with alkaline phosphatase–anti-alkaline phosphatase (APAAP) (1:50 dilution) for 20 min.
9. Repeat steps 6–8 to amplify.
10. Prepare enzyme substrate. New Fuchsin is used with alkaline phosphatase to give a red end-product (*see* **Note 4**). Prepare a working solution by mixing Solutions A and B, then add Solution C, adjust to pH 8.7 with HCl. Mix well and filter onto slides.
11. Incubate for 10–20 min at room temperature until color develops. Monitor color development on wet slides by light microscopy. The color produced by New Fuchsin is insoluble in alcohol and other organic solvents, allowing for the specimens to be dehydrated before cover slipping.
12. Rinse with distilled water.

3.5.3. Washes and Additional Treatments

Depending on the second target, antigen retrieval and additional washes in TBS may be necessary.

3.5.4. Co-localization of a Second Antigen (Peroxidase Detection)

A number of different methods have been developed to localize binding of peroxidase labeled or biotinylated antibodies and to increase the intensity of staining. The system we describe here is based on the avidin–biotin method (*see* **Note 5**). Other perfectly suitable techniques are the peroxidase–anti-peroxidase (PAP) method (*see* **Note 6**) and polymer-based protocols (*see* **Note 7**).

1. Cover sections with peroxidase blocking solution to quench endogenous activity (**Table 5.2**). The most commonly used procedure for suppressing endogenous peroxidase activity in formalin-fixed tissue is the incubation of sections in 3% H_2O_2 for 5–10 min. Methanolic H_2O_2 treatment (11 parts 3% H_2O_2, four parts absolute methanol) for 20 min is also used but is not recommended for specimens where cell surface markers are to be stained. Endogenous peroxidase activity also can be suppressed by a mixture of sodium azide and H_2O_2. However, in most work with formalin-fixed tissue sections, the interpretation of specific staining is not usually impaired by endogenous alkaline phosphatase or peroxidase activity (if the formalin-fixed tissue is rich in blood-containing elements, then to quench endogenous peroxidase activity is

necessary). In the absence of formalin fixation (cell preparations or frozen sections), routine quenching of endogenous alkaline phosphatase and peroxidase is also necessary.

2. Rinse with PBS/Tween 20 (detergent can be used to minimize non-specific binding of reagents) for 3 × 2 min.
3. Incubate sections in avidin solution for 15 min followed by a brief rinse in PBS, and then incubate sections in biotin solution for 15 min (all at room temperature) (*see* **Note 5**).
4. Briefly rinse in PBS and continue the protocol with primary antibody.
5. Incubate sections with primary antibody at appropriate dilution in primary antibody dilution buffer for 1 h at room temperature or overnight at 4°C (*see* **Note 3**).
6. Rinse sections with PBS/Tween 20 for 2 × 2 min.
7. Cover sections with the enzyme solution and incubate for 3–10 min at room temperature. Depending on the enzyme method used, different substrates are available giving different colors. With horseradish peroxidase, 3,3′-diaminobenzidinetetrahydrochloride (DAB) is usually used (*see* **Note 8**). This produces a brown end product that is highly insoluble in alcohol and other organic solvents. Of the several metals and methods used to intensify the optical density of polymerized DAB, gold chloride in combination with silver sulfide appears to be the most successful (*see* **Note 9**). DAB has been classified as a potential carcinogen and therefore should be handled and disposed of with appropriate care.
8. Rinse with distilled water.
9. Counterstain in Harris' hematoxylin, dehydrate, and cover slip with either organic- or aqueous-based medium (*see* **Note 10**).

3.6. Controls

3.6.1. Specificity of Staining

Immunization with an antigen may result in the production of contaminating antibodies, or monoclonal antibodies may have cross-reacting or non-specific binding. Control sections from other organs (e.g., spleen, lymph node) and normal tissue are useful for confirming specificity of staining. Substitution of the antibody with non-immune serum or an irrelevant antibody from the same species at the same protein concentration is used to confirm antibody specificity. Wherever possible, serial sections are labeled using two different antibodies to the same immunogen. Specificity is established by confirming that staining patterns are similar. If available, antibodies can also be pre-absorbed with an excess of purified immunogen overnight, with the supernatant being used for immunoperoxidase staining at the same dilution as primary antibody.

Some matrix proteins, collagen in particular, are not highly immunogenic and give rise to low-titer antisera. This complicates the problem of non-specific binding.

3.6.2. Technical Controls

Specificity of the enzymatic reaction is established by confirming that staining is absent when the primary antiserum is omitted or a better control can be performed by substituting a non-specific immunoglobulin of the same isotype as the primary antibody.

4. Notes

1. Formalin is a saturated solution of formaldehyde, water, and typically another agent, most commonly methanol. In its typical form, formalin is 37% formaldehyde by weight (40% by volume), 6–13% methanol, and the rest water. Formaldehyde (H_2CO) belongs to a class of organic compounds called aldehydes, which are all obtained from the oxidation of alcohol, the most common being methyl alcohol or methanol (CH_3OH). During the oxidation process from methyl alcohol to formaldehyde, a certain level of formic acid is produced and will be found in formaldehyde solutions. Furthermore, since formaldehyde is basically unstable in its basic compound form, further oxidation even in storage is possible, thus producing additional levels of formic acid. To help stabilize formaldehyde, methanol is added to formalin.
2. Microwave or pressure cooker can be used as alternative heating source to replace steamer or water bath (3).
3. Because antigen–antibody reactions reach equilibrium more quickly at 37°C than room temperature, it would seem judicious to incubate the slide at this temperature. Furthermore, it should allow for greater dilution of the antibody and/or a shortened incubation time. However, it is not known whether an increased temperature promotes the antigen–antibody reaction selectively, more than the various reactions that give rise to background. In some cases, a temperature of 4°C is used in combination with overnight or longer incubations. Slides incubated for extended periods should be placed in a humidity chamber to prevent evaporation and drying of tissue sections. In all cases, avoid drying out the slides.
4. In addition to New Fuchsin substrate, the chromogens Fast Red and Fast Blue can be used and produce a bright red or blue end product, respectively. Both are soluble in alcoholic and other organic solvents, so aqueous mounting media must be used.

5. All avidin–biotin methods rely on the strong affinity of avidin or streptavidin for the vitamin biotin. Streptavidin (from *Streptomyces avidinii*) and avidin (from chicken egg) both possess four binding sites for biotin. The biotin molecule is conjugated easily to antibodies and enzymes. In the avidin–biotin complex (ABC) method, secondary antibodies are conjugated to biotin and function as links between tissue-bound primary antibodies and an avidin–biotin–peroxidase complex. In a similar method, the labeled streptavidin–biotin (LSAB) method also utilizes a biotinylated secondary antibody that links primary antibodies to a streptavidin–peroxidase conjugate. In both methods, a single primary antibody subsequently is associated with multiple peroxidase molecules, and because of the large enzyme-to-antibody ratio, a considerable increase in sensitivity is achieved compared to direct peroxidase-conjugate methods. Some tissues may bind avidin, biotinylated horseradish peroxidase or other biotin/avidin system components without prior addition of biotinylated antibody. This binding may be due to endogenous biotin or biotin-binding proteins, lectins, or non-specific binding substances present in the section. If a high background is present using the ABC reagents (or other avidin conjugate) in the absence of biotinylated secondary antibody, pre-treatment of the tissue with avidin, followed by biotin (to block the remaining biotin binding sites on the avidin) may be required.
6. The peroxidase–anti-peroxidase (PAP) method uses an immunological sandwich amplification and the enzyme peroxidase to obtain a signal. A polyclonal immune response is generated against the horseradish peroxidase enzyme which is an immunogenic protein. This antiserum is placed in solution with the enzyme so that immune complexes that form remain soluble. These complexes form with a molar ratio of two molecules of IgG to three molecules of enzyme. Furthermore, the enzymatic activity of the peroxidase is not affected by the attached immunoglobulins.
7. Polymer-based method. The presence of endogenous biotin in tissues can lead to significant background staining in certain tissues. Moreover, with the advent of heat-induced antigen retrieval, the recovery of endogenous biotin can appear as an unwanted artifact. Then, polymer-based immunohistochemical methods that do not rely on biotin have been introduced. These methods utilize a unique technology based on a polymer backbone to which multiple antibodies and enzyme molecules are conjugated. For example, a dextran backbone to which multiple enzyme molecules are attached is now available (EnVision™, Dako). This system contains secondary antibodies with anti-mouse Ig and anti-rabbit Ig specificity. Compared with other systems, the sensitivity of this

system is similar or even slightly greater in most cases. However, because of the large molecular size of the polymer conjugates, in some cases, accessibility to certain epitopes is restricted, presumably due to steric hindrance.

8. In addition to 3,3′-diaminobenzidinetetrahydrochloride (DAB), 3-amino-9-ethylcarbazole (AEC) which forms a rose–red end product, and 4-chloro-11-naphthol (CN) which precipitates as a blue end product, can be used. However, these end products are soluble in alcohol and other organic solvents. Therefore, the specimen must not be dehydrated, exposed to alcoholic counterstains (for example, Harris' hematoxylin), or cover slipped with mounting media containing organic solvents. Instead, an aqueous counterstain and mounting should be used. AEC is susceptible to further oxidation and, when exposed to excessive light, will fade in intensity. Storage in the dark is recommended. CN tends to diffuse from the site of precipitation.
9. Chromogen-enhancement treatments produce a color modification. DAB enhancers contain compounds that continue the DAB reaction, allowing for further enhancement. Enhancers should be applied immediately after incubation with the chromogen/substrate and water wash. Incubation times are determined by the individual laboratory, depending on the hue desired for the chromogen. The end product will be deeper dark brown color. Enhancers are usually heavy metals, which continue the reduction process with elements such as copper, silver, nickel, gold, or cobalt.
10. If a different substrate is used for alkaline phosphatase detection, for example NBT-BCIP, then only aqueous mountant may be used, as solvent-based mountants will degrade the substrate and remove it.

References

1. Shi, S.R., Chaiwun, B., Young, L., Cote, R.J., and Taylor, C.R. (1993) Antigen retrieval technique utilizing citrate buffer or urea solution for immunohistochemical demonstration of androgen receptor in formalin-fixed paraffin sections. *J. Histochem. Cytochem.* **41**, 1599–1604.
2. Kanai, K., Nunoya, T., Shibuya, K., Nakamura, T., and Tajima, M. (1998) Variations in effectiveness of antigen retrieval pretreatments for diagnostic immunohistochemistry. *Res. Vet. Sci.* **64**, 57–61.
3. Brown, R.W. and Chirala, R. (1995) Utility of microwave-citrate antigen retrieval in diagnostic immunohistochemistry. *Mod. Pathol.* **8**, 515–520.
4. Lepreux, S., Bioulac-Sage, P., Gabbiani, G., Sapin, V., Housset, C., Rosenbaum, J., Balabaud, C., and Desmoulière, A. (2004) Cellular retinol-binding protein-1 expression in normal and fibrotic/cirrhotic human liver: different patterns of expression in hepatic stellate cells and (myo)fibroblast subpopulations. *J. Hepatol.* **40**, 774–780.
5. Uchio, K., Tuchweber, B., Manabe, N., Gabbiani, G., Rosenbaum, J., and Desmoulière, A. (2002) Cellular retinol-binding protein-1 expression and modulation during in vivo and in vitro myofibroblastic differentiation of rat hepatic stellate cells and portal fibroblasts. *Lab. Invest.* **82**, 619–628.

Chapter 6

Retrogradely Transported Neuronal Tracers Combined with Immunohistochemistry Using Free-Floating Brain Sections

Emilio Badoer

Abstract

Immunohistochemistry has been used widely for the detection of proteins in brain tissue. The process can be performed on free-floating sections, but thicker sections are required than those required for processing on slides due to the "wear and tear" of the constant agitation that free-floating sections undergo. Immunohistochemical detection of molecules of interest such as receptors, neurotransmitters or intracellular signaling molecules is used to determine the distribution of these molecules in tissues. However, it is often of interest to simultaneously determine where the neurons under investigation may project and whether they are activated by a specific stimulus. In this chapter, we will focus on protocols that we use to combine the detection of (i) Fos-positive neurons to detect increased neuronal activity, (ii) nicotine adenine dinucleotide phosphate-diaphorase (NADPH-d) to detect nitric oxide synthase, and (iii) retrogradely transported tracers to identify specific projections.

Key words: Fos immunohistochemistry, NADPH-diaphorase, retrogradely transported neuroanatomical tract tracing, central nervous system.

1. Introduction

1.1. Immunohistochemistry

Immunohistochemistry has been used widely for the detection of proteins in brain tissue. The process can use sections that vary between 5 and 50 μm in thickness. Although immunohistochemistry can be used on sections that have been mounted onto slides, we describe in this chapter, a method where sections are not adhered to any support and are processed "free-floating" in the buffer. To accommodate the extra wear on the sections brought about by the processing, thicker sections (typically 40–50 μm) are used. It is also important that the sections are well fixed with an appropriate fixative (e.g., 4% paraformaldehyde) for the process to

T.D. Hewitson, I.A. Darby (eds.), *Histology Protocols*, Methods in Molecular Biology 611,
DOI 10.1007/978-1-60327-345-9_6,

be successful. Poorly perfused tissue does not withstand the "stress" of the constant agitation that is used in the "free-floating" conditions.

Immunohistochemical detection of molecules of interest such as receptors, neurotransmitters, or intracellular signaling molecules is an important technique to determine the distribution of those molecules in tissues including the central nervous system. It is often of interest, however, to differentiate the detected neurons even further. In particular, we are often interested in the areas in the central nervous system to which the neurons may project.

1.2. Tracing Neuronal Pathways

There are numerous neuronal tract tracing dyes (tracers) available that upon injection into specific sites are taken up into neurons and transported via axonal transport processes toward the soma (retrograde) or toward the terminal end of neurons (anterograde). Tracers such as biotinylated dextran, cholera toxin B subunit conjugated to gold, and horseradish peroxidase can be visualized by chemical processes and chromogens that allow visualization using light microscopy or even electron microscopy. There are also inherent fluorescent tracers such as fast blue, fluorogold, and diamidino yellow which can be visualized using fluorescent microscopy with lighting and filter conditions that allow the passage of excitation and emission spectra appropriate to each tracer. Additionally, nanospheres conjugated to fluorescent dyes have proved popular in recent years. We have many years of experience with RetroBeads™ from Lumafluor. These beads are available conjugated to rhodamine (red) or fluorescein (green) fluorophores and are effectively taken up by nerve terminals and transported retrogradely to the neuronal cell body. Once in the cell body, they appear to be stable for a considerable time (months) without apparent effect on neuronal viability (*see* **Note 1**). Maximum excitation and emission spectra for rhodamine are 530 and 590 nm, respectively, while for fluorescein the maximum excitation wavelength is 460 nm and the maximum emission spectrum is 505 nm.

1.3. Fos – A Marker of Increased Neuronal Activity

More than two decades ago, the first reports appeared suggesting that the protein product of the *c-fos* proto-oncogene (Fos) could be used to detect increased activity in neurons (1–4). Since then, Fos immunohistochemistry has become widely accepted and is used as a marker for an acute increase in neuronal activity in the central nervous system. Fos is a DNA-binding protein that functions as a component of the mammalian transcription factor, activator protein-1 (AP-1) (5, 6). AP-1 corresponds to several proteins related to Fos that form homodimeric and heterodimeric complexes through a leucine zipper structure. These proteins regulate the expression of many genes containing AP-1 DNA promoter sequence elements.

Proto-oncogenes are normal cellular genes that play a critical role in the regulation of cell growth and differentiation (3, 7). They are also responsible for encoding proteins that function as extracellular growth factors, cell surface receptors, G-proteins, protein kinases, hormone receptors, and transcription factors.

Fos expression can be increased in neurons by a variety of treatments. For example, seizure activity (chemically and electrically induced), kindling, brain injury (ischemic or mechanical), sensory stimulation (noxious, visual, olfactory or somatosensory), stress, learning, and the induction of long-term potentiation (LTP) result in increased expression of immediate-early genes (IEG) within the nervous system (1, 8–11). Activation of specific neurotransmitter receptors results in increased IEG expression within the central nervous system. The temporal profile of the IEG protein, Fos, shows maximum induction within 1 h of the commencement of the stimulus and falls to baseline within 4 h (7, 12–14).

The use of Fos to identify activated neurons following a stimulus is widely utilized because it is relatively easy to carry out using conventional immunohistochemical procedures to reveal Fos-positive neurons. However, only activated cell bodies express Fos; thus, neurons that are inhibited by upstream events will not express Fos. In addition, not all neurons are capable of expressing Fos. We have used this technique in conjunction with retrogradely transported tracers extensively in our work (12, 13, 15–21).

In this chapter we will focus on protocols that we use to combine the detection of (i) Fos-positive neurons, (ii) nicotine adenine dinucleotide phosphate-diaphorase (NADPH-d) to detect nitric oxide synthase, and (iii) retrogradely transported tracers. Generally speaking, the combination of immunohistochemistry and neuroanatomical markers allows us to determine the nature of the neurochemical content, receptor content, or intracellular signaling molecules of specific subgroups of neurons based on their neuroanatomical connections and their responses to specific physiological stimuli. In the specific case we focus on in this chapter, we detect nitrergic neurons projecting to the spinal cord that can be activated by an increase in body temperature.

2. Materials

2.1. Pre-operative Surgical Preparation

1. Anesthetic: Sodium pentobarbitone Nembutal™ (Boehringer Ingelheim, Sydney, NSW, Australia) or Diazepam (Pamlin™, Parnell laboratories, Alexandra, NSW, Australia) and Ketamine HCl (Ketamil™, Troy laboratories, Sydney, NSW, Australia).

2. Buscopan Compositum™ (consisting of a mixture of hyoscine-*N*-butyl bromide (12.5 mg/kg) and dipyrone (0.1 mg/kg); Boehringer Ingelheim)
3. Surgical instruments.
4. Surgical Suture.

2.2. Microinjection of Retrogradely Transported Neuroanatomical Tracers

1. Fine glass pipettes pulled to produce tips of 50 μm using a standard pipette pulling instrument.
2. RetroBeads™ (Lumafluor Inc., Durham, NC, USA). These beads are available conjugated to rhodamine (red) or fluorescein (green) fluorescent dyes (*see* **Note 2**).
3. Standard stereotaxic frames (Stoelting Company, Wood Dale, IL, USA or David Kopf Instruments, Tujunga, CA, USA).

2.3. Post-operative Treatment

1. Buprenorphine HCl 15 μg (Temgesic™, Reckitt and Coleman Pharmaceuticals, NSW, Australia).
2. Oxytetracyclin (200 mg/ml Terramycin™, Provet, Vic, Australia) or chloramphenicol, Chloromycetin™, Parke-Davis, Sydney, NSW, Australia).

2.4. Materials for Immunohistochemistry

1. Phosphate buffer (pH 7.4): A stock solution of 0.1 M phosphate buffer, pH 7.4, can be prepared by dissolving 77.3 g of $NaH_2PO_4.H_2O$ in approximately 2 L of distilled water and 203.7 g of Na_2HPO_4 in a similar volume of distilled water. Combine the two solutions and bring the total volume up to 20 L using distilled water. Store the phosphate buffer at 4°C.
2. Phosphate buffered saline (pH 7.4): 1 L of phosphate buffered saline is prepared by dissolving 8.87 g of NaCl in approximately 500 mL of phosphate buffer (pH 7.4). Add phosphate buffer to adjust the volume of the solution to 1 L.
3. Tris buffer (pH 7.4): Prepare 0.05 M Tris (hydroxymethyl) aminomethane buffer solution (pH 7.4) by dissolving 28.0 g of Trizma base ($C_4H_{11}NO_3$) in approximately 2 L of distilled water. Add 121.2 g of Trizma HCl ($C_4H_{11}NO_3.HCl$) to approximately 2 L of distilled water. Combine the two solutions and bring the total volume up to 20 L with distilled water. Store at 4°C.
4. 4% paraformaldehyde in 0.1 M phosphate buffer (pH 7.4): Make approximately 400–500 mL per rat. Heat approximately half the volume of 0.1 M phosphate buffer pH 7.4 required until the beaker is too hot to touch for more than about 3 s with a gloved hand (70°C maximum). In the fume hood, and wearing gloves, gradually add paraformaldehyde while stirring. Do not allow to boil. When paraformaldehyde is dissolved (approximately 5–10 min), place beaker in ice to cool to 45°C or less (approximately 0.5 h for each 0.5 L).

Filter solution through two Whatman number 1 filter disks (Whatman, Piscataway, NJ, USA). In a measuring cylinder, make up the filtered solution to the required volume with 0.1 M phosphate buffer pH 7.4.

5. Normal horse serum (NHS; Vector Laboratories, Burlingame, CA, USA).
6. Primary antibody: anti-c-fos (Ab-5), (Oncogene, Calbiochem, EMD Chemicals, Inc., Gibbstown, NJ, USA).
7. Secondary antibody: Vector Laboratories affinity purified biotinylated anti-rabbit IgG (*see* **Note 3**).
8. Extravidin™ (Sigma-Aldrich, St. Louis, MI, USA).
9. Diaminobenzidine HCl, (DAB) from (Sigma-Aldrich) (*see* **Note 4**). To prepare 100 mL of 0.05% DAB (3,3′-diaminobenzidine hydrochloride) solution dissolve 50 mg of DAB powder in approximately 80 mL of phosphate buffer (pH 7.4) at room temperature in a fume hood. Use 0.05 M Tris buffer, pH 7.4, if nickel ammonium sulfate intensification is required. Filter the solution (Whatman number 1 filter paper) and adjust the volume to 100 mL with phosphate buffer.
10. Nickel sulfate intensification solution $(NH_4)_2Ni(SO_4)_2$: (Sigma-Aldrich). Nickel intensification requires 40 mg of $(NH_4)_2Ni(SO_4)_2$ dissolved in the 0.05 M Tris buffer prior to filtration. This turns the normal brown reaction product of DAB to a black product.
11. Subbed slides: Place microscope slides into slide holders and soak in 80% ethanol for 3–4 h. Rinse the slides in distilled water. Soak for a further hour in distilled water. Prepare the subbing solution by adding 5 g of gelatin to 1 L of water. Heat this solution to 45°C and stir vigorously until the gelatin is entirely dissolved. Remove the solution from the heat source and add 0.5 g of chromium (III) potassium sulfate, $CrK(SO_4)_2.12H_2O$ and continuously stir until completely dissolved. Filter this solution (Whatman number 1 filter paper) while still warm. Dip the slides into the subbing solution and allow to dry overnight in an oven (60–70°C).
12. Cryogenic embedding medium (Tissue-Tek OCT™; Sakura Finetek, Torrance, CA, USA).
13. Cryostat.
14. DePeX™ (BDH Lab Supplies, Poole, UK) or solvent-based mountant.
15. Nicotine adenine dinucleotide phosphate-diaphorase (NADPH-d), (Sigma-Aldrich) (*see* **Note 5**).
16. Nitroblue tetrazolium (Sigma-Aldrich).

17. Triton X-100 (Sigma-Aldrich).
18. Xylene (Analar; Merck Pty Ltd, VIC, Australia).
16. Surgical instruments includings rongeurs and thin spatulae.
20. Microcentrifuge tubes.

3. Methods

3.1. Pre-operative Surgical Preparation

The procedures described below are for Sprague-Dawley rats (250–350 g).

1. For general anesthesia, administer (i) sodium pentobarbitone [60 mg/kg intraperitoneally (i.p.) initially and top-ups of 20 mg/kg i.p. every 50 min] (Nembutal™ 60 mg/mL) or (ii) diazepam, 5 mg i.p. followed by ketamine HCl, 100 mg/kg i.p.
2. Administer Subcutaneously Compositum™ at a dose of 0.3 mL/kg subcutaneous (s.c.) to prevent excessive salivation.
3. All surgical procedures should be performed under clean, aseptic conditions. Before commencement of the surgery, all instruments being used should be sterilized using a sterilizer or autoclave or soaked in 70% alcohol.

3.2. Injection of Retrogradely Transported Nanospheres

The following is an example of the techniques used to inject the retrogradely transported nanospheres into the brain or the spinal cord. All surgical procedures are performed under general anesthesia, e.g., Nembutal™ (60 mg/kg i.p.) followed by buprenorphine HCl, 15 μg intramuscularly (i.m), for post-operative analgesia. Antibiotic (oxytetracyclin 200 mg/kg or chloramphenicol 0.75 mg s.c.) is administered after surgery.

3.2.1. Brain

1. For injections into the brain, the head of the rat is placed into a stereotaxic apparatus and positioned so that the region to be injected can be accurately approached.
2. For injection into the rostral ventrolateral medulla (RVLM), for example, the head can be flexed approximately 45°C from the horizontal. The dorsal medulla is exposed after retraction of the overlying muscles and occipital membrane.
3. A small part of the occipital bone can be nibbled away to increase the exposure of the medulla. The pressor region of the RVLM can be located functionally by injecting 20 nL of 0.1 M L-glutamate using a glass micropipette.
4. The coordinates for the RVLM using this approach are 1.1–1.3 mm rostral to the calamus scriptorus, 2.0 mm lateral to the midline, and 3.3–3.5 mm ventral to the brain surface.

5. When the pressor site is located, the pipette can be withdrawn and refilled with rhodamine-tagged nanospheres (1:1 dilution with normal saline) and reinserted into the pressor region.
6. A unilateral injection of the tracer (250 nL) can be made into the brain over 10 min and the pipette is not removed for several minutes after completion of the injection.

3.2.2. Spinal Cord

As a second example, injections into the spinal cord can be made by making a 2–3 cm midline incision to expose the vertebrae.

1. A hole approximately 1.5 mm wide and 3 mm long can be made in the dorsal surface of the vertebrae and the underlying spinal cord exposed.
2. The left lateral sulcus is located and used as a landmark for pressure-injecting the rhodamine- or fluorescein-conjugated nanospheres (200 nL) (**Fig. 6.1**).
3. When the pipette is withdrawn, the muscles overlying the wound can be sutured together and the wound closed.

Using the different colored nanospheres injected into two separate regions means that it is possible to use both in the same animal and identify neurons with collaterals projecting to two separate regions of the central nervous system (22). We have also used fast blue and rhodamine-conjugated nanospheres and these work just as well (**Fig. 6.2**).

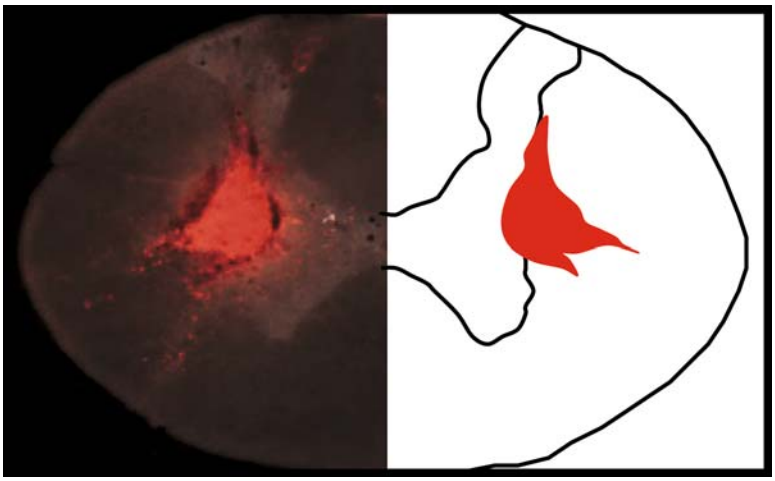

Fig. 6.1. A coronal section of a rat spinal cord showing a discrete injection site of rhodamine-conjugated nanospheres into the intermediolateral cell column (*left panel*). A schematic diagram of the spinal cord showing the anatomical localization of the injection site is shown in the *right panel*.

3.3. Post-operative Treatments

1. Buprenorphine HCl 15 μg is routinely administered i.p. for analgesia at the completion of surgery.
2. The antibiotic oxytetracyclin 200 mg/kg or chloramphenicol 0.75 mg is given s.c. to prevent infection.

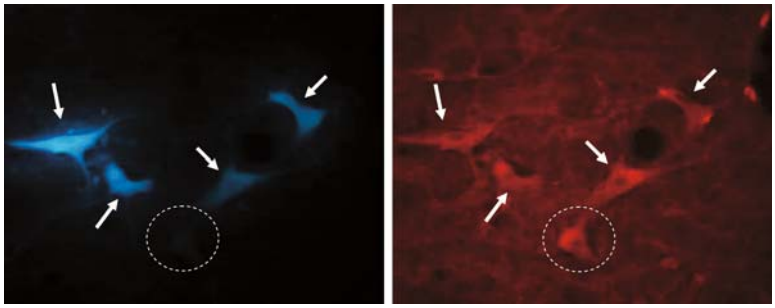

Fig. 6.2. Photomicrographs of a coronal section through the hypothalamus of a rat brain showing neuronal cell bodies labeled with the retrogradely transported neuroanatomical tracers fast blue (*left panel*) and rhodamine-conjugated nanospheres (*right panel*). Fast blue was injected into the spinal cord and the nanospheres were injected into the brainstem in the same animal. Neurons containing both tracers are shown by *arrows* and highlight neurons with collaterals projecting to both sites of injection. The *dashed circle* highlights a neuron containing only the nanospheres and indicates that this neuron does not send collaterals to the sites of injection.

3. At the completion of surgery, if there are signs of wheezing, Buscopan™ (0.015 mL/kg s.c.) can be re-administered.

3.4. Preparation of Tissue and Sectioning

Following the microinjections of tracer, the rats can be housed for a period of several days to months. Depending on the distance to be traveled by the tracer, a minimum time must be allowed for the tracer to be transported to the cell body of the neuron. We routinely allow at least 5 days for intracranial transport.

3.4.1. Perfusion Fixation

1. Histological processing of the animals can be performed after the animals are deeply anesthetized with sodium pentobarbitone (Nembutal™).
2. Perfuse transcardially with phosphate buffered saline (pH 7.4, 450 mL), followed by 4% paraformaldehyde in phosphate buffer (pH 7.4, 450 mL) and 4% paraformaldehyde in phosphate buffer containing 30% sucrose (pH 7.4, 250 mL).

3.4.2. Removing the Rat Brain and Spinal Cord

1. Make a midline incision of the skin extending approximately from between the eyes to the level of T2.
2. Scrape the muscle layers away to reveal the occipital bone and vertebrae. Using *rongeurs*, carefully remove the spongy part of the occipital bone to reveal the cerebellum and then the cerebral hemispheres and brainstem.
3. Peel back the duramater from the brain surface, and make two transverse cuts, one at the level of the olfactory bulb and the other at the caudal end of the medulla.
4. Using a long thin spatula, gently raise the brain and cut the optic nerves.

5. Carefully remove the brain from the skull and post-fix in the fixative solution, 4% paraformaldehyde, for 2 h and then place in phosphate buffer containing 20% sucrose overnight.
6. Similarly, the vertebrae can be cut away to expose the spinal cord which can be carefully removed and post-fixed for 2 h before placing into phosphate buffer containing 20% sucrose overnight. This prevents the tissue from cracking when it is frozen.

3.5. Fos Immunohistochemistry on Floating Sections

1. Cut brain into appropriate blocks, remove dura, freeze in OCT™, and cut using a cryostat (40 μm sections). In our laboratory, we collect every section serially and process appropriate sections.
2. Place the brain sections into containers and wash the sections three times, each 5 min in duration, with 0.1 M phosphate buffer pH 7.4.
3. Incubate with 10% NHS in phosphate buffer, pH 7.4, for 60 min at room temperature.
4. Place a maximum of five sections into a microcentrifuge tube and incubate with rabbit anti-c-fos antibody (1:20,000), NHS (2%), and Triton X-100 (0.3%) in phosphate buffer (pH 7.4) (total volume 400 μL) overnight at room temperature (*see* **Note 6**).
5. Wash again threes times, each 5 min in duration, in phosphate buffer pH 7.4.
6. In microcentrifuge tubes (400 μL per five sections), incubate with biotinylated anti-rabbit antibody (1:600) and NHS (2%) in phosphate buffer pH 7.4 for 60 min at room temperature.
7. Wash again three times, each 5 min in duration, in phosphate buffer pH 7.4.
8. In microcentrifuge tubes, incubate with Extravidin™ (1:400) in phosphate buffer pH 7.4 for 60 min at room temperature.
9. Wash again three times, each 5 min in duration, in phosphate buffer pH 7.4. Alternatively, use 0.05 M Tris buffer, pH 7.4, if nickel ammonium intensification is used and continue as indicated below.
10. Incubate with $(NH_4)_2Ni(SO_4)_2$ (0.04% w/w) and DAB (0.05% w/w) in 0.05 M Tris buffer for 10 min at room temperature on orbital shaker (75 rpm). Inclusion of nickel sulfate intensification solution turns the normal brown reaction product of DAB to a black product
11. Add 5 μL of 30% H_2O_2 which has been diluted 1:4 in 0.05 M Tris buffer. Note that the reaction time after the addition of H_2O_2 can be quite variable and the reaction needs constant monitoring. In our hands, the reaction usually takes approximately 6 min.

12. To stop the reaction, add excess 0.05 M Tris buffer. At this point, you can continue and perform the NADPH staining if required – *see* **Section 3.6** below. Otherwise complete the procedure by mounting the sections as indicated below.
13. Mount sections on subbed slides.
14. Place slides in fume hood, covered by aluminum foil, if rhodamine/fluorescein is present in sections, to dry overnight.
15. Wash slides in distilled water.
16. Allow to dry in fume hood.
17. Cover slip with DePeX™ or solvent-based mountant.
    See **Fig. 6.3** for an example of Fos-positive staining.

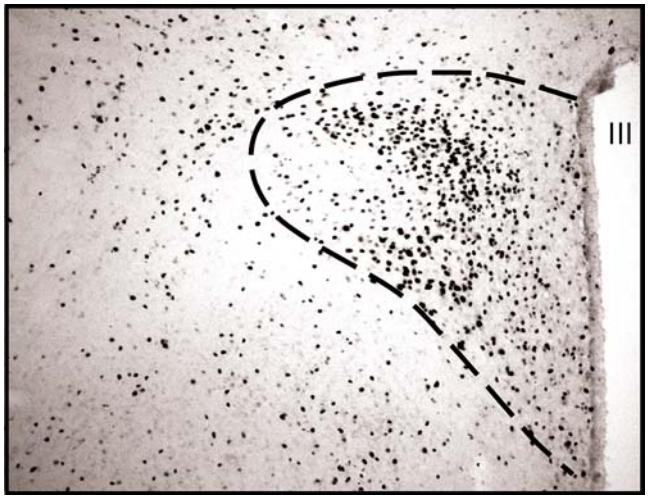

Fig. 6.3. A coronal section through the paraventricular nucleus of the hypothalamus (outlined by the *dashed line*) showing the distribution of Fos-positive nuclei (appear as *dots*). Note: Fos is localized to the nucleus since it forms part of the transcription factor AP-1 and is translocated to the nucleus of the cell. In this instance, the stimulus used to activate neurons was an intravenous infusion of hypertonic saline. Abbreviation: III, third brain ventricle.

3.6. Nicotine Adenine Dinucleotide Phosphate-Diaphorase (NADPH-d) Staining

1. Immediately after the immunohistochemistry procedure to detect Fos, the sections can be incubated in a mixture of 2.5 mg nitroblue tetrazolium, 10 mg β-NADPH, and 0.2% Triton X-100 in 10 mL of 0.05 M Tris buffer.
2. Allow the reaction to proceed for 30–40 min at room temperature (23°C).
3. Examine the intensity of staining before terminating the reaction with 0.05 M Tris buffer washes.
4. Mount the sections onto gelatin-subbed slides and allow to dry.
5. Briefly wash the sections by dipping the slides into distilled water and then re-dry.
6. Dip slides very briefly into xylene before placing a cover slip over the sections using DePex™ mounting medium.

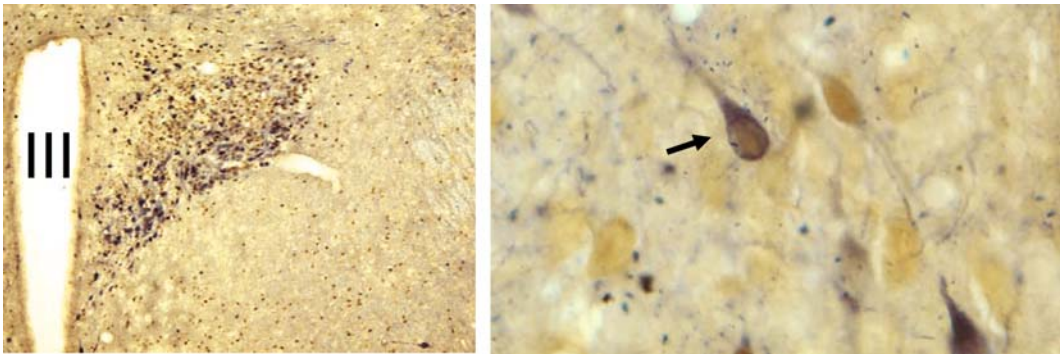

Fig. 6.4. Coronal section through the hypothalamic paraventricular nucleus of a rat brain. On the *left panel* is a low-power photomicrograph showing the distribution of Fos-positive nuclei (*brown*, *solid arrow*) and NADPH-diaphorase-stained neurons (*blue*). On the *right panel* is a high-power photomicrograph highlighting a double-labeled neuron (*arrow*) containing both markers. Abbreviation: III, third ventricle. For color figures see online version at www.springer.com.

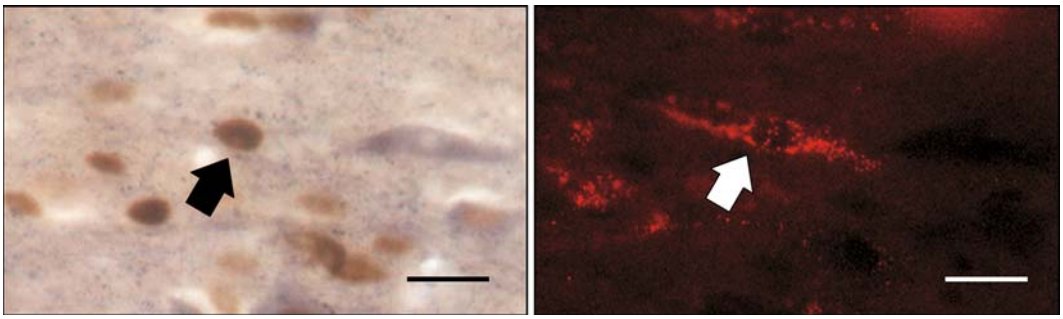

Fig. 6.5. High-power photomicrograph showing a Fos-positive nucleus (*left panel*) viewed using normal bright field lighting and the same view using fluorescent conditions to show rhodamine-conjugated nanospheres (*right panel*). The *arrowed* neuron is double labeled. Bar = 20 μm.

Figure 6.4 is an example of a section that has been processed for Fos-positive neurons and combined with NADPH-d staining. *See* **Fig. 6.5** for an example of staining for Fos in sections that also contain the retrogradely transported tracer, rhodamine-conjugated nanospheres. **Figure 6.6** shows a combination of triple stained sections where the tissue has been processed for Fos, NADPH-d, and contains the retrogradely transported tracer, rhodamine-conjugated nanospheres.

4. Notes

1. Retrogradely transported neuroanatomical tracers vary in their lifespan once injected into an animal. The nanospheres conjugated to rhodamine or fluorescein described in the present chapter have a relatively long lifespan in the animal.

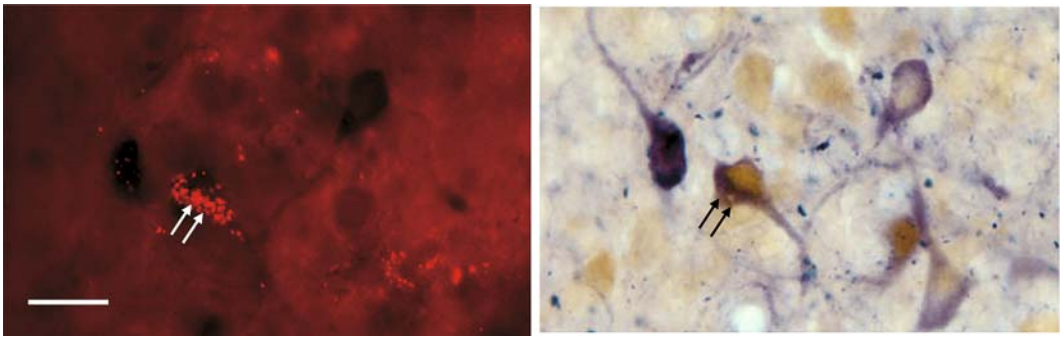

Fig. 6.6. Photomicrographs showing retrogradely labeled neurons (i.e., containing rhodamine) (*left panel*) viewed using fluorescent lighting conditions and the same view observed using bright field illumination showing neurons that have Fos-positive nuclei (*brown*) or NADPH-diaphorase staining (*blue*) or both (*right panel*). *Double arrows* highlight a neuron stained for all three markers. Bar = 20 μm. For color figures see online version at www.springer.com.

2. The nanospheres conjugated to rhodamine or fluorescein described in the present chapter should not be exposed to alcohol or glycerol as this degrades their fluorescence.
3. The secondary antibody must be directed against the IgG of the species in which the primary antibody was raised.
4. Diaminobenzidine HCl is carcinogenic. Ensure that appropriate personal protective clothing and mask are used. Use this compound in a fume hood. At the end of the procedures, neutralize diaminobenzidine with bleach before discarding. Wash all glassware that has come in contact with diaminobenzidine with bleach and then wash all glassware thoroughly.
5. Using 4% paraformaldehyde in conjunction with NADPH-diaphorase staining detects neuronal nitric oxide synthase.
6. Specificity of the primary antibody is important to ensure correct interpretation of the results. The most common way of assessing specificity is to utilize an excess of the protein against which the antibody is directed. Leaving out the primary antibody is also a common practice for specificity. The availability of knockout animals means that testing of the specificity of primary antibodies can be even more rigorously performed, as there should be no binding of the primary antibody in the appropriate knockout animal.

References

1. Sagar, S.M., Sharp, F.R., and Curran, T. (1988) Expression of C-fos protein in the brain: metabolic mapping at the cellular level. *Science* **240**, 1328–1331.
2. Hughes, P., Lawlor, P., and Dragunow, M. (1992) Basal expression of Fos, Fos-related, Jun, and Krox 24 proteins in rat hippocampus. *Mol. Brain Res.* **13**, 355–357.
3. Dragunow, M. and Faull, R. (1989) The use of c-fos as a metabolic marker in neuronal pathway tracing. *J. Neurosci. Methods* **29**, 261–265.

4. Hughes, P. and Dragunow, M. (1995) Induction of immediate-early genes and the control of neurotransmitter-regulated gene expression within the nervous system. *Pharmacol. Rev.* **47**, 133–178.
5. Curran, T., Abate, C., Baker, S., Kerppola, T., and Xanthoudakis, S. (1993) The regulation of c-fos – too much is never enough. *Adv. Second Messenger Phosphoprotein Res.* **28**, 271–277.
6. Kerppola, T. and Curran, T. (1995) Transcription – Zen and the art of Fos and Jun. *Nature* **373**, 199–200.
7. Curran, T. and Morgan, J.I. (1995) Fos: an immediate-early transcription factor in neurons. *J. Neurobiol.* **26**, 403–412.
8. Smeyne, R.J., Vendrell, M., Hayward, M., Baker, S.J., Miao, G.G., Schilling, K., Robertson, L.M., Curran, T., and Morgan, J.I. (1993) Continuous c-fos expression precedes programmed cell death in vivo. *Nature* **363**, 166–169.
9. Morgan, J.I. and Curran, T. (1989) Stimulus-transcription coupling in neurons: role of cellular immediate-early genes. *Trends Neurosci.* **12**, 459–462.
10. Morgan, J.I. and Curran, T. (1991) Proto-oncogene transcription factors and epilepsy. *Trends Pharmacol. Sci.* **12**, 343–349.
11. Morgan, J.I. and Curran, T. (1986) Role of ion influx in the control of c-fos expression. *Nature* **322**, 552–555.
12. Badoer, E., McKinley, M.J., Oldfield, B.J., and McAllen, R.M. (1992) Distribution of hypothalamic, medullary and lamina terminalis neurons expressing Fos after hemorrhage in conscious rats. *Brain Res.* **582**, 323–328.
13. Badoer, E., McKinley, M.J., Oldfield, B.J., and McAllen, R.M. (1993) A comparison of non-hypotensive and hypotensive hemorrhage on Fos expression in spinally-projecting neurons of the paraventricular nucleus and rostral ventrolateral medulla. *Brain Res.* **610**, 216–223.
14. Badoer, E. (1994) The cardiovascular role of the paraventricular nucleus. *Proc. Aust. Physiol. Pharmacol. Soc.* **25**, 20–25.
15. Badoer, E., Oldfield, B.J., and McKinley, M.J. (1993) Haemorrhage-induced production of Fos in neurons of the lamina terminalis: role of endogenous angiotensin II. *Neurosci. Lett.* **159**, 151–154.
16. Badoer, E., McKinley, M.J., Oldfield, B.J., and McAllen, R.M. (1994) Localization of barosensitive neurons in the caudal ventrolateral medulla which project to the rostral ventrolateral medulla. *Brain Res.* **657**, 258–268.
17. Oldfield, B.J., Badoer, E., Hards, D.K., and McKinley, M.J. (1994) Fos production in retrogradely labeled neurons of the lamina terminalis following intravenous infusion of either hypertonic saline or angiotensin II. *Neuroscience* **60**, 255–262.
18. McKinley, M.J., Badoer, E., Vivas, L., and Oldfield, B.J. (1995) Comparison of c-fos expression in the lamina terminalis of conscious rats after intravenous or intracerebroventricular angiotensin. *Brain Res. Bull.* **37**, 131–137.
19. Badoer, E., McKinlay, D., Trigg, L., and McGrath, B.P. (1997) Distribution of activated neurons in the rabbit brain following a volume load. *Neuroscience* **81**, 1065–1077.
20. Badoer, E. and McKinlay, D. (1997) Effect of intravenous angiotensin II on Fos distribution and drinking behaviour in the rabbit. *Am. J. Physiol.* **272**, R1515–R1524.
21. Badoer, E. and Merolli, J. (1998) Neurons in the hypothalamic paraventricular nucleus that project to the rostral ventrolateral medulla are activated by haemorrhage. *Brain Res.* **791**, 317–320.
22. Shafton, A.D., Ryan, A.R., and Badoer, E. (1998) Neurons in the hypothalamic paraventricular nucleus send collaterals to the spinal cord and to the rostral ventrolateral medulla in the rat. *Brain Res.* **801**, 239–243.

Chapter 7

High-Pressure Freezing, Chemical Fixation and Freeze-Substitution for Immuno-electron Microscopy

Christian Mühlfeld

Abstract

This chapter deals with tissue preparation for subsequent detection of molecules in biological samples using immunocytochemistry and transmission electron microscopy. The aim of these methods is to localize specific molecules at high resolution in order to identify their subcellular (or exact extracellular) localization. The methods are based on the use of antibodies or other affinity markers that bind specifically to a molecule of interest and a suitable detection system, e.g. a secondary antibody coupled to a gold particle of 5–15 nm size. Two different ways of sample preparation are described: (1) high-pressure freezing followed by freeze-substitution and immunogold labeling and (2) chemical fixation followed by freeze-substitution and immunogold labeling. Both methods have advantages and disadvantages that influence their utility in a given study design.

Key words: Immunocytochemistry, transmission electron microscopy, high-pressure freezing, freeze-substitution, colloidal gold.

1. Introduction

The aim of combining immunocytochemistry with transmission electron microscopy (immuno-TEM) is to identify the localization(s) of molecules in biological samples at a spatial resolution that cannot be achieved by immunocytochemical light microscopy. The general principles of immuno-TEM (**Fig. 7.1**) are easy to understand but the suitability of a particular method depends on the type of tissue, the antigen itself, fixation and other parameters. This chapter focuses on post-embedding techniques, where immunoreagents are applied to embedded and sectioned material. The chapter does not cover pre-embedding protocols, where immunoreagents are applied to cells and tissues before embedding and

T.D. Hewitson, I.A. Darby (eds.), *Histology Protocols*, Methods in Molecular Biology 611,
DOI 10.1007/978-1-60327-345-9_7,

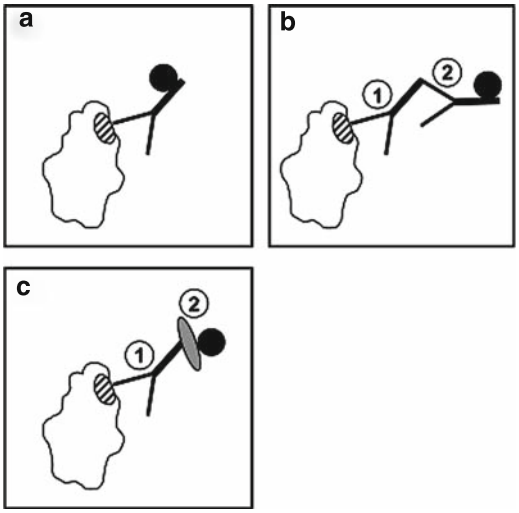

Fig. 7.1. Schematic of the principles of immunocytochemistry. A macromolecule (*lower left corner*) with a specific antigenic region (*hatched area*) is labeled in three different ways. (**a**) An antibody that specifically binds to the antigen of the macromolecule is coupled to a nanogold particle; the latter is visualized in the electron microscope. This method is named direct labeling method and is only rarely used. (**b**) A primary antibody (1) that binds specifically to the antigen of interest is detected by a secondary (2) antibody directed against the Fc region of the primary antibody and carrying a nanogold particle. This is called the indirect labeling method. (**c**) In contrast to **b**, the secondary antibody is replaced by protein **A** (2) coupled to a nanogold particle which binds to the Fc region of the primary antibody (1). This method is useful in various species (see **Note 8**).

sectioning. The use of cryosections for immunogold labeling is also not covered. For background and more comprehensive information, the reader may refer to the listed references (1–4).

Specimen fixation, or immobilization, is a crucial step in immuno-TEM since both morphology and antigenicity can easily be modified from that of the living state. It is therefore useful to aim for the best compromise between preservation of ultrastructure and antigenicity. Specimen immobilization can be obtained by rapid cooling (physical fixation) or by perfusion with/immersion in suitable fixatives (chemical fixation). At ambient pressure, physical fixation of a specimen in liquid nitrogen results in the development of ice crystals (5) that completely destroy the ultrastructure (**Fig. 7.2**). The outer few micrometers of the tissue block may be properly frozen in a state where ice crystals have not formed, but the slow freezing will result in destruction of the rest of the specimen. Using high-pressure freezing (HPF), however, it is possible to avoid the development of ice crystals by vitrifying water up to a depth of several hundred micrometers (**Fig. 7.3**). Detailed literature on the background of high-pressure freezing is available elsewhere (6–11).

After physical fixation, it is most convenient to transfer the specimen to a freeze-substitution (FS) unit for dehydration at low temperature and to embed it in a suitable resin. Chemical fixation

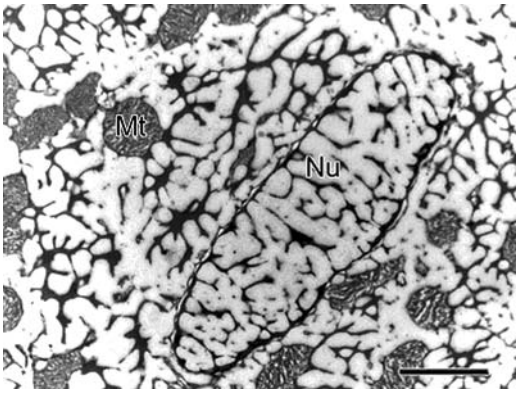

Fig. 7.2. A piece of adult rat myocardium was frozen under ambient pressure and subsequently freeze-substituted in 0.5% uranyl acetate in methanol and embedded in Lowicryl™ HM20. The ultrastructure of the cardiomyocytes is completely destroyed by ice crystals. Mt = mitochondrion, Nu = nucleus. Scale bar = 4 μm.

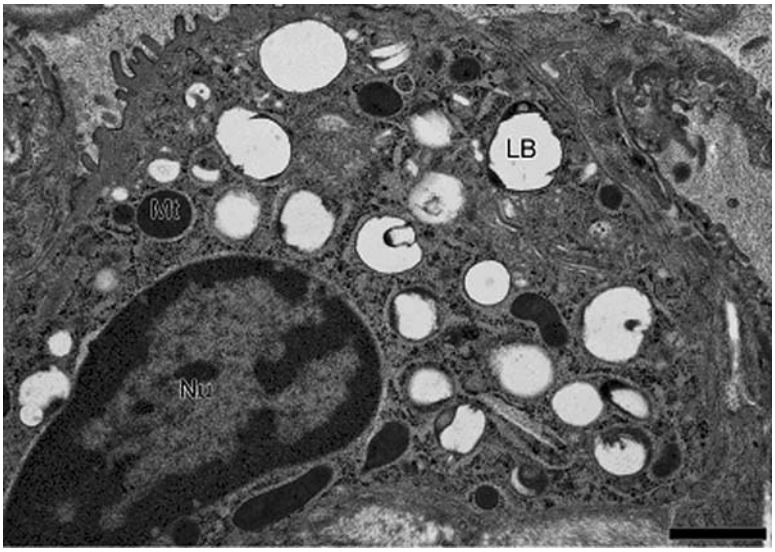

Fig. 7.3. A piece of adult rat lung was high-pressure frozen using a Leica EM PACT2. After freezing, the tissue was substituted in 1% osmium tetroxide in acetone and embedded in Epon. The figure shows an alveolar epithelial type-II cell with a well-preserved ultrastructure. However, the typical organelles of the type-II cells namely the surfactant storing lamellar bodies (LB) are not contained in the section, probably because they have been washed out during substitution. Mt = mitochondrion, Nu = nucleus. Scale bar = 1 μm. Figure reproduced with permission from (10).

using paraformaldehyde with or without small concentrations of glutaraldehyde is frequently used for immuno-TEM, and background information can be obtained from Griffiths (1) and Skepper (3). After chemical fixation, the sample can be cryoprotected, frozen by immersion in liquid nitrogen and then either sectioned

directly at low temperature (2, 12) or embedded by freeze-substitution. Cryoprotection of chemically fixed material can be performed by immersion in a high concentration of saccharose solution, in glycerol or in dimethyl formamide (**Fig. 7.4**). The

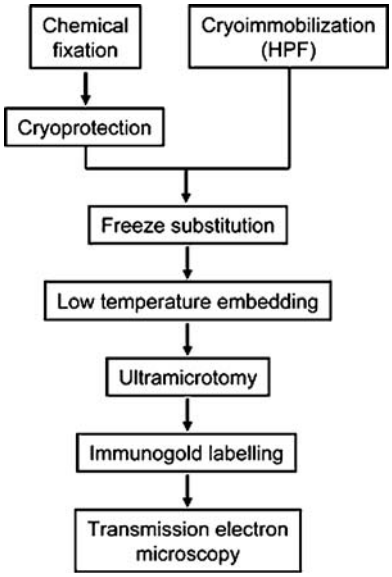

Fig. 7.4. Schematic summary of the workflow for post-embedding electron microscopic immunocytochemistry.

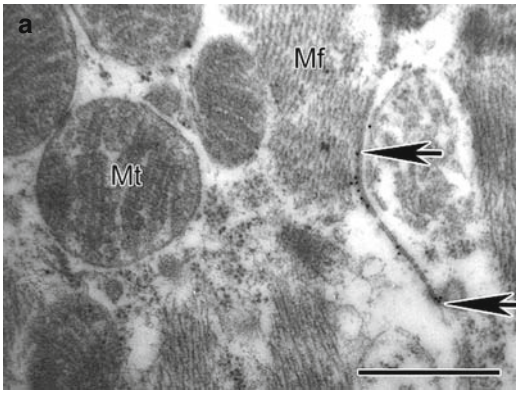

Fig. 7.5. Immunogold labeling of rat myocardium after high-pressure freezing and freeze-substitution using a primary antibody against connexin 43 and a secondary antibody coupled to 10 nm gold particles. (**a**) Connexin 43 hemichannels forming junctions between two cardiomyocytes. Between the *arrows*, the myocyte membranes are close enough for hemichannels to form gap junctions. The gold particle above the upper arrow is located in a section that is not closely attached to the membrane of the adjacent cardiomyocyte. This may either be the labeling of a hemichannel or non-specific labeling. (**b**) Annular gap junctions (AGJ) are intracellular organelles, probably related to the degradation of connexin molecules. In both figures, a strong immunogold labeling is shown with an acceptable ultrastructural preservation. Mt = mitochondrion, Mf = myofibrils. Scale bar = 500 nm.

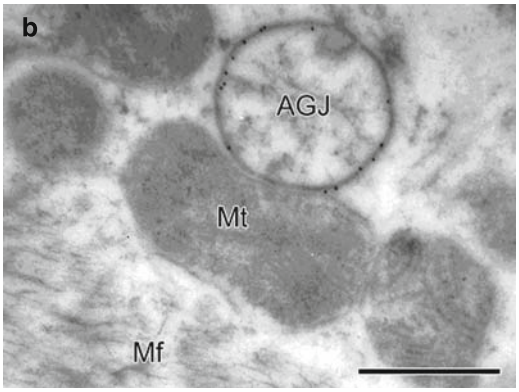

Fig. 7.5. (continued)

progressive lowering of temperature (PLT) method for preparing chemically fixed biological specimens for immunocytochemistry involves immersing specimens in increasing concentrations of ethanol while simultaneously cooling them until they reach a temperature of –50°C. They are then infiltrated with resin and polymerized at low temperature. Information on the PLT method is available elsewhere (13).

The present chapter provides information on two basic scenarios, viz. (1) high-pressure freezing and freeze-substitution (**Fig. 7.5**) and (2) chemical fixation and freeze-substitution (**Fig. 7.6**). These

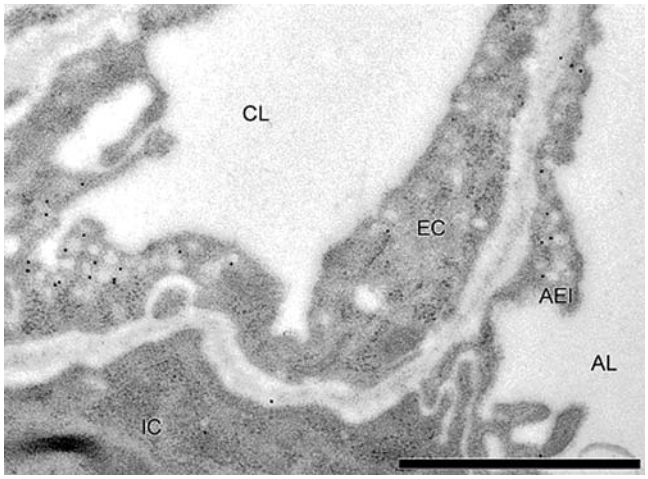

Fig. 7.6. Immunogold labeling of rat lung after chemical fixation and freeze-substitution using a primary antibody against caveolin-1 and a secondary antibody coupled to 10 nm gold particles. Strong labeling was observed for caveolae in capillary endothelium and alveolar epithelium. CL = capillary lumen; EC = endothelial cell; IC = interstitial cell; AEI = alveolar epithelial type-I cell; AL = alveolar lumen. Bar = 1 μm. Figure reproduced with permission from (10).

methods have been used in studies examining the localization of the gap junction protein connexin 43 in rat heart muscle throughout post-natal development (HPF+FS) (14) and the localization of surfactant proteins in the rat and human lung (chemical fixation+FS) (15, 16).

2. Materials

2.1. High-Pressure Freezing Followed by Freeze-Substitution

1. High-pressure freezing device including materials (e.g. Leica EM PACT 2, Leica Microsystems, Wetzlar, Germany; *see* **Note 1**).
2. Cryosubstitution unit (e.g. Leica AFS2).
3. Ultramicrotome for room-temperature thin sectioning.
4. Diamond knife.
5. Liquid nitrogen.
6. 1-hexadecene or 20% bovine serum albumin (BSA) as filler material (*see* **Note 2**).
7. 0.5% uranyl acetate in acetone or methanol (*see* **Note 3**).
8. 100% acetone or methanol (*see* **Note 3**).
9. Lowicryl™ HM20 (Polysciences Inc., Warrington, PA, USA).
10. 100 μm nickel mesh grids.

2.2. Chemical Fixation Followed by Cryosubstitution

1. Cryosubstitution unit (e.g., Leica AFS2).
2. Ultramicrotome for room temperature sectioning.
3. Diamond knife.
4. 4% paraformaldehyde and 0.1% glutaraldehyde in 0.2 M Hepes buffer.
5. 2.3 M saccharose (*see* **Note 4**).
6. 0.5% uranyl acetate in methanol (*see* **Note 5**).
7. 100% methanol (*see* **Note 5**).
8. Lowicryl™ HM20 (Polysciences Inc.).
9. 100-μm nickel mesh grids.

2.3. Immunogold Labeling

1. Parafilm™ (Pechiney Plastic Packaging Company, Minneapolis, MN, USA).
2. Ultrathin sections on grids (40–80 nm).
3. 0.02% glycine in Tris-buffered saline (pH 7.6) (*see* **Note 6**).
4. Blocking buffer (e.g. 5% fetal calf serum, 0.1% Tween 20, 0.25% bovine serum albumin in Tris-buffered saline) (*see* **Note 7**).
5. Primary antibody.

6. Secondary gold-coupled antibody or protein A gold (*see* **Note 8**).
7. Uranyl acetate.

3. Methods

The following procedures describe high-pressure freezing, cryosubstitution and immunogold labeling. Routine TEM procedures such as coating of grids or ultramicrotomy are pre-supposed and the reader may refer to descriptions of these methods in a recent book edited by John Kuo (*see* (4) for formvar coating grids and (17) for resin sectioning).

3.1. High-Pressure Freezing

1. Set-up the high-pressure freezing machine and check that it is working correctly before you prepare your first sample (*see* **Note 9**).
2. Make sure that you have all material for loading the HPF machine at hand: specimen carrier or tubes, microbiopsy transfer system (18), loading device, filler material etc. The equipment necessary for HPF is usually supplied with the machine by the manufacturer.
3. Prepare your tissue samples carefully using a stereomicroscope. Depending on the material you are working with, you may use a microbiopsy needle and transfer system for solid organs, cut small tissue pieces with a razor blade or scalpel (e.g. more delicate tissue such as the lung) or drag cell suspensions by capillary forces into tubes supplied by the manufacturer or cellulose capillary tubes (19) (*see* **Note 10**). Tissue samples should be approximately 200–300 μm in maximal diameter (*see* **Note 11**).
4. Before placing tissue pieces onto flat specimen carriers, it is recommended to dip the carrier into 1-hexadecene or 10–20% BSA dissolved in a medium compatible with the sample to make sure that the sample is surrounded by one of these media and no air or water surrounding the specimen fills the carrier well.
5. Transfer the flat specimen carrier into a pod and insert it into the cryofixation machine.
6. Start freezing process and check the pressure protocol.
7. Keep frozen specimen in liquid nitrogen until beginning of freeze-substitution (*see* **Note 12**).

3.2. Chemical Fixation

1. Prepare chemical fixation solution either immediately before use or use fixative stored at 4°C (*see* **Note 13**).

2. The most rapid and immediate chemical fixation is usually achieved by perfusion of the organ with the fixative. In the case of the lung, infiltration of fixative via the trachea is a suitable alternative. Immersion of tissue pieces in the fixative should only be used when biopsy material or cell cultures are used (*see* **Note 14**).
3. Before the beginning of freeze-substitution, the organ needs to be cut into small specimens (approximately 300–600 μm in diameter) (*see* **Note 15**).
4. Immerse specimens in 2.3 M saccharose for 24 h.
5. Place one specimen at a time onto a metal specimen pin (e.g. with a toothpick or similar) and drop into liquid nitrogen.
6. Keep the frozen specimen in liquid nitrogen until commencing the freeze-substitution protocol.

3.3. Freeze-Substitution

All steps including temperature control are performed automatically by the freeze-substitution unit if the program has been entered. Before adding solutions to the specimen, place the solutions in the cold chamber for temperature adjustment.

1. Set-up the freeze-substitution unit by filling with liquid nitrogen and starting the program at –90°C.
2. Transfer frozen specimens to a suitable test tube in the cold chamber of the freeze-substitution unit. High-pressure frozen samples are transferred on the flat specimen carrier. Make sure that the specimen is not warmed during the transfer.
3. Incubate with 0.5% uranyl acetate in methanol for 72 h (*see* **Note 16**).
4. Raise temperature of the FS unit slowly up to –45°C (e.g. 5°C/h).
5. Wash with methanol for 10 min × 3.
6. Separate high-pressure frozen sample from specimen carrier (*see* **Note 17**) and place specimen back in the test tube.
7. Incubate with methanol/Lowicryl™ HM20 1:1 first and then with methanol/Lowicryl™ HM20 1:2 for 2 h each (*see* **Note 18**).
8. Incubate with pure Lowicryl™ HM20 twice for 2 h.
9. Prepare small slips of paper for identification of the samples and place one label into each test tube (*see* **Note 19**).
10. Seal the test tubes in an air-tight fashion; this is not required in the new AFS, as nitrogen gas fills the chamber (*see* **Note 20**).
11. Place UV lamp above the specimens to induce polymerization of Lowicryl™ HM20 at –45°C.
12. Remove specimens from freeze-substitution unit after 2 days. Polymerization should be complete; however, further polymerization at room temperature is always recommended to

allow full polymerization and to remove the smell. The polymerized resin blocks should have a pink color when they are first removed from under the UV light (*see* **Note 21**).

13. Cut ultrathin sections from the tissue blocks using an ultramicrotome. The ultrathin sections should be mounted on nickel mesh grids and not stained for contrast (*see* **Note 22**).

3.4. Immunogold Labeling

Mount a clean piece of parafilm™ on your workplace by fixing it with a thin layer of water. water (*see* **Note 23**). The following steps are carried out by placing drops of the solutions on the parafilm™ and by floating the grids section-side down on the drops (*see* **Note 24**). Throughout the whole process, the section-side should remain hydrated and the other side should remain dry.

1. Float grids on a drop of 0.02% glycine in Tris-buffered saline for 15 min.
2. Float grids on a drop of blocking buffer for 30 min at room temperature. This step is used to mask non-specific binding sites.
3. Dilute primary antibody in the blocking buffer used in step 2 and centrifuge afterwards (*see* **Note 25**).
4. Prepare a new piece of parafilm™ in a wet chamber and float the grids section-side down on a drop of the diluted primary antibody solution for 10–60 min (*see* **Note 26**).
5. Wash grids 6 × for 5 min each with blocking buffer.
6. Dilute secondary antibody in blocking buffer.
7. Incubate grids with secondary antibody in a wet chamber for 60 min.
8. Wash grids 4 × for 5 min each with distilled water (*see* **Note 27**).
9. Contrast sections by floating grids on drops of 1% aqueous uranyl acetate.
10. Rinse sections with distilled water to remove superfluous uranyl acetate.
11. Dry sections for 4 h at 40°C.

4. Notes

1. There are a number of different commercially available high-pressure freezers, viz. the EM PACT2 (Leica Microsystems, Germany), the HPM 010 (Boeckeler Instruments Inc., USA), the HPM 100 (BAL-TEC AG, Liechtenstein, acquired by

Leica Microsystems) and the HPF Compact 01 (Engineering Office M. Wohlwend, Switzerland). The EM PACT and the HPM systems are the most frequently used high-pressure freezers which are described and compared in detail in (20) (HPM 010) (8), (EM PACT) and (11) (EM PACT2). The new generation of high-pressure freezers (HPM 100, EM PACT2) has several advantages compared to the older versions because they are smaller, consume less liquid nitrogen and are portable. The latter may be of substantial importance when the material cannot be brought to the freezing machine without inappropriate efforts. Another advantage is the availability of rapid transfer systems that allow a quick transfer (for example from live cell experiments) to the freezer facilitating correlative microscopic investigations.

2. During the freezing process, the biological specimen should not be surrounded by water because this will freeze before the sample in the core and delay the heat transfer out of the sample. The space between the specimen and the carrier needs to be filled with a medium that at best also cryoprotects the sample. While 1-hexadecene has been recommended for several years, it seems that 10–20% bovine serum albumin in a medium compatible with the specimen is currently the material of choice (11).
3. Although in the original paper on high-pressure freezing of rat myocardium methanol was used for substituting the high-pressure frozen samples (14), this does not seem to be the substitution medium of choice. As analysed by Monaghan et al. (21), incubation with methanol led to a rapid substitution and well infiltrated and polymerized tissue blocks but the specimens had an extracted appearance in the electron microscope with a lack of membrane and organelle detail. In that study, acetone provided the best ultrastructural preservation during substitution without loss of antigenicity as compared to methanol. Substitution with acetone can be performed with uranyl acetate (0.5%), osmium tetroxide (1%), glutaraldehyde (0.5%) or a combination of the three. Recent evidence suggests that small amounts of water (5%) added to polar substitution media may increase the ultrastructural preservation (22). The choice of a particular substitution medium for immunocytochemistry depends on the preservation of antigenicity and ultrastructure and may therefore vary between the antigens under investigation.
4. When chemically fixed samples are subjected to freeze-substitution, cryoprotection is essential. Infiltration of the tissue with 2.3 M saccharose acts as a strong

cryoprotectant avoiding the development of ice crystals. Other cryoprotectants include 10% glycerol in PBS or 1% dimethyl formamide.

5. If saccharose is being used for cryoprotection, then methanol is the best substitution medium. It is the only solvent among acetone, ethanol and methanol that can successfully substitute sucrose-containing tissues. The other solvents do not dissolve the sugar, and crystals are left in the tissue.
6. Instead of Tris buffer, PBS is the most widely used buffer for immunocytochemistry. PBS has the advantage that copper grids may also be used instead of nickel grids. The Tris–HCl buffer reacts with the copper to produce copper chloride precipitates on the grid and the sections. Therefore, when using Tris–HCl buffer, nickel grids have to be used.
7. If lectins or streptavidin–biotin systems are to be used, then fish skin gelatin at a concentration of 10% is a better blocker.
8. Besides secondary antibodies coupled to gold particles, the use of protein A gold or avidin–biotin systems is a good alternative. Protein A is a natural content of *Staphylococcus aureus* cell walls which binds primarily to the Fc regions of antibodies of a variety of species. If it is coupled to a gold particle, it is a useful detection system when primary antibodies from rabbit, mouse (IgG 2A, 2B) or rat (IgG 2C, IgG1) are used (*see* (1), p. 322). Similarly, the avidin–biotin reaction is a non-immunological detection system.

   If different macromolecules are to be labeled simultaneously, then the combination of an immunological with a non-immunological system may decrease the amount of non-specific staining. Differently sized gold particles distinguish between the molecules.
9. The pressure induced by the HPF device should be around 2,000 bar, a condition that is monitored and recorded by the EMPACT2 and the HPM 100. Before introducing the first tissue sample, it is strongly recommended to perform machine calibrations without tissue and make sure that the machine is working fine.
10. It is useful to learn the different techniques from someone who is experienced with HPF and practice them before using precious tissues. Both when using microbiopsy transfer systems or directly cutting a piece of tissue from an organ, damage can occur to the tissue due to pulling or crushing. This damage can result in morphological artefacts that may protrude to the core of the specimen. Specimen manipulations should be kept to a minimum to avoid post-mortem changes. A realistic aim is 30 s.
11. Use a stereomicroscope to prepare the specimen and make sure it is not too large. Otherwise, the quality of fixation decreases.

12. After freezing by the HPF machine, the pod with the specimen on the carrier directly drops into a liquid nitrogen bath. Afterwards, the specimen, including the carrier, have to be removed from the pod and can be stored within the liquid nitrogen bath in a device with several clearly identified molds. This allows freezing of a sequence of samples without transferring each sample independently to the FS unit. During any manipulation of the specimen, e.g., removing the specimen carrier from the pod, transferring the specimen to a cryotube for storage or to the pre-cooled FS unit, make sure that the specimen has no chance of warming. Use pre-cooled tools at all times.
13. There are many different fixation solutions and the one recommended in the materials section is a good starting point. It contains 4% paraformaldehyde that guarantees a rapid fixation and 0.1% glutaraldehyde that enhances the quality of ultrastructural preservation. Many antibodies work well on tissues fixed with this combination but some will not. Also, some antibodies will work well on tissues fixed at higher glutaraldehyde concentrations. The recommended fixative therefore can be used as a multi-purpose fixative for conventional and immuno-TEM. Each antibody–antigen system will have its own optimal preparation protocols that will have to be worked out empirically.
14. The most useful perfusion fixation techniques for different organs are discussed by Hayat (23).
15. When the results from the specimens are thought to be representative of the whole organ, the samples itself need to be representative of the whole organ, i.e., every part of the organ should have an equal chance of being chosen for further processing. An efficient way to do this is systematic uniform random sampling: The first position from which a sample is taken is chosen randomly, and from that starting position samples are taken at regular intervals (24, 25).
16. Uranyl acetate is a toxic agent that emits α and β radiation. More importantly, uranyl acetate is a heavy metal that can result in severe heavy metal poisoning. Preparation of and working with the methanol–uranyl acetate solution should be performed under a fume hood wearing gloves. Waste uranyl acetate solutions should be disposed of in accordance with the guidelines of the respective authorities.
17. Separating the specimen from the specimen carrier requires a suitable tool such as a fine needle or forceps or self-made devices. The author, for example, uses the edge of a razorblade tied to a toothpick. The new EM PACT specimen carriers are designed to be embedded in place, removing them only after the resin has been polymerized.

18. Lowicryl™ HM20 is member of a family of low-viscosity acrylic resins designed for low-temperature embedding. It can be obtained as a kit or as a pre-mixed preparation. The kit contains the substances crosslinker D (triethylene glycol demethacrylate), monomer E (ethyl methacrylate and *n*-hexyl methacrylate) and initiator C (benzoin methyl ether) which have to be mixed according to the manufacturer's manual. Contact with the components of Lowicryl HM20 as well as the final solution and its vapours should be minimized by working under a fume hood and wearing gloves. Lowicryls™ are known to cause allergies and skin irritations. The resin acts as a solvent that can rapidly penetrate latex gloves. More resilient gloves are recommended (even so, penetration can still occur!).
19. A good way to identify the resins used to embed specimens is to use unique identifier labels made with colored paper, with a different color for each resin.
20. Oxygen inhibits the polymerization process of Lowicryl™. Therefore, polymerization should take place in air-tight sealed test tubes. The workstation in the new AFS unit is filled with nitrogen gas which makes it unnecessary to seal the tubes in an air-tight fashion. However, mixing the resin using a stream of dry nitrogen gas is a good way to remove residual oxygen from the sample.
21. During polymerization, heat is generated in the sample. Since this may affect the antigenicity a suitably low temperature should be used and kept during the initial polymerization. The author usually uses a 48 h polymerization step at –45° C within the substitution unit followed by a few hours to days (depending on the weather) in the sunlight. Room-temperature polymerization can also be performed under the UV light of a laminar flow hood (biosafety hood).
22. The smaller the width of the mesh grid, the easier the immunogold labeling, but also the smaller the amount of tissue between the between the grid bars. Mesh grids of 100–200 μm can be regarded as a good compromise.
23. During the whole process of immunolabeling, it is extremely important to work cleanly. Each washing step may introduce "small" particles to the sample which appear as "large" pieces of dirt under the electron beam.
24. For the transfer from a large to a small drop and vice versa, use forceps. For the transfer between two large drops, use a wire loop.
25. It is recommended to work at primary antibody concentrations of 1–5 μg/ml. However, performing light microscopy before immuno-TEM will enable proper antibody titration to

be performed. This will make it possible to find the optimal concentration for each antibody on sections. Light microscopy immunocytochemistry can easily be performed on resin-embedded sections (13). In general, the best dilution to use for EM immunolabeling is the highest concentration with the lowest signal/noise ratio and has to be determined empirically. It has become a bad habit that many papers only report dilutions of the antibody without reporting the original antibody concentration.

26. As the reported method is an on-section labeling protocol, no time is needed for the antibody to diffuse through the section. Short incubation times with the antibodies may be sufficient to produce effective labeling. Most of the antibodies the author has worked with have delivered good results at room temperature. Sometimes, however, it is worth incubating at 4°C or for longer periods of time.
27. It is necessary to wash the sample with distilled water before staining with uranyl acetate because the remnants of phosphate from the blocking buffer might react with uranyl acetate resulting in large electron-dense precipitations.

Acknowledgements

The author wishes to thank Prof. Paul Webster, House Ear Institute, USA, for his very helpful suggestions to improve this manuscript and to Ms. Karola Michael for technical assistance with the preparation of the graphical work. The author is also thankful to the whole team of the EMBO Practical course "Electron microscopy and stereology in cell biology" held in Paris, September 2004, and the Faculty of Medicine, Georg-August-University Göttingen, whose research grant supported the study on high-pressure freezing of myocardium for immunolocalization of connexin 43.

References

1. Griffiths, G. (1993) *Fine structure immunocytochemistry*. Springer, Berlin, Germany.
2. Liou, W., Geuze, H.J., and Slot, J.W. (1996) Improving structural integrity of cryosections for immunogold labelling. *Histochem. Cell Biol.* **106**, 41–58.
3. Skepper, J.N. (2000) Immunocytochemical strategies for electron microscopy: choice or compromise. *J. Microsc.* **199**, 1–36.
4. Webster, P. and Webster, A. (2007) Cryosectioning fixed and cryoprotected biological material for immunocytochemistry. *Methods Mol. Biol.* **369**, 257–289.
5. Robards, A.W. and Sleytr, U.B. (1985) In: *Low temperature methods in biological electron microscopy*. Elsevier, New York.
6. Moor, H. (1987) Theory and practice of high pressure freezing. In: *Cryotechniques in biological electron microscopy*. Edited by

Steinbrecht R.A. and Zierold, K. Springer, Berlin, 175–191.

7. Shimoni, E. and Müller, M. (1998) On optimizing high-pressure freezing: from heat transfer theory to a new microbiopsy device. *J. Microsc.* **192**, 236–247.
8. Studer, D., Graber, W., Al-Amoudi, A., and Eggli, P. (2001) A new approach for cryofixation by high-pressure freezing. *J. Microsc.* **203**, 285–294.
9. Al-Amoudi, A., Norlen, L.P.O., and Dubochet, J. (2004) Cryo-electron microscopy of vitreous sections of native biological cells and tissues. *J. Struct. Biol.* **148**, 131–135.
10. Mühlfeld, C., Rothen-Rutishauser, B., Vanhecke, D., Blank, F., Gehr, P., and Ochs, M. (2007) Visualization and quantitative analysis of nanoparticles in the respiratory tract by transmission electron microscopy. *Part Fibre Toxicol.* **4**, 11.
11. McDonald, K.L., Morphew, M., Verkade, P., and Müller-Reichert, T. (2007) Recent advances in high-pressure freezing: equipment and specimen-loading methods. *Methods Mol. Biol.* **369**, 143–173.
12. Tokuyasu, K.T. (1973) A technique for ultracryotomy of cell suspensions and tissues. *J. Cell Biol.* **57**, 551–565.
13. Schwarz, H. and Humbel, B.M. (2007) Correlative light and electron microscopy using immunolabeled resin sections. *Methods Mol. Biol.* **369**, 229–256.
14. Mühlfeld, C. and Richter, J. (2006) High-pressure freezing and freeze substitution of rat myocardium for immunogold labelling of connexin 43. *Anat. Rec. A Discov. Mol. Cell. Evol. Biol.* **288**, 1059–1067.
15. Schmiedl, A., Ochs, M., Mühlfeld, C., Johnen, G., and Brasch, F. (2005) Distribution of surfactant proteins in type II pneumocytes of newborn, 14-day old, and adult rats: an immunoelectron microscopic and stereological study. *Histochem. Cell Biol.* **124**, 465–476.
16. Brasch, F., Schimanski, S., Mühlfeld, C., Barlage, S., Langmann, T., Aslanidis, C., Boettcher, A., Dada, A., Schroten, H., Mildenberger, E., Prueter, E., Ballmann, M., Ochs, M., Johnen, G., Griese, M., and Schmitz, G. (2006) Alteration of the pulmonary surfactant system in full-term infants with hereditary ABCA3 deficiency. *Am. J. Respir. Crit. Care Med.* **174**, 571–580.
17. Hagler, H.K. (2007) Ultramicrotomy for biological electron microscopy. *Methods Mol. Biol.* **369**, 67–96.
18. Vanhecke, D., Graber, W., Herrmann, G., Al-Amoudi, A., Eggli, P., and Studer, D. (2003) A rapid microbiopsy system to improve the preservation of biological samples prior to high-pressure freezing. *J. Microsc.* **212**, 3–12.
19. Hohenberg, H., Mannweiler, K., and Müller, M. (1994) High-pressure freezing of cell suspensions in cellulose capillary tubes. *J. Microsc.* **175**, 34–43.
20. McDonald, K. (1999) High-pressure freezing for preservation of high resolution fine structure and antigenicity for immunolabeling. *Methods Mol. Biol.* **117**, 77–97.
21. Monaghan, P., Perusinghe, N., and Müller, M. (1998) High-pressure freezing for immunocytochemistry. *J. Microsc.* **192**, 248–258.
22. Buser, C. and Walther, P. (2008) Freeze-substitution: the addition of water to polar solvents enhances the retention of structures and acts at temperatures around –60°C. *J. Microsc.* **230**, 268–277.
23. Hayat, M. (2000) *Principles and techniques of electron microscopy.* Cambridge University Press, Cambridge.
24. Mayhew, T.M. (2008) Taking tissue samples from the placenta: an illustration of principles and strategies. *Placenta* **29**, 1–14.
25. Mühlfeld, C., Nyengaard, J.R., and Mayhew, T.M. A review of state-of-the-art stereology for better quantitative 3D morphology in cardiac research. *Cardiovasc. Pathol.* (epub ahead of print) doi: 10.1016/j.carpath. 2008.10.015)

Chapter 8

Lectin Histochemistry for Light and Electron Microscopy

Su Ee Wong, Catherine E. Winbanks, Chrishan S. Samuel, and Tim D. Hewitson

Abstract

Glycoconjugates are complex macromolecules present in all tissues throughout the body. Depending on the tissue region, glycoconjugates express different carbohydrate moieties, which can be used to both distinguish cell type and examine changes in cell phenotype.

Although the periodic acid–schiff (PAS) method has long been used to study the distribution of glycoconjugates, the usefulness of the technique is severely limited by its lack of specificity. A more specific technique makes use of the affinity that plant-derived lectins have for different carbohydrate moieties in glycoconjugates. Binding of lectins is therefore a particularly useful adjunct to conventional histology when it is important to characterise cell type. These well-characterised binding patterns have proved particularly valuable in helping us understand the pathogenesis of kidney disease, changes in cell surface carbohydrates on normal and neoplastic cells in tumours, and blood group biology.

When labeled with a reporter molecule such as biotin or gold, lectin binding can be easily identified using light and electron microscopy. In this chapter, we describe the appropriate experimental protocols for light and electron microscopic examination of lectin binding, emphasising their utility in characterising nephron segments in renal disease.

Key words: Lectin, histochemistry, glycoconjugates.

1. Introduction

Glycoconjugates are complex macromolecules expressed ubiquitously throughout the body. Depending on the tissue region, individual cells often express quite different carbohydrate moieties. This expression is both indicative of cell type, and in the case of neoplasma, may change with pathogenesis.

Non-immunohistochemical techniques such as the periodic acid–schiff (PAS) method have previously been utilised to study the distribution of glycoconjugates, but these techniques are limited due to non-specificity (1). More specific techniques rely on the affinity that plant lectins have for the different carbohydrate moieties.

T.D. Hewitson, I.A. Darby (eds.), *Histology Protocols*, Methods in Molecular Biology 611,
DOI 10.1007/978-1-60327-345-9_8, © Humana Press, a part of Springer Science+Business Media, LLC 2010

Lectins are sugar-binding proteins which are specific for the sugar moieties found in glycoproteins and glycolipids. Because lectins interact with domains of complex oligosaccharides (2), they can be used to identify various carbohydrate moieties in a number of tissues throughout the body. This includes skin (3, 4), kidney (5–7), breast (8, 9), cervix (2) and components of the nervous system (10).

As elsewhere, different glycoconjugates are expressed by the various cells present in the vessels, tubules, interstitium and glomeruli of the kidney (5–7). Although there are no specific markers for renal tubules, the distribution of lectin binding sites can be used to characterise nephron segments (**Table 8.1**, **Fig. 8.1**).

Table 8.1
Renal staining characteristics of various lectins, classified by group (I–V) according to broad nephron specificity

Group	Lectin	Abbreviation	Origin	Nephron specificity	Carbohydrate specificity
I	*Tritium vulgaris*	WGA	Wheat germ	All segments of tubules	Neuraminic acid
	Concanavalin ensiformis	ConA	Jack bean	All segments of tubules	Glucose, mannose
II	*Phaseolus vulgaris* leukoagglutinin	PHA-L	Red kidney bean	Brush border of proximal tubules, thick loops of Henle	Galactose
	Phaseolus vulgaris erythroagglutinin	PHA-E	Red kidney bean	Brush border of proximal tubules	Galactose
III	*Dolichos biflorus*	DBA	Horse gram	Collecting ducts	Galactose
	Glycine max	SBA	Soybean	All segments of tubules except proximal tubules	Galactose
	Arachis hypogaea	PNA	Peanut	Distal convoluted tubules and collecting ducts	Galactose
	Sophora japonica	SJA	Japanese pagoda tree	Distal convoluted tubules and most collecting ducts	Galactose
	Bandeiraea simplicifolia I	BSL-I	Griffonia	Distal convoluted tubules and collecting ducts. Some medullary collecting ducts	Galactose, glucose

(continued)

Table 8.1 (continued)

Group	Lectin	Abbreviation	Origin	Nephron specificity	Carbohydrate specificity
IV	*Ulex europaeus* I	UEA-I	Gorse	Apical surfaces of medullary collecting ducts	Fucose
V	*Ricinus communis* I	RCA-I	Castor bean	Proximal tubules and medullary collecting ducts	Galactose

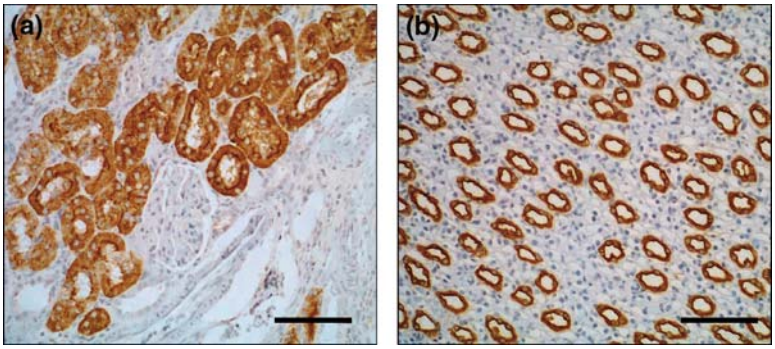

Fig. 8.1. Staining of paraffin-embedded rat kidney sections with biotinylated lectins. (**a**) Staining for PHA-L identifies proximal tubule cells while (**b**) DBA is a specific maker of collecting ducts in the renal papilla. Bar = 100 μm.

The study of lectin binding to these conjugates has therefore proven to be particularly valuable in helping us understand the mechanisms and processes involved in nephrotoxicity.

Interestingly, because the changes in cell morphology and function that lead to neoplasia involve changes to cell surface carbohydrates, lectins have also shown promise in the study of normal and neoplastic cells in tumours including those of the cervix, pituitary, pancreatic and breast carcinomas (2, 6, 11–14). The degree of lectin binding to neoplastic cells can also reflect the histological grade in many cases (10, 15).

The intestine represents another region where lectin staining could be advantageous due to its ability to differentiate between epithelial segments based on the presence of carbohydrate moieties which serve as transport molecules and receptors along the length of the intestine (16). For instance, the luminal surface of the caecum may be identified using Lens culinaris agglutin (LCA) as can regions within the colonic epithelium (16). Throughout the alimentary tract, peanut lectin conjugated to horseradish peroxidase (HRP) has also been shown to identify epithelial sites including at the ultra structural level where peanut lectin was localised to the central Golgi cisternae (17).

Finally, lectins can also identify blood group substances and have therefore been used to identify glycolipids and glycoproteins on red blood cells (18).

In each case, lectin binding is easily visualised directly through the use of lectins labeled with biotin, HRP, or in the case of electron microscopy, conjugated with gold particles.

2. Materials

2.1. Light Microscopy

2.1.1. Fixation and Embedding of Tissue

1. Neutral buffered formalin (Australian Biostain Pty Ltd, Taralgon, VIC, Australia)
2. Ethanol, laboratory grade.
3. Chloroform.
4. Paraffin wax, e.g. Paraplast™ (McCormick Scientific, St Louis, MO, USA).
5. Stainless steel embedding molds.
6. Tissue-embedding rings (Simport, Beloeil, Canada).

2.1.2. 3 APES-Coated Slides

1. Alkaline laboratory detergent, e.g. Pyroneg™ (Johnson Diversey, Smithfield, NSW, Australia).
2. Ethanol, laboratory grade.
3. 3-Aminopropyltriethoxysilane (APES) (Sigma-Aldrich, St. Louis, MO, USA) (see **Note 1**).
4. Acetone.
5. Slide racks.
6. Hair dryer.

2.1.3. Tissue Sectioning

1. Microtome.
2. Heated histological floatation bath.
3. Ethanol, laboratory grade.

2.1.4. Labeling

1. Phosphate buffered saline (1 × PBS), pH 7.4: Prepare 10 × stock solution by dissolving 80 g NaCl, 2 g KCL, 11.5 g disodium hydrogen orthophosphate (Na_2HPO_4-$12H_2O$) and 2 g potassium dihydrogen phosphate (KH_2PO_4) in 900 mL distilled water (d H_2O). Adjust to pH 7.4, and make up to 1 L. Dilute stock 1/10 for use.
2. Ethanol, laboratory grade.
3. HistoClear™ (National Diagnostics, Atlanta, GA, USA).
4. Xylene.

5. Biotinylated or horseradish peroxidase (HRP)-conjugated lectin of interest (**Table 8.1**) (e.g. Sigma-Aidrich).
6. Antibody diluent (e.g. Dako, Glostrup, Denmark).
7. Vectastain™ ABC Elite kit (Vector laboratories, Burlinghame, CA, USA): Prepare working solution by adding two drops of Reagent A to 5 mL of buffer; then add two drops of Reagent B to the mixture. Reagents A and B are supplies in the ABC Kit. Allow the Vectastain™ ABC Reagent to stand for at least 30 min before use. Diluted solutions are stable for 4 days at –4°C.
8. DAB: Add 1 DAB tablet (S-3000 Dako) to 10 mL 1 × PBS and filter the mixture when dissolved. Transfer 2 mL DAB chromogen solution to a clean container and add 1.5 μL 30% H_2O_2 (*see* **Note 2**).
9. Harris' hematoxylin.
10. Scott's tap water.
11. DePex™ (BDH, Poole, UK).
12. Cover slips.

2.2. Electron Microscopy

2.2.1. Preparation of Colloidal Gold

1. Gold chloride crystals (BDH).
2. 1% (w/v) trisodium citrate dehydrate in double dH_2O.

2.2.2. Conjugation of Colloidal Gold to Lectins

1. 0.1 M potassium carbonate.
2. 0.1 M HCl.
3. pH test paper.
4. Unconjugated lectin of interest (E.Y. Laboratories, San Mateo, CA, USA).
5. 0.005 M NaCl.
6. 5% polyethylene glycol (MW 20,000).
7. 0.45-μm syringe filter.
8. 5% glycerol in dH_2O (v/v) containing 0.05% polyethylene glycol (w/v) and 0.01% sodium azide (w/v).

2.2.3. Paraformaldehyde/ Glutaraldehyde Fixative

1. 0.1m phosphate buffer, pH 7.4: Combine 80mL 0.1m Na_2HPO_4 and 20mL NaH_2PO_4.
2. Prepare a solution of 2% paraformaldehyde (w/v) and 2.5% glutaraldehyde (v/v) in 0.1 M phosphate buffer, pH 7.4.
3. Wash buffer 7% w/v sucrose in 1 × PBS.

2.2.4. Embedding and Section Cutting

1. 0.1 M phosphate buffer, pH 7.4.
2. Sucrose.
3. Ethanol.

4. LR Gold resin™ (London Resin Company, Reading, Berkshire, UK).
5. Ultra violet (UV) light box for resin polymerisation.
6. Gelatin-embedding capsules.
7. 300-mesh nickel grids (TAAB Laboratories, Aldermaston, Berkshire, UK).

2.2.5. Post-embedding Labeling with Lectin–Gold Complex

1. BSA/PBS: 0.1% bovine serum albumin in 1 × PBS (w/v), pH 7.4.
2. Lectin–Gold complex.
3. Filter paper.
4. Laboratory squeegee bottle filled with dH_2O.
5. Saturated aqueous solution of uranyl acetate (BDH).

3. Methods

3.1. Light Microscopy

3.1.1. Preparation of Tissue

1. Fix small pieces of human or animal tissue in neutral buffered formalin overnight at room temperature.
2. Dehydrate tissue by passing through graded alcohols 50, 70, 90 and 100% × 2 (1 h each with rotation).
3. Pass tissue through 2 changes of 100% chloroform (1 h each with rotation).
4. Place tissue in molten paraffin-embedding wax (Paraplast™) and leave at 60°C for a minimum of 4 h.
5. Discard primary wax and replace with fresh wax. Infiltrate tissue with fresh wax for 4 h.
6. Embed tissue in wax using tissue embedding rings and stainless steel molds. Remove wax blocks from molds after cooling.

3.1.2. Coating Slides with APES

1. Immerse slides in an alkaline detergent overnight.
2. Rinse slides in running tap water.
3. Wash in sterile distilled water 2 × 5 min.
4. Wash in 95% ethanol 2 × 5 min.
5. Place slides in racks and air dry with a hair dryer.
6. Immerse in 2% solution of APES in acetone for 20 s.
7. Wash in dry acetone 2 × 5 min.
8. Wash twice in dH_2O.
9. Dry slides in a hot air oven (37°C) for 12 h.
10. Store covered at room temperature until use.

3.1.3. Tissue Sectioning

1. Fill the floatation bath with dH_2O and adjust to 50°C.
2. Using a microtome, cut 2-μm sections of the paraffin-embedded tissue.
3. Float the sections in 20% ethanol so that the sections can expand if they have become wrinkled.
4. Transfer sections to the heated floatation bath using an uncoated microscope slide.
5. Pick up sections on an APES-coated microscope slide.
6. Tap slide on bench to remove excess liquid and leave to dry in room temperature until the cutting has been finished.
7. Leave slides in a hot air oven (37°C) overnight.
8. Store slides covered at room temperature.

3.1.4. Labeling

1. De-wax sections and rehydrate fixed tissue by immersing sequentially in xylene (15 min), HistoClear™ (10 min × 1, 5 min × 1) and graded ethanol (100% × 2, 75%, 50%; 15 s each).
2. Wash twice in 1 × PBS for 5 min each.
3. Quench endogenous peroxidase activity for 20 min with 0.3% v/v H_2O_2 in methanol in humidified chamber.
4. Wash twice in 1 × PBS, for 5 min each.
5. Incubate with a 1:50 dilution of biotinylated or HRP-conjugated lectin diluted in antibody diluent for 1 h.
6. Wash twice in 1 × PBS, 5 min each.
7. Incubate for 15 min with ABC Elite Reagent (Vectastain™; Vector).
8. Prepare chromogen peroxidase substrate.
9. Wash twice in 1 × PBS, 5 min each.
10. Develop with DAB chromogen for 2–7 min.
11. Wash in tap water for 2 min.
12. Counterstain with Harris' hematoxylin for 15 s.
13. Wash in tap water for 5 min.
14. Dip 3 × in Scott's tap water,
15. Dehydrate in increasing grades of alcohol, HistoClear™ and xylene.
16. Mount with DePex™ and cover slip.

3.2. Electron Microscopy with Lectin–Gold Complex

For biologists, transmission electron microscopy (EM) offers unparalleled precision in examining ultrastructure. The technique has always been widely used in renal medicine where ultrastructural changes have diagnostic significance. Not surprisingly therefore, the use of lectin-staining techniques in EM offer an important tool in the study of renal pathology.

Lectin–gold complexes can be easily prepared in the laboratory and are useful cytochemical tools for localisation of specific carbohydrates in human or animal tissue.

3.2.1. Preparation of Colloidal Gold

Colloidal gold particles are made by chemical reduction of gold chloride (chloroauric acid) (19). In our experience, 15-nm diameter gold particles are suitable for labeling of kidney sections visualised with a transmission EM. The key step is the production of monodispersed gold particles, without aggregates.

1. An ampoule containing 1.0 g of gold chloride crystals is washed in 100% ethanol, dried and then broken. The broken ampoule, still containing the crystals, is immersed in 50 mL of double distilled water and stored in the dark as 2.0 % gold chloride solution.
2. Freshly prepare a gold solution by adding 0.5 mL of 2.0% gold chloride solution to 79.5 mL of double distilled water in a well-cleaned Erlenmeyer glass flask (*see* **Note 3**).
3. Heat the solution to 60°C in a hot water bath with stirring.
4. Freshly prepare the reducing mixture. Combine 4 mL of 1% trisodium citrate dehydrate and 16 mL of double distilled water for 15 nm colloidal gold particles.
5. Quickly add the reducing mixture to gold solution while stirring.
6. Wait until colloid formation is complete. The color of the solution will change progressively, with the color of the solution indicating particle size. In the case of 15 nm particles, wait for solution to turn bright red (approximately 1 h).
7. Heat the solution to boiling point when appropriate color is reached.

3.2.2. Preparation of Gold–Lectin Complex

1. The pH of the gold solution is adjusted to the isoelectric point for each lectin (**Table 8.2**) with 0.1 M potassium carbonate or 0.1 M hydrochloric acid. The pH should be measured by pH test paper such as litmus paper, since non-stabilised colloidal gold will plug the pore of a pH meter electrode.
2. 100–200 μg of lectin – enough to stabilise 5 mL colloidal gold solution in our experience – is weighed into a plastic container and dissolved in 0.1 mL 0.005 M sodium chloride. Add 5 mL of pH-adjusted colloidal gold solution to this. After 1–2 min, 0.15 mL 5% polyethylene glycol solution is added to stabilise the gold probe.
3. Crude lectin–gold complexes are purified and concentrated by ultracentrifugation. Spin 15-nm colloidal gold at 55,000 *g* for 40 min at 4°C on a 2.5 mL cushion of 5% glycerol containing 0.05% polyethylene glycol and 0.01% sodium azide, filtered through a 0.45-μm syringe filter.

Table 8.2
Isoelectric point of various lectins

Lectin	Abbreviation	Isoelectric point (pH)
Dolichos biflorus agglutinin	DBA	5.0
Griffonia simplicifolia IB (4)	GSI-B_4	5.0
Griffonia simplicifolia lectin II	GS-II	5.0
Helix pomatia agglutinin	HPA	7.4
Arachis hypogaea	PNA	6.3
Glycine max	SBA	6.1
Ulex europaeus	UEA-I	6.3

4. After centrifugation, about 6.5 mL of water-clear supernatant is carefully aspirated and discarded, leaving about 1 mL of condensed sol to be stored at 4°C until use.

3.2.3. Preparation of Tissue

1. Small pieces of human or animal kidney tissue are fixed in paraformaldehyde/glutaraldehyde for 2 h at 4°C (see **Note 4**).
2. Wash with 0.1 M phosphate buffer pH 7.4 containing 7% sucrose (wash buffer) × 3 for 10 min each.
3. Dehydrate in graded ethanol (50, 75, 95 and 100% v/v in dH_2O) for 10 min each.
4. Immerse tissue in equal parts of 100% ethanol and LR Gold™ resin for 30 min, followed by pure LR Gold™ resin for 30 min (*see* **Note 5**).
5. Embed tissue in fresh LR Gold™ and polymerise at 4°C for 24 h in sealed gelatin capsules using UV irradiation.
6. Use standard EM techniques to cut survey sections and select an area of interest.
7. Cut ultrathin sections (silver to pale gold in color) and collect on uncoated 300-mesh nickel grids (*see* **Note 6**).

3.2.4. Lectin–Gold Labeling

1. Pre-treat sections by placing grids, section down, on a drop of BSA/PBS for 5 min at room temperature (*see* **Note 7**).
2. Transfer to a drop of lectin–gold complex solution for 30 min at room temperature (*see* **Note 8**).
3. Wash 3 × by transferring consecutively to three drops of BSA/PBS (5 min each).

4. Use a wash bottle to rinse sections in running dH_2O.
5. Use filter paper to blot excess water, and leave to dry.
6. Stain sections with uranyl acetate for 5 min.
7. Examine using a transmission EM.

3.3. Interpretation

Results resemble the staining patterns routinely seen with immunoperoxidase and immunogold histochemistry. Lectin binding is visualised as brown chromogen, or in the case of gold-conjugates, as electron dense particles (*see* **Note 9**).

4. Notes

1. APES is harmful by ingestion, inhalation and if absorbed by the skin. Adequate ventilation and personal protective equipment are necessary.
2. DAB is moisture and light sensitive and should be stored appropriately. It is also a possible carcinogen and may act as an eye, skin and respiratory irritant. Adequate ventilation and personal protective equipment are necessary.
3. Many investigators suggest that only siliconised glassware should be used in making the gold solution, as unstable colloidal gold will adhere to the uncoated glass. In our experience, however, thoroughly cleaned non-siliconised glassware is adequate.
4. Choice of fixative is very important for carbohydrate binding. Periodate–lysine–paraformaldehyde (PLP), a fixative commonly used for histochemistry in EM, is unsuitable for lectin labeling as it is known to alter carbohydrate structure.
5. Although the epoxy resins have been used extensively as an embedding medium for conventional electron microscopy, they are not suitable for labeling lectins in electron microscopy since they exhibit low water adsorption and many hydrophobic structures, resulting in poor reaction with aqueous reagents. On the other hand, acrylic resins such as Lowicryl™ (Polysciences Inc., Warrington, PA, USA) and LR Gold™ (London Resin) have highly hydrophilic characteristics with good immunhistochemical labeling properties. Ultrathin sections permit full penetration of aqueous solutions. Furthermore, these acrylic resins are polymerised by exposure to ultraviolet light at low temperature; therefore, preservation of binding sites is much better than that in heat-cured epoxy resins (20).

6. The copper grids used in conventional electron microscopy can corrode in the labeling process. Nickel grids are therefore routinely used in post-embedding labeling.
7. In each step, nickel grids should be mounted section face down onto a drop of reagent. Before transferring to next reagent, use a piece of filter paper to gently blot the reagent from the edge of the grid. Drying the grid adequately is essential to reduce background and prevent the grid from sinking into the reagent.
8. Appropriate dilution of lectin–gold complex depends on the stock concentration. As a guide, red colored lectin–gold complexes should be diluted to a pale pink color for use.
9. Although different lectins are highly specific to different carbohydrate moieties, the various carbohydrates may themselves be expressed by multiple cell types. In these circumstances, a combination of lectins may be necessary. For instance, in the kidney, since *Arachis hypogaea* agglutinin (PNA) stains both distal tubules and collecting ducts, and *Dolichos biflorus* agglutinin (DBA) stains collecting ducts, those tubules staining for PNA only are distal tubules.

References

1. Spicer, S.S., Schulte, B. A., Thomopoulos, G. N., Parmley, R. A., and Takagi, M. (1979) Cytochemistry of complex carbohydrates by light and electron microscopy. Available methods and their application. In *Connective Tissue Diseases* (Wagner, B.M, Fleichmaier, R., and Kaufman, N., eds.). Williams and Wilkins, Baltimore, MD. pp. 163–211.
2. Byrne, P., Williams, A., and Rollason, T. (1989) Studies of lectin binding to the human cervix uteri: I. Normal cervix. *Histochem. J.* **21**, 311–322.
3. Ookusa, Y., Takata, K., Nagashima, M., and Hirano, H. (1983) Distribution of glycoconjugates in normal human skin using biotinyl lectins and avidin-horseradish peroxidase. *Histochemistry* **79**, 1–7.
4. Skerrow, C. J. and Bell, C. M. (1985) Lectin-binding abnormalities in the stromal and epithelial components of basal cell carcinoma. *Br. J. Cancer* **52**, 117–122.
5. Holthofer, H., Virtanen, I., Pettersson, E., Tornroth, T., Alfthan, O., Linder, E., and Miettinen, A. (1981) Lectins as fluorescence microscopic markers for saccharides in the human kidney. *Lab. Invest.* **45**, 391–399.
6. Truong, L.D., Phung, V.T., Yoshikawa, Y., and Mattioli, C.A. (1988) Glycoconjugates in normal human kidney. A histochemical study using 13 biotinylated lectins. *Histochemistry* **90**, 51–60.
7. Kanwar, Y.S., Rosenzweig, L.J., and Jakubowski, M.L. (1983) Distribution of de novo synthesized sulfated glycosaminoglycans in the glomerular basement membrane and mesangial matrix. *Lab. Invest.* **49**, 216–225.
8. Leathem, A., Dokal, I., and Atkins, N. (1983) Lectin binding to normal and malignant breast tissue. *Diagn. Histopathol.* **6**, 171–180.
9. Walker, R. A. (1984) The binding of peroxidase-labelled lectins to human breast epithelium. I – Normal, hyperplastic and lactating breast. *J. Pathol.* **142**, 279–291.
10. Wang, X. C., Kochi, N., Tani, E., Kaba, K., Matsumoto, T., and Shindo, H. (1989) Lectin histochemistry of human gliomas. *Acta Neuropathol.* **79**, 176–182.
11. Byrne, P., Williams, A., and Rollason, T. (1989) Studies of lectin binding to the human cervix uteri: II. Cervical intraepithelial neoplasia and invasive squamous carcinoma. *Histochem. J.* **21**, 323–336.
12. Hori, T., Nishiyama, F., Anno, Y., Adachi, S., Numata, H., Hokama, Y., Muraoka, K., and Hirano, H. (1985) Difference of lectin

binding sites of secretory granules between normal pituitary and adenoma cells. *Acta Neuropathol.* **66**, 177–183.

13. Raedler, A., Schmiegel, W. H., Raedler, E., Arndt, R., and Thiele, H. G. (1983) Lectin-defined cell surface glycoconjugates of pancreatic cancer cells and their nonmalignant counterparts. *Exp. Cell Biol.* **51**, 19–28.
14. Walker, R. A. (1984) The binding of peroxidase-labelled lectins to human breast epithelium. III – Altered fucose-binding patterns of breast carcinomas and their significance. *J. Pathol.* **144**, 109–117.
15. Boland, C. R., Chen, Y. F., Rinderle, S. J., Resau, J. H., Luk, G. D., Lynch, H. T., and Goldstein, I. J. (1991) Use of the lectin from Amaranthus caudatus as a histochemical probe of proliferating colonic epithelial cells. *Cancer Res.* **51**, 657–665.
16. Alroy, J., Goyal, V., Lukacs, N. W., Taylor, R. L., Strout, R. G., Ward, H. D., and Pereira, M. E. (1989) Glycoconjugates of the intestinal epithelium of the domestic fowl (Gallus domesticus): a lectin histochemistry study. *Histochem. J.* **21**, 187–193.
17. Sato, A. and Spicer, S. S. (1982) Ultrastructural visualization of galactosyl residues in various alimentary epithelial cells with the peanut lectin-horseradish peroxidase procedure. *Histochemistry* **73**, 607–624.
18. Nakajima, M., Ito, N., Nishi, K., Okamura, Y., and Hirota, T. (1988) Cytochemical localization of blood group substances in human salivary glands using lectin-gold complexes. *J. Histochem. Cytochem.* **36**, 337–348.
19. Hughes, D. (2005) Preparation of colloidal gold probes. *Methods Mol. Biol.* **295**, 155–172.
20. Roth, J. (1984) The protein A-gold technique for antigen localization in tissue sections by light and electron microscopy. In *Immunolabelling for Electron Microscopy* (Polak, J.M. and Varndell, I.M., eds.). Elsevier Science Publishers, Amsterdam, The Netherlands, pp. 113–121.

Chapter 9

Duplex In Situ Hybridization in the Study of Gene Co-regulation in the Vertebrate Brain

Raphael Pinaud and Jin K. Jeong

Abstract

We describe here a high-sensitivity in situ hybridization protocol, optimized for fresh-frozen brain sections, that enables the detection of two transcripts, at single cell resolution. Riboprobes directed against two mRNAs of interest are synthesized with nucleotides tagged with different haptens (digoxigenin- or biotin-UTP), via in vitro transcription, hybridized simultaneously to brain sections, and independently detected through immunocytochemistry. Sequential detection of each probe involves peroxidase-mediated precipitation of tyramide-linked fluorophores of separate emission wavelengths. In addition, we demonstrate how classic non-fluorescent chromogens, such as 3,3′-diaminobenzidine, can be successfully combined with fluorescence-based detection, to yield reliable detection of two transcript populations. We provide examples of representative results obtained with this protocol and describe necessary controls. Additionally, we discuss common problems associated with this methodology, and detail troubleshooting recommendations. Although this method has been optimized for brain sections, it may be useful to detect two mRNA species in a variety of tissues.

Key words: Duplex in situ hybridization, dISH, double fluorescence in situ hybridization, dFISH, non-radioactive riboprobes, digoxigenin, biotin, tyramide, 3, 3′-diaminobenzidine.

1. Introduction

The study of gene regulatory events has uncovered fundamental aspects of the anatomical and functional organization of brain circuits in both health and disease states (1–9). Much of our current knowledge of these processes has resulted from the analysis of gene expression patterns via histological approaches in brain sections. In this regard, in situ hybridization, a technique that allows for the detection of specific native mRNAs via complementary binding of tagged DNA or RNA probes, has been a leading

T.D. Hewitson, I.A. Darby (eds.), *Histology Protocols*, Methods in Molecular Biology 611,
DOI 10.1007/978-1-60327-345-9_9,

approach used to study brain gene regulation. Unlike other powerful RNA analytical methods, such as northern blots, in situ hybridization in brain sections preserves tissue morphology thereby enabling mRNA expression studies at single-cell resolution (10–13). Traditionally, radioactively labeled probes (e.g., ^{33}P or ^{35}S) have been used; however, more recent approaches involving hapten-based tags have provided a non-radioactive alternative for in situ hybridization protocols (13–16). In addition to minimizing procedural safety concerns, in situ hybridization with hapten-labeled probes offers significant methodological advantages over radioactive protocols, including the ability to simultaneously detect multiple mRNA species in single cells. This is typically accomplished by co-hybridizing probes labeled with different haptens (most commonly digoxigenin, fluorescein, and biotin) and, subsequently, detecting each of them separately via immunocytochemical detection through independent peroxidase-coupled antibodies and chromogenic substrates. Furthermore, this approach can be combined with fluorescent nuclear markers such as DAPI or Hoechst.

In this chapter, we describe a duplex in situ hybridization protocol (dISH) that allows for the simultaneous detection of virtually any two transcripts in fresh-frozen brain sections. We have used this protocol to study gene co-regulation in the context of determining the neurochemical and functional properties of sensory circuits in the vertebrate brain (13, 17, 18). Even though our over-arching goal is to apply this method to study the co-regulation of brain gene expression programs, it is expected that our protocol will be useful for research conducted in a wide array of applications and preparations.

2. Materials

2.1. Tissue Preparation and Sectioning

1. Surgical dissecting instruments.
2. Embedding molds.
3. Cryogenic embedding medium (e.g., Tissue-Tek™ OCT, Sakura Finetek, Torrance, CA, USA).
4. Freezing bath consisting of a dry ice/ethanol paste.
5. Cryostat.
6. Superfrost™ Plus slides (Thermo-Fisher Scientific, Fremont, CA, USA).

2.2. Riboprobes and Hybridization

1. Diethyl pyrocarbonate (DEPC)-treated water: For RNase-free water, add 1 mL of DEPC (*see* **Note 1**) to 1 L of deionized water and stir overnight at room temperature in a fume hood. Autoclave the solution on the following day.

2. Suitable restriction endonuclease enzyme with accompanying buffer.
3. QIAquick™ PCR Purification Kit (Qiagen, Valencia, CA, USA).
4. 10 × Tris–acetate EDTA buffer (TAE): To prepare a 10 × stock, mix 48.4 g Tris base with 11.42 mL glacial acetic acid and 20 mL 0.5 M EDTA (pH 8.0) and make up to 1 L.
5. Formaldehyde (*see* **Note 1**).
6. Appropriate RNA polymerases (we mainly use T3 and T7 polymerase).
7. Probe labeling buffer stock (also known as Ribo12 buffer): Prepare 1 mL of a 5 × stock with a final concentration of 50 mM DTT, 200 mM Tris–HCl, 30 mM $MgCl_2$, 50 mM NaCl, 10 mM spermidine. Store at –20°C.
8. Tris–HCl (stock; 1 M, pH 7.5).
9. $MgCl_2$ (stock; 1 M).
10. Spermidine (stock; 1 M).
11. DIG RNA labeling mix (Roche Diagnostics, Madison, WI, USA).
12. Biotin RNA labeling mix (Roche Diagnostics).
13. RNasin ribonuclease inhibitor (Promega, Madison, WI, USA).
14. Bovine serum albumin (BSA) (stock; 20 μg/μL, store at –20°C).
15. Dithiothreitol (DTT) (stock; 20 μg/μL, store at –20°C).
16. Sephadex™ G-50 (Amersham, Pittsburgh, PA, USA).
17. EDTA, 0.5 M, pH 8.0.
18. Column washing buffer: 50 mL with a final composition of 10 mM Tris–HCl, 0.15 M NaCl, 0.05 mM EDTA, 50 μg/μL tRNA, and 0.1% SDS in 50 mL DEPC-treated water. Store at room temperature.
19. Column-blocking buffer: 50 mL with a final composition of 10 mM Tris–HCl, 50 mM NaCl, 0.1 mM EDTA in DEPC-treated water. Store at room temperature.
20. Wax sealing film (e.g., Parafilm™).
21. Sodium dodecyl sulfate (SDS) (stock; 20%).
22. Transfer (t)RNA: Prepare a stock solution of 20 μg/μL (t)RNA (Invitrogen, Carlsbad, CA, USA) and store at –20°C.
23. 10 × MOPS solution (VWR, Lutterworth, Leicestershire, UK; toxic substance).
24. 4% Paraformaldehyde (w/v) fixative: In a fume hood, add 8 g of paraformaldehyde (VWR) (*see* **Note 1**) to 150 mL of DEPC-treated water and heat to 60°C while stirring. Ensure

that the temperature does not exceed 65°C. Add two drops of 10 M NaOH. When the solution becomes clear, adjust the pH to 7.4 and allow it to cool down. Subsequently, dissolve 0.44 g of sodium phosphate monobasic and 2.4 g of sodium phosphate dibasic anhydrous into the solution, and bring volume up to 200 mL using DEPC-treated water.

25. Phosphate buffered saline (PBS).
26. Ethanol.
27. NaOH (stock; 10 M).
28. Triethanolamine.
29. Acetic anhydride (*see* **Note 1**).
30. Sodium chloride, sodium hydrogen phosphate EDTA buffer (SSPE) (stock; 20 × , VWR).
31. Formamide (VWR) (*see* **Note 1**).
32. PolyA (stock; 20 μg/μL, Invitrogen, store at –20°C)
33. Mineral oil (VWR).
34. Chloroform (VWR, organic solvent)
35. Deionized formamide (Sigma-Aldrich, St Louis, MO, USA; toxic substance, aliquot and store at –20°C)
36. Hydrogen peroxide (30% Stock; VWR) (*see* **Note 1**).
37. 2 × pre-hybridization buffer (Sigma-Aldrich).
38. Hybridization solution: Mix 50% formamide, 2 × SSPE, 2 μg/μL tRNA, 1 μg/μL BSA, and 1 μg/μL poly A in DEPC-treated water.
39. Acetylation solution: Add 2.7 mL of triethanolamine to 200 mL of DEPC-treated water and mix well. Next, add 0.5 mL of acetic anhydride to the solution and mix well.
40. TNT washing buffer: Mix 60 mL of 1 M Tris–HCl, 18 mL of 5 M NaCl, and 1.8 mL of Triton X-100 in 600 mL of DEPC-treated water for three washes (3 × 200 mL volume for a small plastic container). Ensure that Triton X-100 has gone into solution before proceeding.
41. TNB blocking buffer: To make 1 mL of TNB buffer, mix 100 μL of 1 M Tris–HCl, 415 μL of 20 μg/μL BSA, 30 μL of 5 M NaCl, 3 μL of Triton X-100, and 452 μL of DEPC-treated water. We use 150 μL of TNB per slide; final volumes needed can be calculated accordingly.
42. Tween 20.
43. Triton X-100 (J.T. Baker, Phillipsburg, NJ, USA).
44. Anti-DIG HRP conjugated (Roche Diagnostics).
45. Anti-biotin peroxidase conjugated (Vector Laboratories, Burlinghame, CA, USA).

46. TSA detection kits with HRP streptavidin and tyramide-coupled Alexa™ Fluor 594 and 488 (Invitrogen). The Alexa-conjugated tyramide-working solutions should be prepared as follows: add 1 μL of 30% hydrogen peroxide to 200 μL of amplification buffer (both solutions provided by the kit's manufacturer). Prepare a 1:100 dilution of this solution in amplification buffer to an adequate volume that will cover all sections in the experiment. Add 1:100 to 1:200 of the Alexa™ fluorophore of choice (either Alexa™-488 or -594) depending on probe abundance to generate a working solution.
47. Diaminobenzidine (DAB) substrate kit for peroxidase (Vector Laboratories). To prepare working solution, sequentially mix two drops of stock buffer solution, seven drops of DAB solution, two drops of hydrogen peroxide solution, and two drops of nickel solution (all provided in kit) in 5 mL of distilled water. DAB is a carcinogen (*see* **Note 1**).
48. Hoechst (stock; 2 mg/mL, VWR, store at –4°C).
49. Vectashield™ mounting medium (for epifluorescence microscopy; Vector Laboratories).
50. ProLong™ gold antifade reagent (for confocal microscopy; Invitrogen).
51. UV transilluminator.

3. Methods

Below we detail the methodology associated with tissue preparation and sectioning (*see* **Section 3.1**), generation and purification of riboprobes (*see* **Section 3.2**), assessment of quality and yield of labeled riboprobes (*see* **Section 3.3**), fixation and acetylation of sections (*see* **Section 3.4**), hybridization (*see* **Section 3.5**), post-hybridization washes (*see* **Section 3.6**), and riboprobe detection (*see* **Section 3.7**).

Our dISH protocol is optimized to be completed within 2 days. The first day encompasses the production and purification of riboprobes (2.5 h), and the fixation, acetylation, dehydration, and hybridization steps (~1.5 h). The second day of our method includes post-hybridization washes (3.5 h) and the sequential immunocytochemical detection of each probe (~9 h). Importantly, prior to attempting dISH, we recommend optimizing in situ hybridization conditions for each probe separately. Specifically, efforts should be focused at carefully determining optimal hybridization and washing temperatures (via radioactive or non-

radioactive in situ hybridization approaches; (*see* 18, 19), and working dilutions and incubation times for antibodies and detection systems, which can be determined via single probe ISH, using the protocol detailed below. Finally, this protocol is optimized for probes that range from 0.5 to 1.5 Kb in size, but has been successfully used for larger probes, provided that hybridization and detection conditions are adjusted accordingly (*see* **Section 4**).

3.1. Tissue Preparation and Sectioning

1. Following the animal's decapitation, rapidly extract the brain from the skull, and place it into adequate plastic mold that allows for approximately 2–5 mm of space around all edges of the brain at its widest point. Cover the brain with a minimum amount of embedding medium (e.g., Tissue-Tek™ OCT) so as to fully cover the tissue.
2. Rapidly freeze brains by placing the plastic mold in a dry-ice/ethanol bath. After embedding medium solidifies, brains can be stored at −80°C until use (*see* **Note 2**) or immediately sectioned on a cryostat.
3. Obtain 10–12-μm thick brain sections on a cryostat. Two to three sections should be thaw-mounted on charged Superfrost™ Plus slides (*see* **Note 3**).

3.2. Preparation and Purification of Riboprobes

Below we detail the preparation and purification of a single riboprobe. For dISH, the preparation of each probe involves the same methodology, except that one probe is labeled with DIG-tagged UTP and the other with biotin-tagged UTP. Consequently, while the former involves the use of a DIG-labeling mix, the latter requires a biotin-labeling mix.

1. Digest 3 μg of plasmid carrying the cDNA of interest using the appropriate restriction enzyme.
2. Purify the linearized or excised DNA using the QIAquick™ PCR Purification Kit, following the manufacturer's instructions.
3. Run 2 μL of purified DNA on a 1% agarose gel containing ethidium bromide for the assessment of quality and quantity of the template cDNA (*see* **Note 4**). cDNA yield may also be assessed by spectrophotometry.
4. Add 1 μg of purified cDNA template, 2 μL of 5 × probe labeling buffer, 1 μL of 10 × DIG (or biotin)-labeling mix, 0.5 μL of RNasin, and 1 μL of the appropriate RNA polymerase to a 1.5-mL microcentrifuge tube. Bring the final volume of solution to 10 μL using RNase-free DEPC-treated water.
5. Incubate the solution in a water bath at 37°C for 1 h.
6. Add 0.5 μL of appropriate RNA polymerase to the solution and incubate for an additional hour.

7. Add 1 μL of tRNA solution (stock at 20 μg/μL).
8. Bring the volume of solution to 50 μL with blocking buffer.
9. Purify each labeled probe on Sephadex™ G-50 spin columns (*see* **Note 5**). To prepare and use columns, follow the following procedure.
   (a) Hydrate 2–4 g of Sephadex™ G-50 powder with 200 mL of RNase-free DEPC-treated water at room temperature; mix the solution well and let the suspension precipitate. This step is also necessary to remove dextran from the Sephadex™ powder. Subsequently, remove excess water with a clean glass pipette. Repeat this process five to ten times.
   (b) After the last hydration step, remove the DEPC-treated water and suspend the Sephadex™ G-50 beads in TE buffer (10 mM Tris–HCl, pH 7.5; 1 mM EDTA, pH 7.5) in a 1:1 ratio. This solution allows for the long-term storage of the beads at 4°C until use.
   (c) To generate columns, place a layer of autoclaved glass wool into a sterile 1-mL syringe and compress it with the plunger several times until it is compacted at the bottom.
   (d) Place syringe into a 15-mL cell culture tube, fill it with the Sephadex™ G-50 solution described above, and centrifuge for 30 s at 112 *g*.
   (e) Repeat this procedure to pack Sephadex™ G-50 beads into the syringe. Once the syringe is almost filled with beads, hydrate column with 200 μL of washing buffer, and centrifuge it for 2 min at 112 *g*.
   (f) Subsequently, apply 200 μL of blocking buffer to the column and centrifuge it for 2 min at 112 *g*. Repeat this step four to five times. Columns can now be stored at –4°C until use after sealing with Parafilm™.
   (g) Before use, equilibrate columns with 50 μL of column-blocking buffer and centrifuge it for 3 min at 447 *g*. Repeat this step until column is equilibrated such that the full 50 μL is obtained after centrifugation.

3.3. Assessment of Quality and Yield of Labeled Riboprobes

1. Prepare 1% agarose–formaldehyde RNA gel (*see* **Note 6** for method).
2. Load 2 μL of purified riboprobe on gel at 60 mV for 30 min (see **Note 7**).
3. Assess the size and quality of labeled probe on a UV transilluminator. Due to DIG incorporation, probe yield cannot be accurately estimated on a spectrophotometer. We, therefore, estimate yield based on visual inspection of our samples on the formaldehyde–agarose gel.

3.4. Fixation, Acetylation, and Dehydration of Sections

All procedures for the fixation and acetylation of brain sections are conducted at room temperature in a fume hood.

1. Remove sections from the –80°C freezer and allow them to air-dry for 30 min.
2. Fix sections in freshly made 4% paraformaldehyde for 5 min (*see* **Note 8**).
3. Wash sections twice in phosphate buffered saline (PBS; 2 min each).
4. Dehydrate sections through incubation in a standard alcohol series (70, 95, 95, 100 and 100%; 2 min each) and allow them to air-dry.
5. Incubate sections in acetylation solution for 10 min (*see* **Note 9**).
6. Wash sections three times in 2 × SSPE for 2 min each.
7. Dehydrate sections once again by sequentially incubating them in a series of graded ethanol (70, 95, 95, and 100%; 2 min each). Allow sections to air-dry.

3.5. Hybridization of Riboprobes

Total amount of hybridization solution should be calculated as described in **Note 10**. As indicated previously, optimal hybridization conditions should be established for each probe separately before attempting dISH. Additionally, a pre-hybridization step can be included to decrease background and, therefore, enhance signal-to-noise, if necessary (*see* **Note 11**).

1. Prepare an adequate volume of hybridization solution, using stock solutions stored at –80°C.
2. Add adequate volumes of each riboprobe (at 1 ng/μL) to the final hybridization solution (*see* **Note 12**).
3. Apply 16 μL of hybridization solution to each section and use glass cover slips to cover tissue. Ensure that the hybridization solution evenly and completely covers the tissue, and that it is free of bubbles.
4. Place slides in a metal slide holder. Slowly immerse slide holder, vertically, in a mineral oil bath set to 65°C (or other appropriate hybridization temperature), such that cover slips face up. Sections should remain in this bath overnight.

3.6. Post-hybridization Washes

Unless otherwise indicated, washes should be carried out at the same temperature as the hybridization step (i.e., 65°C; *see* **Note 13**).

1. The following day, carefully remove the slide holder from the mineral oil bath. Rinse the metal holder and the slides in chloroform twice (*see* **Note 14**).
2. Place slides in a 2 × SSPE solution. Cover slips should detach in a matter of 3–5 min (*see* **Note 15**).
3. Rinse sections in a new 2 × SSPE solution at room temperature for 1 h.

4. Incubate sections in a solution of 2 × SSPE plus 50% formamide at 65°C (or hybridization temperature of choice) for 1.5 h.
5. Incubate sections twice in a 0.1 × SSPE solution at 65°C (or hybridization temperature of choice; 30 min each).

3.7. Riboprobe Detection

The detection of each probe for dISH requires ~9 h from this point on. We recommend conclusion of the procedure in a single day. However, if necessary, these steps can be separated into 2 days at **Section 3.7**, step 8. All procedures described below are conducted at room temperature.

1. Incubate sections in TNT buffer with 0.3% hydrogen peroxide for 10 min.
2. Wash sections three times in TNT buffer (10 min each).
3. Rapidly dry glass surrounding the sections with tissue paper, and draw a well around the sections with DAKO pen (*see* **Note 16**). Ensure that sections do not dehydrate during this step.
4. Incubate sections in TNB buffer for 30 min in a humid chamber (*see* **Note 17**).
5. Discard TNB buffer by tilting slides. Incubate sections in a solution containing peroxidase-conjugated anti-DIG antibody in TNB buffer (1:200 to 1:400 dilution) in a humid chamber for 2 h (*see* **Note 18**).
6. Wash sections three times in TNT buffer (5 min each).
7. Incubate sections in an Alexa™-594-conjugated tyramide-working solution containing H_2O_2, in a humid chamber for 1 h (*see* **Note 19** and **Note 20**).
8. Wash sections three times in TNT buffer (5 min each) (**Fig. 9.1**, and *see* **Note 21**).
9. Incubate sections in TNT buffer containing 0.3% hydrogen peroxide solution for 10–30 min (*see* **Note 22** for this critical step).
10. Wash sections three times in TNT buffer (10 min each).
11. Incubate the sections in a solution containing peroxidase-conjugated anti-biotin antibody in TNB buffer (1:200 to 1:800 dilution, depending on probe abundance) in a humid chamber for 2 h.
12. Wash sections three times in TNT buffer (5 min each).
13. Incubate slides in a solution containing either Alexa™-488-conjugated tyramide (*see* **Note 19**) or DAB-working solution (*see* **Note 23**) for 0.5–1 h in a humid chamber.
14. Wash sections three times in TNT buffer (5 min each).
15. Incubate the sections in a Hoechst solution (1:1000 in TNT buffer) for 10 min in a humid chamber.

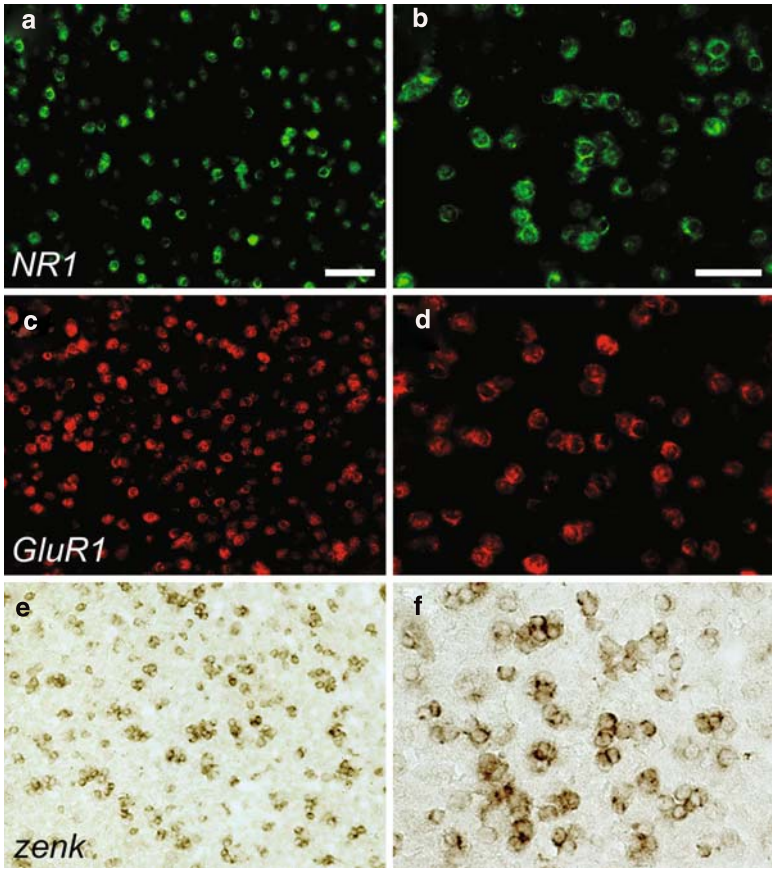

Fig. 9.1. Representative results obtained with fluorescence- (**a**–**d**) and diaminobenzidine-mediated (**e**–**f**) detection of single transcripts via in situ hybridization, using hapten-labeled riboprobes. Low- (*left*) and high-power (*right*) photomicrographs depicting the expression of *NR1* (**a**, **b**), a fundamental subunit of glutamatergic NMDA receptors, *GluR1*, a subunit of the AMPA-type of glutamate receptors (**c**, **d**), and the immediate *zenk* (**e**, **f**), in the auditory forebrain of a songbird stimulated with 30 min of a playback of a medley of conspecific songs. All riboprobes used to detect these transcripts were labeled with digoxigenin and detected via immunocytochemical approaches using peroxidase-mediated precipitation of tyramide coupled to Alexa™-488 (**a**–**b**) or Alexa™-594 (**c**–**d**), and diaminobenzidine (**e**–**f**). Scale bars (in μm): 50 (**a**, **c**, **e**) and 25 (**b**, **d**, **f**).

16. Wash sections three times in TNT buffer (5 min each).
17. Cover slip sections with Vectashield™ (for epifluorescence microscopy) or ProLong™ antifade (for confocal microscopy) mounting medium (**Fig. 9.2**).

4. Notes

1. This reagent is toxic. Use in a fume cabinet and exercise caution when handling.

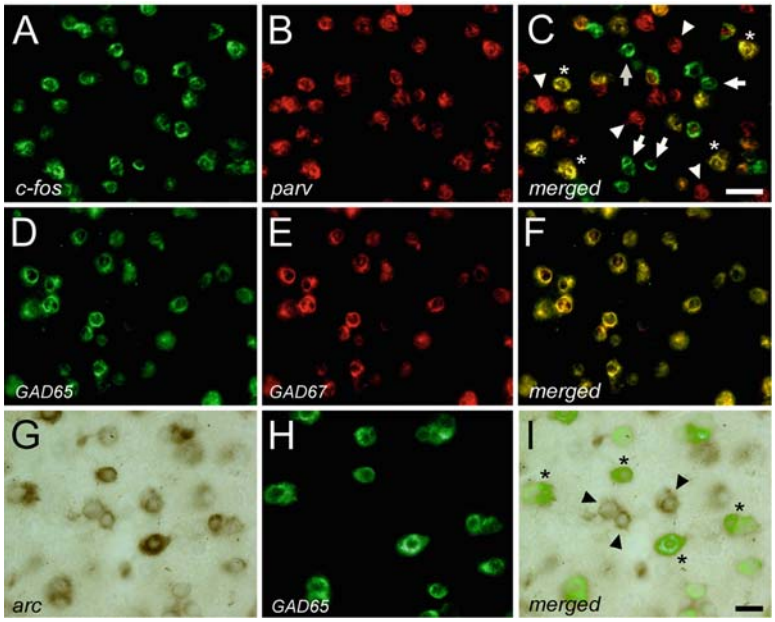

Fig. 9.2. Representative duplex in situ hybridization results in the songbird auditory forebrain. Detection of two transcript populations at single-cell resolution can be achieved through double-fluorescence in-situ hybridization (**A**–**F**) or through a combination of fluorescence- and non-fluorescence-based detection systems (**G**–**I**). Whereas, hearing-activated neurons exhibit the expression of the immediate early gene c-fos (**A**), a sub-population of inhibitory neurons can be detected by the expression the mRNA that encodes for the calcium-binding protein parvalbumin (**B**). Cells expressing both transcripts (**C**; *asterisks*) can be inferred to be song-responsive inhibitory neurons. Note the presence of neurons positive only for c-fos (*arrows*) or parvalbumin (*arrowheads*). Auditory "cortical" neurons fully co-express transcripts associated with the 65 kDa (**D**) and the 67 kDa (**E**) isoforms of the glutamic acid decarboxylase (GAD) genes, which encode for the enzymes responsible for the biosynthesis of GABA, the main inhibitory neurotransmitter in the vertebrate brain. Song-driven neurons also display a robust expression of the immediate early gene *arc* (**G**). A sub-population of these neurons co-expresses GAD65 (**H**), indicating the presence of hearing-activated inhibitory cells (**I**). Arc-positive/GAD65-negative neurons highlight the presence of putative song-responsive excitatory neurons (*arrowheads*). Importantly, while our duplex in situ hybridization protocol is optimized for detection of two riboprobes with fluorescence-based detection systems (i.e., Alexa-488 (**A**, **D**) and Alexa-594 (**B**, **E**)), we demonstrate here that non-fluorescence-based detection systems such as diaminobenzidine (**G**), can be combined with fluorescence-based detection (H; Alexa-488), to yield reliable detection of two mRNA populations at single-cell resolution (**I**). Scale bars (in mm): 25 (**A**–**F**); 10 (**G**–**I**).

2. All surgical tools should be sterilized before use. We typically store a bottle of embedding medium (e.g., Tissue-Tek™ OCT) in the refrigerator to facilitate rapid brain freezing. Following extraction, brains are placed into a thin plastic mold and covered with embedding medium. We use a dry-ice/ethanol (or propanol) bath for quick freezing, which is made by crushing dry-ice to powder and mixing it with ethanol until the mixture has a paste-like consistency. Plastic molds containing brains included in embedding medium are then inserted into this bath. Under this configuration, brains are typically frozen in less than 2 min. Frozen brains in the plastic molds can be stored and maintained at –80°C for several years.

3. In our experience, adequate cryostat sectioning temperatures range between –18 and –25°C. If brain blocks are maintained in a –80°C freezer, place them into the cryostat chamber 30 min before sectioning to equilibrate block temperature.
4. To prepare a 1% DNA agarose gel, add 1 g of agarose to 100 mL 1 × TAE and microwave the solution to dissolve the agarose. Subsequently, add 2 μL of a 10 mg/mL solution of ethidium bromide to the agarose solution when it has cooled down to ~60°C. Mix the solution well, pour it on the gel casting unit, and wait until gel polymerizes. Ethidium bromide is a carcinogenic substance; protect skin by wearing gloves and have separate ethidium bromide disposable containers. DNA samples to be loaded in the gel consist of a mixture of 2 μL of DNA sample, 1 μL of 6 × loading dye, and 3 μL of distilled water. An adjacent lane should be loaded with a DNA molecular size marker. Run the gel at 70 mV for 30 min and inspect samples on a UV transilluminator. DNA concentration should be determined via spectrophotometric analysis.
5. Although we prepare our own columns, purification of riboprobes can be conducted in commercially available spin columns.
6. For the preparation of a 1% RNA agarose gel, dissolve 0.3 g of molecular biology-grade agarose in 23 mL of DEPC-treated water on a microwave. Cool solution down to 60°C, add 3.3 mL of 10 × MOPS, and 5.7 mL of formaldehyde. Mix the solution well and pour solution into gel caster.
7. RNA gels yield significantly better results if run within a cold room or in a container with ice.
8. It is important to prepare a fresh fixative solution on the day of the hybridization step.
9. We highlight here that the acetylation solution loses its stability only a few minutes after the addition of acetic anhydride. It is, therefore, critical to incubate sections in this solution immediately after its preparation.
10. The total volume of hybridization solution will directly depend on the number of slides included in the experiment, as well as the number of sections per slide. We use 16 μL of hybridization solution per brain section.
11. To prepare the pre-hybridization working solution, dilute 2 × pre-hybridization buffer with deionized formamide stock (1:1 dilution). Apply 100 μL of the pre-hybridization working solution to each slide, cover slip sections, and incubate slides in a humid chamber at room temperature for 30 min. Cover slips should be removed in a 2 × SSPE solution.

12. The concentration of each riboprobe in the hybridization solution should be 1 ng/μL.
13. In the event of high background, increase stringency of washing steps by increasing the incubation time in the second wash (2 × SSPE plus 50% formamide), and/or by decreasing the salt concentration of the final wash (from 0.1 × to 0.05 × SSPE).
14. Drip excess oil from the slide rack on a paper towel. Subsequently, rinse the slide rack in two separate containers containing chloroform (five to six times, each) to remove the remaining oil.
15. Cover slips should easily detach from sections in the 2 × SSPE solution. Do not attempt to physically remove cover slips, as this will likely damage tissue sections. Under normal conditions, cover slips should detach from tissue in the 2 × SSPE solution within 5 min.
16. Carefully and rapidly dry the glass surrounding the sections with tissue paper. Next, create a well with DAKO pen ensuring that sections do not dry during this process.
17. We use a regular microscope slide box (100 slide capacity) as a humid chamber. First, we place paper towel on the floor of the box, and soak it with DEPC-treated water. Slides rest above the wet paper towel by placing them flat with either edge rested upon the vertical slots on the sides of the slide box compartments. In the correct position, the slide will bridge the two rows of vertical slots. It is good practice to leave approximately 1 mm space between each slide.
18. Antibodies should be carefully titrated prior to attempting dISH. We routinely use 1:200–1:400 antibody dilutions (in TNB) in our laboratory depending on probe abundance.
19. Working solution dilution of the Alexa™ fluorophore of choice (either Alexa™-488 or -594) depends on probe abundance.
20. In our experience, non-specific/high-background signals are often associated with problems in the detection step, more specifically, the peroxidase-mediated precipitation of tyramide/Alexa dyes. Typically, a significant increase in washing schedules after enzymatic probe detection remediates these problems. Before attempting dISH, ensure proper titration of the detection substrate for each probe separately.
21. Check the quality of probe signal by briefly inspecting sections under fluorescence microscopy during the washing step. Only proceed to the next step on the dISH protocol when satisfactory signal is achieved with the first probe. Alternatively, add extra "testing" slides to the experiment such that

the quality of the first probe detection can be assessed prior to proceeding on to the detection of the second probe (at **Section 3.7**, step 8). At this point in the protocol, extra slides can be cover slipped with Vectashield™ and inspected under epifluorescence microscopy.

22. The incubation of sections in this solution of H_2O_2 is arguably the most important step in the successful implementation of dISH. This step is necessary to inactivate peroxidase activity associated with the detection of the first riboprobe, such that the second detection system exclusively and reliably detects the second probe. In general, a 10-min incubation using fresh H_2O_2 reliably abolishes peroxidase activity associated with the first probe. It is important, however, to carefully control this step. We usually add "testing slides," which proceed to **Section 3.7**, step 9 (inactivation step), except that instead of being subjected to incubation with the second antibody, these sections are directly incubated with the second tyramide/Alexa™ solution. If peroxidase inactivation was successful, incubation in this second solution should yield *no signal*. Conversely, in the event that the second fluorophore yields measurable signals, it can be concluded that the peroxidase inactivation associated with the first probe was not complete and, therefore, false-positive double-labeled cells will likely occur. If these control sections yield false-positives, return sections to the H_2O_2 solution for additional incubation time. Alternatively, higher concentrations of H_2O_2 can be used (we have successfully used up to 0.5% H_2O_2).
23. We use the DAB substrate kit from Vector Laboratories. The manufacturer's protocol suggests to sequentially mix two drops of stock buffer solution, four drops of DAB solution, two drops of hydrogen peroxide solution, and two drops of nickel solution (all provided in kit) in 5 mL of distilled water to make a working buffer. We found that using seven drops of DAB (instead of four), rapidly differentiates the signal from noise which leads to strong deposition of DAB with virtually non-existent background. Incubation times in the DAB solution vary significantly for different genes. It is, therefore, important to optimize the DAB detection for each gene separately prior to using this approach in a dISH experimental configuration.

References

1. Pinaud, R. and Tremere, L.A. (2006) *Immediate early genes in sensory processing, cognitive performance and neurological disorders*, Pinaud, R. and Tremere, L.A. (eds.), Springer-Verlag, New York.
2. Pinaud, R., Tremere, L.A., and De Weerd, P. (2005) *Plasticity in the visual system: from genes to circuits*, Pinaud, R., Tremere, L.A., and De Weerd, P. (eds.), Springer-Verlag, New York.

3. Pinaud, R. (2004) Experience-dependent immediate early gene expression in the adult central nervous system: evidence from enriched-environment studies. *Int. J. Neurosci.* **114**, 321–333.
4. Ooi, L. and Wood, I.C. (2008) Regulation of gene expression in the nervous system. *Biochem. J.* **414**, 327–341.
5. Navarro, X., Vivo, M., and Valero-Cabre, A. (2007) Neural plasticity after peripheral nerve injury and regeneration. *Prog. Neurobiol.* **82**, 163–201.
6. Bading, H. (1999) Nuclear calcium-activated gene expression: possible roles in neuronal plasticity and epileptogenesis. *Epilepsy Res.* **36**, 225–231.
7. Thomas, G.M. and Huganir, R.L. (2004) MAPK cascade signalling and synaptic plasticity. *Nat. Rev. Neurosci.* **5**, 173–183.
8. Cohen, S. and Greenberg, M.E. (2008) Communication between the synapse and the nucleus in neuronal development, plasticity, and disease. *Annu. Rev. Cell Dev. Biol.* **24**, 183–209.
9. Greene, J.G. (2006) Gene expression profiles of brain dopamine neurons and relevance to neuropsychiatric disease. *J. Physiol.* **575**, 411–416.
10. Jin, L. and Lloyd, R.V. (1997) In situ hybridization: methods and applications. *J. Clin. Lab. Anal.* **11**, 2–9.
11. Stoler, M.H. (1990) In situ hybridization. *Clin. Lab. Med.* **10**, 215–236.
12. Komminoth, P. and Werner, M. (1997) Target and signal amplification: approaches to increase the sensitivity of in situ hybridization. *Histochem. Cell Biol.* **108**, 325–333.
13. Pinaud, R., Velho, T.A., Jeong, J.K., Tremere, L.A., Leão, R.M., von Gersdorff, H., and Mello, C.V. (2004) GABAergic neurons participate in the brain's response to birdsong auditory stimulation. *Eur. J. Neurosci.* **20**, 1318–1330.
14. Kessler, C. (1991) The digoxigenin:anti-digoxigenin (DIG) technology – a survey on the concept and realization of a novel bioanalytical indicator system. *Mol. Cell. Probes* **5**, 161–205.
15. Panoskaltsis-Mortari, A. and Bucy, R.P. (1995) In situ hybridization with digoxigenin-labeled RNA probes: facts and artifacts. *Biotechniques* **18**, 300–307.
16. Qian, X. and Lloyd, R.V. (2003) Recent developments in signal amplification methods for in situ hybridization. *Diagn. Mol. Pathol.* **12**, 1–13.
17. Velho, T.A., Pinaud, R., Rodrigues, P.V., and Mello, C.V. (2005) Co-induction of activity-dependent genes in songbirds. *Eur. J. Neurosci.* **22**, 1667–1678.
18. Pinaud, R., Mello, C.V., Velho, T.A., Wynne, R.D., and Tremere, L.A. (2008) Detection of two mRNA species at single-cell resolution by double-fluorescence in situ hybridization. *Nat. Protoc.* **3**, 1370–1379.
19. Mello, C.V., Jarvis, E.D., Denisenko, N., and Rivas, M. (1997) Isolation of song-regulated genes in the brain of songbirds. *Methods Mol. Biol.* **85**, 205–217.

Chapter 10

Special Stains for Extracellular Matrix

Andréa Monte-Alto-Costa and Luís Cristóvão Porto

Abstract

Extracellular matrix and cells are the components of connective tissue. Extracellular matrix provides tissue with tensile strength, elasticity, and resistance to compressive forces. Although immunohistochemistry is often used to study matrix constituents, a number of basic histological techniques can be used to describe the qualitative and quantitative presence and arrangement of matrix components. This chapter details specific staining techniques used for the study of extracellular matrix, explaining the rationale of each.

Key words: Extracellular matrix, histology, collagen, elastic system, reticular fibers.

1. Introduction

Extracellular matrix (ECM) and cells are the components of all connective tissue. The functions of connective tissues are a reflection of both the cells and extracellular matrix present. ECM provides tissue with structural support and tensile strength, elasticity, and resistance to compressive forces. Matrix provides a substrate for cell anchorage, acting as a scaffold for cell migration during embryonic development and wound repair. In addition to its structural properties, ECM constitutes directly the physical microenvironment in which cells live. It provides a medium for exchange, defense, protection, and storage (fat, cytokines, growth factors, etc.), and is therefore responsible for transmitting environmental signals to cells, which affect essentially all aspects of a cell's life, including proliferation, differentiation, and death.

Extracellular matrix comprises fibers, glycosaminoglycans, proteoglycans, and glycoproteins. Classically, connective tissue fibers have been classified as collagen, reticular or reticulin and elastic system. Although we now know that reticular fibers are a

T.D. Hewitson, I.A. Darby (eds.), *Histology Protocols*, Methods in Molecular Biology 611,
DOI 10.1007/978-1-60327-345-9_10,

type of collagenous fiber, some histologists still use this term for historical reasons. Elastic, elavnin and oxytalan fibers are referred to here as elastin containing fibers.

A common feature in a diverse range of chronic human diseases is the ongoing accumulation of excess connective tissue, and the replacement of tissue parenchyma by ECM, a process termed fibrosis or sclerosis. This has substantial clinical implications and serves as a prognostic indicator in many organs. The identification and understanding of matrix turnover is therefore an important histological objective.

For many years, histochemistry has provided a number of specific and useful techniques to describe the presence and arrangement of matrix components (*see* **Chapters 4** and **5**). The recent widespread interest in the pathogenesis of fibrosis and sclerosis has seen the application of specific immunohistochemical staining to the study of ECM components. However, special histological stains are still routinely and widely used in both research and diagnostic pathology laboratories to describe quantitative and qualitative alterations in ECM matrix composition and arrangement in different situations. This chapter describes how these techniques can be applied to the study of ECM through example and by explaining the rationale of each stain.

2. Materials

2.1. General Materials

1. Paraffin solvent for dewaxing (e.g., xylene).
2. Ethanol.
3. Forceps.
4. Coplin Jars.
5. Slide racks and staining jars.
6. Harris' hematoxylin (Sigma-Aldrich, St. Louis, MI, USA).

2.2. Trichrome Staining

Trichromic solution: Dissolve 0.6 g of cromotrop 2R (Sigma-Aldrich), 0.3 g of fast green (Sigma-Aldrich), and 0.6 g phosphotungstic acid in 10 mL of distilled H_2O (dH_2O). Add 1 mL of glacial acetic acid.

2.3. Weigert's Resorcin-Fuchsin Stain

1. Resorcin-fuchsin solution: Add 2 g of basic fuchsin (Sigma-Aldrich) and 4 g of resorcin (Sigma-Aldrich) to 200 mL of boiling dH_2O. Add 25 mL of a 30% w/v aqueous ferric chloride and continue boiling for 2–5 min. Cool and filter. Dissolve the precipitate in 200 mL of warm 95% ethanol. Cool and add 4 mL of concentrated HCl.

2. 1% w/v solution of Orange G (Sigma-Aldrich) in dH_2O (optional).

2.4. Unna's Orcein Staining

1. Orcein solution: Dissolve 1 g of orcein (Sigma-Aldrich) in 100 mL of ethanol, and add 0.7 mL of concentrated HCl.
2. Saturated aqueous picric acid (1.2% w/v) (Sigma-Aldrich) (*see* **Note 1**)

2.5. Sirius-Red Staining

Sirius red solution: Dissolve 3 g of Sirius Red F3BA (Sigma-Aldrich) in 100 mL of saturated picric acid solution (Sigma-Aldrich) (pH 2.0) (*see* **Note 1**).

2.6. Periodic Acid Schiff

1. Schiff's reagent: Dissolve 1 g of basic fuchsin (Sigma-Aldrich) in 200 mL of boiling dH_2O. Cool the solution to 70°C and add 2 g of sodium metabisulphite. Cool to room temperature. Add 10 mL of 1 N HCl. Leave for 24 h in the dark. Add 2 g of activated charcoal, mix, and filter. Store at 4°C in a dark flask. Solution should be clear or light yellow. Stable for 4–5 months (*see* **Notes 2** and **3**).
2. 1% w/v solution of periodic acid in dH_2O.

2.7. Gomori's Stain

1. 1% w/v solution of potassium permanganate in dH_2O.
2. 2% w/v solution of potassium metabisulphite in dH_2O.
3. 2% w/v iron alum in 2% w/v solution of potassium metabisulphite in dH_2O.
4. Silver solution: Add 40 mL of 10% silver nitrate to 10 mL of 10% w/v aqueous potassium hydroxide solution. Allow precipitate to settle and decant supernatant. Wash the precipitate many times with dH_2O. Add 28% ammonia (drop by drop) until the precipitate has dissolved. Add again 10% silver nitrate solution (drop by drop) until little precipitate remains. Dilute to 100 mL, filter, and store in a dark bottle.
5. 4% formalin.
6. 0.2% w/v solution of gold chloride (Sigma-Aldrich) in dH_2O.
7. 2% w/v solution of sodium thiosulphate in 2% w/v solution of potassium metabisulphite in dH_2O.

3. Methods

3.1. Gomori's Trichrome

The term trichrome is a general term used to describe a series of staining techniques for connective tissue (1). In trichrome staining, less porous structures are stained by dyes with smaller

molecules, and the more porous are stained by dyes with larger molecules, that displace smaller molecules when necessary. For example, red blood cells are less porous than muscle cells that in turn are less porous than collagen molecules. To correctly stain collagen fibers, the staining procedure should be performed at acidic pH (1.5–3.0). Phosphotungstic and phosphomolybidic are dyes with large molecules that stain collagen fibers (2).

3.1.1. Staining Method

1. Dewax sections and bring to 90% ethanol.
2. Stain with Harris' hematoxylin for 3 min.
3. Wash in tap water, 3 min.
4. Stain in trichromic solution for 10 min.
5. Wash in dH_2O.
6. Dehydrate through ethanol.
7. Clear in xylene.
8. Cover slip using mounting medium.

3.1.2. Results

Typical results of staining are shown in **Fig. 10.1**. Keratin, cytoplasm, and muscle stain purple to red, collagen stains green with nuclei black to blue (*see* **Notes 4** and **5**).

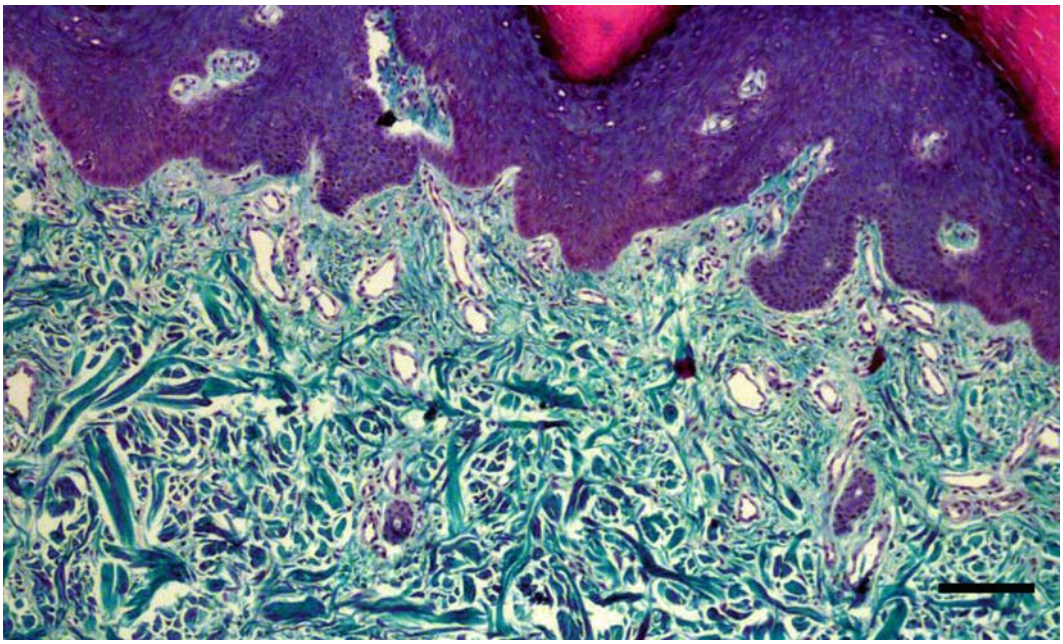

Fig. 10.1. Thick skin stained with Gomori's trichrome. Bar = 100 μm.

3.2. Weigert's Resorcin-Fuchsin

The resorcin-fuchsin solution is a complex that binds to elastin-containing fibers, staining fibers black to brown (3). The staining is thought to be due to the formation of hydrogen bonds between the elastin-containing fiber and the phenol group of resorcin (4).

Fibers containing only microfibrils (formerly termed oxytalan fibers) may be visualized if sections are oxidized before staining. Those fibers probably contain a reduced component of elastin-containing fibers that is reactive only after oxidation (5).

3.2.1. Staining Method

1. Dewax sections and bring to 90% ethanol.
2. Stain in a coplin jar filled with resorcin-fuchsin solution for 1 h (*see* **Note 6**).
3. Rinse in 90% ethanol.
4. Rinse in dH_2O.
5. Counterstain in Orange G 1% (optional).
6. Rinse in dH_2O.
7. Dehydrate through ethanol.
8. Clear in xylene.
9. Mount.

3.2.2. Results

Results are illustrated in **Fig. 10.2**. Elastin-containing fibers stain black to brown. In this case, counterstaining with Orange G results in an orange background (*see* **Note 7**).

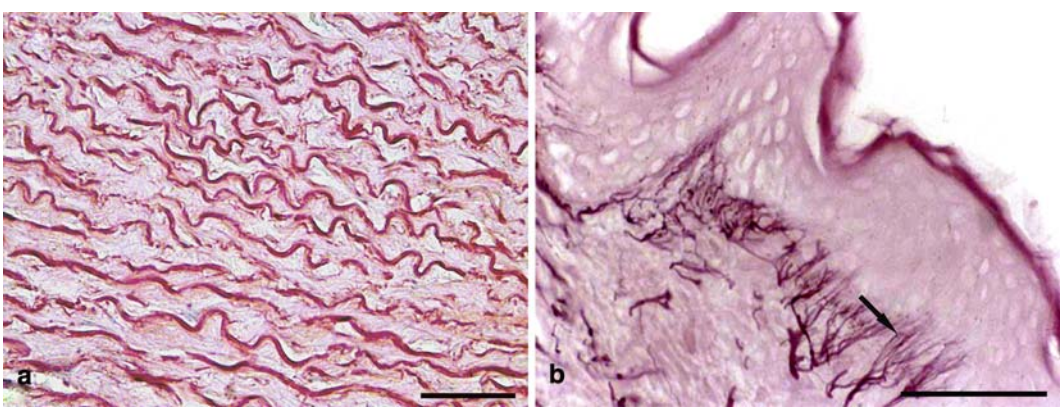

Fig. 10.2. (**a**) Aorta stained with Unna's orcein. Elastic lamellae are stained. (**b**). Skin stained with Weigert's resorcin-fuchsin, with prior oxidation. Thin elastin containing fibers are visualized only after oxidation. Bar = 50 μm.

3.3. Unna's Orcein

Little is known about the mechanism of staining involving elastin-containing fibers and orcein, a naturally occurring vegetable dye (6, 7). It has however been shown that staining is inhibited by the presence of urea, a strong hydrogen bonding agent, in the staining solution. It is therefore suggested that hydrogen bonding is responsible for elastin staining (8).

3.3.1. Staining Method

1. Dewax sections and bring to ethanol 90%.
2. Stain in orcein solution for 1 h.
3. Rinse in distilled water.
4. Counterstain in saturated picric acid solution for 30 s.
5. Rinse in dH_2O.
6. Dehydrate through graded ethanol.
7. Clear in xylene.
8. Mount.

3.3.2. Results

Elastin-containing fibers stain dark brown and collagen fibers light brown (**Fig. 10.2**).

3.4. Sirius-Red Staining

Sirius red in an anionic dye that stains collagen through reaction of its sulphonic groups with basic groups of collagen molecules (9). Dye molecules arrange parallel to collagen fibers, resulting in collagen birefringence. The role of picric acid is not well understood, but since in the absence of picric acid the entire tissue stains red, we presume that its function is to prevent indiscriminate staining of non-collagenous structures (9). Sirius red staining is frequently used as a basis for quantitative studies of fibrosis (10).

3.4.1. Staining Method

1. Dewax sections and bring to water.
2. Stain with sirius red solution, in a coplin jar, for 1 hr.
3. Rinse in two baths of 0.01 N hydrochloric acid, 1 min each.
4. Rinse in dH_2O.
5. Counterstain in Harris hematoxylin (optional).
6. Rinse in distilled water.
7. Dehydrate through graded ethanol.
8. Clear in xylene.
9. Mount.

3.4.2. Results

Fibrillar collagen stains red and nuclei purple (if counterstain is performed). If observed under polarization, birefringent collagen fibers will be visible on a black background. Individual fibers will range in color from green, to yellow to red depending on their thickness (thin, intermediate, and thick, respectively) (**Fig. 10.3**).

3.5. Periodic Acid Schiff

This technique is appropriated to indicate the presence of carbohydrates in tissues (11). As basement membranes are rich in carbohydrates, it is a useful technique to point out basement membranes. The reaction is based on oxidation that periodic acid induces in carbon–carbon ligation, forming aldehydes that react with acid fuchsin, which in turn combine with pararosanilin that becomes magenta (12).

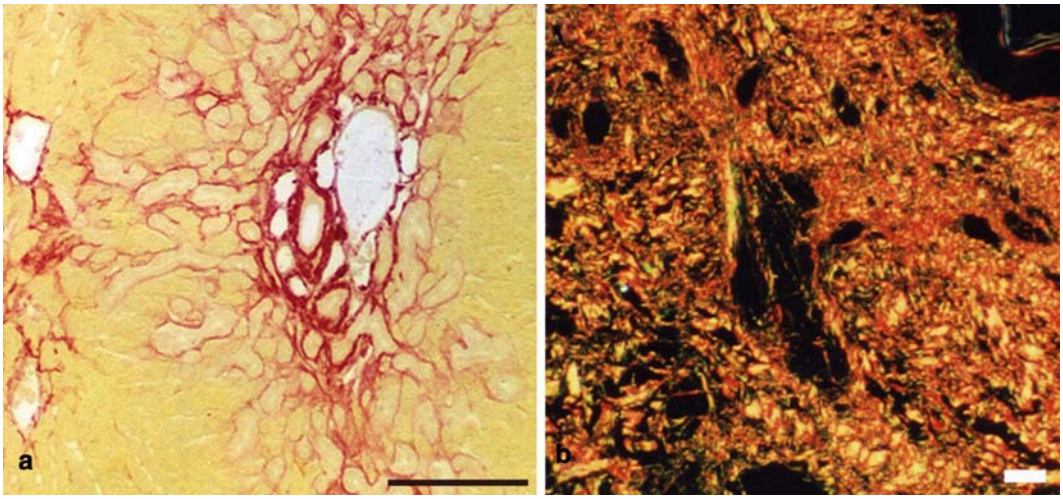

Fig. 10.3. (**a**) Fibrotic liver stained with sirius-red, visualized without polarization. Fibrillar collagen is in *black*. (**b**) Normal skin stained with sirius-red, visualized with polarization. Depending on fiber diameter, the refringent color varies. Bar = 150 μm.

3.5.1. Staining Method

1. Dewax sections and bring to water.
2. Incubate in 1% periodic acid for 10 min.
3. Rinse in distilled water, three times.
4. Cover with Schiff's reagent for 10 min.
5. Wash in running tap water.
6. Counterstain in Harris' hematoxylin (optional).
7. Rinse in distilled water.
8. Dehydrate through ethanol.
9. Clear in xylene.
10. Mount.

3.5.2. Results

Glycogen and other carbohydrates stain magenta and nuclei purple (if counterstaining is performed).

3.6. Gomori's Method for Reticulin

As reticular fibers are very thin, conventional stains are not suitable to demonstrate them (13). Metal impregnation techniques are indicate since they provide contrast that allows visualization of the thin reticular fibers. Pretreatment of sections with heavy metal salt solutions improves the affinity of reticular fibers to silver salts. The treatment of sections with a reducing agent converts silver in unreduced form, taken by tissue in metallic silver that is deposited. Sodium thiosulfate treatment removes any unreacted silver. Treatment with gold chloride solution stabilizes the silver and increases the contrast (8).

3.6.1. Staining Method

1. Dewax sections and bring to water.
2. Treat sections with 1% potassium permanganate solution for 2 min.
3. Rinse in tap water.
4. Bleach in 2% potassium metabisulphite solution.
5. Rinse in tap water.
6. Treat sections with 2% iron alum solution for 2 min.
7. Wash several times in distilled water.
8. Incubate, in a coplin jar, with silver solution, for 1 min (*see* **Notes 8** and **9**).
9. Wash several times in distilled water.
10. Treat with 4% formalin for 3 min (*see* **Note 10**).
11. Rinse in tap water.
12. Tone in 0.2% gold chloride solution for 10 min.
13. Rinse in tap water.
14. Treat with 2% metabisulphite solution, 1 min.
15. Rinse in tap water.
16. Treat with 2% sodium thiosulphate solution, 1 min.
17. Rinse in tap water.
18. Dehydrate through ethanol.
19. Clear in xylene.
20. Mount.

3.6.2. Results

Reticular fibers stain black and nuclei grey (**Fig. 10.4**).

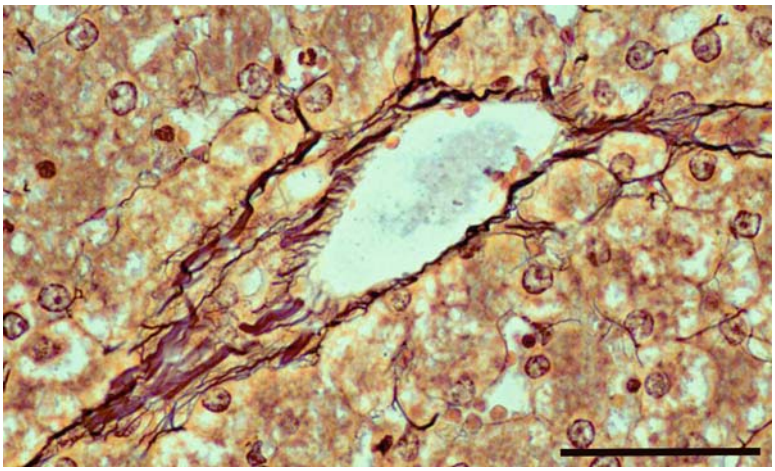

Fig. 10.4. Liver stained with Gomori's method for reticulin. Reticular fibers are stained in *black*. Bar= 50 μm.

4. Notes

1. Picric acid crystals are highly explosive when dry. It is therefore best handled as a commercial-prepared saturated aqueous solution (1.2% w/v).
2. If Schiff's reagent is not clear, add sodium metabisulphite and filter again.
3. Schiff's reagent can be prepared using 1 N acetic acid replacing hydrochloric acid. In this case, it should be added to hot solution of basic fuchsin before adding sodium metabisulphite.
4. Light green can be replaced by aniline blue. In this case, collagen will stain in blue.
5. If sections are too red, differentiate in 100 ml of 1% acetic acid containing 0.7 g of phosphotungstic acid.
6. Excess of ferrous salt may disturb staining; so use freshly prepared ferric chloride solution. Ferric nitrate can replace ferric chloride, since it is free from ferrous salt.
7. After oxidation, by exposition to 10% potassium monopersulphate for 40 min before staining, fibers containing microfibrils and not elastin will stain in black to brown (**Fig. 10.2b**).
8. Acid-clean coplin jar after use with silver solution.
9. Use clean plastic forceps to move slides from one bath to another.
10. Discard formalin solution after 10–12 sections.

References

1. Gomori, G. (1950) A rapid one-step trichrome stain. *Am. J. Clin. Pathol.* **20**, 661–664.
2. Bradbury, P. and Gordon, K. (1977) Connective tissue and stains. In: Bancroft, J.D., Stevens, A., eds. *Theory and Practice of Histological Techniques.* Churchill Livingstone, London. pp. 95–112.
3. Weigert, C. (1898) Ueber eine methode zur Farbung elasticher Fasern. *Zentralbl. Allg. Pathol.* **9**, 289–292.
4. Sheehan, D.C. and Hrapchak, B.B. (1973) Theory and Practice of Histotechnology. Mosby Company, St Louis, MO.
5. Fullmer, H.M. and Lillie, R.D. (1958) The oxytalan fiber: a previously undescribed connective tissue fiber. *J. Histochem. Cytochem.* **6**, 425–430.
6. Lillie, R.D. (1969) Exploration of dye chemistry in Taenzer Unna orcein type elastin staining. *Histochemie* **19**, 1–12.
7. Puchtler, H. and Meloan, S.N. (1979) Orcein, collastin and pseudo-elastica: a reinvestigation of Unna's concepts. *Histochemistry* **64**, 119–130.
8. Bradbury, P. and Rae, K. (1996) Connective tissues and stains. In: Bancroft, J.D., Stevens, A. eds. Theory and Practice of Histological Techniques, 4th edition. Churchill Livingstone, New York. pp. 113–137.
9. Junqueira, L.C., Bignolas, G., and Brentani, R.R. (1979) Picrosirius staining plus polarization microscopy, a specific method for collagen detection in tissue sections. *Histochem. J.* **11**, 447–455.

10. Whittaker, P., Kloner, R.A., Boughner, D.R., and Pickering, J.G. (1994) Quantitative assessment of myocardial collagen with picrosirius red staining and circularly polarized light. *Basic Res. Cardiol.* **89**, 397–410.
11. Mc Manus, J.F. (1948) Histological and histochemical uses of periodic acid. *Stain Technol.* **23**, 99–108.
12. Cook, H.C. (1977) Carbohydrates. In: Bancroft, J.D., Stevens, A., eds. Theory and Practice of Histological Techniques. Churchill Livingstone, London. pp. 141–167.
13. Gomori, G. (1937) Silver impregnation reticulum in paraffin sections. *Am. J. Pathol.* **13**, 993–1002.

Chapter 11

Active Staining of Mouse Embryos for Magnetic Resonance Microscopy

Alexandra Petiet and G. Allan Johnson

Abstract

Magnetic resonance histology (MRH) has found considerable application in structural phenotyping in the mouse embryo. MRH employs the same fundamental principles as clinical MRI, albeit with spatial resolution up to six orders of magnitude higher than that in clinical studies. Critical to obtaining this enormous gain in resolution is the need to enhance the weak signal from these microscopic voxels. This has been accomplished through the use of active staining, a method to simultaneously fix the embryonic/fetal tissues, while reducing the spin lattice relaxation time (T1). We describe here the methods that allow one to balance the fixation, which reduces the nuclear magnetic resonance (NMR) signal, with the enhancement of signal derived from the reduction in T1. Methods are included to cover the ranges of embryonic specimens from E10.5 through E19.5.

Key words: Magnetic resonance microscopy, embryos, active staining.

1. Introduction

Histology as defined by Webster's dictionary is "the branch of biology concerned with the microscopic structure of tissue." The vast majority of the histology studies today, and the focus of much of this book, employ conventional optical or electron microscopes. Magnetic resonance histology (MRH) was first suggested by Johnson et al. in the early 1990s (1, 2). MRH differs from conventional optical methods in four major ways: (a) MRH is non-destructive: there is no physical sectioning required such that the tissue under study remains physically intact; (b) the contrast in the MR histology images is dependent on the protons (mostly water) in the tissue and how those protons are bound. This, in turn, provides a rich bounty of contrast mechanisms to differentiate

T.D. Hewitson, I.A. Darby (eds.), *Histology Protocols*, Methods in Molecular Biology 611,
DOI 10.1007/978-1-60327-345-9_11,

structures and pathology based on the same parameters that have made MRI so successful in the clinical domain – such as spin lattice relaxation (T1), spin–spin relaxation (T2), diffusion, and proton density. The underlying physics of these "proton stains" (2) is beyond the scope of this chapter. The interested reader is referred to several excellent texts (3–5); (c) MRH provides three-dimensional images; and (d) MRH is inherently digital.

MRH is based on the same physical principles as clinical MR imaging (MRI). However, MRH differs from MRI in several respects. MRI studies of post-mortem specimens have been performed using clinical systems (6). But, clinical systems are typically limited to spatial resolution in the order of 1 mm. Systems designed for MRH provide spatial resolution down to 10 μm. Since MRI and MRH are tomographic (three-dimensional) imaging systems, spatial resolution is most appropriately stated in terms of the voxel volumes. Thus, the dedicated systems, with $(10\ \mu m)^3$ voxels (voxel volume = 1 pl) are encoding the signal from voxels that are 1,000,000 × smaller than the clinical systems at 1 mm^3 (voxel volume 1 μL). To achieve this increase in spatial resolution, systems designed for MRH differ significantly from clinical MRI systems. The first major difference is in the magnetic gradient coils. Spatial encoding in MRI/MRH is achieved through the application of a magnetic field gradient (7). In order to achieve the higher resolution, MR microscopes use much stronger gradients. The typical MRI system achieves gradients of ~50 mT/m. The gradients on an MR microscope can be 60 × greater (3,000 mT/m). Technical constraints limit the volume over which such gradients can be sustained, so the magnets used for these studies are much smaller bore (60–120 mm) than the 1 m bore of a clinical magnet. This, of course, limits the size of the specimen that can be studied.

Since the voxels are 1 million times smaller, the signal is 1 million times weaker. Thus, a major focus in MR histology is increasing the sensitivity. This is achieved in three ways. First, MRH systems use much stronger magnets: clinical MRI systems operate at 0.5–3.0T, while MRH systems work at 7.0–22.0T. Second, since the MRI/MRH signal is a radiofrequency (rf) signal that is captured by the rf probe that holds the specimen, careful design of the probe is essential to optimize the sensitivity. But, this also (like the gradient coil) limits the size of the specimen. Smaller radiofrequency coils provide greater sensitivity required for higher spatial resolution. The third approach to enhancing sensitivity is the use of active staining (8), which is the focus of this chapter. The signal in MR histology is derived from protons (usually water) in the tissue. The nuclear magnetic resonance (NMR) phenomenon, upon which MRI/MRH is based, exploits the interaction of a radiofrequency pulse to excite these protons. Once excited, the protons return a signal, the strength of which is dependent on

intrinsic factors in the tissues and extrinsic variables that are set in the scan protocol (3). For example, for a T1-weighted sequence, the signal S from a tissue is given by equation [1]:

$$S_i = PD_i(1 - e^{-TR/T1_i}) \quad [1]$$

where PD_i, the proton density in tissue i, and $T1_i$, the spin lattice relaxation for tissue i, are intrinsic for that tissue, and TR is the extrinsic parameter that one sets in the scanning sequence. **Figure 11.1** shows a graph of the signal for two tissues with differing spin lattice relaxation times. Tissue A (dotted line) has a shorter T1 than tissue B (solid line). At TR1, the signal from tissue A is much greater than it is from tissue B. Active staining is the process of radically reducing spin lattice relaxation time through the induction of a chemical agent.

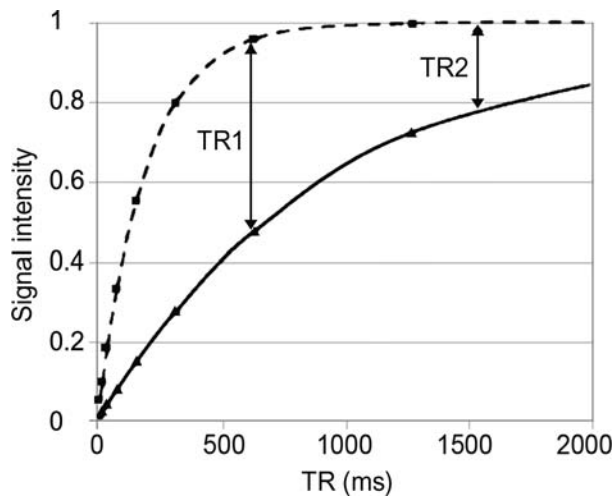

Fig. 11.1. Signal intensity as a function of TR for two tissues with different T1. The *solid line* shows the signal from a tissue with long T1. Active staining reduces the T1 yielding the recovery curve shown by the *dotted line*. With active staining, one can use much shorter TR and still recover the majority of the signal.

Figure 11.2 shows both the impact of changing the extrinsic variable (TR) and the intrinsic tissue parameters (T1). Figure 11.2a–d shows images of a formalin-fixed mouse brain acquired with TR of 20, 40, 80, and 160 ms. Figure 11.2e–h shows an identical series for a mouse brain that has been actively stained (9). These images are acquired at very low spatial resolution to allow quick comparison of the consequence of active staining. The signal enhancement from active staining is 8.4-times greater than the signal from formalin-fixation only at TR = 40ms. The benefits of active staining are clear: under optimized conditions, one can realize gain in signal-to-noise, gain in spatial resolution, and gain in contrast. Here, we describe the methods we employ with specific focus on the mouse embryo.

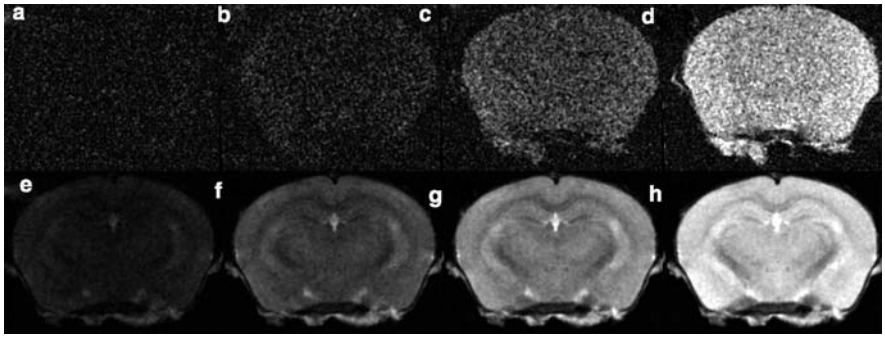

Fig. 11.2. (**a**–**d**) MR microscopy images from a formalin-fixed mouse brain (at TR= 20, 40, 80, and 160 ms, respectively) show increasing signal with longer TR. (**e**–**h**) MR microscopy images of an actively stained mouse brain (at TR= 20, 40, 80, and 160 ms, respectively) show a much enhanced signal (reproduced from (9) with permission of *NeuroImage*).

2. Materials

2.1. Preparation of the Fixing-Staining Solution

1. Bouin's solution (LabChem Inc., Pittsburgh, PA, USA) (*see* **Note 1**).
2. Gadoteridol (ProHance™, Bracco Diagnostics Inc., Princeton, NJ, USA), 0.5 M (*see* **Note 2**).
3. Eppendorf tubes for embryos of crown-rump length (CRL) $\sim \leq 5$ mm.
4. 15 mL jars for embryos of ~ 5 mm $\leq$ CRL ≤ 17 mm (*see* **Note 3**).
5. 30 mL containers for fetuses of CRL $\sim > 17$ mm.

2.2. Preparation of the Storage Solution

1. Phosphate buffered saline (PBS).
2. Gadoteridol (ProHance™, Bracco Diagnostics Inc), 0.5 M.
3. Eppendorf tubes for embryos of CRL $\sim \leq 5$ mm.
4. 15 mL jars for embryos of ~ 5 mm $\leq$ CRL ≤ 17 mm (*see* **Note 3**).
5. 30 mL containers for fetuses of CRL $\sim > 17$ mm.

3. Methods

3.1. Immersion Fixation-Staining of E10.5–E18.5

1. Dilute some ProHance™ in Bouin's solution at 1:20 (v:v, i.e., 25 mM) and prepare 15–30 mL per embryo/fetus, depending on the size (*see* **Notes 1, 2,** and **4**) (**Fig. 11.3**).

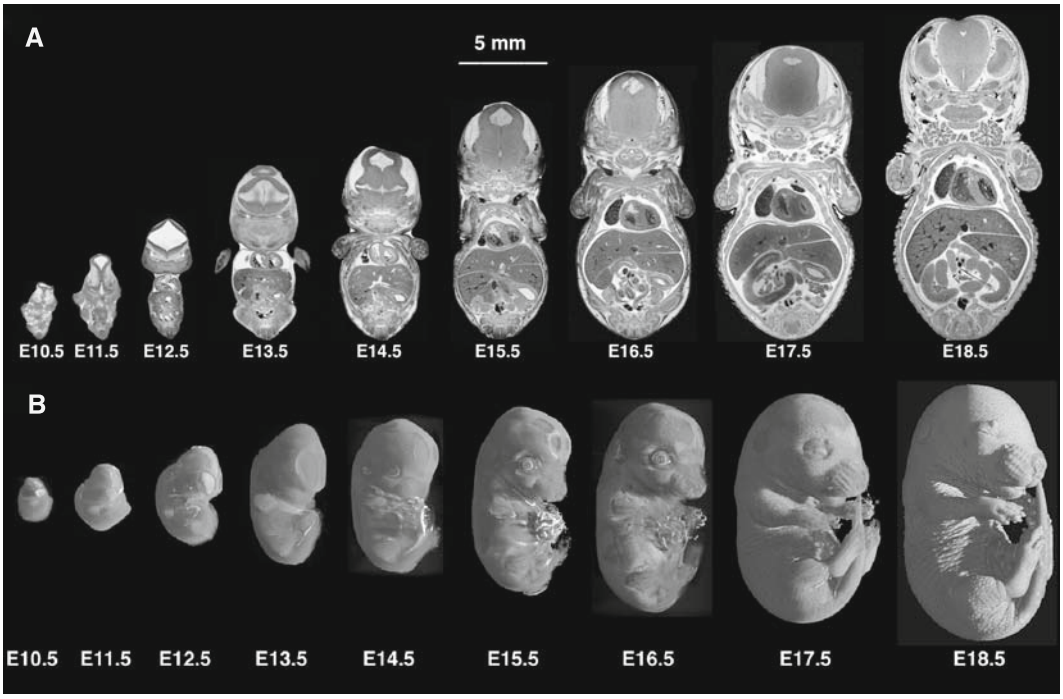

Fig. 11.3. Embryos from E10.5 to E18.5: (**a**) mid-coronal slices and (**b**) rendered volumes. The contrast across images is very similar and many small structures are clearly identifiable. These data are part of an extensive database of the developing mouse (11) available online at http://www.civm.duhs.duke.edu/devatlas/index.html.

2. After hysterectomy of the anesthetized pregnant mouse, dissect out the first embryo/fetus in a Petri dish filled with ice-cold saline and cut the placenta off if you do not need it. Drop the embryo/fetus in a jar with the fixing-staining solution at room temperature. See **Table 11.1** for immersion durations (*see* **Notes 5**–*7*).

Table 11.1
Immersion durations as a function of the size of the specimen (± 0.5 mm) and reduced T1 values

Stage	E10.5	E11.5	E12.5	E13.5	E14.5	E15.5	E16.5	E17.5	E18.5
CRL (mm)	4	5	7.5	9.5	11	12	13	15	16.5
Immersion duration	10 min	10 min	30 min	30 min	1 h	2 h	4 h	9 h	24 h
T1 (ms)	35	53	40	80	53	87	85	70	50

3.2. Immersion Fixation-Staining of E19.5

Late-stage fetuses are viable, so care should be taken not to fix them if their heart is still beating (**Fig. 11.4**). The fetuses can be intraperitoneally (i.p.) injected with diluted anesthetics at lethal dose prior to fixation.

Another issue arises from the impermeable skin that does not allow the reagents to penetrate. This can be overcome by several injections of the fixing-staining solution prior to a 24-h immersion

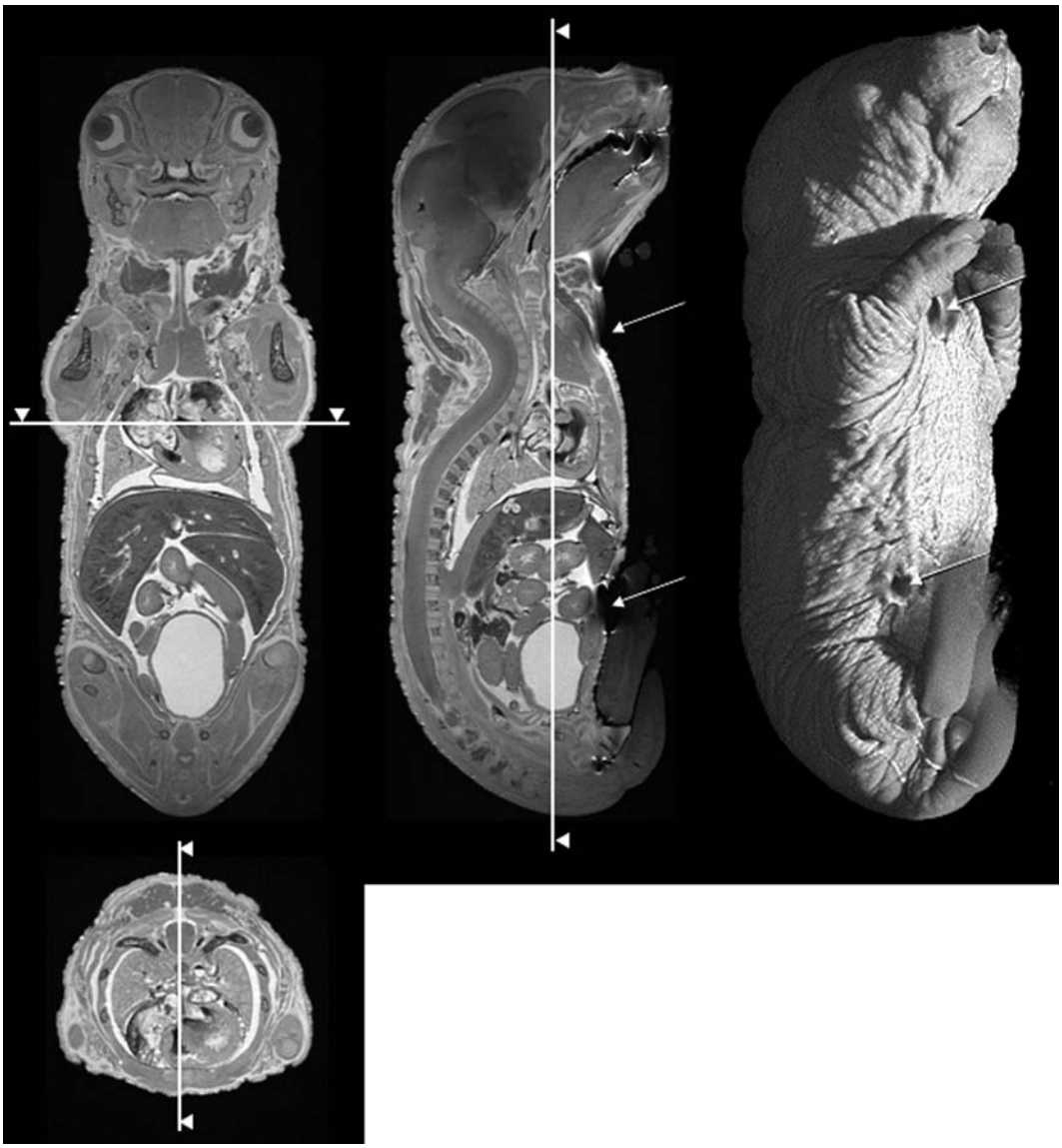

Fig. 11.4. E19.5 fetus prepared with i.p. injections of ProHance™: Bouin's solution at 1:20 followed by an overnight immersion in the same mixture. High signal-to-noise ratio (SNR) and contrast-to-noise ratio (CNR) were achieved uniformly throughout the body with no significant tissue damage or image artifact. The *arrows point* to the sites of injection (neck and lower abdomen).

(30-mL container): i.p. in the abdomen to help penetration in the lower body parts or subcutaneous in the neck to help penetration in the head (*see* **Notes 5–7**).

3.3. Long-Term Storage of Fixed-Stained Specimens

The staining process is designed to reduce the spin lattice relaxation time (T1), thereby increasing the MR signal (*see* **Note 8**). This is accomplished by the gradual diffusion of the contrast agent into the tissues. But, the cross-linking that accompanies the fixation has detrimental impact on the MR signal that arises from reduction of a second critical MR parameter, the spin–spin relaxation time, T2 (10). Fixation beyond the time required for the contrast agent to diffuse into the tissue is not recommended. **Figure 11.5** shows a comparison between two fetuses fixed for 3.5 and 24 h, respectively. The fixation and staining can be stabilized after the appropriate fixation time by immersion in a PBS/contrast agent solution with a low concentration of contrast agent (to avoid over-staining of the tissues). A dilution of 1:200 ProHance™: PBS should be used and the specimens should be stored at 4°C. Specimens can be stored for several weeks in this solution.

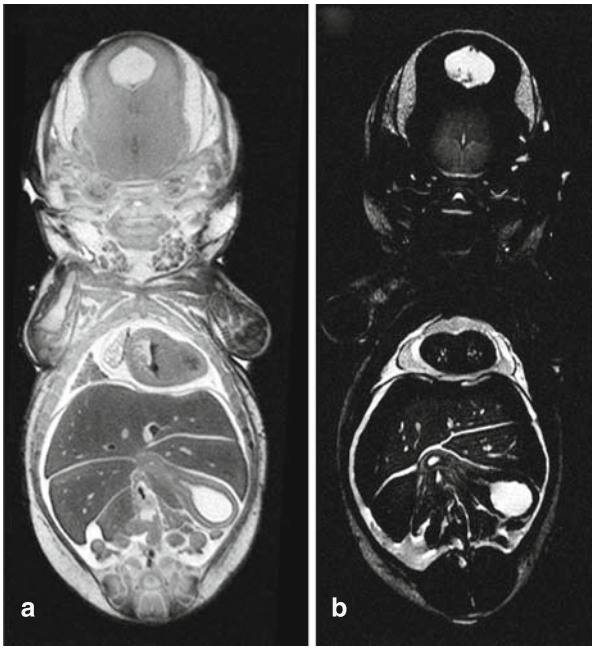

Fig. 11.5. Coronal slices from 3D acquisitions (3D spin warp, TR/TE = 100 ms/5.5 ms, FOV = 20 × 10 × 10 mm, matrix size = 1024 × 512 × 512) of E18.5 rat fetus immersed for (**a**) 3.5 h and (**b**) 24 h. Note the strong signal from the fluid in the ventricle indicating that the T1 has been reduced in both cases. But the extended immersion also reduces T2 (in **b**) resulting in much lower MR signal (1) (reproduced from (10) with permission of the *J. Magn. Reson. Imaging*).

4. Notes

1. Other fixative agents, such as formalin, can also be used. We have chosen Bouin's because picric acid aids the diffusion of the contrast agent into the tissues. Other fixatives will permeate the tissue at different rates, so the immersion times will need to be adjusted. In addition, the cross-linking that causes reduction in T2 may be different, so the results may vary from those shown here.
2. Other paramagnetic contrast agents such as gadopentetate dimeglumine (Magnevist™, Bayer Schering Pharma, Berlin, Germany) or gadoterate meglumine (Dotarem™, Guerbet, France) can also be used, though one needs to be cognizant of potential chemical reactions. For example, $MnCl_2$, a potential, inexpensive stain, may precipitate in some fixatives.
3. For the fixation solution, it is generally recommended to use 15–20 × the volume of the specimen, but 15 mL is sufficient for most stages.
4. MR is generally sensitive to water protons. Fixatives that remove all the water (e.g., alcohol) remove the source of the MR signal. While there are protons in alcohol that do yield an NMR signal, they are not chemically equivalent and this can lead to severe artifacts in the MR images.

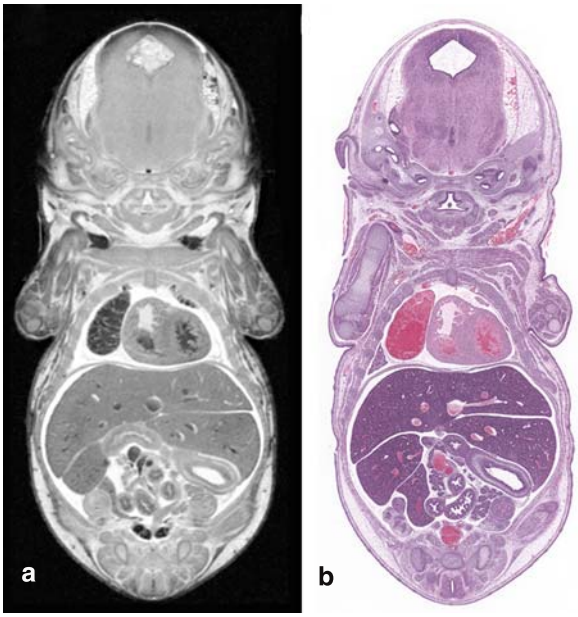

Fig. 11.6. Coronal slices of (**a**) MR histology and (**b**) conventional histology (hematoxylin and eosin stain) of the same E16.5 mouse fetus. The specimen was fixed for 4 h and stored for 2 months prior to sectioning.

5. This method can be extended to rat embryos/fetuses/pups and to all mouse strains, as well.
6. This method can also be used for fixing-staining other tissue types of comparable sizes (e.g., mouse brains). However, where possible, perfusion fixation provides better results (10).
7. Active staining has been used for much larger specimens, e.g., post-natal mice, whole adult mice, and isolated organs (8). While immersion fixation is possible, larger specimens will require much longer immersion times and as with all fixation, the quality of the fixation (and staining) can be improved with direct perfusion.
8. This method is compatible with post-histological analysis of the fixed tissues (**Fig. 11.6**). Paramagnetic contrast agents have no known interferences with most routine (e.g., hematoxylin and eosin Nissl) histological staining.

References

1. Johnson, G.A., Maronpot, R.R., and Redington, R.W. (1990) MR microscopy as a new histologic tool. *Invest. Radiol.* **25**, 1361.
2. Johnson, G.A., Benveniste, H., Black, R.D., Hedlund, L.W., Maronpot, R.R., and Smith, B.R. (1993) Histology by magnetic resonance microscopy. *Magn. Reson. Q.* **9**, 1–30.
3. Wehrli, F.W., Shaw, D., and Kneeland, J.B. (eds) (1988) *Biomedical magnetic resonance imaging: Principles, methodology, and applications.* VCH, New York, p. 601.
4. Callaghan, P.T. (1994) *Principles of nuclear magnetic resonance microscopy.* Oxford University Press, Oxford, p. 492.
5. Haacke, E.M., Brown, R.W., Thompson, M.R., and Venkatesan, R. (eds) (1999) *Magnetic resonance imaging: Physical principles and sequence design.* Wiley-Liss, New York, p. 914.
6. Boyko, O.B., Alston, S.R., Fuller, G.N., Hulette, C.M., Johnson, G.A., and Burger, P.C. (1994) Utility of postmortem magnetic resonance (MR) imaging in clinical neuropathology. *Arch. Pathol. Lab. Med.* **118**, 219–225.
7. Lauterbur, P.C. (1973) Image formation by induced local interactions – examples employing nuclear magnetic resonance. *Nature* **242**, 190–191.
8. Johnson, G.A., Cofer, G.P., Gewalt, S.L., and Hedlund, L.W. (2002) Morphologic phenotyping with magnetic resonance microscopy: The visible mouse. *Radiology* **222**, 789–793.
9. Johnson, G.A., Ali-Sharief, A., Badea, A., Brandenburg, J., Cofer, G., Fubara, B., Gewalt, S., Hedlund, L.W., and Upchurch, L. (2007) High-throughput morphologic phenotyping of the mouse brain with magnetic resonance histology. *NeuroImage* **37**, 82–89.
10. Petiet, A., Hedlund, L.W., and Johnson, G.A. (2007) Staining methods for magnetic resonance microscopy of the rat fetus. *J. Magn. Reson. Imaging* **25**, 1192–1198.
11. Petiet, A.E., Kaufman, M.H., Goddeeris, M.M., Brandenburg, J., Elmore, S.A., and Johnson, G.A. (2008) High-resolution magnetic resonance histology of the embryonic and neonatal mouse: A 4D atlas and morphologic database. *Proc. Natl. Acad. Sci. USA* **105**, 12331–12336.

Chapter 12

Immunohistochemical Detection of Tumour Hypoxia

Richard J. Young and Andreas Möller

Abstract

In this chapter, we describe the use of immunohistochemical methods to detect hypoxia in tumour tissue sections, utilising antibodies specific for endogenous proteins hypoxia inducible factor 1 alpha (Hif1α) and glucose transporter 1 (Glut-1) and the exogenous compound pimonidazole (Pim). Immunohistochemistry is routinely used both diagnostically and in research to label and identify specific cellular proteins of interest. The methods described here enable staining of hypoxic cells and tissue in formalin-fixed paraffin-embedded (FFPE) tumour tissue sections that can then be visualised either using chromogenic or fluorescence detection. All three methods can be used on human, xenograft, or mouse tumour tissue.

Key words: Hypoxia, tumour, immunohistochemistry, pimonidazole, Hif1α, Glut-1.

1. Introduction

Hypoxia, or low oxygen, is a common phenomenon in many solid tumours (1). Hypoxia results from an imbalance between the supply and consumption of oxygen, whereby the rate of oxygen consumption by tumour cells exceeds the oxygen supply. This occurs as a result of poorly functioning, abnormal tumour vasculature which leads to limited tissue perfusion and diffusion of oxygen, and through the rapid proliferative rate of tumour cells (2). Hypoxia is known to be an adverse prognostic factor in human cancers due to hypoxic tumour cells exhibiting increased resistance to chemotherapy and radiotherapy (3). The targeting of hypoxia has been an area of intense investigation for many years; however, clinical efforts have been slowed by an inability to accurately identify patients who would most benefit from hypoxia-targeted therapies (4).

Several techniques are available for measurement of tumour oxygenation, including needle electrodes, positron emission tomography (PET) imaging, and endogenous and exogenous

T.D. Hewitson, I.A. Darby (eds.), *Histology Protocols*, Methods in Molecular Biology 611,
DOI 10.1007/978-1-60327-345-9_12,

hypoxia markers (2). Endogenous hypoxia markers are proteins that are induced or altered in expression by hypoxic exposure. They have potential as markers of tumour hypoxia as they are non-invasive and can be assessed on archival materials. Two of the most commonly used endogenous markers of hypoxia are hypoxia inducible factor 1 alpha (Hif1α) and glucose transporter 1 (Glut-1) (5). Hif1α is described as a master protein for the regulation of the cellular response to hypoxia, given that when hypoxia occurs, Hif1α is quickly stabilised and enables the activation of many genes essential to the cellular adaptation to low oxygen conditions (6). Glut-1, which plays a critical role in the transport of glucose into cells, is one of the genes activated by Hif1α. The Glut-1 protein is a membrane-bound transporter that has a high affinity for glucose, and is therefore the main pathway by which glucose enters the cell. Under hypoxic conditions, these transporter proteins play an important role as hypoxic cells are highly dependent upon glucose as their energy source (7).

Exogenous compounds such as pimonidazole (Pim) can also be used for the detection of tissue hypoxia. Pim belongs to a group of 2-nitroimidazole compounds which at oxygen tensions below 10 mmHg undergoes a nitroreductase catalysed single-electron reduction and binds covalently to macromolecular cellular components in hypoxic cells (8). Specific antibodies raised against pimonidazole-protein adducts allow visualisation of tissue hypoxia through immunohistochemical detection.

Through immunohistochemistry (IHC), which utilises the specific binding of antibodies to antigens, proteins of interest can be localised and visualised specifically within a tissue section, a powerful tool for diagnosis of disease processes, such as cancer. In this chapter, we will describe the methods utilised in our laboratories for detecting tumour hypoxia using antibodies directed against Pim, Hif1α and Glut-1. All three of these detection methods are robust and enable visualisation either chromogenically or fluorescently in human, xenograft and mouse FFPE tumour tissue sections.

2. Materials

2.1. Tissue Collection

1. Surgical instruments (scissors, forceps).
2. Ethanol.

2.2. Fixation and Processing for Formalin-Fixed Paraffin-Embedded (FFPE) Tissue

1. 10% Neutral buffered formalin (10% NBF).
2. Paraffin-embedding wax.
3. Processing cassettes.
4. Ethanol.

2.3. Section Preparation for FFPE Sections

1. Microscope slides (Superfrost™ Plus; Thermo-Fisher Scientific, Fremont, CA, USA).
2. Slide racks.

2.4. Immunohistochemistry

1. Histolene or xylene.
2. Ethanol.
3. Wash buffer: 50 mM Tris/HCl buffer.
4. Antibody diluent (Dako, Glostrup, Denmark).
5. Hydrogen peroxide (H_2O_2).
6. Antigen retrieval solutions (ARS) (*see* **Sections 2.5–2.7**; **Table 12.1**).
7. Primary antibodies (*see* **Sections 2.5–2.7**; **Table 12.1**).
8. Hydrophobic wax pen.
9. Secondary antibodies for chromogenic or fluorescent detection (*see* **Sections 2.5–2.7**; **Table 12.1**).
10. Entellan™ mounting media (ProSciTech, Thuringowa, Qld, Australia).
11. Cover slips.

Table 12.1
Summary of antigen retrieval solutions and antibody dilutions

Marker	Antigen retrieval solution	Primary antibody (dilution)	Secondary antibody for chromogenic detection (dilution)	Secondary antibody for fluorescent detection (dilution)
Pim	10 mM sodium citrate (pH 6.0)	Hypoxyprobe™ 1-Mab1 FITC conjugate (1:400)	Mouse anti-FITC (1:400)	Not required
Hif1α	100 mM Tris/ 10 mM EDTA/ 0.5% Tween solution (pH 9.0)	Mouse monoclonal anti-Hif1α (1:200)	EnVision™+ System-HRP anti-mouse (ready to use)	AlexaFluor™ 488 goat anti-mouse (1:500)
Glut-1	10 mM sodium citrate (pH 6.0)	Rabbit polyclonal anti-Glut-1 (1:200)	EnVision+™ System-HRP anti-rabbit (ready to use)	AlexaFluor™ 568 goat anti-rabbit (1:500)

2.5. Pimonidazole

2.5.1. Pimonidazole Preparation and Injection

1. Pimonidazole (Millipore, Billerica, MA, USA).
2. Saline.
3. 0.3-mL insulin syringe (for injection).

2.5.2. Pimonidazole Histochemistry

1. ARS: 10 mM sodium citrate (pH 6.0).
2. Primary antibody: Hypoxyprobe™ 1-Mab1 conjugated to fluorescein isothiocyanate (FITC) (Millipore).

2.5.2.1. Chromogenic Detection

1. Secondary antibody/detection: Mouse anti FITC (Millipore).
2. Dako liquid 3,3′-diaminobenzidine (DAB) (Dako).

2.5.2.2. Fluorescent Detection

1. Prolong-Gold™ with Dapi (Molecular Probes, Invitrogen, Carlsbad, CA, USA).

2.6. Hif1α Immunohistochemistry

1. ARS: 100 mM Tris/10 mM EDTA/0.5% Tween solution (pH 9.0).
2. Primary antibody: Mouse monoclonal anti-Hif1α (Novus Biologicals, Littleton, CO, USA).

2.6.1. Chromogenic Detection

1. Secondary antibody/detection: EnVision+™ System-horseradish peroxidase conjugated (HRP) anti-mouse (Dako).
2. Dako liquid DAB (Dako).

2.6.2. Fluorescent Detection

1. Secondary antibody/detection: AlexaFluor™ 488 goat anti-mouse (Molecular Probes, Invitrogen).
2. Prolong-Gold™ with Dapi (Molecular Probes, Invitrogen).

2.7. Glut-1 Immunohistochemistry

1. ARS: 10 mM sodium citrate (pH 6.0).
2. Primary antibody: Rabbit polyclonal anti-Glut1 (Lab Vision, Thermo-Fisher Scientific).

2.7.1. Chromogenic Detection

1. Secondary antibody/detection: EnVision™ + System-HRP anti-rabbit (Dako).
2. Dako liquid DAB (Dako).

2.7.2. Fluorescent Detection

1. Secondary antibody/detection – AlexaFluor™ 568 goat anti-rabbit (Molecular Probes, Invitrogen).
2. Prolong-Gold™ with Dapi.

3. Methods

3.1. Pimonidazole Injection

1. Freshly prepare pimonidazole at 60 mg/kg by dissolving in required volume of saline.
2. Three hours prior to sacrifice, inject pimonidazole via intravenous tail vein injection.

3.2. Collection, Fixation, Processing and Embedding of Tissue

1. Sacrifice mouse, carefully remove tumour, cut into two halves.
2. Place each half in a processing cassette and immerse in 10% NBF, leave overnight and then place into 70% ethanol.
3. Dehydrate tissue through the following solutions $2 \times 70\%$ ethanol (30 min each), $4 \times 100\%$ alcohol (1 h each), $4 \times$ histolene or xylene (1 h each), $4 \times$ paraffin wax at approximately 58°C (1 h each).
4. Ensuring correct orientation of the tissue (i.e. cut surface face down), embed the tissue in wax using the stainless steel molds. Place the molds on ice for 15 min and then remove the paraffin block from the mold.

3.3. Tissue Sectioning

1. Fill a small shallow container with distilled H_2O and prepare a water bath at 50°C.
2. Cut 3–4 μm sections of the paraffin-embedded tissue on a microtome.
3. Float the sections on the surface of the warmed H_2O bath. Pick up the section on a Superfrost™ Plus-coated glass slide. The section should flatten onto the slide and have no creases or folds.
4. Stand the section vertically until dry, then incubate overnight at 37°C.

3.4. Immunohistochemistry

In each IHC experiment, always include a positive control of a tissue section with known positive staining for each antibody to be tested. If the positive control section stains as expected, then you can be confident that the procedure has worked and all "test" sections have stained appropriately. Also, always include a negative control, a "test" section which is treated the same as the other "test" slides but for which the primary antibody is omitted. This section should have no staining at the end of the procedure, demonstrating that any positive staining is real and specific.

The following method is used for Pim, Hif1α and Glut-1 IHC on FFPE sections (*see* **Note 1**), using the relevant ARS, primary antibody and secondary antibody/detection for each, as specified.

3.4.1. Deparaffinising, Antigen Retrieval and Primary Antibody Incubation

1. Dewax slides (3×5 min) in histolene or xylene, rehydrate through graded ethanol (70, 90, 100%) and wash (2×5 min) in distilled H_2O.
2. Place the slides in a slide rack and place into a container that allows the sections to be fully immersed in appropriate ARS (**Table 12.1**). Place container into a pressure cooker and set for 2 min at approximately 125°C, 15–18 pounds per square inch (PSI), then cool to 90°C, before opening.
3. Rinse slides in distilled water for 5 min (*see* **Note 2**).

4. Incubate slides in 3% H_2O_2 in water for 10 min to block endogenous peroxidase activity.
5. Using a wax pen, draw a circle around the tissue section. This enables the solutions in the following steps to be used in small volumes and ensures that the tissue section is always covered by solution (*see* **Note 3**).
6. Dilute relevant primary antibody (**Table 12.1**) to recommended dilution using antibody diluent.
7. Incubate slides with diluted primary antibody for 60 min at room temp (*see* **Note 4**) in a humidified chamber (*see* **Note 5**). The volume of antibody required is determined by the size of the tissue section; typically 200 μL will cover most sections adequately.
8. Rinse twice in 50 mM Tris/HCl buffer for 5 min.
9. For chromogenic detection, follow **Section 3.4.2**; for fluorescent detection, follow **Section 3.4.3**.

3.4.2. Chromogenic Detection – Secondary Antibody Incubation, DAB and Counterstain

1. Incubate slides with a species-matched HRP-conjugated secondary antibody (**Table 12.1**) for 60 min at room temperature in a humidified chamber.
2. Rinse twice in 50 mM Tris/HCl buffer for 5 min.
3. Incubate sections in liquid DAB for 10 min.
4. Rinse in distilled water.
5. Counterstain for 10–30 s with hematoxylin (*see* **Note 6**).
6. Dehydrate through 5 × 100% ethanol (2 min each), clear in 3 × histolene or xylene (2 min each), mount with mounting media and cover slip.
7. Visualise using a light microscope.

3.4.3. Fluorescent Detection – Secondary Antibody Incubation and Dapi

1. Incubate slides with a species-matched fluorescent secondary antibody (**Table 12.1**) diluted in antibody diluent for 60 min at room temperature in a humidified chamber
2. Rinse twice in 50 mM Tris/HCl buffer for 5 min.
3. Mount sections with Prolong-Gold™ Dapi (*see* **Note 7**).
4. Visualise on a fluorescence microscope.
5. Store sections horizontally on a slide tray wrapped in foil at 4°C to preserve fluorescence.

3.5. Interpretation of Results

Positive chromogenic DAB staining should appear as a dark brown color against the light blue/purple of the hematoxylin counterstain. Staining intensity will vary depending on whether the antibody localises to nucleus, cytoplasm or membrane and depending on the number of positive cells.

Positive fluorescent staining should appear as red or green (or color of secondary antibody) against a blue (Dapi) background.

3.5.1. Pimonidazole

The staining pattern for Pim staining appears as strong nuclear and cytoplasmic staining and can often appear as a gradient of weak staining on the outer edge of hypoxic areas through to intense staining at the centre of the hypoxic area (*see* **Figs. 12.1–12.3**).

3.5.2. Hif1α

Hif1α-positive staining appears as nuclear-staining pattern (*see* **Figs. 12.1 and 12.4**). The intensity can be variable and is often weak. Hif1α typically does not label as many cells as Pim.

3.5.3. Glut-1

The Glut-1 staining pattern is strong membranous and cytoplasmic staining and generally appears very similar in appearance to pimonidazole staining (*see* **Figs. 12.2–12.4**).

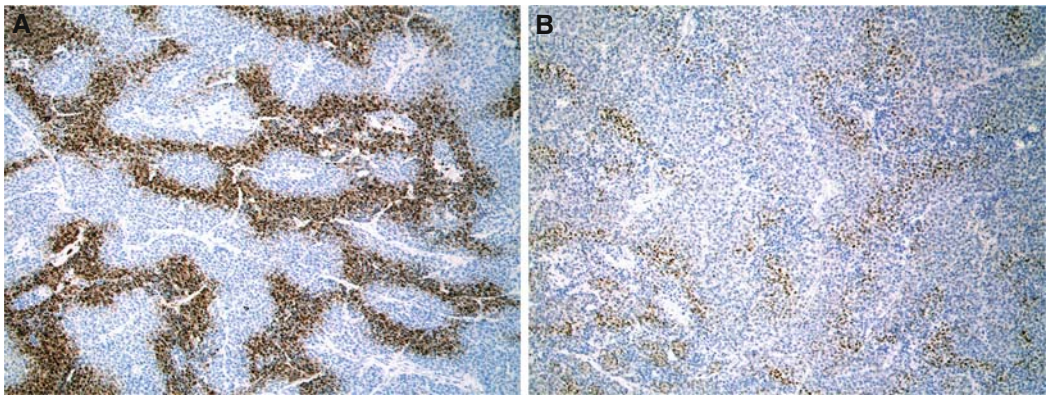

Fig. 12.1. Examples of Pim and Hif1α chromogenic IHC staining in a transplanted mouse Her2/Neu breast cancer model. (**a**) Pim, (**b**) Hif1α (× 10 magnification).

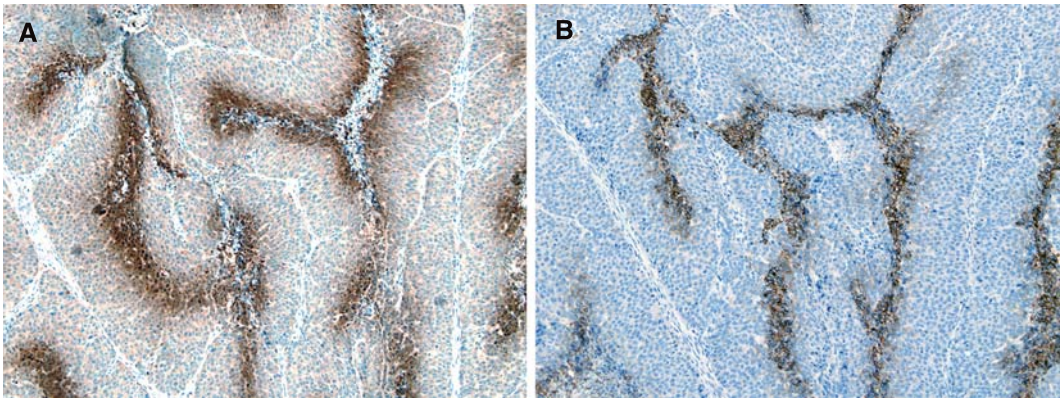

Fig. 12.2. Examples of Pim and Glut-1 chromogenic IHC staining in a spontaneous mouse Polyoma Middle T (PyMT) breast cancer model. (**a**) Pim, (**b**) Glut-1 (× 10 magnification).

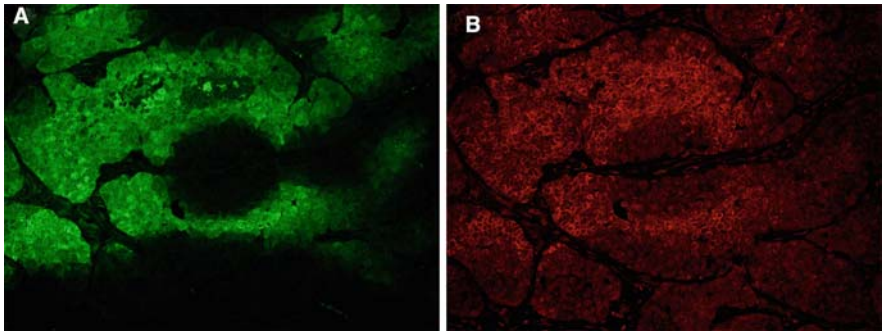

Fig. 12.3. Examples of Pim and Glut-1 fluorescent staining in a transplanted mouse Her2/Neu breast cancer model. (**a**) Pim, (**b**) Glut-1 ($\times$ 20 magnification).

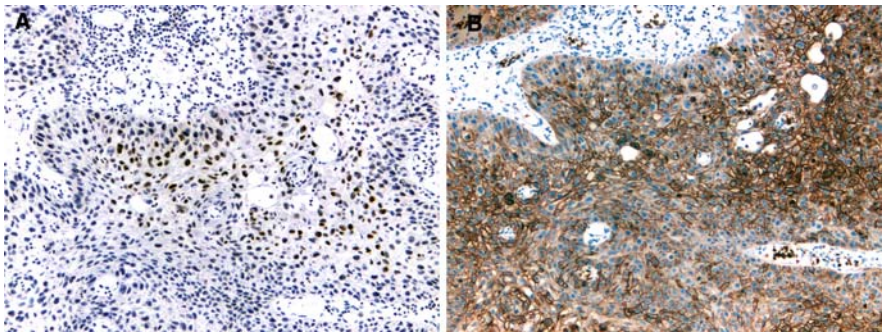

Fig. 12.4. Examples of Hif1α and Glut-1 chromogenic IHC staining in human head and neck cancer. (**a**) Hif1α, (**b**) Glut-1 ($\times$ 10 magnification).

4. Notes

1. The preceding methods for all three antibodies can also be used on frozen sections (with some modifications) with very good results. A major disadvantage of frozen sections is that the morphology of frozen sections is inferior to FFPE. We have limited the methods in this chapter to describing IHC on FFPE sections.
2. It is essential that the tissue sections never dry out during the procedure. Therefore, due to the small volume of liquid placed on the sections for several steps, it is important to perform all incubations in a humidified chamber.
3. An alternative to using a wax pen is to place a cover slip over the slide after each solution is added. This spreads the solution over the entire section. Care must be taken when removing the cover slip between incubations so as not to scratch the tissue section.

4. Incubation times and temperatures can vary between antibodies. Many IHC methods suggest overnight incubations at 4°C. Optimal conditions should be determined by the user.
5. A plastic container and lid, with a moist paper towel on the bottom, is an effective humidified chamber.
6. The length of time to counterstain in hematoxylin will vary and should be determined by the user. The counterstain should ideally be a weak blue/purple color which allows identification of non-stained tissue/cells and provides a contrast to the brown DAB-positive staining.
7. Prolong-Gold™ acts as a preservative for the fluorescence and should enable fluorescently labeled sections to be kept for several months at 4°C. To avoid leakage, slides can be sealed with nail polish around the edge of the cover slip.

References

1. Troost, E.G., Laverman, P., Philippens, M.E.P., Lok, J., van der Kogel, A.J., Oyen, W.J.G., Boerman, O.C., Kaanders, J.H.A.M., and Bussink, J. (2008) Correlation of [18F]FMISO autoradiography and pimonidazole immunohistochemistry in human head and neck carcinoma xenografts. *Eur. J. Nucl. Med. Mol. Imaging* **35**, 1803–1811.
2. Ljungkvist, A.S.E., Bussink, J., Kaanders, J.H.A.M., and van der Kogel, A.J. (2007) Dynamics of tumor hypoxia measured with bioreductive hypoxic cell markers. *Radiat. Res.* **167**, 127–145.
3. Le, Q. (2007) Identifying and targeting hypoxia in head and neck cancer: a brief overview of current approaches. *Int. J. Radiat. Oncol. Biol. Phys.* **69**, S56–S58.
4. Rischin, D., Fisher, R., Peters, L., Corry, J., and Hicks, R. (2007) Hypoxia in head and neck cancer: studies with hypoxic cytotoxins. *Int. J. Radiat. Oncol. Biol. Phys.*, **69**, S61–S63.
5. Vordermark, D. and Brown, M. (2003) Endogenous markers of tumor hypoxia: predictors of clinical radiation resistance? *Strahlenther. Onkol.* **179**, 801–811.
6. He, F., Xuelong, D., Bixiu, W., Yueping, L., Xiaorong, S., Ligang, X., Akiko, M., Huang, Y., Chen, Q., Zanzonico, P.B., Ling, C.C., and Lil, G.C. (2008) Noninvasive molecular imaging of hypoxia in human xenografts: comparing hypoxia-induced gene expression with endogenous and exogenous hypoxia markers. *Cancer Res.* **68**, 8597–8606.
7. Tian, M., Zhang, H., Nakasone, Y., Mogi, K., and Endo, K. (2004) Expression of Glut-1 and Glut-3 in untreated oral squamous cell carcinoma compared with FDG accumulation in a PET study. *Eur. J. Nucl. Med. Mol. Imaging* **31**, 5–12.
8. Solomon, B., Binns, D., Roselt, P., Weibe, L.I., McArthur, G.A., Cullinane, C., and Hicks, R.J. (2005) Modulation of intratumoral hypoxia by the epidermal growth factor receptor inhibitor gefitinib detected using small animal PET imaging. *Mol. Cancer. Ther.* **4**, 1417–1422.

Chapter 13

In Situ Localization of Apoptosis Using TUNEL

Tim D. Hewitson and Ian A. Darby

Abstract

Apoptosis is an important process both in normal biology and in various pathologies and disease states. Apoptosis in tissue or cells can be detected in a number of ways. In tissue sections, electron microscopy can identify apoptosis by cellular and nuclear morphology, and in live cells, changes in the membrane and membrane permeability allow apoptosis and necrosis to be observed. Histologically, apoptosis is best detected using the partial DNA degradation that is present in apoptotic cell nuclei. Terminal transferase-mediated UTP nick end-labeling (TUNEL) has been used successfully for detection of DNA degradation in paraffin-embedded tissue sections and can be combined with immunohistochemistry if desired to allow more precise identification of apoptotic cells.

Key words: TUNEL, apoptosis, DNA fragmentation, necrosis.

1. Introduction

Apoptosis is a morphologically distinct form of "programmed" cell death. It has a role in such processes as embryogenesis, immune regulation, and defence against viruses and can also be induced by a variety of physical and chemical stimuli (1). Importantly apoptosis leads to the safe removal of cells by phagocytosis, whereas in contrast, necrosis provokes tissue injury and inflammation. Apoptotic cell death is associated with a number of biochemical and morphological changes including de novo gene expression, condensation of chromatin, and DNA degradation. Many attempts have been made to utilize these changes in the identification of apoptosis, with varying degrees of success. Although a number of specific gene products are now known to be associated with apoptosis (2), histochemical studies still rely on the specific morphological changes that occur during this process.

T.D. Hewitson, I.A. Darby (eds.), *Histology Protocols*, Methods in Molecular Biology 611,
DOI 10.1007/978-1-60327-345-9_13,

These have been defined as the sequential condensation of nuclear chromatin, formation of membrane-bound cell fragments termed apoptotic bodies, and finally engulfment by professional and recruited phagocytes. Although these criteria are easily recognized in tissue sections viewed by electron microscopy (**Fig. 13.1**), the relative rarity of its occurrence makes its quantitation by this means problematic. Activation of endonuclease activity during the process of cell death (3) causes DNA fragmentation in apoptotic cells. This produces a characteristic ladder of oligonucleosome-sized DNA fragments on agarose gel electrophoresis. While applicable to pure cell populations, gel electrophoresis is difficult to apply to in situ studies with mixed cell populations.

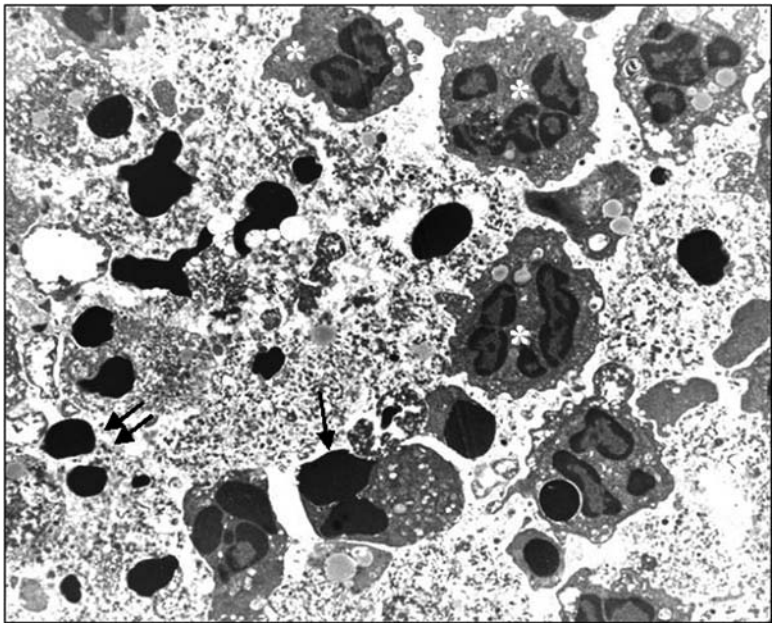

Fig. 13.1. Electron micrograph of polymorphonuclear granulocyte apoptosis in a rat model of experimental renal infection. Resolution of tubulointerstitial nephritis occurs through apoptosis of inflammatory cells and drainage of apoptotic cells through the tubular lumen. The various stages of polymorph apoptosis are labeled. Several normal polymorphs are visible with irregular outlines and granular appearance of nuclear chromatin (*white asterisk*). The increased electron density of chromatin can be seen in the early stages of budding (*single arrow*), while numerous apoptotic bodies (*double arrows*) are distributed throughout the lumen.

The presence of DNA fragmentation has however now been adapted to the in vivo identification of apoptosis. Apoptotic cells may be localized by the in situ labeling of this fragmented DNA using terminal transferase-mediated UTP nick end-labeling (TUNEL) (4). In this technique, labeled-dUTP is attached to the 3′ end of these breaks by terminal transferase (TdT) and is

then detected using immunohistochemical techniques. TUNEL has been used successfully to study apoptosis in a diverse range of biological systems including among others, developmental biology (5), immunoselection (6), wound healing (7), and glomerulonephritis (8).

It is however important to remember that DNA fragmentation is not confined to apoptosis exclusively. Fragmentation of DNA is also found in the late stages of necrosis, although the nuclear floculation and diffuse labeling pattern result in differences in histological appearance compared to apoptosis (*see* **Figs. 13.2 and 13.3**). Several in vitro studies have however confirmed that end-labeling of fragmented DNA correlates with the incidence of apoptosis, as measured by other parameters (9). Furthermore, there are some data to suggest that single-strand DNA breaks, as in necrosis, are labeled less easily than the double-stranded fragmentation in apoptosis (10).

Other techniques can be used to help confirm that observed staining for TUNEL is indeed apoptosis. Immunohistochemical staining for effector proteins in apoptosis such as activated caspase-3 has been used with success and shown to correlate well with apoptosis shown by TUNEL. Similarly, staining for proteins that have been cleaved by caspases such as cytokeratin have also been shown to correlate well with apoptosis (11, 12).

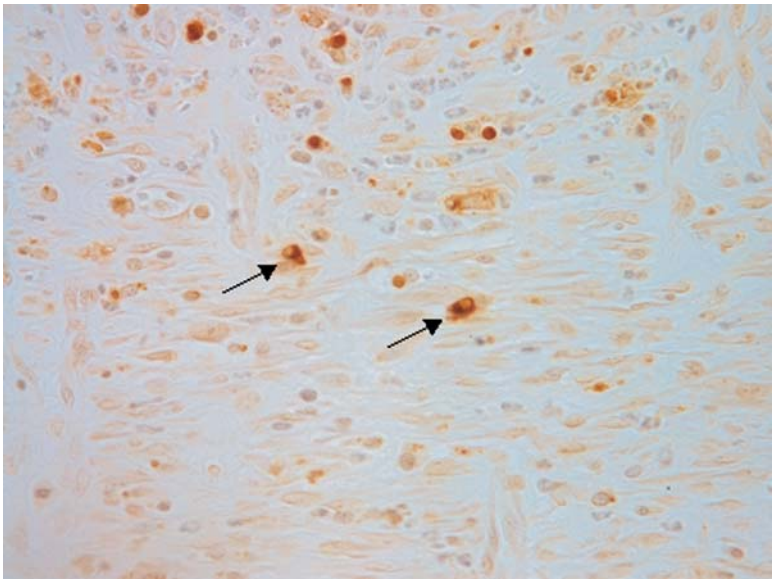

Fig. 13.2. TUNEL staining of an experimental wound showing several positive cells including some cells (*arrowed*) that show classical morphology of apoptosis with pyknotic nuclei and marginalized chromatin.

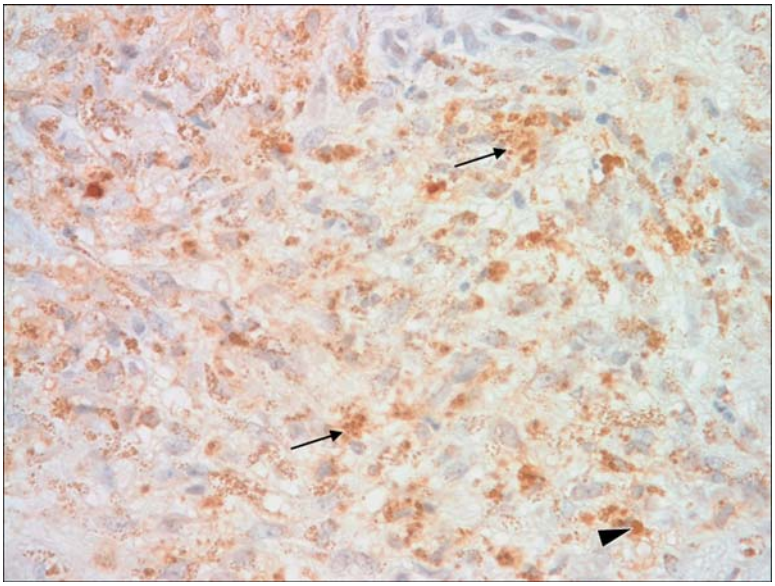

Fig. 13.3. TUNEL staining of human chronic wound tissue showing scattered positive staining in brown; however, the majority of TUNEL-positive structures do not appear to be condensed pyknotic nuclei (*arrow head*) but rather scattered and diffuse granular structures (*arrows*) suggesting TUNEL in this section is detecting necrosis.

Recent studies have identified autophagy as another form of cell death used to remove unwanted or transformed cells. Autophagy is accompanied by expression of specific genes including beclin-1 and this may be used to identify this form of cell death (13).

In summary, despite the limitations of the TUNEL method, the judicious use of this technique may aid considerably in the identification and quantitation of apoptosis in situ. Here we describe how to perform TUNEL staining on sections. Commercial kits are available that will perform TUNEL with a variety of labels and can be used to adapt the technique to other applications such as flow cytometry (*see* **Note 1**).

2. Materials

2.1. TUNEL on Paraffin-Embedded Tissue

1. Paraffin-embedded sections of 10% neutral buffered formalin or 4% paraformaldehyde-fixed tissue collected onto 3′-aminopropyltriethoxysilane (Sigma-Aldrich, St Louis, MO, USA) coated slides (*see* **Notes 2** and **3**). A positive control tissue section should be included to verify that the TUNEL reaction has worked (*see* **Note 4**).
2. Proteinase K (Sigma-Aldrich): stock solution of 20 mg/mL made up in distilled water and Sigma-Aldrich stored at –20°C.

3. Biotin-labeled dUTP (Roche Diagnostics, Penzberg, Germany).
4. Terminal deoxynucleotidyl transferase (TdT) (25 U/μL) (Roche) (*see* **Note 5**).
5. Buffer 1: sodium chloride (30 mL of 5 M stock), sodium citrate (15 mL of 1 M stock), and distilled water added to a total volume of 500 mL (final composition 0.3 M sodium chloride, 0.03 M sodium citrate).
6. Tris/EDTA (TE) buffer: Tris–HCI, pH 7.4 (0.5 mL of 2 M stock), EDTA, pH 8.0 (20 μL of 0.5 M stock), distilled water to 100 mL (final composition 0.01 M Tris, 0.0001 M EDTA).
7. TdT buffer: 15.0 g of sodium cacodylate, 0.119 g of cobalt chloride, 15 mL of 1 M stock Tris–HCI, and distilled water added to a total volume of 500 mL (final composition: 140 mM cacodylate, 1 mM cobalt chloride, 30 mM Tris).
8. Phosphate-buffered saline (PBS), pH 7.2.
9. Vector ABC Elite staining kit (Vector laboratories, Burlingame, CA, USA).
10. Chromogen substrate: 4 mL of 3.3′-diaminobenzidine tetrahydrochloride (DAB) (DAKO, Glostrup, Denmark) mixed with 3 μL of 30% H_2O_2. An equivalent commercial preparation (e.g., metal-enhanced diaminobenzidine [DAB], Pierce, Rockford, EL, USA) may be substituted.
11. Humidified staining tray.
12. Microscope.
13. Staining racks and baths.
14. Wax pen (DAKO or equivalent).
15. Harris' hematoxylin.
16. Scott's tap water: 20 g of $MgSO_4$–$7H_2O$, 3.5 g of $NaHCO_3$, made up to I L with distilled water (final concentrations: 0.081 M of $MgSO_4$, 0.041 M of $NaHC0_3$).
17. DNase I (Promega, Madison, WI, USA).
18. Absolute ethanol.
19. Xylene.
20. 0.45 μM Syringe filter.
21. Depex™ (BDH, Poole, UK) or other nonaqueous mounting media.

2.2. Additional Materials for Combined Immunohistochemistry and TUNEL

1. Tris-buffered saline (TBS), pH 7.4 (25 mM Tris base, 0.9% NaCl, adjust pH to 7.4 with HCl).
2. Primary cell-specific antisera (e.g., leukocyte marker).

3. Alkaline phosphatase–anti-alkaline phosphatase complex (DAKO).
4. Alkaline phosphatase-conjugated anti-IgG serum (species specific for primary antiserum) (DAKO).
5. Fast red substrate (Sigma-Aldrich).
6. Aquamount™ (BDH) or other aqueous mounting media.

3. Methods

3.1. TUNEL Protocol

1. Heat paraffin-embedded tissue sections in a 60°C oven for 10 min.
2. Dewax tissue sections by transferring slides immediately to a xylene bath for 5 min.
3. Rehydrate tissue in graded (100, 75, 50%) alcohols and wash in distilled water for 5 min.
4. Digest sections by treatment with proteinase K (1 μL of 20 μg/mL stock in 1,000 μL of TE buffer) for 15 min at room temperature (*see* **Note 6**).
5. Wash tissue sections in TdT buffer for 5 min.
6. Outline the section with a wax pen to create a hydrophobic barrier around the tissue section, thereby reducing the volume of reagents required.
7. Incubate sections at 37°C with 1 μL of biotin-labeled dUTP and 1 μL of TdT in 100 μL of TdT buffer for 30 min in a humid atmosphere.
8. Wash in buffer 1 to terminate the reaction.
9. Detect in situ incorporation of biotinylated dUTP by incubating sections with biotin horseradish peroxidase complex (ABC Elite kit) for 15 min or according to the manufacturer's instructions.
10. Wash in PBS 2 × 5 min.
11. Develop reaction product by staining with DAB/H_2O_2 substrate for 3–7 min at room temperature. Most DAB solutions made from DAB in powder or tablet form should be filtered through a 0.45-μm syringe filter prior to use. Monitor DAB/H_2O_2 on wet slides using a microscope with a low-power (×10) objective.
12. Terminate the staining by rinsing in distilled water when the ratio of positive staining of apoptotic nuclei to background staining is maximal.
13. Wash in distilled water (5 min).

14. Counterstain sections with Harris' hematoxylin (1–2 min depending on strength of hematoxylin), rinse in tap water, dip briefly in Scott's tap water (3 ×) until the sections are visibly "blued," and wash in tap water for 5 min.
15. Finally, dehydrate in graded (50, 75, 100%) alcohols, rinse in xylene, and mount with Depex™.

3.2. Combined Immunohistochemistry and TUNEL Protocol

The TUNEL technique can be combined with immunohistochemistry for cytoplasmic or surface markers to identify apoptotic cell phenotype (6) and/or phagocytosis of apoptotic bodies (14).

1. Follow the TUNEL protocol in **Section 3.1** for steps 1–11 inclusive.
2. Wash in TBS (*see* **Note 7**) for 3 min × 2.
3. Incubate with primary antiserum for 1 h at room temperature in a humidified container (determine appropriate dilution empirically).
4. Wash sections in TBS for 3 min × 2.
5. Incubate for 20 min with alkaline phosphatase-conjugated anti-IgG serum (species specific for primary antiserum) (1:50 dilution in TBS).
6. Wash in TBS for 3 min × 2.
7. Incubate for 20 min with alkaline phosphatase–anti-alkaline phosphatase complex (1:50 dilution in TBS).
8. Wash in TBS 3 min × 2 for 3 min × 2.
9. Detect alkaline phosphatase reaction product by incubation with fast red substrate for 10–20 min at room temperature. Monitor substrate reaction microscopically, terminating the reaction by washing in distilled water for 5 min.
10. Counterstain sections as described previously.
11. Mount sections in Aquamount™ (*see* **Note 8**).
12. View by light microscopy (*see* **Note 9**).

4. Notes

1. Commercial kits for performing apoptosis labeling by TUNEL using a number of different detection techniques are available. These allow TUNEL to be preformed on sections or cultured cells and detection by either colorimetric or fluorescent methods (e.g., Deadend™, Promega, Madison, WI, USA)

2. 4% paraformaldehyde or paraformaldehyde–lysine–periodate (PLP) may be substituted for neutral buffered formalin. Fixatives that denature DNA (e.g., mercuric formalin) may result in artifactual labeling of nuclei and are therefore unsuitable for TUNEL.

   False-positive labeling is an artifact associated with any delay between retrieval of tissue and fixation.

3. 3′-Aminopropyltriethoxysilane (APES) coating of slides: Pretreatment of microscope slides with APES prevents sections falling off during protease digestion. Importantly it also avoids having to "bake" sections in a hot oven, as is often routinely used in histology laboratories to ensure adherence of the tissue.

   APES-coated slides can be prepared by sequentially washing microscope slides in (a) dilute laboratory detergent overnight, (b) running tap water for 3 h, (c) distilled water for 2×5 min, and (d) 95% alcohol for 2×5 min. Slides are then air dried before being dipped in a freshly prepared 2% solution of APES (Sigma-Aldrich) in 100% acetone (BDH) for 10 s. Slides are then washed in (a) acetone for 2×5 min and (b) distilled water for 2×5 min and air dried at 40°C in a hot air oven for 12 h. Slides may be stored at room temperature in a dust-free container until use. Alternatively, commercially coated or charged slides such as Superfrost plus slides (Menzel Glaser, Braunschweig, Germany) can be used.

4. Positive controls consist of TUNEL labeling of rat ovary or lymph node sections and of tissue sections pretreated with DNase I at a concentration of 1 μg/mL TBS for 5 min. TUNEL labeling of tissue sections in the absence of TdT is used as a negative control. DNase digestion results in positive labeling of all nuclei (4), while the TUNEL reaction in the absence of TdT leaves all nuclei unlabeled. Sections of small intestine may not be a suitable positive control. Despite Gavrieli et al. (4) describing labeling of the intestinal villus in their original description of the TUNEL method, doubts have been raised about the specificity of this reaction (9).

5. In situ end-labeling (ISEL) as described by Wijsman et al. (15) is a variant of the above technique where the enzyme Klenow DNA polymerase I is substituted for terminal deoxynucleotidyl transferase (TdT). There is some evidence that TdT is preferable to DNA polymerase because more favorable kinetics are reflected in shorter incubation times (16).

6. Optimal concentration and time of protease digestion may have to be established empirically for individual tissues. Microwave treatment has been substituted for protease digestion by some investigators (17). Overdigestion using proteinase K may result in false-positive results; therefore digestion times need to be established for each tissue.

7. Tris-buffered saline is used in all washes in the double labeling procedure as phosphate-buffered saline is incompatible with subsequent alkaline phosphatase detection.
8. Avoid section dehydration or solvent-based mountants as they will remove fast red reaction product.
9. The definition of apoptosis is still essentially based on morphological criteria. The presence of apoptosis may therefore need to be substantiated by electron microscopy (**Fig. 13.1**) or the identification of morphological features in TUNEL-positive cells. Apoptotic cells are often recognizable on light microscopy as condensed TUNEL-positive chromatin with marginalized dense staining chromatin or a positive nucleus lying within a "halo" of what was the cell cytoplasm. Such a phenomenon is presumably due to the contraction of cell cytoplasm in combination with the rapid kinetics of apoptosis. Apoptotic cells are usually expressed as a proportion (%) of total cell number or as the number of apoptotic cells per unit area (e.g., 10×0.25 μm fields).

   Kinetic studies have suggested that apoptotic cells are histologically recognizable for 0.5–2.0 h before clearance (8). Identification of a low rate of apoptosis therefore still indicates the removal of a significant proportion of the cell population. For example, if apoptotic bodies are visible for 2 h, a 1% incidence of visible apoptosis may represent clearance of up to 12% of cells within 24 h. This study highlights that for statistical validity it is necessary to examine sufficient nuclei (at least 1,000) when enumerating the incidence of apoptosis.

References

1. Ueda, N. and Shah, N. (1994) Apoptosis. *J. Lab. Clin. Med.* **124**, 169–177.
2. Martin, D.A. and Elkon, K.B. (2004) Mechanisms of apoptosis. *Rheum. Dis. Clin. North Am.* **30**, 441–454.
3. Arends, M.J., Morris, R.G., and Wyllie, A.H. (1990) Apoptosis: the role of endonuclease. *Am. J. Pathol.* **136**, 593–608.
4. Gavrieli, Y., Shermm, Y., and Ben-Sasson, S. (1992) Identification of programmed cell death in situ via specific labeling of nuclear DNA fragmentation. *J. Cell Biol.* **119**, 493–501.
5. Fekete, D.M., Homburger, S.A., Waring, M.T., Riedl, A.E., and Garcia, L.F. (1997) Involvement of programmed cell death in morphogenesis of the vertebrate inner ear. *Development* **124**, 2451–2461.
6. Smith, K.G.C., Hewitson, T.D., Nossal, G.J.V., and Tarlinton, D.M. (1996) The phenotype and fate of the antibody-forming cells of the splenic foci. *Eur. J. Immunol.* **26**, 444–448.
7. Darby, I.A., Bisucci, T, Hewitson, T.D., and MacLellan, D.G. (1997) Apoptosis is increased in a model of diabetes-impaired wound healing in genetically diabetic mice. *Int. J. Biochem. Cell Biol.* **29**, 191–200.
8. Baker, A.J., Mooney, A., Hughes, I., Lombardi, D., Johnson, R.J., and Savill, J. (1994) Mesangial cell apoptosis: the major mechanism for resolution of glomerular hypercellularity in experimental mesangial proliferative nephritis. *J. Clin. Invest.* **94**, 2105–2116.
9. Ansari, B., Coates, P.J., Greenstein, B.D., and Hall, P.A. (1993) In situ end labeling detects DNA strand breaks in apoptosis and other physiological and pathological states. *J. Pathol.* **170**, 1–8.

10. Hockenbery, D. (1995) Defining apoptosis. *Am. J. Pathol.* **146**, 16–19.
11. Duan, W.R., Garner, D.S., Williams, S.D., Funckes-Shippy, C.L., Spath, I.S., and Blomme, E.A. (2003) Comparison of immunohistochemistry for activated caspase-3 and cleaved cytokeratin 18 with the TUNEL method for quantification of apoptosis in histological sections of PC-3 subcutaneous xenografts. *J. Pathol.* **199**, 221–228.
12. Gown, A.M. and Willingham, M.C. (2002) Improved detection of apoptotic cells in archival paraffin sections: immunohistochemistry using antibodies to cleaved caspase-3. *J. Histochem. Cytochem.* **50**, 449–454.
13. Høyer-Hansen, M., Bastholm, L., Mathiasen, I.S., Elling, F., and Jäättelä, M. (2005) Vitamin D analog EB1089 triggers dramatic lysosomal changes and Beclin 1-mediated autophagic cell death. *Cell Death Differ.* **12**, 1297–1309.
14. Hewitson, T.D., Smith, K.G.C., and Becker, G.J. (1996) Apoptosis and resolution of experimental renal infective tubulointerstitial nephritis. *Nephrology* **2**, 127–132.
15. Wijsman, J.H., Jonker, R.R., Keijzer, R., Van de Velde, C.J.H., Comelisse, C.J., and Van Dierendonck, J.H. (1993) A new method to detect apoptosis in paraffin sections: in situ end-labeling of fragmented DNA. *J. Histochem. Cytochem.* **41**, 7–12.
16. Gorczym, W., Gong, J., and Darzynkiewicz, Z. (1993) Detection of DNA strand breaks in individual apoptotic cells by the in situ terminal deoxynucleotidyl transferase and nick translation assays. *Cancer Res.* **53**, 1945–1951.
17. Strater, J., Gunthem, A.R., Bruderlein, S., and Moller, P. (1995) Microwave irradiation of paraffin-embedded tissue sensitizes the TUNEL method for in situ detection of apoptotic cells. *Histochemistry* **103**, 157–160.

Part III

Imaging Techniques

Chapter 14

Use of Confocal Microscopy for Three-Dimensional Imaging of Neurons in the Spinal Cord

Martin Stebbing, Simon Potocnik, Pinglu Ye, and Emilio Badoer

Abstract

Confocal microscopy provides a powerful and efficient tool for studying the morphology of cells. Here we describe its use to study the morphology of neurons in the dorsal horn of the spinal cord either following electrophysiological studies in live tissue slices or in neurons filled with dye in fixed tissue sections following identification using retrograde tracing. The methods are broadly applicable to other cell types and can be combined with multiple label immunohistochemistry to study cellular constituents or with subsequent DAB staining to produce a permanent mount.

Key words: Confocal microscopy, immunohistochemistry, spinal cord, neuron.

1. Introduction

Understanding the function of complex cells invariably requires a detailed analysis of their cellular structure and often their intracellular architecture. Three-dimensional studies of complex cellular morphology once involved a tedious, frustrating process of serial sectioning, processing and visualization of multiple histological sections, and manual or mostly manual reconstruction. The advent of confocal microscopy and optical sectioning techniques has since revolutionized the study of cellular morphology and made possible the visualization and fine localization of multiple epitopes and cellular markers within and around cells without serial sectioning (**Figs. 14.1 and 14.2**).

Confocal microscopy, while technically complex, relies on the simple principle that an appropriately placed pinhole will only pass light from a single thin focal plane. In this respect, a confocal

T.D. Hewitson, I.A. Darby (eds.), *Histology Protocols*, Methods in Molecular Biology 611,
DOI 10.1007/978-1-60327-345-9_14,

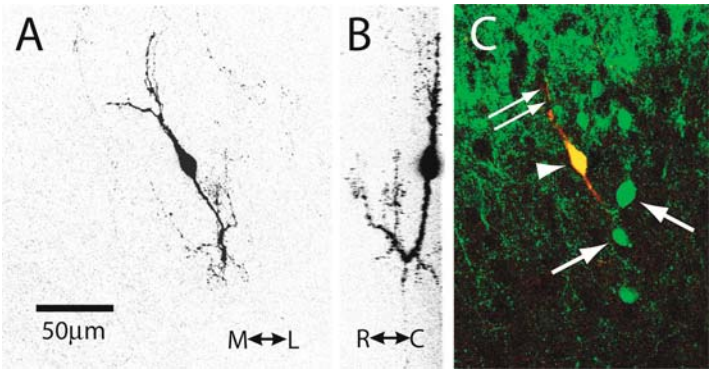

Fig. 14.1. (**a**, **b**) Three-dimensional reconstruction of a rat spinal dorsal horn neuron filled with biocytin from two different angles. The original fluorescent image has been inverted to better show fine detail of cellular processes. M↔L indicates mediolateral direction, R↔C indicates rostrocaudal dimension. (**c**) The same neuron shown in *red* (*double arrows*) overlayed with immunohistochemical staining for calbindin, a calcium-binding protein in *green* (*arrows*). Colocalization is shown in *yellow* (*arrow head*). The images were taken using a Biorad MRC 100 microscope mounted on a Zeiss Axioskop microscope.

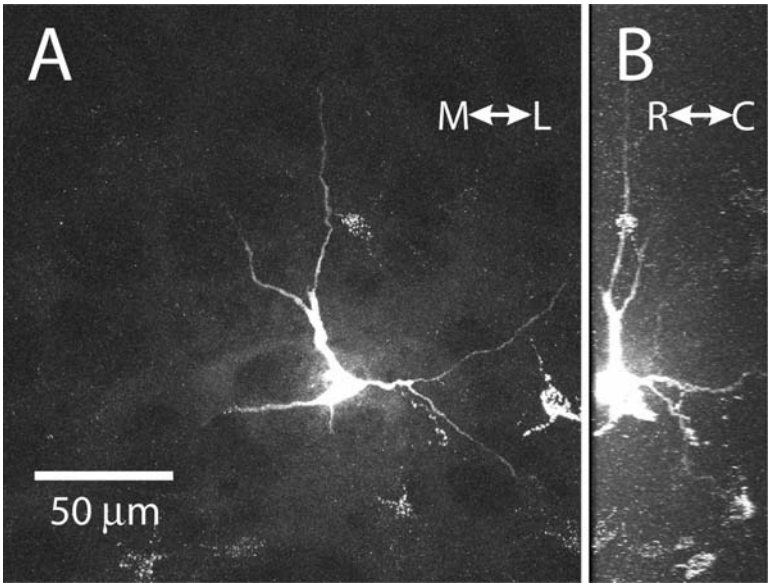

Fig. 14.2. Confocal *z*-stack of a spinal cord neuron filled with Lucifer *yellow* in a fixed tissue section following retrograde labeling from the dorsal column nuclei (*see* **Chapter 6** for a description of the retrograde tracing method). Note the presence of another retrogradely labeled neuron in the same image. Two different aspects of the same cell are shown in **a** and **b**.

microscope is much like a simple "pinhole camera." This property allows a confocal attachment to a conventional light microscope to obtain an "optical section" of the preparation being viewed. By alternately capturing an image and then moving the focus of the

microscope, a series of optical sections defining the three-dimensional structure of the preparation can be obtained. If the size of the pinhole is changed, the thickness of each optical section can be varied. The two main types of confocal microscopes currently available differ principally in the way that they obtain an image. Laser scanning confocals build up an image by scanning a laser across a preparation containing fluorescent molecules and detecting the emitted light from each pixel in the image in turn using sensitive photomultipliers. Spinning disc confocal microscopes detect the light coming from a preparation using a CCD camera but use multiple pinholes arranged in a disc that spins in order to scan the preparation and build up an image.

When combined with electrophysiological recordings and cell filling, confocal microscopy can be used to characterize single cells functionally, morphologically, and chemically (1). This chapter describes the use of these techniques to study the properties of the most complex cells in the body, that is neurons. The techniques discussed have most commonly and successfully been applied to neurons. Nevertheless, they should be applicable to any complex cells that require detailed morphological analysis. The drawback of using fluorescent preparations is that the prolonged imaging required to study the fine detail of cellular morphology can cause fluorophores to fade, although this is less of a problem with the advent of new fluorescent molecules such as quantum dots. We describe here a method for converting fluorescent preparations to permanent histological stains following fluorescence imaging (2). With this technique, it is possible to add fine structural characterization to the suite of techniques that can be applied to a single cell (3).

While a discussion of the complex methods involved in electrophysiological characterization of cells is beyond the scope of this chapter, the principle of using a microelectrode to fill individual cells with a marker or fluorescent dye to delineate the extent of a cell's membrane is more simple. While this is usually done in live cells in tissue slices, it can also be successfully carried out in fixed tissue via intracellular iontophoresis (4). The advantage of individually injecting cells in complex preparations is that only a single cell is labeled, meaning any stained structures can be more readily attributed to that one cell. Other ways to delineate a cell's membrane for confocal analysis include using antibodies to cell surface markers, which are usually raised to the intracellular domain of membrane proteins such as receptors, or lectins that bind to specific carbohydrate moieties on the outside surface of cells. Again in living cells, cell permeant dyes (e.g., acetomethoxy-esters) are available that cross the cell membrane and are modified by intracellular enzymes such that they become trapped and can also be used to delineate the extent of the cell membrane. The development of fluorescent dyes and GFP-expressing proteins that are specifically localized to particular cellular organelles has meant that subcellular morphologies can be studied in a similar way.

2. Materials

2.1. Preparation of Tissue Slices and Intracellular Injection of Dye

1. Dissecting instruments, for instance toothed forceps for holding cord, pointed laminectomy scissors (e.g., Fine Science Tools, Foster City, CA, USA), fine forceps, and fine spring scissors.
2. Agar for blocking.
3. Fast-drying cyanoacrylate tissue glue, e.g., Vet Bond™ (3 M, St. Paul, MN, USA) or similar fast-drying, low-viscosity cyanoacrylate adhesive.
4. Vibrating tissue slicer – various brands are available. For us, Vibratome brand slices (Vibratome™, St Louis, MO, USA) have been the most successful for producing viable spinal cord slices from rate up to 35 days of age.
5. Cutting solution consisting of artificial cerebrospinal fluid (ACSF) with sucrose substituted for NaCl – composition: 252 mM sucrose, 2.5 mM KCl, 2 mM $CaCl_2$, 2 mM $MgCl_2$, 10 mM glucose, 26 mM $NaHCO_3$, 1.2 mM NaH_2PO_4, and 5 mM kynurenic acid, pH 7.4 (5).
6. Recording solution (ACSF) consisting of 127 mM NaCl, 2.5 mM KCl, 1.2 mM NaH_2PO_4, 26 mM $NaHCO_3$, 1.3 mM $MgSO_4$, 2.5 mM $CaCl_2$, and 25 mM D-glucose, pH 7.4.
7. Recording chamber and tissue slice harp (*see* **Note 1**).
8. Fixed-stage upright microscope fitted with infrared differential interference contrast (Nomarsky) optics.
9. Vibration isolation table.
10. Microelectrode puller.
11. Electrode glass with filament (World Precision Instruments, Sarasota, FL, UK) (*see* **Note 2**).
12. Micromanipulator, e.g., Sutter (Novato, CA, USA) or Narashigi (Tokyo, Japan).
13. Microelectrode amplifier to allow electrophysiological recordings and/or iontophoresis of intracellular marker.
14. Electrode filling solution either 0.5–5.0 M KCl for intracellular electrodes or artificial intracellular solution for patch electrodes. Many types of solution are used depending on the study. For example: 130 mM potassium gluconate, 1 mM $MgCl_2$, 2 mM $CaCl_2$, 10 mM HEPES, 10 mM EGTA, 4 mM Mg-ATP, 0.3 mM Na-GTP, 0.15% biocytin, pH 7.2, 290–300 mOsm.
15. Intracellular marker substance such as biocytin (0.15% for patch electrodes, 1% for sharp microelectrodes, neurobiotin or Lucifer yellow (lithium salt)).

2.2. Fixation of Tissues and Multiple Label Immunohistochemistry

1. Cells in tissues filled with biocytin/neurobiotin or biotinlyated primary antibody or lectin to mark cell membrane.
2. Streptavidin-linked fluorescent probe, e.g., Streptavidin Texas Red (Invitrogen, Carlsbad, CA, USA).
3. Secondary antibodies.
4. Zamboni's fixative: 2% formaldehyde plus 0.2% picric acid in 0.1 M sodium phosphate buffer, pH 7.0.
5. Dimethyl sulfoxide (DMSO) (*see* **Note 3**).
6. Phosphate buffered saline (PBS), filtered.
7. Microscope slides.
8. Aqueous mounting medium, e.g., buffered glycerol or commercial fluorescent mounting medium such as Fluomount™ (Dako, Glostrup, Denmark).
9. Staining tray.

2.3. Confocal Imaging of Fixed Cells

1. Laser scanning confocal microscope (*see* **Note 4**).
2. High numerical aperture, long working distance objective to suit mounting medium used (*see* **Note 5**).
3. 3-D modeling software, e.g., ImageJ (NIH, freeware) or commercial equivalent (e.g., NIS Elements, Nikon Inc., Tokyo, Japan).

2.4. Processing of Fluorescent Specimens to Produce a Permanent Stain

1. Streptavidin antibody (*see* **Note 6**).
2. Goat anti-streptavidin antiserum coupled to biotin (Vector Laboratories, Burlingame, CA, USA), diluted 1:50 at room temperature.
3. Avidin–biotin–horseradish peroxidase kit (Vectastain™, Vector Laboratories) to localize biotin.
4. Diaminobenzidine–4HCl.
5. Hydrogen peroxide.
6. Microscope with camera lucida attachment for drawing neurons OR deconvolution microscope.

3. Methods

3.1. Preparation of Tissue Slices and Intracellular Injection of Dye

Here, we describe the process of making spinal cord sections and filling cells with a dye to allow morphological analyses.

1. Remove tissue from animal as quickly as possible. When preparing spinal cord slices, this involves decapitation, taping the animal to the dissecting surface – dorsum uppermost, and removal of the skin on the back and the fat pad between the shoulder blades.

2. The spinal column is cut through at a high thoracic level and a dorsal laminectomy performed by holding up the cut end of the spinal cord and dorsal edge of the canal using the toothed forceps, inserting one point of the scissors into the canal ventral to the cord and making cuts through the bone on either side ventral and lateral to the cord. Then by alternatively cutting through the muscle and then the bone on either side of the cord, it can be quickly removed along with a dorsal section of muscle and bone. This is then placed in a dissecting dish filled with cooled cutting solution and the spinal cord carefully removed from the underlying bone and muscle using fine forceps and fine spring scissors.
3. Cut the desired length of cord and glue it to the agar block using the tissue glue (*see* **Note 7**).
4. Glue agar block to cutting chamber of vibrating slicer and fill chamber with ice-cold cutting solution.
5. Cut sections at 250–300 μm thick depending on age of animal and degree of myelination.
6. Mount sections in chamber on microscope, hold down with tissue harp, and perfuse with recording solution.
7. Visualize cells to be filled under DIC optics, taking care to focus condenser and adjust optical elements to achieve optimum viewing conditions.
8. Mount electrode on micromanipulator and advance to cell and either impale (sharp microelectrode) or form seal and break through to whole cell mode (patch electrode). A very useful description of how to patch clamp recordings from brain slices has previously been published (6).
9. Allow time for dye to diffuse into cell (patch electrodes) or iontophorese dye by applying negative current (biocytin, Lucifer yellow) or positive current (neurobiotin) (*see* **Note 8**).
10. Make a sketch to show approximate location of cell within tissue slice.
11. Nick or otherwise mark tissue so that the orientation of the slice is clear.
12. If structural studies are to be performed, or if certain peptides are to be localized, it may prove useful to keep the tissue viable by incubating in culture medium, e.g., DMEM bubbled with 95% O_2/5% CO_2 for 1 h or longer before fixation.

3.2. Fixation of Tissues and Multiple Label Immunohistochemistry

1. Fix in Zamboni's fixative or paraformaldedyde for 4 h (or overnight), depending on secondary epitopes to be localized.
2. Clear and permeabilize tissue by placing for 3×10 min washes in DMSO.
3. Wash tissue in 3×10 min in filtered PBS.

4. Place tissue in staining tray and dry around edges with filter paper to remove excess PBS.
5. Apply primary antibody to localize desired epitopes and incubate overnight at room temperature or for 48 h at 4°C if non-specific background staining is a problem.
6. Wash 3 × 10 min in filtered PBS.
7. Apply mixture of fluorescent-linked secondary antibody and fluorescent streptavidin and incubate for 90 min at room temperature.
8. Wash 3 × 10 minutes in filtered PBS.
9. Dry and mount in buffered glycerol.
10. Cover slip with No. 1 cover slip or thinner.

3.3. Confocal Imaging of Fixed Cells

1. Mount slide on confocal microscope and find cell of interest at low power using fluorescent lamp and the drawing prepared earlier to record the cell location in the tissue (*see* **Section 3.1**, step 10).
2. View at higher power – for large fields of processes, best results are obtained using 40 × magnification. If terminal fields are larger, then multiple images can be stitched together or images taken with a high numerical aperture (NA) 20 × lens. Smaller cells can be viewed at 60 × , but a 100 × lens is not usually recommended due to the reduced working distance and is rendered unnecessary with high NA lenses and the ability of many confocal microscopes to scan smaller areas thus producing an "optical" zoom effect.
3. Use the microscope's "live" imaging/fast-scanning feature to roughly adjust laser power and photomultiplier gain and determine the extent in the *z* dimension or depth of processes that can be imaged.
4. Set appropriate pinhole aperture for desired optical section thickness. In a microscope without a continuous variable pinhole, this is usually close to the thickness of the airy disc for the lens to be used. For a microscope with a continuous variable pinhole, this setting is a compromise that will depend on (a) the thickness of the cell's processes and the size of the cellular features being imaged and (b) the total size of the cell and its processes, since thinner optical sections mean larger *z*-stacks, more imaging time and greater fading of fluorophores. Most confocal microscopes come with software that will suggest an appropriate optical section thickness and *z*-step size based on the numerical aperture of the lens – this is a good starting point.
5. As a compromise, set the gain and laser power to optimum levels at the centre of *z* range. In general, when taking large *z*-stacks it is preferable to move the focal plane in the direction

from the deep in the tissue to more superficial. In this way, the hardest to detect structures deep in the tissue are bleached less before being imaged. For very large *z*-stacks, if this does not produce adequate results, two separate *z*-stacks may need to be taken using different gain settings (*see* **Note 9**).

3.4. Processing of Fluorescent Specimens to Produce a Permanent Stain

The drawback of using fluorescent preparations is that the prolonged imaging required to study the fine detail of cellular morphology can cause fluorescence to fade. We therefore routinely convert fluorescent preparations to permanent histological stains after fluorescence imaging.

1. Soak slides in PBS with gentle shaking until cover slip is removed.
2. Wash tissue 3 × 10 min in filtered PBS to remove mounting medium.
3. Incubate with goat anti-streptavidin antibody 1:50 overnight at room temperature.
4. Wash 3 × 10 min in filtered PBS.
5. Visualize using Vectastain™ DAB kit as per instructions.

4. Notes

1. Small perfusion chambers suitable for slice work with matching harps for holding down tissue slices are available for purchase from several companies. If workshop facilities are available, baths can also be produced from inexpensive materials such as Perspex. We make tissue harps from small pieces of bent platinum or stainless steel wire using laddered nylon stockings to form the harp strings.
2. Electrode glass with a wire filament allows very fine electrodes to be filled with solution by capillary action much faster than electrodes without a filament, which may require soaking in solution for longer periods to achieve filling with solution.
3. While Triton™ is also useful for permeabilizing tissue, we have found DMSO to be superior for thicker tissue sections and whole mounts. It also obviates the need for using the detergent in antibody incubations meaning that surface tension remains intact and smaller amounts of antibody are required to cover the tissue. It is compatible with most peptide epitopes.
4. Spinning disc confocal systems are adequate for imaging in thin sections and cultured cells. High-end microscopes may even be superior to laser scanning systems for studying

intracellular organelles. They are not, however, as useful for studying complex cells in thick tissue specimens, since they are not able to exclude all out of focus light from thick fluorescent specimens.

5. High-quality images depend not only on high-quality optics but also on matching the optics to the sample and the mounting medium. Some lenses have collars that can be adjusted to correct for the mounting medium and or cover slip used. Others are specially designed for particular mounting mediums such as buffered glycerol.
6. A "bridge" method using a biotin–HRP conjugate has also been described for converting fluorescently labeled streptavidin to a permanent reaction product (3). We have found the streptavidin antibody method to give better results and be more reliable (2).
7. Generally in order to properly adhere, tissue must be relatively dry, i.e., without large droplets of solution. The agar block should also be dry before application of the glue. A very thin layer of glue must be applied to the block and tissue held vertically and touched once only to the agar surface held vertically in the correct position. Tissue will generally not stick again if the first attempt is unsuccessful.
8. Biocytin and Lucifer yellow require negative current to iontophorese into cells. This is useful since holding cells hyperpolarised with negative current is a common method of stabilizing a recording, and so cells will fill with dye during the recording process. Neurobiotin requires positive current, which can also be useful if you only want to fill certain cell types during sharp microelectrode recordings. Thus cells will not fill with dye while applying negative current to stabilize recordings (7).
9. Confocal microscopes theoretically allow optical sections to be taken at depths into the sample as far as the working distance of the lens will allow. Practically, the strength of the in-focus fluorescent signal entering the pinhole is substantially reduced at deeper focal planes as the majority of the light is scattered by shallower elements in the tissue. This means that laser power and photomultiplier gain must be increased in order to detect light emitted from elements deep in the tissue. This in turn means that for long *z*-stacks, gains that allow detection of deep elements will cause saturation of the detectors for shallower optical sections. Only a few confocal applications allow scaling of gain settings depending on tissue depth, although some do allow creation of macros that can achieve the same effect with a little effort and technical expertise. In this case, imaging the sample at great depths can cause

bleaching of the superficial depths, so that images should be undertaken from shallow to deep rather than vice versa as stated earlier.

References

1. Balasubramanyan, S., Stemkowski, P.L., Stebbing, M.J., and Smith, P.A. (2006) Sciatic chronic constriction injury produces cell-type-specific changes in the electrophysiological properties of rat substantia gelatinosa neurons. *J. Neurophysiol.* **96**, 579–590.
2. Furness, J.B., Robbins, H.L., Xiao, J., Stebbing, M.J., and Nurgali, K. (2004) Projections and chemistry of Dogiel type II neurons in the mouse colon. *Cell Tissue Res.* **317**, 1–12.
3. Young, H.M., Kunze, W.A., Pompolo, S., Furness, J.B., and Bornstein, J.C. (1994) Combined intracellular injection of Neurobiotin and pre-embedding immunocytochemistry using silver-intensified gold probes in myenteric neurons. *J. Neurosci. Methods* **51**, 39–45.
4. Buhl, E.H. and Lubke, J. (1989) Intracellular lucifer yellow injection in fixed brain slices combined with retrograde tracing, light and electron microscopy. *Neuroscience* **28**, 3–16.
5. Chery, N. and de Koninck, Y. (1999) Junctional versus extrajunctional glycine and GABA(A) receptor-mediated IPSCs in identified lamina I neurons of the adult rat spinal cord. *J. Neurosci.* **19**, 7342–7355.
6. Sakmann, B. and Stuart, G. (1995) Patch-pipette recordings from the soma, dendrites, and axon of neurons in brain slices. *In* Single-Channel Recording, Sakmann, B. and Neher, E. (Eds). Plenum Press, New York.
7. Kunze, W.A., Furness, J.B., and Bornstein, J.C. (1993) Simultaneous intracellular recordings from enteric neurons reveal that myenteric AH neurons transmit via slow excitatory postsynaptic potentials. *Neuroscience* **55**, 685–694.

Chapter 15

High-Resolution Confocal Imaging in Tissue

Verena C. Wimmer and Andreas Möller

Abstract

Laser scanning microscopy is playing a major role in visualization of biological structures and processes. However, as images are degraded due to blurring, noise, and color shifts, quantitative interpretation of confocal images can be difficult. In this chapter, we detail a procedure that involves acquisition of high-resolution confocal image stacks in tissue sections and the subsequent deconvolution process. Data generated using these methods can be used for reliable quantification of cell biological and tissue interactions, e.g., colocalization analyses or 3D reconstructions.

Key words: Confocal imaging, deconvolution, beads, point spread function, neuronal.

1. Introduction

The analysis of cell biological processes and tissue organization relies on visualization using microscopic techniques. Although fluorescence microscopy is widely used for localization of antibody labeling, a major drawback is out of focus blur caused by illumination of the full depth of the tissue section.

Laser scanning confocal microscopy has been an important tool to investigate sub-cellular processes as it offers a number of inherent advantages that solve this deficiency: illumination of a single point of the specimen at any one time with a focused laser beam ensures that illumination intensity drops off rapidly above and below the plane of focus, the short depth of fields allows optical sectioning, and the aptly named pinhole rejects fluorescence coming from out of focus planes (1).

Importantly, confocal microscopy not only allows acquisition of qualitative data in a snapshot experiment but it also enables the collection of quantitative data (2, 3). However, quantification of

T.D. Hewitson, I.A. Darby (eds.), *Histology Protocols*, Methods in Molecular Biology 611,
DOI 10.1007/978-1-60327-345-9_15,

confocal images is not straightforward. Errors are introduced due to physical limitations of the laser scanning microscope, e.g., light diffraction, noise, chromatic errors etc (4, 5). Therefore, careful data collection and post-acquisition processing are imperative in order to obtain reliable information from the experiment. Deconvolution, i.e., mathematical recovery of the original signal from degraded observations, is instrumental in removing noise and improving contrast and resolution of confocal image stacks, in particular in the Z-axis (6).

There are large amounts of protocols on how to obtain, process, and label cells and tissues for confocal laser scanning microscopy, including publications in this book series. This chapter will focus on acquisition and deconvolution of high-resolution confocal image stacks which can form a basis for further analyses, e.g., 3D reconstruction and colocalization analysis (7, 8). This process involves correct mounting of labeled tissue samples, in this case neuronal tissue, as well as "ideal" image acquisition based on the Nyquist-Shannon sampling theory (9) and deconvolution using an experimentally measured point spread function (PSF) (**Fig. 15.1**) (10).

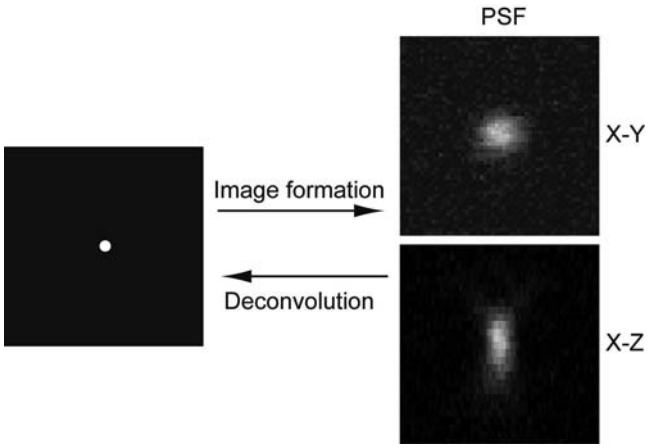

Fig. 15.1. Blurring of a point-like object (*left*) by the optical instrument creating the point spread function (PSF) shown on the *right* in X–Y and X–Z. Please note: the point is spread "longer" in Z than in X and Y, i.e., the axial resolution is worse than the lateral resolution.

2. Materials

2.1. Tissue

Fluorescently labeled vibratome or cryostat-cut free-floating tissue sections.

2.2. Mounting

1. 0.1 M phosphate buffer (PB), pH7.4.
2. SlowFade™ Antifade Kit (Invitrogen, Carlsbad, CA, USA) or similar mounting medium (*see* **Note 1**).

3. Glass microscope slides.
4. Cover slips with defined thickness (0.17 or 0.22 mm, depending on the working distance of lens used; Warner Instruments, Hamden, CT, USA).
5. Nail polish, to seal edges of cover slips.
6. Filter paper, cut into triangles.
7. Fine forceps.
8. TetraSpeck™ Fluorescent Microspheres Size Kit (Invitrogen).

2.3. Imaging

1. Confocal microscope.
2. Immersion oil (oil or glycerol depending on lens).
3. Lens tissues.
4. Ethanol.
5. Deconvolution software. e.g., Huygens Essential Deconvolution Software (SVI, Hilversum, The Netherlands).

3. Methods

The starting point for methods described in this chapter is fluorescently labeled tissue sections. Labeling can be achieved by a number of standard techniques, including immunohistochemistry, viral gene expression systems, or DNA transfection.

The use of vibratome or cryostat sections depends on the scientific question and the type of labeling. Fresh frozen or lightly fixed tissue can be processed for cryostat sectioning; this can be advantageous as immunogenicity and antibody penetration are better. On the other hand, for reconstruction of large cells, to study neuronal pathways or for postprocessing of acute tissue (e.g., after electrophysiological recordings or pharmacological experiments), thicker vibratome sections are preferable (7).

As a rule of thumb, the maximal penetration depth in tissue with a confocal microscope is 100–120 μm. Therefore, if your sections are thicker you will not be able to resolve structures deeper than 100–120 μm.

3.1. Mounting of Vibratome Sections (>50 μm thickness)

1. Prepare a flotation bath by filling a shallow glass or plastic container (approximately 10 × 15 cm in size) with 0.1 M PB.
2. Transfer section from washing buffer into this container.
3. Using fine forceps, gently push section to the surface – it will spread due to the surface tension.
4. Insert an untreated glass slide into container and maneuver section onto the glass; slowly remove slide from buffer and dry surplus buffer using lint-free tissues.

5. Set aside to dry further. Do not allow the tissue surface to dry out but make sure that "puddles" of buffer evaporate.
6. Pipette one to two drops of SlowFade™ Antifade on top of a section; holding a cover slip at an oblique angle (using your fingertip on the slide and fine forceps), gently lower it down onto the section.
7. Place filter paper next to the edge of the cover slip so that redundant mounting medium can be absorbed (*see* **Note 2**).
8. Seal the edges of the cover slip with nail polish and let dry in the dark.
9. The slides can be stored at −20°C for up to 3 months (*see* **Note 3**).

3.2. Mounting of Cryo Sections

Follow steps 6–9, **Section 3.1**.

3.3. Mounting of Tetraspeck™ Fluorescent Beads

This step is only necessary if you need to determine the specific point spread function (PSF) of your confocal microscope (*see* **Note 4**), e.g., using a deconvolution software like Huygens Essential. The use of a theoretical PSF is possible; however, it does not account for extra distortions introduced, for example, by suboptimal microscope configuration or deviations in the light path (11).

1. Dilute *subresolution* fluorescent coated beads (Tetraspeck™ Microspheres, Invitrogen) with a diameter of 100–200 nm 1:10 or 1:20 in distilled water (5).
2. Vortex or sonicate to suspend the beads well.
3. Pipette 5 μL of the Tetraspeck™ solution onto a clean slide and spread with the pipette tip. Let dry.
4. Add 5–10 μL of SlowFade™ Antifade (in any case the same mounting medium you use for the tissue sample) and cover slip as described in **Section 3.1**, steps 6–9.

3.4. Imaging of Fluorescent Beads

The various confocal acquisition software differ slightly with respect to the design of the user interface. Therefore, we describe the principles of image acquisition rather than single steps for a particular software program. These principles, however, can easily be implemented in all commonly used confocal microscopes.

1. Beads should be acquired with the same microscopic parameters that will later be used to image the experimental sample, i.e., a reliable deconvolution can only be achieved with a PSF extracted from beads which have been recorded with the same lens, magnification, voxel size, pinhole diameter etc.
2. Generally, voxel sizes (*see* **Note 5**) should be 50–60 nm in X/Y and 100–120 nm in the Z-axis (**Section 3.5**, step 6). Voxel sizes are derived from lens magnification and electronic zoom and are readily displayed in most confocal acquisition software.

3. Beads have to be well apart from each other to reliably extract the PSF. Record 1–10 beads per image in channels matched with the fluorophores used in your specimen (Tetraspeck™ beads are labeled in four different colors: 360/430 nm (blue), 505/515 nm (green), 560/580 nm (orange), and 660/680 nm (dark red)).
4. Apply 16 × Kalman averaging (*see* **Note 6**) and avoid clipping of the image (*see* **Note 7**).
5. Record image stacks containing the whole beads with two to three images without signal on top and bottom (35–50 frames).

3.5. High-Resolution Imaging of Sample Tissue Using Confocal Microscopy

1. Apply immersion medium (oil or glycerol, depending on the lens used; the higher the numerical aperture (NA) of the objective the better) to the objective, place slide in sample holder.
2. Focus on the region of interest and choose the channels to be used as required in the respective confocal acquisition program based on the fluorophores used in your staining (*see* **Note 8**).
3. Adjust the laser intensity and detector voltage for each channel (*see* **Note 9**), use gain control in moderation as it increases the noise.
4. The pinhole can usually be set to "airy disc" (*see* **Note 10**).
5. Importantly, ensure that the image is not clipped (*see* **Note 7**). Make sure to set the dark levels correctly.
6. Record an image stack by adjusting the voxel size to the Nyquist sampling distance in X and Y and set the Z-step. The Nyquist sampling distance represents "ideal sampling" based on the Nyquist-Shannon sampling theory and depends on the respective confocal microscope and lens (*see* **Note 11**). Nyquist calculators are available online. The voxel size is adjusted by (a) increasing the electronic zoom, (b) adjusting the number of pixels per frame or (c) both (*see* **Notes 12** and **13**).
7. Filtering (e.g., Kalman) is not necessary (*see* **Notes 6** and **14**).
8. Save image stack for subsequent processing.

3.6. Deconvolution

Numerous deconvolution programs are available, e.g., ImageJ plugins (http://bigwww.epfl.ch/demo/deconvolution3D/) or AutoQuantX (Media Cybernetics, Bethesda, MD, USA). In our laboratory, we use Huygens Essential Deconvolution Software (SVI) which also allows for simple extraction of measured PSFs from bead image stacks. Therefore, we will describe deconvolution with Huygens Essential as an example.

1. *If you are using a theoretical PSF, skip steps 1 and 2.* Load bead stacks into Huygens and follow the prompts of the wizard. Make sure to adjust the refractive index and the

backprojected pinhole diameter correctly (a calculator for the backprojected pinhole diameter can be found on http://www.svi.nl/).

2. Huygens Essential will extract an experimentally measured PSF.
3. Load one of the data stacks and follow the prompts of the wizard. Again, adjust refractive index and the backprojected pinhole diameter. Inspect the image histogram for clipping (sharp peak at the right end of the histogram, *see* **Note 15**).
4. Carefully estimate the signal-to-noise ratio (SNR) of your images and test different settings (*see* **Note 16**).

Figure 15.2 illustrates the effect of deconvolution.

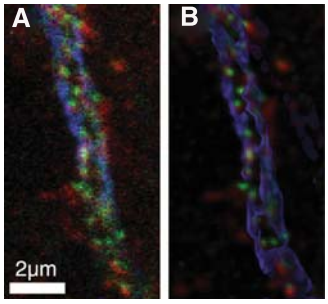

Fig. 15.2. Effect of deconvolution. *Green*: Immunostaining against GABA receptor subunit gamma2; *Blue*: anti-Ankyrin-immunostain; *Red*: immunostaining against Gad67 (**a**) raw image, (**b**) deconvolved image. (For color images, see online version)

3.7. Color Shift Correction

Light of different wavelengths travels in different optical paths within a microscope setup. Therefore, recorded channels can be spatially shifted relative to another (**Fig. 15.3**). This color shift can

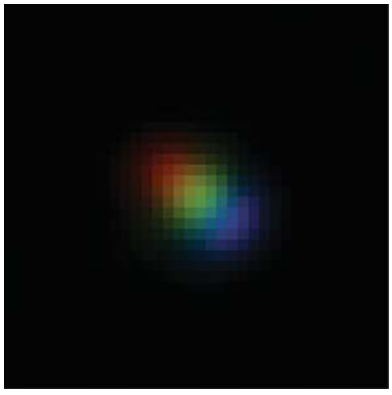

Fig. 15.3. Effect of color shift. Multicolored bead imaged using 405, 473, and 594 nm excitation wavelengths.

dramatically affect downstream analyses, in particular colocalization analysis (3, 4). Therefore, it is necessary to correct this shift which is possible in several confocal acquisition software, e.g., Olympus Fluoview™, or in the freeware version of Huygens *Professional* Deconvolution Software.

1. Load an image stack, launch operations window.
2. Use the "shift" command in the "manipulations" drop-down menu to correct color shifts between channels.

4. Notes

1. To avoid extensive spherical aberration caused by refractive index mismatches, use mounting and immersion media with similar refractive indices.
2. When lightly touching the cover slip with forceps, no SlowFade™ Antifade should ooze out. If the tissue sections are thick, then use spacers. It is important that the cover slip does not move as this causes movement artifacts when doing Z scans. For large Z-stacks that require scanning deep within the sample, we recommend to let the mounting medium penetrate for several hours before imaging. Otherwise the refractive index changes gradually between surface and center of the tissue, causing spherical errors.
3. Mounting media containing glycerol, e.g., SlowFade™ Antifade, do not freeze and can be stored at –20°C which to some degree protects the fluorescent labeling. Other mounting media, e.g., most hard-setting ones, have to be stored at 4°C.
4. The PSF describes how the image of a single point-like object is blurred by the optical system (**Fig. 15.1**). The PSF is very important for the image formation process (12). Deconvolution removes the light "spread" by the PSF, creating a sharper image while being scientifically exact (**Fig. 15.1**). Therefore, deconvolution is different from simple image enhancement.
5. A voxel is the three-dimensional "volume" version of a pixel; a pixel (the smallest unit of an image defining its resolution) has two dimensions (X and Y), while a voxel has three (X, Y, and Z). In a confocal microscope X and Y are determined by the frame resolution, whereas Z is defined by the Z-step. The voxel size is also linked with the sampling density: the sampling density for a given volume is higher, the smaller the voxel size.
6. Kalman filtering refers to repetitive scanning and averaging of the same image frame, either in line scan or frame scan mode.

7. Clipping occurs when the dynamic range of the input signal exceeds that of the analog-to-digital converter. In practice, this leads to "saturation" of very bright structures, i.e., all bright regions are represented by one identical intensity value and internal structures can no longer be identified. Clipping has a negative effect on the results of the deconvolution.

   Clipping can be visualized by using a high–low look-up table available in most confocal acquisition programs. To properly adjust the dynamic range for a Z-stack, it is necessary to find the brightest plane first by focusing up and down.

8. Most confocal microscopes offer a wide range of predefined laser/mirror/filter-combinations for common fluorescent proteins and dyes, e.g., GFP and its variants, Cy3/5, FITC, Alexa-dyes etc. If no predetermined channel settings are available, choose laser, filters, and dichroic mirrors using excitation–emission spectra of your dyes. Such spectra are available online.

9. It is recommended to balance laser intensity and detector voltage, i.e., avoid high laser intensities in combination with very low voltages (results in excessive bleaching) and vice versa (increases the noise). For large Z-stacks or imaging deep within the tissue, it can be necessary to increase laser intensity and detector voltage with depth. Most confocal acquisition software provide this option.

10. For low-fluorescent samples, the pinhole size can be increased. However, the pinhole size affects deconvolution and, therefore, identical pinhole sizes have to be used for beads and tissue samples.

11. The PSF is the smallest unit that a confocal microscope can resolve (*see* **Fig. 15.1**). Deconvolution works at the level of PSFs, i.e., the sampling density has to be high enough to image individual PSFs so that the program can "disentangle" them (http://www.svi.nl/). The Nyquist-Shannon theorem explains exactly how great the sampling density (*see* **Note 5**) has to be to record *all* information from a sample, based on the realization that the sampling frequency must be greater than twice the band width of the input signal in order to be able to reconstruct the original perfectly from the sampled version.

12. If voxel sizes are very large, information is lost and deconvolution may not be possible.

13. In practice, for example, if bleaching is an issue, voxel sizes can be increased up to 1.7 times the Nyquist size.

14. Kalman filtering improves the image quality; however, it is time consuming, increases bleaching, and unnecessary for images that are going to be deconvolved.

15. This information will help you to improve image acquisition for subsequent experiments.
16. If the SNR is too high, then the images will be "over-deconvolved," often resulting in background artifacts. If the SNR is chosen too low, then the result of deconvolution might not be satisfying.

References

1. Tekola, P., Zhu, Q., and Baak, J.P. (1994) Confocal laser microscopy and image processing for three-dimensional microscopy: technical principles and an application to breast cancer. *Hum. Pathol.* **25**, 12–21.
2. Diaz-Zamboni, J.E., Adur, J.F., Vicente, N., Fiorucci, M.P., Izaguirre, M.F., and Casco, V.H. (2008) 3D automatic quantification applied to optically sectioned images to improve microscopy analysis. *Eur. J. Histochem.* **52**, 115–126.
3. Ronneberger, O., Baddeley, D., Scheipl, F., Verveer, P.J., Burkhardt, H., Cremer, C., Fahrmeir, L., Cremer, T., and Joffe, B. (2008) Spatial quantitative analysis of fluorescently labeled nuclear structures: problems, methods, pitfalls. *Chromosome Res.* **16**, 523–562.
4. Manders, E.M.M. (1977) Chromatic shift in multicolour confocal microscopy. *J. Microsc.* **185**, 321–328.
5. Yoo, H., Song, I., and Gweon, D.G. (2006) Measurement and restoration of the point spread function of fluorescence confocal microscopy. *J. Microsc.* **221**, 172–176.
6. Landmann, L. (2002) Deconvolution improves colocalization analysis of multiple fluorochromes in 3D confocal data sets more than filtering techniques. *J. Microsc.* **208**, 134–147.
7. Wouterlood, F.G. (2005) 3-D reconstruction of neurons from multichannel confocal laser scanning image series. *Curr. Protoc. Neurosci.*. Editorial board, Jacqueline N Crawley, Chapter 2: Unit 2.8.
8. Landmann, L. and Marbet, P. (2004) Colocalization analysis yields superior results after image restoration. *Microsc. Res. Tech.* **64**, 103–112.
9. Shannon, C.E. (1949) Communication in the presence of noise. *Proc. Inst. Radio Eng.* **37**, 11.
10. Murray, J.M., Appleton, P.L., Swedlow, J.R., and Waters, J.C. (2007) Evaluating performance in three-dimensional fluorescence microscopy. *J. Microsc.* **228**, 390–405.
11. Anlauf, E. and Derouiche, A. (2009) A practical calibration procedure for fluorescence colocalization at the single organelle level. *J. Microsc.* **233**, 225–233.
12. Dusch, E., Dorval, T., Vincent, N., Wachsmuth, M. and Genovesio, A. (2007) Three-dimensional point spread function model for line-scanning confocal microscope with high-aperture objective. *J. Microsc.* **228**, 132–138.

Chapter 16

Software-Based Stacking Techniques to Enhance Depth of Field and Dynamic Range in Digital Photomicrography

Jörg Piper

Abstract

Several software solutions are powerful tools to enhance the depth of field and improve focus in digital photomicrography. By these means, the focal depth can be fundamentally optimized so that three-dimensional structures within specimens can be documented with superior quality. Thus, images can be created in light microscopy which will be comparable with scanning electron micrographs. The remaining sharpness will no longer be dependent on the specimen's vertical dimension or its range in regional thickness. Moreover, any potential lack of definition associated with loss of planarity and unsteadiness in the visual accommodation can be mitigated or eliminated so that the contour sharpness and resolution can be strongly enhanced.

Through the use of complementary software, ultrahigh ranges in brightness and contrast (the so-called high-dynamic range) can be corrected so that the final images will also be free from locally over- or underexposed zones. Furthermore, fine detail in low natural contrast can be visualized in much higher clarity. Fundamental enhancements of the global visual information will result from both techniques.

Key words: Image processing, light microscopy, photomicrography, depth of field, focal depth, dynamic range, three-dimensional reconstructions, 3D-imaging, sharpness, resolution, HDR, DRI.

1. Introduction

Limitations in focal depth and sharpness are fundamental problems in light microscopy and photomicrography, especially at high magnifications and in specimens with a large local thickness. The higher the magnification, the lower the remaining focal depth will be, both visually and in still-images (1). Because of this, it is often impossible to obtain a sharp focus over the full depth of a specimen. Additional lack of definition can result from spherical

T.D. Hewitson, I.A. Darby (eds.), *Histology Protocols*, Methods in Molecular Biology 611,
DOI 10.1007/978-1-60327-345-9_16,

and chromatical aberration, unsteadiness in the visual accommodation, high ranges in local brightness and contrast, noise and other artifacts.

Using conventional techniques, the depth of focus can be enhanced when the image is taken with a low-magnification lens. After photography, a smaller region of interest can be cropped from the total image in a second step. Alternatively, the three-dimensional structure of a specimen can be shown by a video clip when the stage is moved slowly up and down. In both cases, the resolution is lower than in still-images taken at a higher magnification.

Existing ultrahigh or very low ranges in brightness and contrast cannot be processed by CCD sensors, screens, beamers, or print media; they are quality-limiting factors in all conventional techniques for still-images or video processing (2, 3).

These technical problems can be solved with the help of several specific software solutions for post-processing, when the specimen is taken in multiple single images of focal plane or exposure. Of course, utilizable image sequences can only be created in sessile specimens, which do not move during the procedure.

To enhance the depth of field, it is necessary to take a vertical stack of images consisting of several single images, with different planes of focus. With suitable stacking software, the respective single images can be superimposed so that only regions in focus will contribute to the resulting reconstructed image. The final image will be free from any lack of distinction, and will be independent of the specimen's vertical dimension and the magnification, focal depth, and planarity of the respective lenses. As deep focus images can be created at maximum magnification and resolution, they show much more detail than corresponding views cropped from low-magnification images.

In order to enhance the visible range of contrast (dynamic range), a sequence has to be created consisting of various single images at different exposures. After this, all single images have to be superimposed using software for HDR or DRI imaging (HDR = high-dynamic range rendering, DRI = dynamic range increase, synonym: exposure blending). The techniques (HDR and DRI) are different in their algorithms; nevertheless, visible improvements of the dynamic range can be obtained in digital photomicrographs by both methods. The resulting images are free from any over- or underexposed zones, and in most cases, they show much more visible detail.

Deep focus stacking techniques and HDR/DRI imaging can also be combined with each other. In this way, the resulting final images will be optimized in sharpness and resolving power as well as in global contrast and brightness.

The purpose of this chapter is to provide the user with a detailed guide of how to apply these principles in the preparation of photomicrographs.

2. Materials

2.1. Software

Based on high-resolution still-images, the following freeware and shareware software solutions for deep-focus stacking and HDR/DRI techniques have been tested for photomicrography:

1. Stacking software for enhancements of focal depth: Combine Z 5 (4), Picolay (5), Helicon Focus (6).
2. Software for HDR/DRI techniques: DRI-Tool (7), Image Stacker (8), Easy HDR Basic and Pro (9), Picturenaut (10), Photomatix Pro (11, 12).

Basic characteristics of the tested software are compared in **Table 16.1**.

2.2. Digital Camera

In all techniques, digital photomicrographs can be taken with standard cameras or camera modules. The images presented in this paper were taken with a 7.1 MP Olympus Camedia C-7070 digital camera equipped with a Leica Vario Photo Ocular. Widely used images file formats, including TIF/TIFF and JPG/JPEG, can be processed by all software.

2.3. Computer

The image processing procedures need substantial computer resources when high-resolution images have to be rendered. Thus, a modern computer should be used fitted out with up-to-date hardware components, especially when a large number of single images have to be rendered (*see* **Note 1**).

3. Methods

3.1. Stacking Techniques for Enhancement of Focal Depth

1. To obtain a digital scan from the respective specimen, the stage of the microscope has to be moved up or down in tiny steps so that the plane of focus passes across the specimen. Thus, a vertical stack or sequence of images can be achieved, each with a very shallow focal depth. For the best results, it is important that all relevant structures within all focal planes of interest are clearly seen (sharp) in at least one single image of the complete sequence. The image sequence should be saved in a special folder.
2. In a second step, the respective stacking software has to be started. All versions of such software work in a comparable way. At first, the folder containing the single images has to be opened and all single images suitable for processing have to be marked. Next, the stacking procedure has to be started. The various software solutions differ in their algorithms and presets. Thus, the specific characteristics of the specimen or

Table 16.1
Some characteristics of the tested software

Software	Size	Installation required	Price	Methods	Shade depth	Formats of final images (optional)	Minimum operating system	Manual interactive processing
Combine Z 5	348 KB	No	Freeware	Deep-focus stacking	Like single image	TIF, JPG, BMP, GIF, PNG	Windows 98	No
Picolay	512 KB	No	Freeware	Deep-focus stacking	Like single image	JPG	Windows 98	Yes
Helicon focus	10.7 MB	Yes	Circa 200 US$	Deep-focus stacking	Like single image	TIF, JPG, BMP, PNG, PSD	Windows XP	Yes
DRI-Tool	1.00 MB	No	Freeware	DRI	Like single images	TIF	Windows 95	No
Image stacker	0.97 MB	No	Freeware	DRI	Like single images	TIF	Windows 95	No
Easy-HDR basic	1.36 MB	Yes	Freeware	HDRI	24 bit	TIF, JPG, BMP	Windows 95	Yes
Easy-HDR Pro	1.75 MB	Yes	Circa 50 US$	HDRI	24 bit	TIF, JPG, BMP	Windows 95	Yes
Picturenaut	4.37 MB	No	Freeware	HDRI	8, 16, 32 bit	TIF	Windows 2000	Yes
Photomatix pro	13.9 MB	Yes	Circa 150 US$	DRI, HDRI	8, 16 bit	TIF, JPG, BMP	Windows XP, Mac 05 ×	Yes

the illumination mode may determine which software or preset will lead to the best results (*see* **Notes 2–4**). To obtain optimal reconstructions, the specimen can also be successively stacked using different software so that the best reconstruction can be selected.

In principle, the stacking procedure works as follows: at first, color saturation, white balance, and brightness are re-adjusted; artifacts are reduced. Then, all images are properly aligned so that they are congruent with each other. Finally, the in-focus parts of all single images are selected and composed to a reconstruction being completely in focus.

As an example for the computer-based workflow, **Fig. 16.1** shows some views of the main screen in the software Helicon Focus. The complete sequence consisting of six single images is arranged in thumbnails; a single image (top) and the final reconstruction (bottom) are shown in full size.

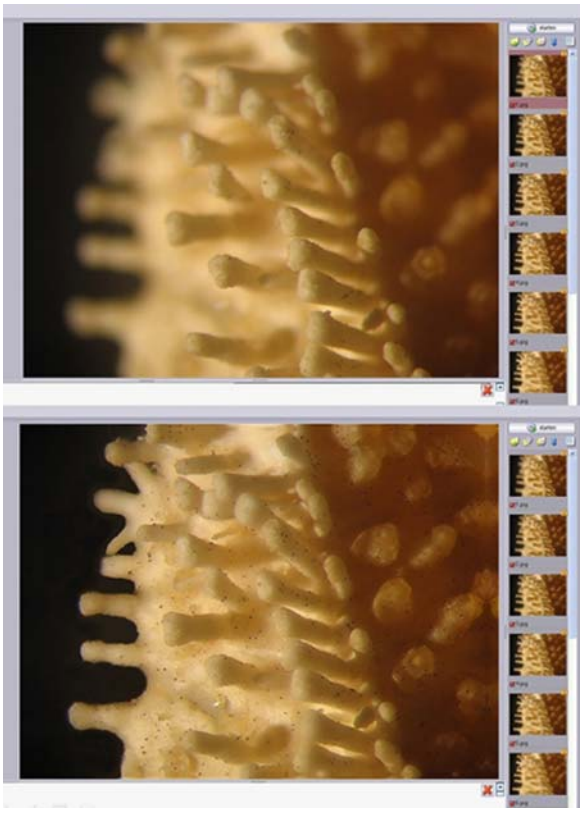

Fig. 16.1. Main screen in Helicon Focus, arm of a starfish, stereo microscope, epi-illumination, objective 2.5 ×, ocular 10 ×, HFW: 6 mm, sequence of six single images with different focal planes (*right margin*). *Top*: initial situation, showing a representative single image in full screen. *Bottom*: final three-dimensional reconstruction.

3.1.1. Combine Z 5

This freeware leads to high-quality results based on three optional presets (macros).

1. *Do Stack* is the standard macro for most purposes promising very good results in most cases.
2. *Do Average and Filter* is an alternative preset leading to reconstructions with ultrahigh contrast and sharpness.
3. *Stack Only* is an easy-working preset making superposition of single images without any corrections or alignments. Therefore, this macro can only be used when the respective single images are properly pre-aligned.
4. Two macros can be used for data saving, *Save Frame/Picture As* and *Save Rectangle As*. When the original image is saved in full size, both macros work in a nearly identical manner. The focal plane can differ marginally, when an image is simultaneously saved as frame/picture and rectangle. In this case, the final sharpness can be enhanced furthermore, when both reconstructed images (frame and rectangle) are stacked again in a second step (double stacking). For double stacking, frames and rectangles must be in equal size (*see* **Note 5**).

Figure 16.2 shows an example of low-magnifying deep-focus images in epi-illumination.

Fig. 16.2. May bug, stereo microscope, epi-illumination, objective 1 ×, ocular 10 ×, HFW: 17 mm, vertical depth: circa 12 mm, superposition of 14 single images, example of a single image (*left*), and final reconstruction (*right*). Software: Combine Z 5.

A new version of Combine has recently been developed (Combine ZT). When still-images are superimposed in photomicrography, reconstructions created with Combine ZT often seem to be lower in quality than rendered with Combine Z 5 (*see* **Notes 6** and **7**).

3.1.2. Picolay

Five presets are implemented in this freeware so that five separate reconstructions are created from each image sequence when stacked in automatic run; an extraordinary variety of reconstruction effects can result (*see* **Note 4**).

First, an average of all images with enhanced sharpness and contrast is generated. Second, a reconstruction is made containing the brightest pixels on each position. Third, a corresponding reconstruction is created based on the darkest pixels at all positions. Moreover, a picture with the sharpest areas in the stack is saved. Finally, all reconstructions generated before are superimposed with each other.

All tests were carried out by use of the Picolay version 2007-07-16. In September 2008, a new release has been developed (version 2008-09-19). However, for photomicrography, the prior version is preferred (*see* **Note 8**).

3.1.3. Helicon Focus

This software is based on one preset leading to useful results in most cases being comparable with the macro *Do Stack* in Combine Z 5.

In Helicon Focus, the progress of image processing and the resulting reconstructed images are permanently presented in life-view mode, also in high-resolution images. In monochromatic light, Helicon Focus is preferred (*see* **Note 2**).

3.2. HDR and DRI Techniques

When an image sequence is created consisting of various single images taken in different exposure, the images can be rendered in two different ways: high-dynamic range rendering (HDR) and dynamic range increase (DRI, synonym: exposure blending).

In HDR techniques, the three color channels corresponding with red, green, and blue, and the alpha channel corresponding with the transparency, are transformed from 8 to 32 bit. Moreover, all tonal values are coded as floating point data. In this way, the number of tonal values can be enlarged from 256 (usual in 8-bit images) up to circa 4.3 thousand million graduations per channel. A high-dynamic range image is therefore reconstructed; in most cases, its dynamic range is approximately 10,000:1 or 100,000:1. Conversely, laptop, computer, and TV screens have a visible dynamic range of about 1:100 or 1:500, photo prints circa 1:32 or 1:64, digital cameras about 1:1,000, and analogue camera films up to 1:10,000. When the dynamic range is 10,000:1 or lower, the corresponding image is defined as a low-dynamic range image (LDR) (2, 3).

HDR images can neither be printed out nor observed on a usual screen in a satisfactory manner because their dynamic ranges are too high. Therefore, HDR images have to be transformed into new LDR images; this separate step in image processing is called tone mapping. When the tone mapping is adequately carried out, the resulting final image shows a maximum of detail and fine structures in an optimized clarity over the full range of luminance, and it is free from any visible over- or underexposed zones.

When DRI/exposure blending is carried out, the tonal values remain constant in all single images; HDR images are not created, so tone mapping is not necessary. Software-based, all zones being

well exposed are directly extracted from the image stack and composed to a new image. Thus, pre-existing high differences in brightness and contrast can be reduced.

To obtain an HDR or DRI reconstruction, it is necessary to firstly take an image sequence consisting of several single images in variable exposure. Normally, the difference in exposure between two successive single images should be 1 or 2 EV-values, as recommended by most users and software producers. The number of images per sequence necessary for a successful rendering procedure is dependent on the dynamic range of the scene. All relevant details within the specimen should be properly exposed at least in one image of the sequence, regardless of whether they are dark, highlights, or midtones details. The single images of a sequence should be saved in a special folder as described above.

After this, the HDR or DRI software has to be started. Now, the folder containing the respective image sequence is opened. All single images being suitable for rendering have to be selected and marked within their folder. Finally, the image processing is started. The majority of software solutions offer several presets and modifications of various parameters so that a lot of different final images can be reconstructed. In this way, the visual character of image reconstructions can be optimally adjusted for all details of interest.

Figure 16.3 shows the principle of the computer-based workflow in Photomatix Pro. Three single images taken in high, medium, and low exposure were rendered into an HDR image and tone-mapped using the *Tone Compressor*. The resulting final image is well balanced in all zones. Within the HDR image, a rectangle can be drawn by the user which should contain representative details in different brightness. Now, the tone mapping can be regulated by a virtual switchboard. All effects achievable by tone mapping can be controlled in the rectangle.

3.2.1. DRI-Tool and Image Stacker

These freeware products for DRI rendering have minor differences in their designs, but they lead to identical results. When the single images are selected from the respective image stack, the software creates a reconstructed DRI image in an automatic run. Thus, the mode of image processing cannot be influenced by the user. The results of reconstructions can only be modified when different single images are pre-selected for rendering.

3.2.2. Easy HDR Basic and Pro

The freeware Easy HDR Basic is capable of creating HDR images which can be manually transformed into new LDR images. The character of reconstructions can be modified by the user with the help of a preview tool. Thus, several relevant parameters can be adjusted when the tone mapping is carried out (gradation, histogram, white and black point, gamma, saturation); additional image filtering is also implemented (Gaussian blur, sharpen, median and bilateral filter, color adjust, white balance).

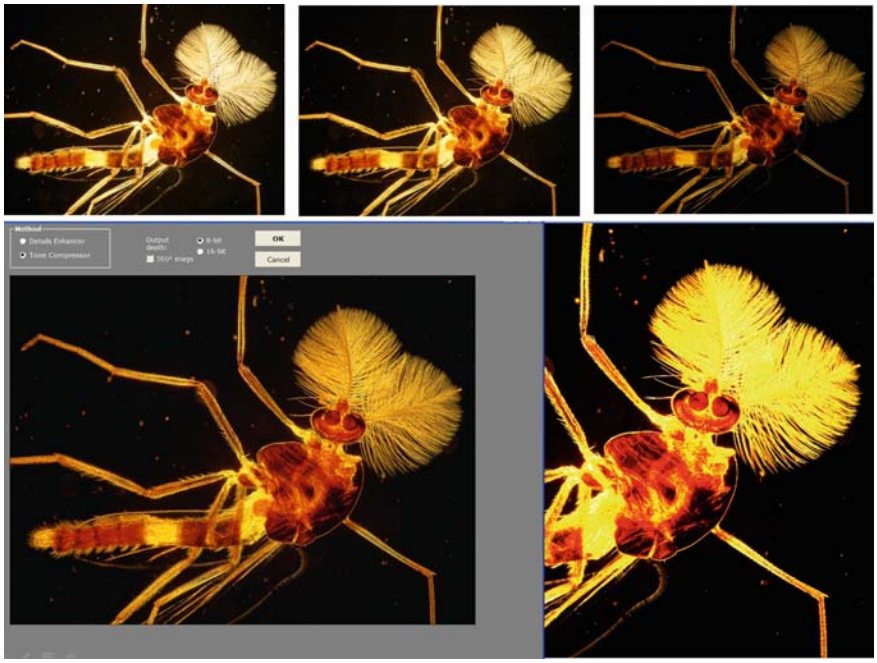

Fig. 16.3. HDR imaging with Photomatix Pro, *top*: three single images taken in high, medium, and low exposure, *bottom*: original HDR-image (*right*), final result created by tone mapping based on the Tone Compressor (*left*).

The shareware version (Easy HDR Pro) is additionally fitted out with a mask mode, so that the strength of tonal equalizing, the intensity of contrast compression, brightness, smoothness, and edge rendering can be adjusted. Thus, resulting final images may be more balanced than with Easy HDR basic.

3.2.3. Picturenaut

Picturenaut is an HDR-based freeware comparable to Easy HDR Pro. For HDR rendering, this software offers two variant modes, the *adaptive logarithmical mode* and the *photoreceptor physiology mode*. In the first mode, the following parameters can be manually modified while the tone mapping is carried out: exposure correction, equalization of light and shadow, mean brightness, contrast and histogram-based gradation. In a similar manner, the other rendering mode allows modifications of exposure correction, dynamic compression, color saturation, contrast and histogram-based gradation. In our experience, both variants lead to comparable results.

EXIF data are required when Picturenaut is used (*see* **Note 9**).

3.2.4. Photomatix Pro

Photomatix is the only software designed for HDR as well as for DRI techniques. Thus, an image stack can be rendered in both modes so that the best result can be selected.

In HDR-technique, tone mapping can be processed in two different ways, based on the *Details Enhancer* or the *Tone Compressor* (*see* **Notes 10** and **11**).

1. When the *Details Enhancer* is used, a maximum number of parameters can be manually influenced by the user: strength of contrast enhancements, color saturation, light smoothing, luminosity, white and black point, gamma, color temperature, saturation of highlights and shadows, micro-contrast, micro-smoothing, contrast enhancements' in highlights and shadows, shadows clipping.
2. The *Tone Compressor* works more simply so that a lower number of parameters can be modified in the tone-mapping procedure: brightness, tonal range, contrast adaptation, white and black point, color temperature, and color saturation.

For reconstructions based on DRI or exposure blending, several macros are implemented. Three macros exist for automatic run: *average* (global averaging), *highlights and shadows* for two images, and *highlights and shadows* for more than two images. Both of the latter macros lead to enhanced contrast and clarity in the dark and bright zones. For manually controlled DRI reconstructions, two separate macros are available: *highlights and shadows adjust* and *highlights and shadows intensive*.

1. In the *adjust mode*, the blending point (weighting given to the overexposed versus underexposed images) and radius (adjustment of sharpness) can be regulated.
2. In the *intensive mode*, the intensity of tonal equalizing can be pre-selected (*light* or *enhanced*); moreover, the precision of image rendering can be selected so that potential halo artifacts may be reduced more exactly.

3.3. Special Techniques in Image Stacking

In some situations, special techniques can be used for further improvements of three-dimensional reconstructions.

3.3.1. Special Techniques for Enhancements of Focal Depth

3.3.1.1. Double and Multiple Stacking

Sharpness and focal depth can be often enhanced furthermore when two or more separate reconstructions made from an identical view are superimposed with each other in a second step. This procedure can also be repeated so that the final sharpness and depth of field can be successively improved. Of course, it is also possible to create the first stack using one particular software and the following stack by another.

Figure 16.4 shows a radiolarian in dark-field illumination reconstructed by triple stacking. At first, two stacks were carried out with Combine Z 5 (macros: *Do Stack* and *Do Average and*

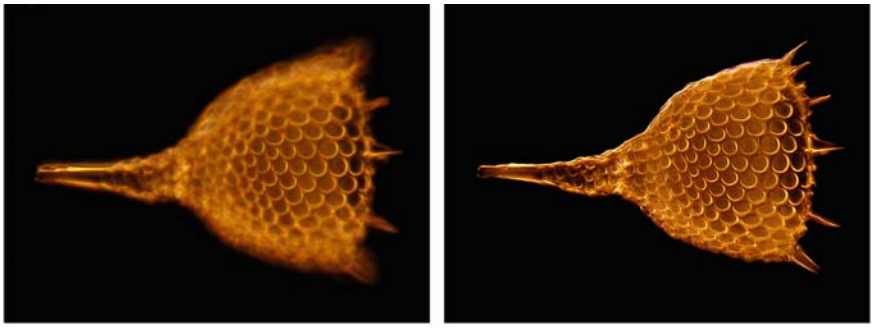

Fig. 16.4. Radiolarian, oblique dark-field illumination, objective iris 20 ×, ocular 10 ×, HFW: 0.26 mm, example of a single image (*left*), superposition of 12 single images by multiple stacking (*right*), Software: Combine Z 5 and Picolay (further explanations in the text).

Filter). Following this, two resulting reconstructions were stacked with Picolay. Finally, two Picolay-based reconstructions were stacked again with Combine Z 5 (macro: *Do Stack*).

3.3.1.2. Sandwich Techniques

Specimens can also be photographed and stacked in identical views when illuminated by different light sources, colors, or illuminating modes. In additional steps, the corresponding reconstructions can be superimposed as sandwiches by double or multiple stacking.

Thus, a specimen can be sequentially photographed in red-yellow bulb and blue flash light, in complementary monochrome color filtering or otherwise different illumination techniques. These different images can be superimposed with each other. Because of the combination of different color temperatures, complementary colors of different illumination effects, new characters of contrast will occur, sometimes comparable with solarization, so that fine structures, such as fine detail within crystallizations, are accentuated furthermore. In some cases, more details in structure will be recognizable than in the initial images (**Fig. 16.5**).

3.3.1.3. Monochromatic Light

Sharpness and resolution in single images and stacks can be maximized by monochromatic light, as any potential chromatic aberration is completely eliminated. In green light, interpolation artifacts are minimized in digital images, as the majority of pixels are sensitive to green color. According to the so-called Bayer mode, 50% of all pixels are sensitive to green and 25% to red or blue. Therefore, monochromatic green light can lead to optimal results, when digital images are intended to be created in black and white. In monochromatic stacks, marginal structures of cell membranes can be visible in an extraordinary clarity, as sharpness and resolution are fundamentally improved.

3.3.1.4. Digitized Interference Contrast

Interference contrast is a very suitable technique for three-dimensional imaging in transparent specimens. However, on the other hand, the depth of focus is minimized in interference contrast, as

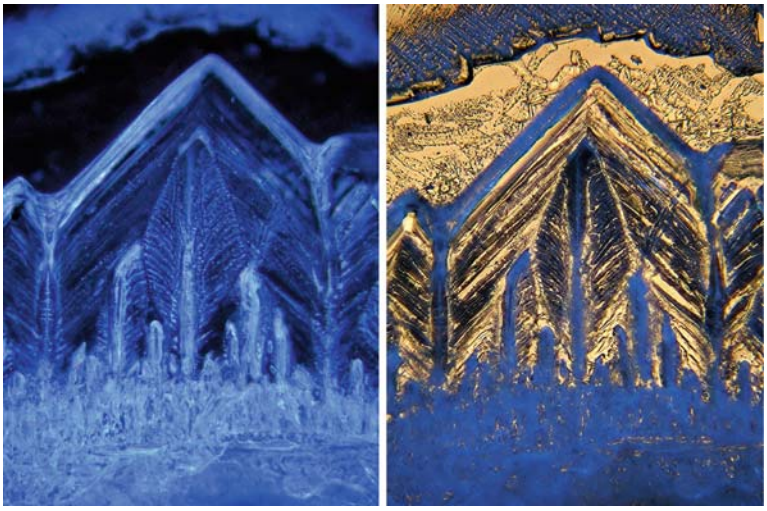

Fig. 16.5. Crystallization of alum, objective 10 ×, ocular 6.3 ×, HFW: 1.3 mm. On the left is a single image in epi-illumination (epi-dark field), filtered in *blue* (*brightly illuminated*). The right image is an example of multiple stacking, superposition of transmitted bright-field and *blue* filtered epi-dark-field, 18 single images per sequence (*right*). Software: Combine Z 5.

the vertical resolution is lower than in most other illumination modes. Therefore, especially in interference contrast, the three-dimensional aspect of transparent specimens can be fundamentally improved when stacking techniques are carried out. The transparent nature of specimens can often be presented best when the background is turned into black by software-based post-processing (**Fig. 16.6**).

3.3.2. Special Techniques in HDR and DRI Imaging

3.3.2.1. Color Contrast Mode

When the software Photomatix Pro is used, existing high or very low differences in brightness can also be transformed into different colors being nearly equal with regard to their luminance. Fine detail can therefore be enhanced in very dark or bright regions and final images can be observed or printed out in optimum quality.

Figure 16.7 shows native low-contrast structures within a living diatom cell taken in luminance contrast (13). Two single images were processed by triple stacking using Combine Z 5 and Picolay as described above. The final deep-focus reconstruction was rendered with Photomatix Pro in order to achieve high-color contrast.

3.3.2.2. Brightening and Contrast Equalization in Dark-Field Images

In dark field, specimens are usually illuminated in high intensity so that they appear as bright luminescent bodies situated in a black background. Thus, dark-field illumination is normally affected with ultrahigh ranges in contrast and brightness. Using Photomatix Pro in particular, the usual black background can be brightened in dark-field images so that pre-existing high differences in brightness of background and specimens are mitigated or equalized.

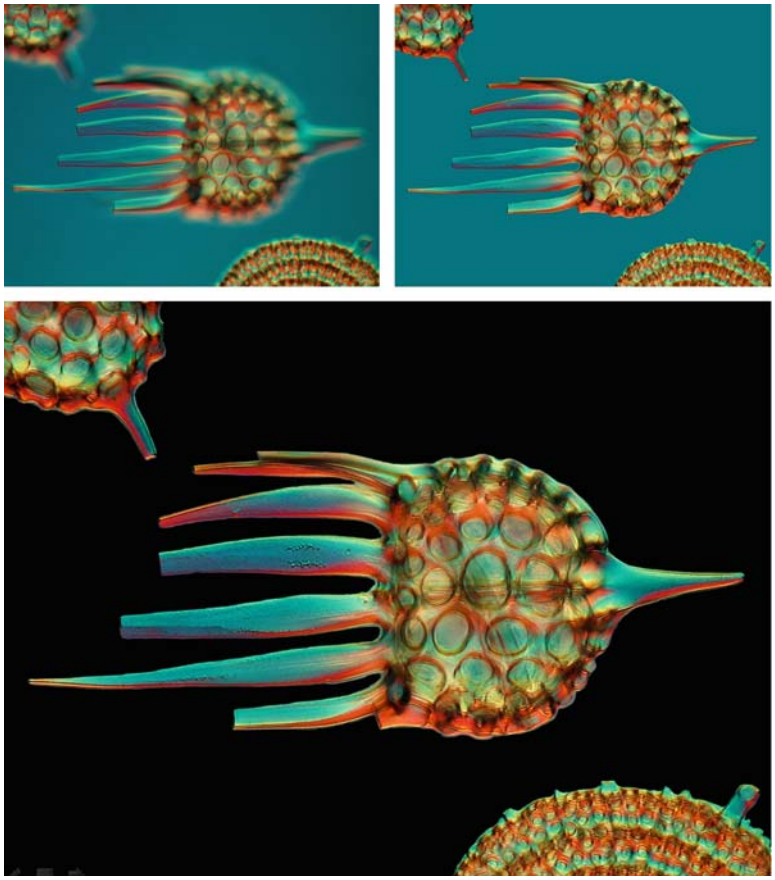

Fig. 16.6. Radiolarian, single image and deep-focus reconstruction, based on 20 single images taken in conventional interference contrast (*top*), digitized dark-field interference contrast (*bottom*), objective 16 ×, ocular 12.5 ×, HFW: 0.26 mm. Software: Combine Z 5.

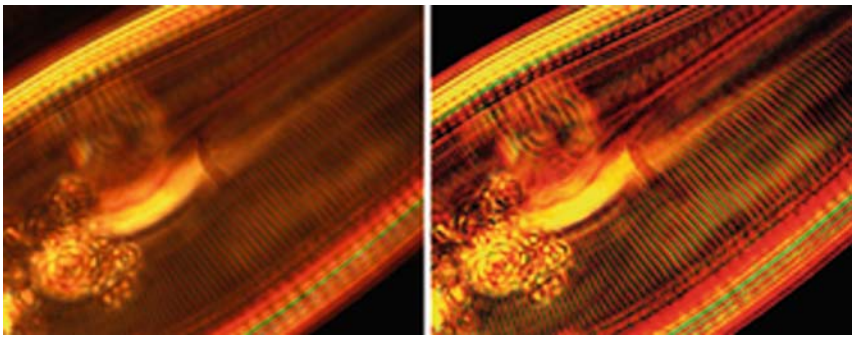

Fig. 16.7. Fine lamellar structures within a native diatom cell, axial illumination in luminance contrast (13), mirror objective 50 ×, ocular 12.5 ×, HFW: circa 0.1 mm, stack from two single images using Combine Z 5 (*left*), enhancement of the dynamic range with Photomatix Pro in order to obtain color contrast (*right*).

Thus, rendered images can often be presented or printed in better quality than the original versions. Moreover, the luminance of colors and the plasticity of transparent specimens can be improved, and ultrahigh contrast within the specimen itself can also be mitigated.

The same techniques can also be successfully carried out in polarized light when anisotropic specimens are examined while polarizer and analyzer are in crossed position (**Fig. 16.8**).

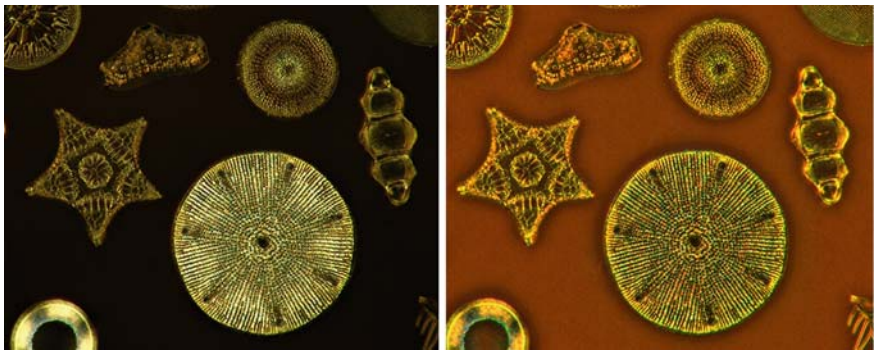

Fig. 16.8. Deep-focus stacking and HDR rendering in polarized light, crossed polarizers, quarter lambda compensator, objective 32 ×, ocular 10 ×, HFW: 0.5 mm, 15 single images per deep focus stack, range of exposure: 4 EV-values, exemplary single image stack (*left*), HDR reconstruction from five separate image stacks taken in different exposure (*right*), Software: Combine Z 5, Photomatix Pro/Details Enhancer (further explanations in the text).

3.3.2.3. Bicolor Monochromatic Imaging

When transparent or semitransparent specimens are simultaneously illuminated in epi-illumination and transmitted light, fine detail can be accentuated when both illuminating light beams are filtered in different colors. To obtain optimal results, monochromatic narrow band filters are preferred. Also, resulting bicolor contrast effects can be fundamentally enhanced when two or more single images taken in different exposure are rendered in HDR techniques (**Fig. 16.9**).

3.3.2.4. Three-Shot Techniques

When specimens are successively photographed in monochrome red, green, and blue light (RGB splitting), the respective three monochrome images can be superimposed as an authentic true color image when processed with DRI-Tool or Image Stacker (*see* **Note 12**). As a result of this, separation, balance, and purity of colors can be optimized, and deviations in color tinge minimized. Moreover, all existing advantages of monochromatic light illumination can be transferred into the reconstructed true color images so that any lack of distinction associated with chromatic aberration is eliminated. If necessary, several quality-determining parameters (e.g., gradation, histogram, brightness, contrast, color saturation) can be separately adjusted for each single color channel by use of

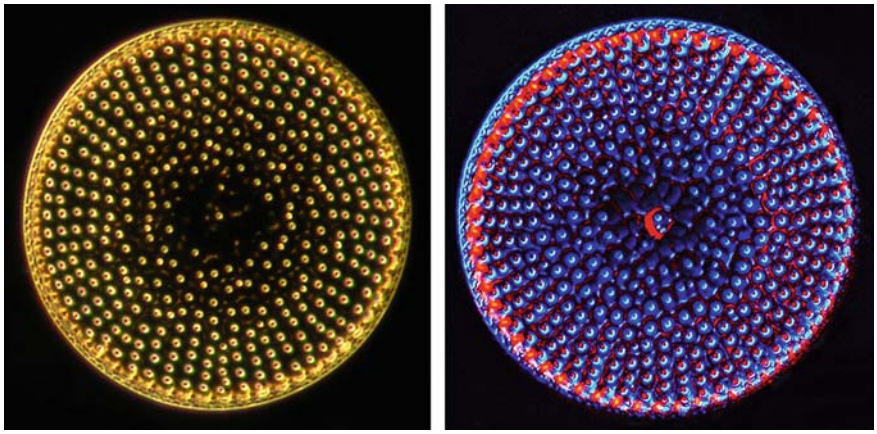

Fig. 16.9. Diatom shell, single image in conventional dark field (*left*), final reconstruction in superimposed dark field (*right*), based on transmitted monochromatic blue light (λ = 486 nm) and red epi-illumination, objective 20 $\times$, ocular 10 $\times$, HFW: 0.15 mm, superposition of 10 single images per stack, multiple stacking and HDR rendering. Software: first, multiple stacking was carried out with Picolay and Combine Z 5 (*see* legend for **Fig. 16.4**), then, two resulting deep focus reconstructions were rendered with Photomatix Pro in order to enhance the visible dynamic range.

common image-processing software. All in all, the reconstructed three-shot color images will appear in apochromatic quality even with non-apochromatic optical equipment.

Figure 16.10 shows an example of an image taken with a special achromatic objective for long-working distance affected with several optical compromises. RGB splitting and superposition of three monochrome RGB images lead to visible improvements of the global image quality. Not only the purity of colors but also the sharpness and contrast enhanced significantly.

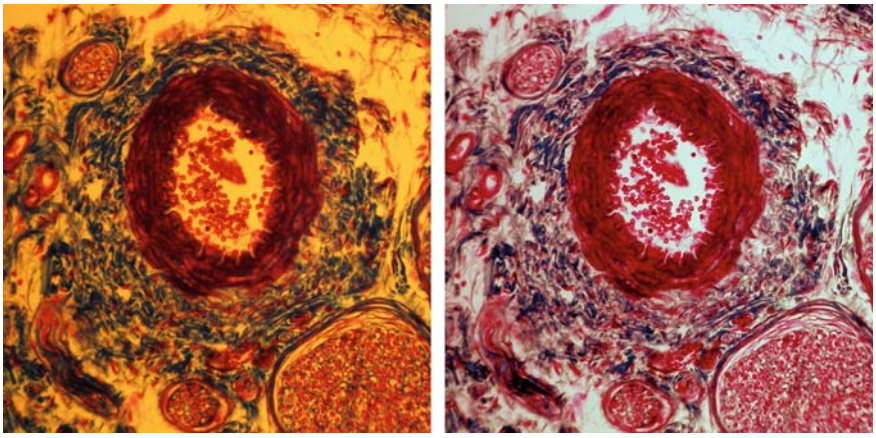

Fig. 16.10. Stained section of a mouse embryo, bright field, bulb light, special objective for long-working distance L 20 $\times$, ocular 10 $\times$, HFW: 0.30 mm, single-shot image (*left*), three-shot reconstruction (*right*), created by superposition of three single images filtered in monochromatic *red*, *green*, and *blue* light (λ = 486, 540, 656 nm). Software: DRI-Tool (further explanation in the text). In the left image, the background is yellow, and the red and blue stained tissues have little sharpness and contrast. In the right image, the background is pure white, and the blue or red stained tissues show greater clarity because of the high grade tonal values, improved contrast, sharpness and resolution.

4. Notes

1. All tested-software solutions lead to final reconstructions of high-resolution material within a few seconds or minutes when up-to-date computers are used. When the size of single images is doubled, the processing time is mostly doubled, in some cases nearly tripled. The processing time increases nearly in proportion to the number of single images, and it is also dependent on the respective software and the respective preset selected by the user.
2. Picolay and Combine Z 5 (macros: *Do Stack* and *Do Average and Filter*) are mostly not capable of superimposing single images taken in monochromatic light. Therefore, in this case, it is preferable to use Helicon Focus, or the Macro *Stack only* in Combine Z 5.
3. In multicolor images, Combine Z 5 leads to the best results in most cases. The standard macros *Do Stack* and *Do average and Filter* should be carried out successively so that the best reconstruction can be selected.
4. When specimens are affected by bright dust particles, other disturbing artificial structures or bright halo artifacts, the use of Picolay is preferred. In such cases, the reconstructions based on the darkest pixels at all positions will mostly lead to the best results, because the respective bright artifacts may appear in lower brightness or will no longer be visible.
5. All single images must always be equal in size when any software-based superposition has to be carried out. This fact is especially important for successive double or multiple stacking when two or more reconstructions differing in size have to be stacked again. In this case, the respective reconstructions have to be cut into identical size before the stacking procedure can be started.
6. In the middle of 2008, Combine ZT, a new version of Combine freeware, became available. This newest release is designed for Windows XP; the additional installation of a batch file is needed to run it. In our own experience, the prior Combine Z 5 software leads to more exact alignment of single images and superior contour sharpness in the final image reconstructions, especially with a stereo microscope when single images are shifting. Therefore, Combine Z 5 seems to offer superior results in photomicrography when still-images have to be stacked.
7. When light microscopes are equipped with digital video modules or digital compact cameras used for producing of video clips, three-dimensional specimens can also be stacked by

video techniques. For this purpose, the stage has to be moved very slowly from the top to the bottom or in reverse direction while the video clip is taken. The number of video frames is determined by the local thickness of the specimen, the speed of stage lifting, and the frame rate of the video camera. Circa 250–500 frames are usual for one stack. Now, the Combine ZT software can be used for video stacking as follows: first, the video has to be converted into the wmv file format (windows media video). The freeware software Prism Video Converter is well suited to this task (14). Afterwards, all single frames of the wmv video can be extracted using Combine ZT. When the arrow keys (*up* and *down*) are pressed, the user can scroll the video frames. Now, the stacking procedure can be directly started in the same way as described for still-images. Alternatively, all video frames can be exported from Combine ZT into a separate folder and saved as TIF, JPG, BMP, GIF, or PNG files. In this case, these image files can be stacked using all variants of stacking software described in this paper (e.g., Combine Z 5, Picolay, and Helicon Focus). The size of video frames is much lower than in usual high-resolution still-images. Thus, video-based three-dimensional reconstructions need to be optimized for full-screen presentations or prints with the help of specialist software which enlarges small digital images with suitable interpolation techniques. In our experience, the shareware PhotoZoom Pro gives the best results in digital image enlargement (15).

8. Recently, a new release of the Picolay software has been developed (version 2008-09-19). This release is designed for all relevant Windows versions (Windows 98 or higher). According to our initial experience in this, the prior version leads to comparable results in most cases, but works faster and is more comfortable to use than the latest release. Thus, in our opinion, the 2007 version is preferable for photomicrography.
9. In contrast to other HDR or DRI software, Picturenaut does not work if the original EXIF data from the single images are not available. Thus, Picturenaut cannot be used for reconstructions when the respective single images were pre-processed by other software so that their EXIF data are missing. EXIF data are also deleted by all stacking software used for enhancing the focal depth. Therefore, this software cannot be combined with Picturenaut, and three-dimensional reconstructions taken at different exposures cannot be rendered in HDR using Picturenaut.
10. In high-dynamic range constellations, the software Photomatix Pro produces the best final results in most cases. The nature of the specimen will determine if the *Details Enhancer* or the *Tone Compressor* will work most effectively. On some occasions, the *Details Enhancer* may produce too much detail

or artificial "pseudo-detail" which does not really exist in the specimen. In this case, the *Tone Compressor* or other software solutions will lead to more authentic results.

11. The fine detail in low contrast can also be visibly enhanced by Photomatix Pro, even when a particular image is taken twice in identical or nearly identical exposure. For this purpose, HDR techniques should be used (*Details Enhancer* or *Tone Compressor*).
12. When true color images have to be reconstructed based on three-shot techniques, only DRI-Tool or Image Stacker is capable of rendering well-balanced colors. The other software solutions will produce multicolor sandwiches instead of authentic true color images.

Acknowledgements

The author thanks Timm Piper for the images shown in **Fig. 16.7** and Eberhard Raap for some excellent preparations from radiolarians and diatoms.

References

1. Hart, J. (2003) 3D Microscopy and high-magnification macro-photography: Digital reconstruction and depth-of-field expansion. University of Colorado. http://www.crystalcanyons.net/pages/TechNotes/3DMicroMacro.shtm
2. Wikipedia (2008) High Dynamic Range Rendering. http://en.wikipedia.org/wiki/High_dynamic_range_rendering
3. Wikipedia (2008) High Dynamic Range Imaging. http://en.wikipedia.org/wiki/High_Dynamic_Range
4. Hedley, A. (2006) CombineZ5. My software to combine pictures to increase depth of focus. http://www.hadleyweb.pwp.blueyonder.co.uk/index.htm
5. Cyprionka, H. (2007) Picolay – freeware for generating improved images from picture series. http://www.picolay.de
6. Heliconsoft (2007) Helicon Focus. http://www.heliconfocus.com/heliconfocus.html
7. Gross, S. and Hartl, B. (2008) Enhancements of visible dynamic ranges using DRI-Tool (in German). http://www.traumflieger.de/desktop/DRI_tool.php
8. Hartl, B. (2008) Image Stacker (in German). http://www.pixel-treff.net/ Daten/ ImageStacker.exe
9. Okonek, B. (2008) EasyHDR, always properly exposed images by exposure blending and tone mapping. http://www.easyhdr.com/index.php
10. Mehl, M. (2008) Picturenaut, HDRI-generator, tone mapping (in German). http://www.hdrlabs.com/picturenaut/index.html
11. HDR Soft (2008) Photomatix. http://www.hdrsoft.com
12. Sasso, F. (2008) How to create HDR-photos-HDR/Photomatix tutorial. http://abduzeedo.com/how-create-hdr-photos-hdrphotomatix-tutorial
13. Piper, J. (2007) Luminance contrast – a new visible light technique for examining transparent specimens. *Micros. Today*, **15**, 26–34.
14. NCH Software (2008) Prism Video Converter. http://prism-video-converter.en.softonic.com/download
15. Brueckner, S., Benvista Ltd. (2008) PhotoZoom Pro. http://photozoom-pro.en.softonic.com/

Chapter 17

Image Analysis and Quantitative Morphology

Carlos Alberto Mandarim-de-Lacerda, Caroline Fernandes-Santos, and Marcia Barbosa Aguila

Abstract

Quantitative studies are increasingly found in the literature, particularly in the fields of development/evolution, pathology, and neurosciences. Image digitalization converts tissue images into a numeric form by dividing them into very small regions termed *picture elements* or *pixels*. Image analysis allows automatic morphometry of digitalized images, and stereology aims to understand the structural inner three-dimensional arrangement based on the analysis of slices showing two-dimensional information. To quantify morphological structures in an unbiased and reproducible manner, appropriate isotropic and uniform random sampling of sections, and updated stereological tools are needed. Through the correct use of stereology, a quantitative study can be performed with little effort; efficiency in stereology means as little counting as possible (little work), low cost (section preparation), but still good accuracy. This short text provides a background guide for non-expert morphologists.

Key words: Image analysis, morphometry, stereology, volume density, surface density, length density, disector.

1. Introduction

Morphologists are habitually interested in form and composition of structures at macro, meso, microscopic, and ultrastructural levels. Although genetic and molecular techniques help biological and biomedical researchers, quantitative approaches are still required to answer questions about numerical alterations of tissues, cells, or cellular organelles, and to better understand the correlation between morphology and function.

Quantitative studies have several scientific advantages over qualitative studies. First, results are numerical (not subjective); therefore, results are reproducible and easier for different laboratories to verify at any time. Second, inter-group comparisons (age,

T.D. Hewitson, I.A. Darby (eds.), *Histology Protocols*, Methods in Molecular Biology 611,
DOI 10.1007/978-1-60327-345-9_17,

species, drug actions, manipulations, etc.) are easily separated out, making these methods particularly useful for hypothesis testing. Third, the fastidious work commonly associated with quantitative studies is largely eliminated with the strict sampling strategy and the computer-aided analysis of modern quantification. Fourth, the well-established theoretical background means that the method is well accepted. Finally, little training is required for relatively inexperienced researchers.

Despite arguments to the contrary, the nomenclature *morphometry* and *stereology* do not describe the same method (1). Most authors consider morphometry a two-dimensional quantitative method that uses a caliper (mainly a caliper micrometer, a gauge with a calibrated micrometer screw for the measurement of thin objects under microscopic observation). Stereology does not use a caliper (and does not perform a direct measurement), but rather is a test-system usually comprised of test-points or test-lines over a known frame (test-area). The challenge in stereology is to understand the structural inner three-dimensional arrangement based on the analysis of slices that only show two-dimensional information (**Fig. 17.1**).

Morphometry determines lengths, perimeters, areas, and can easily be realized using appropriate image analysis software. Stereology estimates densities; the most interesting are the densities per volume: volume density (V_V), length density (L_V), surface

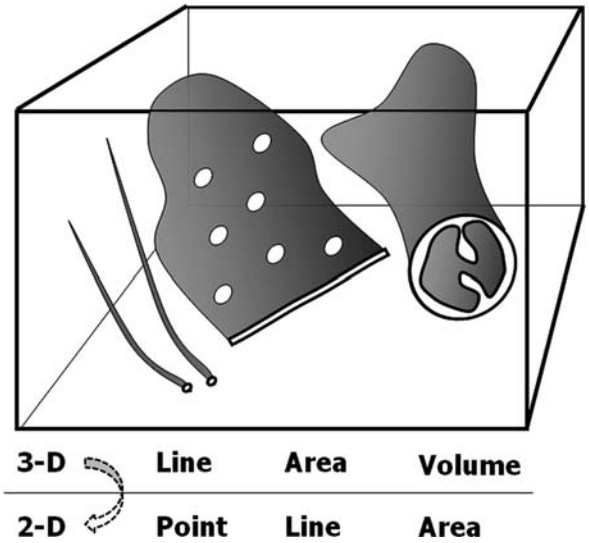

Fig. 17.1. Correlation between three-dimensional structures and two-dimensional images seen on section slices: *lines* (microtubules) appear as points, *areas* (endoplasmic reticulum) appear as *lines*, and *volumes* (mitochondria) appear as *areas*. The challenge of stereology is to recover three-dimensional information based on two-dimensional "counts."

density (S_V), and numerical density (N_V). Densities per area can also be estimated and informative; area density (A_A) and numerical density per area (N_A or Q_A) are the parameters most frequently estimated (2). All indices are estimated by the application of specific formulae (described below). However, the accuracy of calculations is based on statistical principles (sample size, randomization, and tissue isotropy). The aim of the sampling design is to obtain the maximum amount of quantitative structural information at a given total cost or effort. The variation between different individuals (the biological variation) is the major determinant of overall efficiency, whereas the variation between single microscopic features is immaterial. However, spending additional time and/or money in order to increase the precision of the individual measurements is not warranted in almost all studies emphasizing biological results. This could be summarized simply as do more less well (3).

2. Image Analysis

2.1. System Calibration

Image digitalization converts tissue images into a numeric form by dividing them into very small regions called *picture elements* or *pixels*. Length is determined by the number of pixels along a line, area as the number of pixels within an outlined area, and so forth. Nevertheless, it is necessary to correlate pixels with a metric system in order to obtain true measurements. A caliper micrometer – a glass slide having 1-mm rule divided into a hundred parts or 1 mm/100 (i.e., 10 μm) – is used to calibrate the system. In order to create a calibration, first a digital image of the caliper is acquired for each microscope objective (× 40 objective shown in **Fig. 17.2**). After that, a straight line is drawn over the micrometric rule, allowing the software to correlate its length with the number of pixels in it. Finally, the number of micrometers represented by the line (in this example, 50 μm) is loaded into the software program, so that it generates the calibration for the 40 × objective.

We must highlight that the calibration must be created for each objective. So, when measuring by image analysis, the only requirement is to identify for the software which objective was used to acquire the image, to ensure that the results represent a true value.

2.2. Measurement

Specialist software packages for image analysis have the tools required for morphometric analysis. Some examples of the morphometric tools in Image Pro™ Plus (Media Cybernetics Inc., Bethesda, MD, USA) are given below.

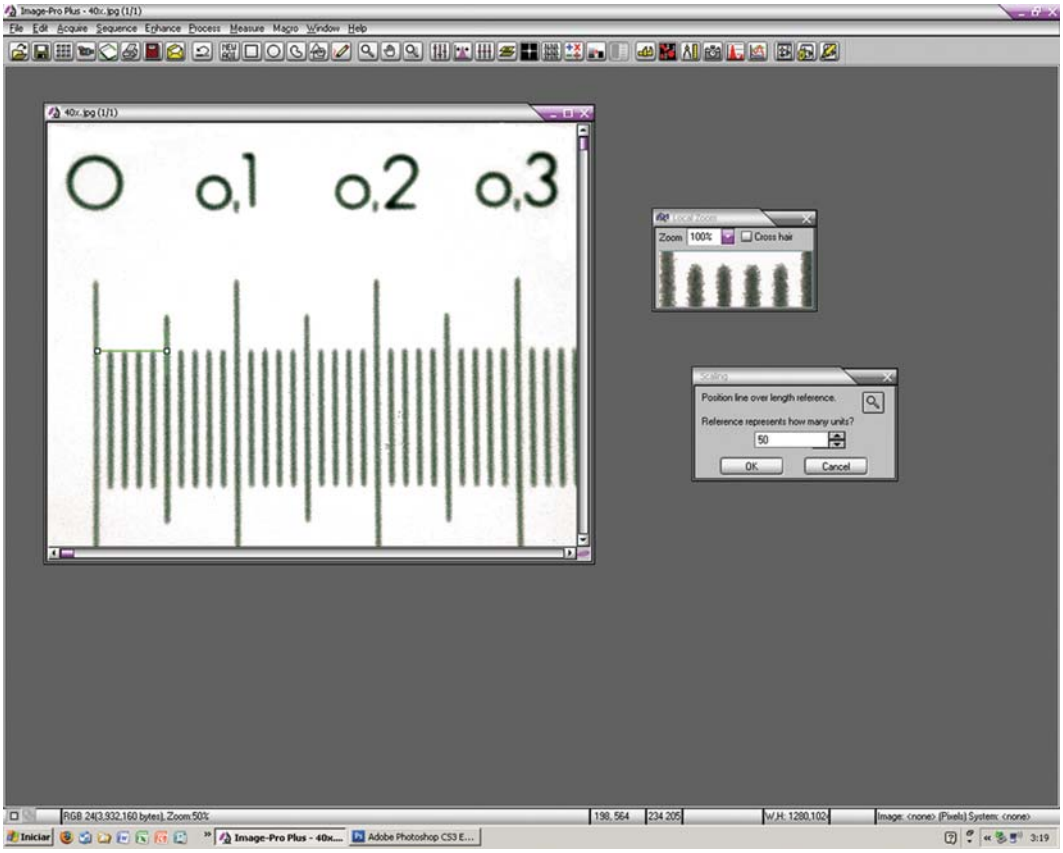

Fig. 17.2. Calibration of the × 40 objective using a caliper – slice micrometer (Image Pro™ Plus program). Each division measures 10 μm. The distance of 50 μm was measured (*left side*) and entered into the program.

2.2.1. Area

The area of a structure is obtained by drawing over its external outline. Tools referred to as *circle*, *rectangle*, and *polygon* can all be used for delineating area, depending on the shape of the structure. Area is easily calculated within these geometrical forms, as it correlates with the number of enclosed pixels.

For instance, the renal glomerulus has a nearly spherical shape; its cross-sectional transverse area can be measured by drawing a circle over its capsule. The area of a pancreatic islet, which is nearly round in shape, can be measured by drawing a polygon over its outline. In the example shown in **Fig. 17.3**, the outer cross-sectional area of an arterial branch was obtained by drawing over the adventitia layer. The software may also determine the arterial diameter (length, in the box), based on the circular shape of the artery.

2.2.2. Length

Length is measured by drawing a straight line on the structure, which can be used to assess the thickness of the artery wall and its lumen diameter (4). The diameter of other structures such as a renal glomerulus, adipose cells, and pancreatic islets can also be measured using this tool (**Fig. 17.4**).

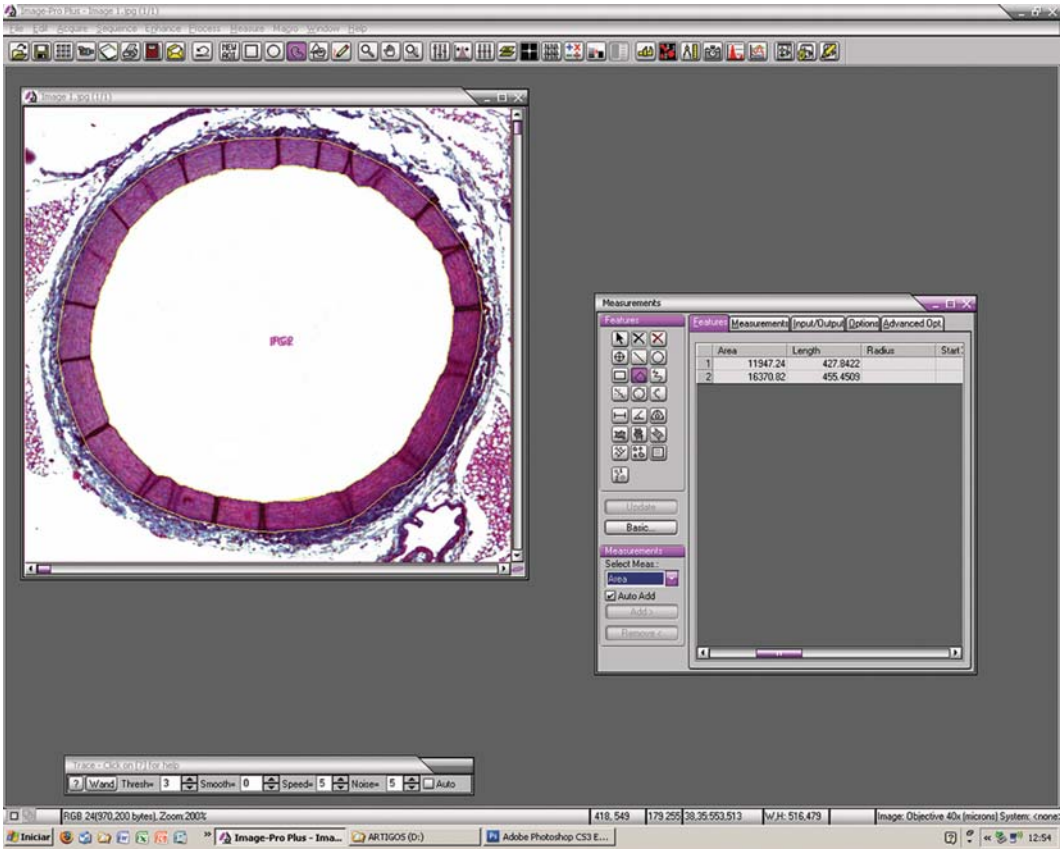

Fig. 17.3. After system calibration, an arterial cross section has been delineated with a circle from the measured area tool in Image Pro™ Plus.

Beyond measuring area, the *polygon tool* also measures length. For instance, a polygon drawn over the arterial intima layer shows its lumen perimeter (**Fig. 17.3**). In the kidney, the area of polygons enclosing either cortex or medulla can be used to help assess the cortex-to-medulla ratio (5).

2.2.3. Another Strategy for Measuring with Image Analysis

Length and area help in assessing more complex parameters (**Fig. 17.4**). In this case, the cross-sectional area of the aorta media layer is assessed by two polygons drawn over the limit between intima and media layers (P1), and another over the limit between media and adventitia layers (P2). Each polygon delineates one area (calculated by the software), and these areas are referred to as A1 and A2, where A1 (lumen area) is enclosed by A2 (lumen area plus tunica media area). Thus, the result of subtracting A1 from A2 represents the cross-sectional area of the media layer.

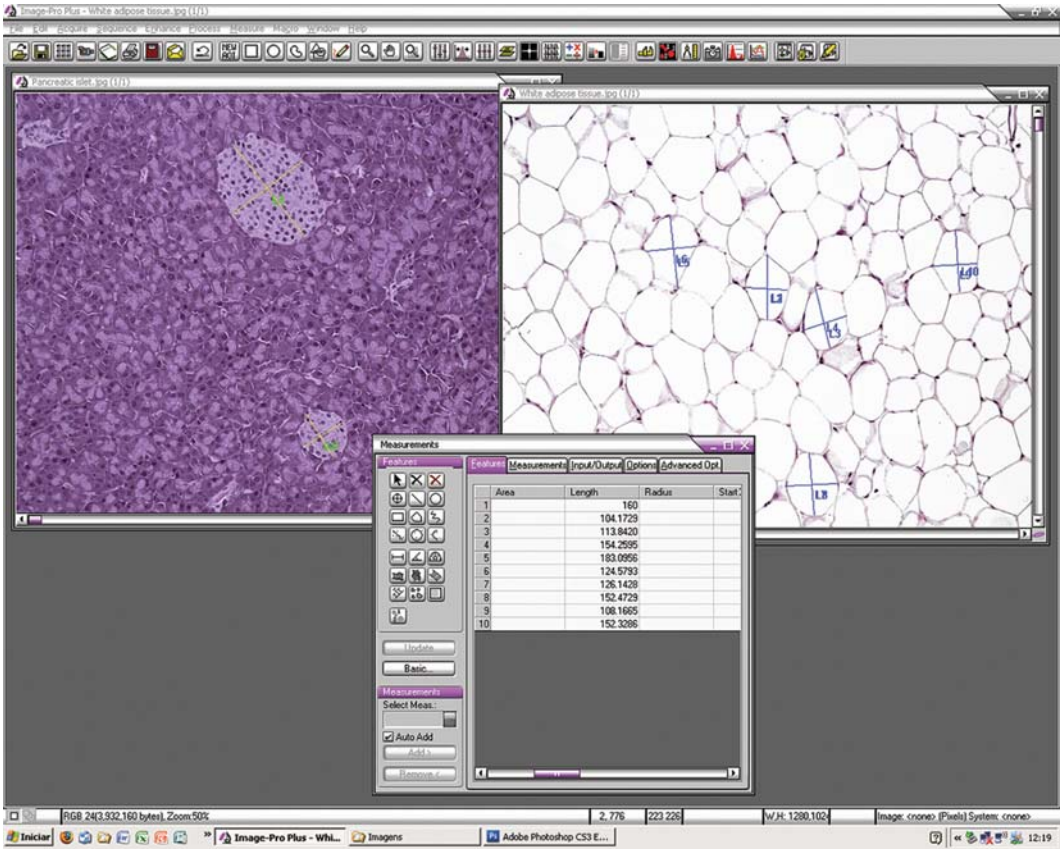

Fig. 17.4. Major and minor diameters of mice pancreatic islet and adipocytes measured with Image Pro™ Plus.

3. Image Segmentation and Quantification

The object of interest should be split from the background by image segmentation. *Segmentation* is the process by which colors on the image are identified and then isolated from the image as a whole. It is performed using their color characteristics. *Thresholding* is a tool used for segmentation, which works by reducing color images to just black and white. This is done by specifying a range of intensities to be emphasized (set to white, 1) and converting all others to black (0).

3.1. Tissue Stain

Objects that will be segmented must have a color as different as possible from the remaining tissue to facilitate pixel selection by the software. If other structures contain pixels similar to those found in the object of interest, they are segmented too, creating background.

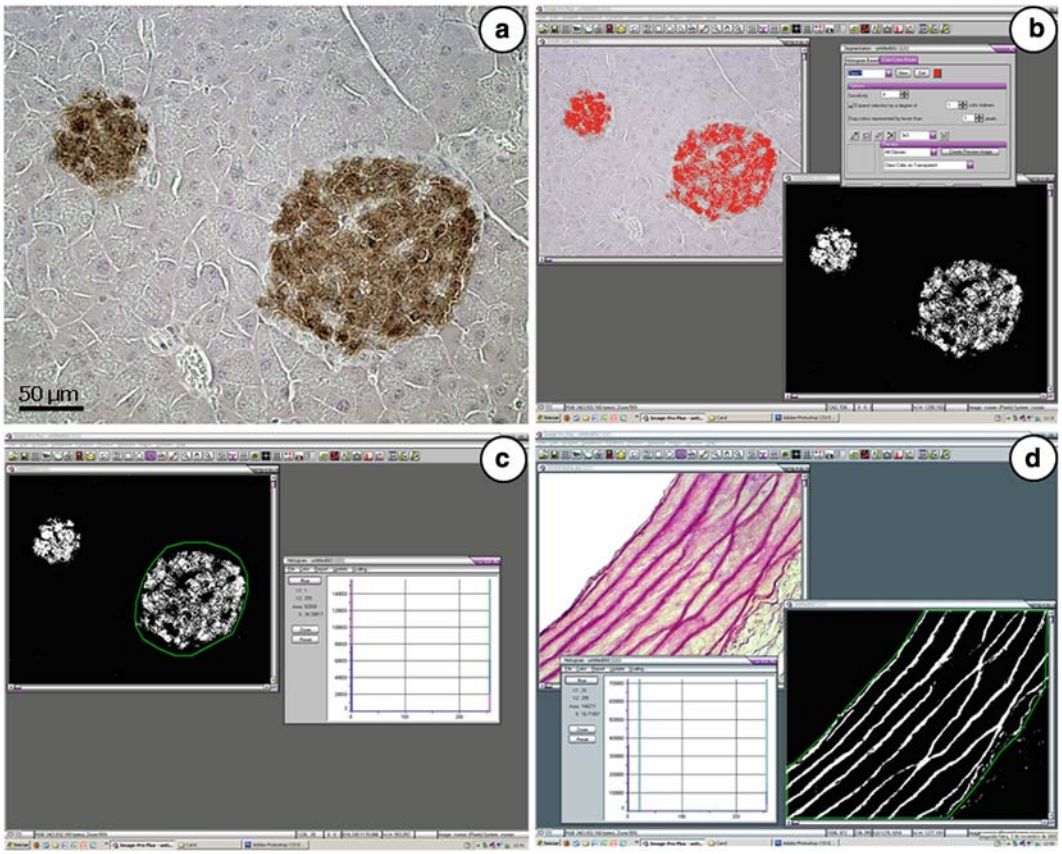

Fig. 17.5. Digital image segmentation and quantification: (**a**) pancreatic islet marked with anti-insulin antibody (dark staining-*brown color*, beta cell); (**b**) segmentation box opened (color-cube-based mode) and a new mask was applied by selecting all pixels of varying levels of *brown color* (*red color*), then a new image in *black* and *white* was generated; (**c**) in this *black* and *white* image, the islet outline was drawn using the AOI tool, so that we measured the density area of insulin stain per islet (as percentage); (**d**) rat aorta stained by orcinol (*upper box*) to mark elastic fibers in *pink color* (*upper left image*). After segmentation (*dark staining*), we quantified the density per area of elastic fibers – a polygon was drawn (AOI tool) on the segmented image delineating the media layer of the aorta. Inside this area, we determined both percentage and area of elastic fibers (*left lower box*).

3.2. Image Capture

It is important to ensure that all digital images to be analyzed are acquired under the same conditions of light and white balance (Image Pro™ Plus allows it to be adjusted before image acquisition). The aim is to avoid great differences in color intensity between images.

3.3. Segmentation

Segmentation can be performed using either histogram-based (HB) or color-cube-based (CCB) options available on the Image Pro™ Plus software. In the first case, a histogram displays all pixels contained in the image based on RGB or HIS color models. Selecting the range of pixels representing the object of interest, the software generates a new image in black and white, where the range of pixels for the object of interest is represented as white and the remaining tissue as black.

However, the HB segmentation option allows only segmentation of nearby pixels. The CCB segmentation is better than HB segmentation, since we can manually choose which pixels need to be segmented. **Figure 17.5 s**hows the segmentation of insulin-stained pancreatic islets in a mouse (brown color in the original, **Fig. 17.5a**). The segmentation box is opened in CCB mode (**Fig. 17.5b**). After selecting all pixels representing varying levels of brown, the new mask tool is applied so that a new image is generated in black and white, where white is the insulin stain and black is the remaining tissue.

3.4. Quantification

The image histogram tool allows the quantification of the amount of white/black colors in the segmented image. It has a scale ranging from 0 to 255 – 0 is white, 255 is black, and the remaining scale, 1–254, shows varied levels of gray, according to the standard gray scale. As the segmented image does not contain gray colors, 0 and 255 show the total percentage of white and black color, respectively, and their sum is 100%. If the image is properly calibrated, the histogram also gives the area occupied by each color. Returning to the example of insulin stain, the islet outline can be drawn using the *area of interest* (AOI) tool, so that the percentage will represent the density area per islet of insulin stain (**Fig. 17.5c**).

Rat aortic wall stained with orcinol shows elastic fibers as pink, while the remaining tissue has a quite different color (**Fig. 17.5d**). In order to quantify the density per area of elastic fibers, the pink color is selected, then segmented. In the segmented image, a polygon is drawn (AOI tool) so that the media layer is delineated. Inside this area, both percentage and area of elastic fibers are determined (histogram tool) (4).

4. Stereology

4.1. Volume

Frequently we need to estimate the volume of an entire organ or parts of an organ. This measurement is essential to estimate absolute stereological quantities. Two main methods are normally used for this estimate, the *liquid displacement* (or submersion) method, and application of Cavalieri's principle.

In the submersion method, volume is measured by weighing the amount of isotonic saline displaced (W) by an organ volume (6). As the specific gravity (σ) of isotonic saline is 1.0048, the volume (V) is obtained by $V = W/\sigma$ or simply $V \approx W$ (7). Normally, weight is measured in grams and needs to be transformed into a volume unit like cubic millimeters (remember: 1 g is equal to 10^3 mm^3).

The volume of an arbitrary-shaped object can be estimated in an unbiased manner from the product of the distance between planes, and the sum of areas on systematic-random sections through the object, as demonstrated by the Italian mathematician Bonaventura Cavalieri (1598–1647). Areas can be measured by *point counting*, so volume will be indirectly estimated without any measurement. It is a useful method for analyzing microscopic structures enmeshed into a tissue like the heart conduction system (8) or organs in vivo by computed tomography or magnetic resonance (9).

4.2. Delesse's Principle

The Delesse's principle is based on homogenous structures, in stereological terms, *isotropic and uniform random* (IUR) sections (*see* **Section 4.5**). In a rock composed of different minerals, the area occupied by any given mineral on a surface of a rock section is proportional to the volume of the mineral in the rock. Only in this case, we can accept the equal ratios:

$$\frac{P_P}{P_T} = \frac{L_L}{L_T} = \frac{A_A}{A_T} = \frac{V_V}{V_T}$$

that means, in IUR sections, the ratio between the partial points (P_P) counted on a section in relation to the total possible points or test-points (P_T) is equivalent to the ratio among lengths (partial, L_L, to total length, L_T), areas (partial, A_A, to total area, A_T), and volumes (partial, V_V, to total volume, V_T). Consequently, we can estimate the length fraction, the area fraction, or the volume fraction of a structure just by "point counting." The volume fraction or volume density (V_V) is a powerful robust stereological estimate, i.e., V_V could be estimated even when it cannot be proved that the start of the object is an IUR section.

4.3. Holmes Effect

The ideal specimen is an infinitely thin section. The area occupied by any given component may be overestimated. To the eye placed above the section, the image of the component will appear to occupy a larger area on the surface of the section than it in fact does. In the case of particles with good contrast, it is usual to make some allowance for the Holmes effect if the mean diameter of the particle is less than 12 times the section thickness. Consequently, stereological estimates must take into account the Holmes effect. A mathematical correction for the Holmes effect can be done, although it is preferable to use thin sections and so not require a correction. In practice, sections of not more than 3-μm thickness are suitable for most stereological procedures (an exception to the use of thin sections is the *disector* method, where sections over 20 μm in thickness can be used – *see* **Section 4.7**).

4.4. Buffon's Needle Problem

In modern stereology, the question *what is the probability that a randomly placed line will intersect a grid of parallel lines?* is similar to the ancient needle problem of Buffon (Georges-Louis Leclerc "Count of Buffon," eighteenth-century French naturalist). Based on this, the surface density (S_V) of a structure can be estimated:

$$S_V = \frac{2 * I}{L_T} (\mathrm{mm}^2/\mathrm{mm}^3)$$

where, I is the number of intersections of the object boundary with the lines of the test-system and L_T is the total length of the lines. The estimate for S_V is a reasonable, but not robust estimate; it should only be used with IUR sections, and this condition needs to be satisfied first.

4.5. Producing IUR Sections

An organ has homogeneous – *isotropic* or not orientated – structure when we are not able to decide the orientation of the section by observing its histological appearance; otherwise, the organ has heterogeneous – *anisotropic* or orientated – structure. IUR sections are the basis of stereology. In organs with homogeneous structure (liver, salivary glands, etc.), no particular procedure is needed to obtain IUR sections. Otherwise, two main methods have been proposed: the *orientator* (10) and the *vertical sections* (11).

4.5.1. Orientator

The *orientator* is an unbiased, design-based approach for stereological estimation using IUR sections. No special technical equipment is necessary. *Orientator* can be generated without difficulty in large specimens; we have investigated human skeletal muscle, myocardium, placenta, and gut tissue. Slight practical modifications extend the application of this method to smaller organs like rat hearts. At the ultrastructural level, a correction procedure for the loss of anisotropic mitochondrial membranes due to oblique orientation of the electron beam has been suggested.

The *orientator* design can be obtained initially by cutting the organ at random; the organ part is then placed on this cut and, again at random, cut with a perpendicular section to the first plane. The specimen is again placed on the new cut surface and a new random orientation is defined by cutting the organ part in a perpendicular section to the plane. The last cut is considered uniformly isotropic – it means without reference to the position of the specimen in the first cut, the last surface has an orientation that varies from all possible ones.

4.5.2. Vertical Sections

Vertical sections are plane sections longitudinal to a fixed (but arbitrary) axial direction. Examples are sections of a cylinder parallel to the central axis and sections of a flat slab normal to the plane of the slab. *Vertical sections* of any object can be generated by placing the object on a table and taking sections

perpendicular to the plane of the table. Stereology's standard methods assume IUR sections, and they are not applicable to this kind of biased sampling. However, using specially designed test-systems (cycloid arcs test-system, *see* **Section 4.6**), an unbiased estimate of surface area can be obtained. No assumptions are necessary about the shape or orientation distribution of the structure. *Vertical section* stereology is valid on the same terms as standard stereological methods for isotropic random sections. The vertical axis direction is freely chosen, which makes the sampling procedure simple.

4.6. Test-Systems and Data Acquisition

We use test-lines, test-points, and a known frame (test-area) to gather information from two-dimensional slices. All together, lines, points, and frame compose a test-system. Usually, test-systems have known line length (L_T), total points (P_T), and test-area (A_T). We need this information to estimate (we use ":=" to highlight that it is an estimate!):

$$\text{volume density}: V_V := P_P/P_T(\text{mm}^0 \text{ or } \%),$$
$$\text{length density}: L_V := 2 * Q_A(\text{mm/mm}^3),$$
$$\text{surface density}: S_V := 2 * I/L_T(\text{mm}^2/\text{mm}^3)$$

Test-systems are used by superimposing on images. A test-system can be mounted into the microscope's eyepiece, drawn in acetate and put over glossy prints (this is normally the case with electron micrographs), superimposed on a monitor screen in video-microscopic system, or produced by software. Regardless of the method, lines and points hitting tissue objects and the number of objects in the frame are counted, to get enough information to undertake the stereological calculation.

Figure 17.6a shows a classic test-system named *multipurpose test-system* or M42. In this test-system, the short line length, d, is used to calibrate the system: $A_T = 36.36d^2$, $L_T = 21d$ and $P_T = 42$ (12).

Another test-system composed of *cycloid arcs* is particularly useful with *vertical sections* and stratified samples (skin, mucosa, cerebral cortex, etc.) (**Fig. 17.6b**) (13). If S_V does not need to be estimated – remember that S_V is not robust, requires IUR sections and, therefore, a major effort (great cost) is usually necessary to estimate S_V – a test-system without test-lines could be used (like the example in **Fig. 17.6c**), allowing easy and fast counts with no accuracy loss.

Since the Danish stereologist Hans Gundersen demonstrated the *edge effect* of the frames (A_T) causing overestimation in the counts, two borders of A_T have been systematically considered *forbidden*, and all objects hit by these borders are not considered in the counts (**Fig. 17.6d**) (14).

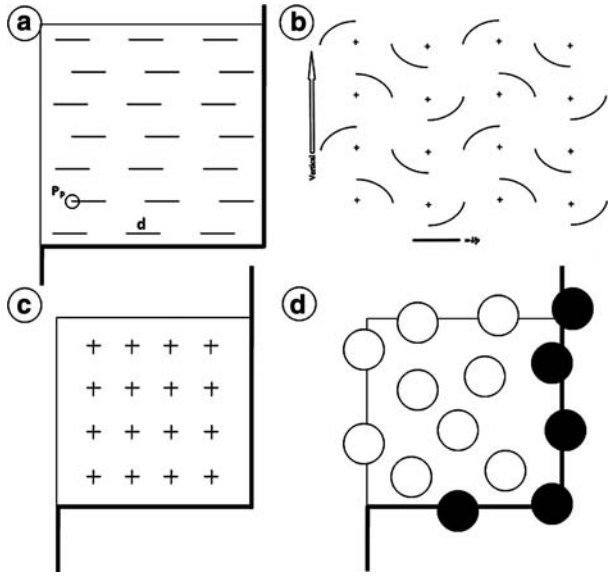

Fig. 17.6. Test-systems usually used in stereology: (**a**) M42 test-system – it has 21 *short lines* of known length (**d**) with two test-points in each extremity (P_P, 42 test-points in total). The test-area is 36.36d^2. The *thicker lines* are "forbidden" (see explanation in figure **d**); (**b**) cycloid arcs test-system – crosses are test-points (n=16). The cycloid arc length is defined as the *short line* (l/p). The system should be aligned on vertical sections using the *arrow* (*left side*); (**c**) P36 test-system has 36 test-points and no test-line – it allows fast counting and can be applied appropriately to majority of uses; (**d**) test frame for profile counting – *thicker line* represents "forbidden line" – all structures hitting this line are not considered. In the schema, white circles only should be counted.

4.7. Estimation of Object Quantity

The object's quantity estimation is a critical issue in stereology. This is partially answered with the estimate of the object's number within a frame (Q_A or N_A), but it is not enough to when studying three-dimensional structures. Instead, over many years great effort has gone into finding an unbiased reproducible method to estimate the numerical density (N_V) of objects – we recommend classic textbooks for a detailed discussion about the older methods (1, 7, 15). A major change in our thinking about estimation of object quantity in three dimensions of space occurred with the *disector* method (note that the word "*disector*" has only one *s* according to its first description) (16).

Figure 17.7 shows the basic principles of the *disector* method in which N_V is obtained in sets of two parallel sections with a known separation (thickness). To avoid overestimation of counts, one plane – look up or look down – should be considered *forbidden* and counts should be made on a single plane (therefore this count is named Q_A^-). For instance, if the look-down plane is considered forbidden, no objects hit by this plane should be counted. Counts are made into a frame of known area A_T

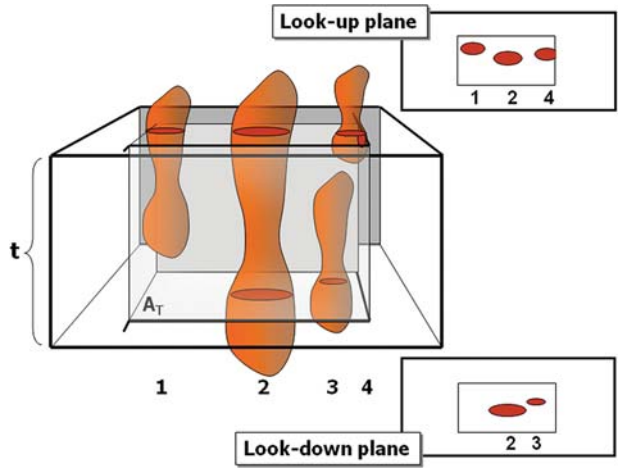

Fig. 17.7. Disector is the union of a reference plane with an unbiased counting frame of area A_T and a look-up plane at distance t apart. The schema exemplifies the *optical disector* with four different objects in the test space-volume (calculated as $A_T * t$). All objects hitting the *forbidden line* (*thick line*) or appearing in both focal planes are not considered – in practice, one focal plane is forbidden. In the example, we suggest the look-down plane as the forbidden plane. In *right side* up and down, we see the schema of the slices with the object profiles. *Up slice* shows objects 1, 2, and 4. *Down slice* shows objects 2 and 3. In the *up slice*, object 4 hits the *forbidden line*. Therefore, only object 1 should be counted.

(considering the forbidden line and its extensions as described before). So, a test-volume is constructed (the product of A_T and thickness), count within this test-volume are considered unbiased. The *disector* can be optical or physical.

4.7.1. Optical Disector

Counts should be made from thick sections and observed by light microscope adapted with an axis-z mobile stage (this is important to exactly determine the distance between the up and down planes of the *disector* or thickness t).

4.7.2. Physical Disector

Counts should be made using photomicrographs, or electron micrographs, of both up and down planes (this is the only way to use the *disector* method with transmission electron microscopy).

The numerical density of the objects (N_V) is estimated as:

$$N_V = \frac{Q_A^-}{t * A_T} (1/\text{mm}^3)$$

The absolute number of objects (N) could be estimated if the organ volume is known (V, Scherle's method of water displacement or Cavalieri's method as already described):

$$N = N_V * V(\text{mm}^0)$$

4.7.3. Fractionator

The *fractionator* is another unbiased method used to quantify the object number. It uses the same counting principles as manual counting of blood cells (blood is diluted many times and, at the end, blood cells are counted in this diluted sample, then the number must be multiplied by the dilutions, allowing the number of cells estimated in the intact blood). With the *fractionator*, the same process occurs. The organ is completely sliced, a known fraction of slices is taken (for example, one of every three slices) and cut away in strips, a known fraction of strips (for example, one of every four strips) is taken and cut away in fragments, a known fraction of the fragments (for example, one of every five fragments) is embedded and serially sectioned. Finally, a known fraction of the sections is analyzed (for example, one of every three sections) and all objects are counted in these chosen sections. This counted number ($N_{[\text{counted}]}$) must be multiplied by fractions to recompose the absolute number of objects ($N_{[\text{objects}]}$) in the organ.

$$N_{[\text{objects}]} = N_{[\text{counted}]} * 3 * 4 * 5 * 3$$

Acknowledgments

The authors participate in the Post-Graduate Program of Human and Experimental Biology (www.bhex.uerj.br), State University of Rio de Janeiro, Brazil. The author's laboratory is sponsored by grants from CNPq (Brazilian National Council for Science and Technology, www.cnpq.br) and FAPERJ (Rio de Janeiro Foundation for Science and Research, www.fapaerj.br).

References

1. Aherne, W.A. and Dunnill, M.S. (1982) *Morphometry*. Edward Arnold Publishers, London.
2. Mandarim-de-Lacerda, C.A. (2003) Stereological tools in biomedical research. *An. Acad. Bras. Cienc.* **75**, 469–486.
3. Gundersen, H.J. and Osterby, R. (1981) Optimizing sampling efficiency of stereological studies in biology: or 'do more less well!'. *J. Microsc.* **121**, 65–73.
4. Torres, T.S., Silva, G.D., Aguila, M.B., Carvalho, J.J., and Mandarim-de-Lacerda, C.A. (2008) Effects of rosiglitazone (a peroxysome proliferator-activated receptor gamma agonist) on the blood pressure and aortic structure in metabolically programmed (perinatal low protein) rats. *Hypertens. Res.* **31**, 965–975.
5. Catta-Preta, M., Oliveira, D.A., Mandarim-de-Lacerda, C.A., and Aguila, M.B. (2006) Adult cardiorenal benefits from postnatal fish oil supplement in rat offspring of low-protein pregnancies. *Life Sci.* **80**, 219–229.
6. Scherle, W. (1970) A simple method for volumetry of organs in quantitative stereology. *Mikroskopie* **26**, 57–60.
7. Weibel, E.R. (1979) *Stereological Methods. Practical Methods for Biological Morphometry*. Academic Press, New York.
8. Mandarim-de-Lacerda, C.A. and Penteado, C.V. (1988) Topographical and morphometrical study of the atrioventricular junctional area of the cardiac conduction system in the *Macaca fascicularis* Raffles, 1821. *Anat. Anz.* **167**, 57–61.

9. Acer, N., Bayar, B., Basaloglu, H., Oner, E., Bayar, K., and Sankur, S. (2008) Unbiased estimation of the calcaneus volume using the Cavalieri principle on computed tomography images. *Ann. Anat.* **190**, 452–460.
10. Mattfeldt, T., Mall, G., Gharehbaghi, H., and Moller, P. (1990) Estimation of surface area and length with the orientator. *J. Microsc.* **159**, 301–317.
11. Baddeley, A.J., Gundersen, H.J., and Cruz-Orive, L.M. (1986) Estimation of surface area from vertical sections *J. Microsc.* **142**, 259–276.
12. Weibel, E.R., Kistler, G.S., and Scherle, W.F. (1966) Practical stereological methods for morphometric cytology *J. Cell. Biol.* **30**, 23–38.
13. Gundersen, H.J.G., Bendtsen, T.F., Korbo, L., Marcussen, N., Moller, A., Nielsen, K., Nyengaard, J.R., Pakkenberg, B., Sorensen, F.B., Vesterby, A., and West, M.J. (1988) Some new, simple and efficient stereological methods and their use in pathological research and diagnosis. *APMIS* **96**, 379–394.
14. Gundersen, H.J. (1977) Notes on the estimation of the numerical density of arbitrary profiles: the edge effect. *J. Microsc.* **111**, 219–227.
15. Elias, H., Hyde, D.M., and Scheaffer, R.L. (1983) *A Guide to Practical Stereology*. Karger, Basel, Switzerland.
16. Sterio, D.C. (1984) The unbiased estimation of number and sizes of arbitrary particles using the disector *J. Microsc.* **134**, 127–136.

Subject Index

T.D. Hewitson, I.A. Darby (eds.), *Histology Protocols,* Methods in Molecular Biology 611,
DOI 10.1007/978-1-60327-345-9, © Humana Press, a part of Springer Science+Business Media, LLC 2010

T

U

V

W